Interoceptive chemosensory functions of neurons in contact with the cerebrospinal fluid

Hugo Marnas

Sorbonne Université

Ecole doctorale « Cerveau, Cognition, Comportement »

Institut du Cerveau (ICM)

Laboratoire Signalisation Sensorielle Spinale

Interoceptive chemosensory functions of neurons in contact with the cerebrospinal fluid

Par **Hugo Marnas**

Thèse de doctorat de Neurosciences

Dirigée par Claire Wyart

Présentée et soutenue publiquement le 22 novembre 2021

Devant un jury composé de :

Rapporteur	Nicolas WANAVERBECQ, MCU
Rapporteur	Bertrand COSTE, CR
Examinatrice	Elim HONG, CR
Examinateur	Guillaume DUMENIL, DR
Examinatrice	Sylvie RETAUX, DR
Examinateur	Stéphane GASMAN, DR
Directrice de thèse	Claire WYART, DR

Cette thèse est dédiée à mon père.

Résumé

Pour assurer leur survie et leur reproduction, les organismes vivants s'adaptent constamment à leur environnement en sondant des signaux externes et internes. La détection des signaux sensoriels externes est effectuée par des cellules réceptrices spécialisées qui convertissent les informations sensorielles en signaux électrochimiques envoyés au système nerveux central. Les neurones sensoriels situés dans les organes sensoriels tels que les yeux ou la peau détectent une diversité de stimuli, qu'ils soient photoniques, mécaniques, chimiques, thermiques ou nocifs. La perception des signaux sensoriels externes de l'environnement est appelée "extéroception" et a fait l'objet de nombreuses recherches. En revanche, sa contrepartie, "l'interoception" ou la sensation des modalités sensorielles internes provenant du corps, est moins comprise.

L'interoception comprend différents sens, dont la proprioception définie comme la perception de la position du corps. Les neurones sensoriels détectant les signaux internes et externes sont principalement situés dans les ganglions du trijumeau et de la racine dorsale. Le ganglion trigéminal est responsable de la sensibilité du visage, tandis que les ganglions de la racine dorsale sont des groupes de neurones sensoriels détectant les signaux internes et externes mécaniques, chimiques, thermiques et nocifs du corps. Classiquement cependant, la proprioception n'implique pas la position de la colonne vertébrale dans le tronc. Existe-t-il des cellules sensorielles spécifiques qui détectent la position de la colonne vertébrale ? Au cours de la dernière décennie, les neurones de contact du liquide cérébrospinal (NcLCS) sont apparus comme des capteurs potentiels de la position de la colonne vertébrale. Il a notamment été démontré que les NcLCS détectent la flexion de la queue chez le poisson zèbre et la lamproie, et qu'ils modulent à leur tour la locomotion et la posture. Chez le poisson zèbre, la modulation de la locomotion par les NcLCS repose sur la libération du neurotransmetteur acide γ-aminobutyrique (GABA) et du neuropeptide Somatostatine1.1, mettant en évidence les fonctions neurosécrétrices des NcLCS. L'ensemble de ces observations suggère que les NcLCS pourraient représenter un nouveau type de neurones intéroceptifs responsables de la détection de la position et du mouvement de la colonne vertébrale et capables de neurosécrétion. Cependant, les fonctions chimiosensorielles des NcLCS n'ont pas été étudiées *in vivo*.

Pour étudier les propriétés chimiosensorielles des NcLCS, j'ai analysé leur profil transcriptomique à la recherche de chimiorécepteurs d'intérêt. J'ai découvert que les NcLCS expriment une grande variété de récepteurs de signaux chimiosensoriels tels que des neuromodulateurs, des neuropeptides, des hormones, et étonnamment des facteurs liés à l'immunité. Suite à cette observation, j'ai contribué à l'étude du rôle des NcLCS dans l'immunité innée lors d'une infection bactérienne. J'ai développé un protocole de culture de cellules primaires me permettant de tester et de surveiller les réponses des NcLCS lorsqu'ils sont exposés à des signaux chimiques candidats *in vitro*. J'ai montré que les NcLCS répondent de manière robuste à des métabolites bactériens pathogènes connus. Ce résultat a été confirmé *in vivo* où l'invasion bactérienne du LCS provoque une activation forte et prolongée des NcLCS. Enfin, nous avons montré que les NcLCS participent à la survie de l'hôte lors d'une infection bactérienne en régulant à la hausse l'expression de cytokines et de composants du complément impliqués dans l'immunité innée. Dans l'ensemble, mes travaux ont contribué à établir que les NcLCS sont des neurones chimiosensoriels intéroceptifs critiques qui détectent les métabolites bactériens pendant une infection et favorisent l'immunité innée de l'hôte.

Abstract

To ensure their survival and reproduction, living organisms constantly adapt to their environment by probing external and internal cues. Sensing of external sensory cues is performed by specialized receptor cells that convert sensory information into electrochemical signals sent to the central nervous system. Sensory neurons located in sensory organs such as the eyes or the skin detect a diversity of stimuli, ranging from photonic, mechanical, chemical, thermal or noxious stimuli. The perception of external sensory cues from the environment is referred to as 'exteroception' and has been considerably investigated. In contrast, its counterpart – 'interoception' or the sensation of internal sensory modalities coming from the body – has remained elusive.

Interoception comprises different senses, including proprioception defined as the perception of body position. Sensory neurons detecting internal and external cues are mainly located in the trigeminal and dorsal root ganglia. The trigeminal ganglion is responsible for face sensitivity, while dorsal root ganglia are clusters of sensory neurons detecting internal and external mechanical, chemical, thermal and noxious cues from the body. Classically however, proprioception does not entail spine position in the trunk. Are there specific sensory cells that detect the position of the spine? In the last decade, the cerebrospinal-fluid contacting neurons (CSF-cNs) have emerged as candidate sensors of spine position. Notably, CSF-cNs have been shown to detect spinal tail bending in zebrafish and lamprey and to, in turn, modulate locomotion and posture. In zebrafish, CSF-cN modulation of locomotion relies on the release of the γ-aminobutyric acid (GABA) neurotransmitter and the Somatostatin1.1 neuropeptide, highlighting neurosecretory functions of CSF-cNs. Together, these observations suggest that CSF-cNs might represent a new type of interoceptive neurons responsible for the detection of spine position and movement, and capable of neurosecretion. However, chemosensory functions of CSF-cNs have not been investigated *in vivo*.

To investigate CSF-cN chemosensory properties, I analyzed their transcriptomic profile looking for chemoreceptors of interest. I found that CSF-cNs express a large variety of receptors for chemosensory cues such as neuromodulators, neuropeptides, hormones and, surprisingly, immune-related factors. Following this observation, I contributed to the investigation of the role of CSF-cNs in innate immunity upon bacterial infection. I developed a protocol of primary cell culture allowing me to test and monitor CSF-cN responses when exposed to candidate chemical cues *in vitro*. I showed that CSF-cNs robustly respond to known pathogenic bacterial metabolites. This result was confirmed *in vivo* where a bacterial invasion of the CSF elicits strong and prolonged activation of CSF-cNs. Finally, we showed that CSF-cNs participate in host survival during bacterial infection through the up-regulation of the expression of cytokines and complement components involved in innate immunity. Altogether, my work helped establish CSF-cNs as critical interoceptive chemosensory neurons that detect bacterial metabolites during infection and promote host innate immunity.

Acknowledgments

Après quatre années de dur labeur, j'arrive finalement au terme de cette thèse qui aura été riche en enseignements et en rencontres. Je souhaite remercier ici toutes les personnes qui ont participé, de près ou de loin, à ce périple qu'est le doctorat.

First of all, I would like to thank all the members of the jury for my PhD defense, for the great discussion we had during the defense. Particularly, I thank Nicolas Wanaverbecq and Bertrand Coste, my two "rapporteurs", for their insightful feedback that allowed me to improve my PhD manuscript as well as consider all the potential perspectives of my project. I also wanted to thank Stéphane Gasman and Isabelle Lihrmann for advising me during the thesis advisory committees and providing me feedback that allowed me to go in the correct direction during all my PhD.

Bien évidemment, un immense merci à toi Claire, sans qui rien de tout cela n'aurait été possible. Tu as décidé de me faire faire confiance depuis le tout début lors de mon stage de Master, et tu n'as cessé d'avoir confiance en moi depuis même dans certains moments où, soyons honnête, je ne me faisais moi-même pas confiance. Merci pour toute l'énergie et toute l'aide que tu m'as données, j'ai beaucoup grandi à tes côtés. I would like to thank all the members of the Wyart team that helped me during these four years. Thank you to the first generation of people that I have met for only a few months but that welcomed me perfectly when I arrived in the lab. Pierre-Luc, merci pour ta gentillesse, ton esprit positif et tes discussions philosophiques. Andy, thank you for all your advice, I have been happy to work with you on the meningitis project and hopefully one day we will publish this paper! Yasmine, merci pour tous tes conseils en culture cellulaire et ta gentillesse à toute épreuve, j'ai toujours pu trouver en toi le soutien dont j'avais besoin. Julian, merci pour toute ton aide avec tous types d'expériences, je me suis toujours tourné vers toi quand j'avais besoin d'un peu d'aide et tu as toujours répondu présent. Adeline, merci pour ton aide et ton soutien, tu as réalisé l'exploit de me faire un peu mieux apprécier l'électrophysiologie et ça, ce n'est pas rien ! Martin, thank you for all your good ideas for experiments during lab meetings. Adna, thank you for the positive attitude that you kept in any circumstances. Olivier, nos chemins ne se sont pas croisés beaucoup, mais merci pour ces sessions de baskets mémorables. Ming-Yue, thank you for all your support that was essential to me as we were doing our PhD in parallel. Feng, tu fais partie des premières personnes que j'ai rencontrées dans le laboratoire, tu m'as aidé et supervisé durant tout mon stage de Master, et je pense pouvoir dire sans risque que tu fais à présent parti de mes amis les plus chers, merci pour tout.

Laura, merci de m'avoir soutenu et compris dans les moments difficiles et ce même en étant loin. Finissant ta thèse quand je commençais la mienne, tu as toujours été un modèle pour moi que j'ai suivi tout au long de ma thèse et j'espère que tu vas semer, sur ton chemin, les plus beaux avocatiers. Yezza, merci pour toute l'énergie que tu as mise dans la gestion de l'équipe, ainsi que pour tes repas et thés toujours superbement bien préparés. Mathilde, merci pour ton énergie (très) débordante et ton aide à toute épreuve. Maha, thank you for being there when I needed to complain about everything, our discussions were always of good help for me to keep going in a good direction. Gautam, thank you for your support, our projects were not related but you always provided good advice. Faustine, merci pour ta gentillesse et ton soutien, notamment pendant l'écriture du manuscrit. Cilia, thank you for your support during the last steps of my thesis. Joana, thank you for your kindness and your help when I needed it.

Monica, Bogdan, Antoine, Sophie et Camille, merci pour toute votre aide avec la plateforme poissons, ma thèse n'aurait certainement pas ou se faire sans vous. Florence, Aurélie, merci pour votre aide avec le FACS, qui aura été cauchemardesque du début à la fin, mais qui finalement m'aura beaucoup appris. Charlotte, merci pour ton soutien même en dehors du laboratoire et de la science, mes discussions avec toi m'ont toujours été très utiles pour relativiser. Marina, merci d'avoir été une super voisine de box en culture, et pour toutes nos discussions sur nos projets en général. Kin Ki, thank you for all your support and your help with the meningitis project. We put a lot of effort together in this project and hopefully, this will lead to an awesome publication!

Je remercie aussi tous les gens qui m'ont soutenu de l'extérieur. Merci à tous mes amis de (très) longue date pour tout votre soutien ces dernières années, et même depuis La Xavière si on y réfléchit bien. Charles, merci pour toutes ces conversations sur tout et rien, ça a toujours été très important pour moi (Poufsouffle represents!). À tous mes amis de la fac, Floriane, Bryann, Séréna, Malala, Clémentine, Caroline, merci pour tout votre soutien, et à toutes ces conversations à se plaindre et à décider qui a la situation la plus dramatique, merci. Agnès, merci pour absolument tout, je te considère vraiment comme de ma famille depuis toutes ces années, et ton soutien m'est inestimable.

Enfin, je souhaiterais remercier ma famille, qui m'a évidemment soutenu depuis le tout début, et m'a permis d'être là où je suis aujourd'hui. Votre présence à mes côtés a toujours été un moteur puissant pour moi, même si j'ai malheureusement toujours été mauvais pour vous le faire ressentir. J'espère que vous mesurez l'importance que vous avez pour moi, car elle est incommensurable. Merci à vous, du fond du cœur.

Table of Contents

Main Abbreviations

aCSF: artificial cerebrospinal fluid
ASIC: Acid-sensing ion channel
ATP: Adenosine triphosphate
CaP: Caudal primary motoneurons
CGRP: Calcitonin-gene related peptide
CoPa: Commissural primary ascending interneurons
CSF: Cerebrospinal fluid
CSF-cNs: Cerebrospinal fluid-contacting neurons
DCX: Doublecortin
DIV: Day *in vitro*
DMEM: Dulbecco's modified Eagle's medium
Dpf: Day post fertilization
DRG: Dorsal root ganglia
FACS: Fluorescence-activated cell sorting
FRAP: Fluoride-resistant acid phosphatase activity
GABA: Gamma-aminobutyric acid
GPCR: G protein-coupled receptors
GTO: Golgi tendon organ
HBSS: Hanks' Balanced Salt Solution
HTMR: High-threshold mechanoreceptor
IA: Intermediately adapting
IB_4: Isolectin B_4
ICC: Immunocytochemistry
IFN: Interferon
IHC: Immunohistochemistry
LH: Luteinizing hormone
LTMR: Low-threshold mechanoreceptor
MAP: Mitogen-activated protein
MAP2: Microtubule-associated protein 2
NGF: Nerve growth factor
NKBa: Neurokinins Ba
NKB-RPa: NKB-Related Peptide a
NPC: Natriuretic peptide C
PBS: Phosphate-buffered saline
PFT: Pore forming toxin
PKD2L1: Polycystic kidney disease 2-like 1
PLC: Phospholipase C
PSA-NCAM: Polysialylated neural cell adhesion molecule
RA: Rapidly adapting
RF: Reissner fiber
SA: Slowly adapting
SCO: Subcomissural organ
T2R: Taste receptor of type 2
TLR: Toll-like receptors
TNF-*α :* Tumor necrosis factor alpha
TrkA: Tyrosine kinase A
TRP: Transient receptor potential
VIP: Vasointestinal peptide
WT: Wild type

Introduction

Preamble

All living organisms need for their survival and reproduction to analyze, understand and adapt to their environment by sensing external and internal cues. Sensing and integration of external sensory stimuli by the brain and spinal cord go through sensory neurons located in different sensory organs. In the eye, the retina contains photoreceptors detecting photons, and information is transmitted to the lateral geniculate nucleus (LGN) through optic nerves and ultimately information reaches the primary visual cortex to create a visual scene (Kandel *et al.*, 2012). Animals rely on this visual system to identify objects in their environment. The skin is the main biological substrate of touch, as it is highly innervated by sensory neurons called mechanoreceptors that detect mechanical deformations of the skin (Handler and Ginty, 2021). Touch is essential for exploration and discovery of the external environment, but also for interacting with conspecifics. Mechanosensation is not only associated with touch: it is also crucial for the audition, with sensory hair cells in the ear that are activated after stimulation from mechanical vibrations of sounds (Fettiplace and Hackney, 2006), allowing detection of predators or conspecifics – as well as for proprioception, informing about the perception of our body in space (Tuthill and Azim, 2018). The skin is also an organ detecting thermal stimuli through thermal sensory cells called thermoreceptors, crucial for probing seasonal external temperature changes for example (Zhang, 2015). In addition, the skin senses external pain cues through sensory cells called nociceptors, playing the defensive role of detecting mechanical, thermal and chemical noxious stimuli (Purves *et al.*, 2001): this is referred to as ‘nociception’. Chemoreceptors are sensory cells sensing chemical substances and involved in olfaction and gustation, essential senses providing information on predators or conspecifics as well as nutritional information and danger in the environment. Olfactory chemoreceptors located in the nasal cavity detect chemicals in the gaseous state such as odors and pheromones, while taste receptors in structures called taste buds on the tongue sense aqueous chemical substances. Chemoreceptors also project nerve endings directly to the skin to detect potential noxious chemicals from the external environment. Sensation by sensory organs of these sensory modalities coming from the external environment has been extensively investigated and is classified as ’exteroception’. But what about sensory stimuli coming directly from within the body, such as pain or internal temperature changes?

Internal sensory information coming from inside the body is referred to as 'interoception', providing information about the internal state of the body. Interoception comprises different senses such as proprioception, nociception or visceral sensations (Robinson and Gebhart, 2008). Proprioception is the perception of body position through receptors located in skeletal muscles, tendons and joints. Indeed, specific mechanoreceptors are located in muscle spindles in skeletal muscles, Golgi tendon organs as well as joints. These structures detect muscle contractions, tensions on the tendons and joint torsion to provide information about limb position or velocity. Nociception plays a defensive role by detecting noxious stimuli. On top of detecting exteroceptive noxious stimuli at the skin, nociceptors detect damaging mechanical, thermal and chemical stimuli from other organs such as muscles, tendons and joints, and relay the signal to the brain. Nociceptors specifically located in internal organs, such as the gastrointestinal tract, carry visceral sensations (Robinson and Gebhart, 2008). Interoceptive sensory neurons detecting internal and external cues are mainly located in the trigeminal ganglia and the dorsal root ganglia (DRG) (Kandel *et al.*, 2012). The trigeminal ganglia contain the cell bodies of the trigeminal nerve responsible for face sensitivity. The trigeminal nerve is composed of three major sensory branches, namely the ophthalmic, the maxillary and the mandibular nerves, allowing detection of thermal, mechanical and pain cues from the face. The DRG, analog to the trigeminal ganglia, are clusters of sensory neurons located alongside the spinal cord that detect both interoceptive and exteroceptive thermal, mechanical, chemical and noxious cues from the body. DRG sensory neurons are described as polymodal neurons, meaning that they can encode different types of sensory inputs, such as thermal and mechanical stimuli. Trigeminal and dorsal root ganglia are considered as the main interoceptive sensory organs, but are they the only ones responsible for the detection of internal sensory stimuli?

Until recently, proprioception was described solely as informing on limb position but not the position of the spine in the trunk. Are there sensory cells that detect the position of the spine?

A century ago, Kolmer and Agduhr described cells in contact with the cerebrospinal fluid in the spinal cord in over a hundred vertebrates. These cells, called cerebrospinal fluid-contacting neurons (CSF-cNs) (Kolmer, 1921, 1931; Agduhr, 1922), are gamma-aminobutyric acid (GABA)-ergic neurons bearing an apical extension bathing into the cerebrospinal fluid (CSF), and expressing specifically the transient receptor potential channel polycystic kidney disease 2-like 1 (PKD2L1) in the spinal cord of mice (Huang *et al.*, 2006; Orts-Del'Immagine *et al.*, 2016), macaque (Djenoune *et al.*, 2014) and zebrafish (Djenoune *et al.*, 2014; Sternberg *et al.*, 2018). In the last decade, it has been shown that CSF-cNs

respond to hypo-osmotic shocks (Orts-Del'Immagine *et al.*, 2012) as well as direct fluid pressure applying (Jalalvand, Robertson, Wallén, *et al.*, 2016), suggesting that CSF-cNs could function as mechanosensory cells detecting changes in CSF flow. In zebrafish, CSF-cNs respond *in vivo* to lateral (Böhm *et al.*, 2016) and longitudinal (Hubbard *et al.*, 2016) spinal bending at the concave side, meaning that these cells respond to mechanical compression of the spinal cord. As the embryonic activity of CSF-cNs *in vivo* correlates with CSF flow (Sternberg *et al.*, 2018), and CSF-cNs respond to fluid-pressure applying of CSF *in vitro* (Jalalvand, Robertson, Wallén, *et al.*, 2016), it was hypothesized that CSF-cNs detect changes of CSF flow in the central canal after spinal binding. However, a recent study showed that CSF-cN mechanosensory properties require the Reissner fiber (RF) (Orts-Del'Immagine *et al.*, 2020), an aggregation of the subcomissural organ (SCO)-spondin protein starting from the sub commissural organ in the third brain ventricle and going to the end of the spinal cord. The RF is under tension at rest in the central canal, which means that spinal bending can lead to an asymmetry with the RF being closer to the side of the bending. Electron microscopy investigations showed that the RF is in close vicinity with the CSF-cN apical extension in the central canal (Orts-Del'Immagine *et al.*, 2020). Then, the RF has been suggested to either interact directly with CSF-cN apical extension or to increase the CSF flow sensed by CSF-cNs.

In response to mechanical stimuli of the spine, CSF-cNs release neurotransmitters to modulate locomotion and posture. The first evidence that CSF-cNs could modulate locomotion originated from the optogenetic activation of these neurons that induced slow swim bouts in zebrafish (Wyart *et al.*, 2009). Taking advantage of the specific marker Pkd2l1, it was shown in zebrafish that CSF-cNs modulate slow locomotion in a state-dependent manner by extending GABAergic synapses onto V0-v interneurons, an essential component of slow locomotion (Fidelin *et al.*, 2015). A recent study showed that Somatostatin1.1 is also involved in the modulation of locomotion by inhibiting slow locomotion in zebrafish (Quan *et al.*, 2020). CSF-cNs also project GABAergic synapses onto caudal primary (CaP) motoneurons and commissural primary ascending (CoPa) interneurons that are fast motor neurons and excitatory sensory interneurons of the escape circuit, respectively (Hubbard *et al.*, 2016; Djenoune *et al.*, 2017), suggesting a role in modulation of fast locomotion. Ventral CSF-cNs directly silence the CaP motoneurons that innervate fast skeletal muscles (Hubbard *et al.*, 2016). During fast locomotion, silencing of CSF-cN neurotransmission induces postural defects (Hubbard *et al.*, 2016). Recently, investigations on rostralmost CSF-cNs showed that they send projections to the caudal hindbrain, synapsing onto occipital motoneurons responsible for the control of head position (Wu *et al.*, 2021). Rostralmost CSF-cNs send projections into the brain stem as well, forming axo-axonic synapses onto reticulospinal

neurons, that send descending information to central pattern generators in the spinal cord to control voluntary movements (Wu *et al.*, 2021). Ablation of rostralmost spinal CSF-cNs induced postural control defects, with rolling events occurring more frequently during acousto-vestibular (A-V) induced escapes (Wu *et al.*, 2021). This result suggests that rostralmost CSF-cNs maintain fish stability during escape behavior by sending information to occipital and spinal motoneurons. Altogether, these results show that CSF-cNs form an interoceptive system requiring the RF to detect spinal mechanical cues and, in turn, modulate slow and fast locomotion, as well as posture through the release of neurotransmitters such as GABA and Somatostatin1.1.

Recent studies also provided evidence that CSF-cNs respond to pH variations in mice (Huang *et al.*, 2006; Orts-Del'Immagine *et al.*, 2012, 2016), lamprey (Jalalvand, Robertson, Tostivint, *et al.*, 2016) and zebrafish (unpublished data, Böhm thesis, 2017), suggesting that CSF-cNs can sense pH variations of the CSF. Investigations in mice showed that CSF-cNs also detect neuromodulators such as acetylcholine (Corns *et al.*, 2015; Johnson *et al.*, 2020) and adenosine triphosphate (ATP) (Stoeckel *et al.*, 2003; Johnson *et al.*, 2020). It was hypothesized that considering their location and direct contact with the CSF, CSF-cNs could sense CSF content and respond to chemical stimuli, potentially by secreting molecules in the CSF to change its composition. Yet, there is no evidence about a physiological chemosensory role of CSF-cNs. During my PhD, I investigated chemosensory properties of the CSF-cNs in zebrafish and found that CSF-cNs respond to bacterial metabolites during CSF bacterial infection, and in turn promote innate immunity by releasing peptides and cytokines to improve host survival.

In this manuscript, I first introduce the DRG and the recent CSF-cNs spinal interoceptive system and their different sensory properties. A second part is dedicated to the results obtained during the PhD, with a first chapter describing the primary cell culture protocol developed to investigate the chemosensory functions of the CSF-cNs; a second chapter dedicated to the analysis of CSF-cN transcriptome to find and test *in vitro* receptors for chemical agonists in CSF-cNs; and a third chapter corresponding to the main publication of this PhD showing the chemosensory role of CSF-cNs in the detection of bacterial metabolites during CSF bacterial infection. The last part of the manuscript is a general discussion about the different results obtained and the perspectives we can make.

1/ Classical view: sensory information solely comes from the periphery to the spinal cord

1.1) Dorsal root ganglia neurons

Dorsal root ganglia are clusters of primary sensory neurons located alongside the spinal cord, at the level of the intervertebral foramen (Daroff and Aminoff, 2014). DRG sensory neurons are first-order neurons, meaning the first neurons to receive sensory stimuli – such as mechanical, chemical or thermal stimuli - at the periphery and are responsible for conveying the signal to the central nervous system. DRG sensory neurons are pseudo-unipolar type neurons with one process divided in a 'T-like' fashion into one 'distal' axonal branch that extends to the periphery, and another 'proximal' branch that penetrates the spinal cord (**Figure 1**).

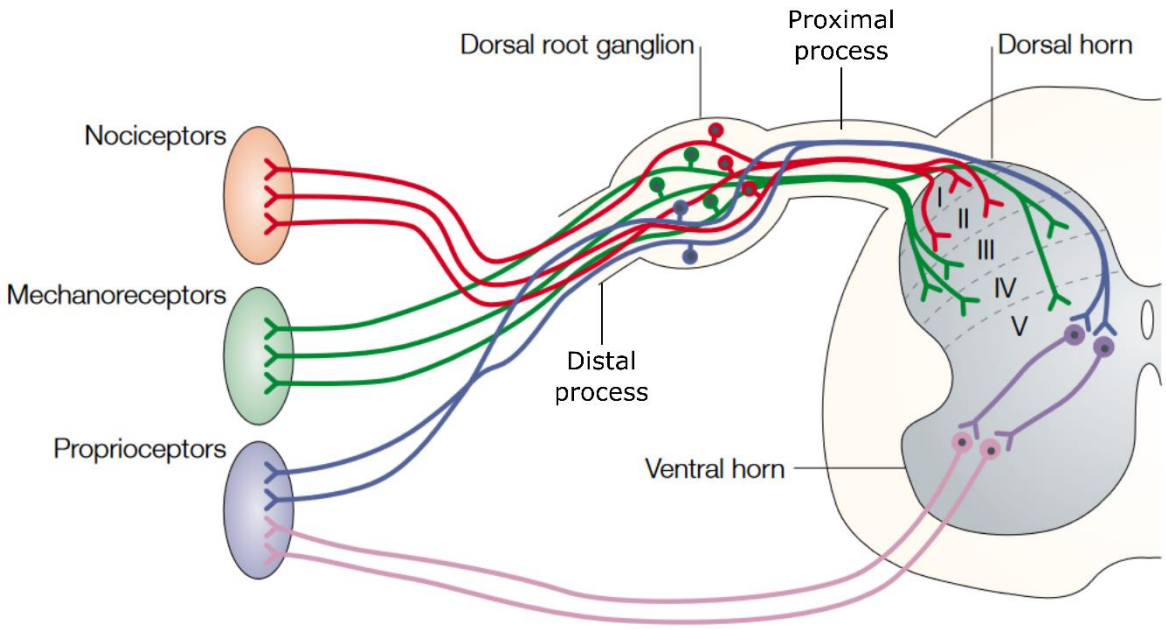

Figure 1. DRG sensory fibers organization. Schematics of neuronal circuits in a mice spinal cord at embryonic day 18. The axons of sensory neurons project from the dorsal root ganglia to specific laminae in the dorsal horn as well as the periphery. Pain and temperature are sensed by nociceptive neurons (red), and the messages are conveyed to laminae I and II. Touch is mediated by mechanoreceptors (green) in the periphery, which connect to laminae III, IV and V. Proprioception is mediated by the sensory neurons that project through the dorsal horn to the ventrally located motor neurons (shown in blue). The motor neurons also connect directly back to the muscle in the periphery to drive movement (pink). Roman numerals indicate the laminae of the dorsal horn. Adapted from (Caspary and Anderson, 2003).

Sensory cells form a heterogeneous population of sensory neurons, with specific fiber myelination and diameter. Myelination consists of fatty sheets surrounding the nerve fiber and acting as an isolator to increase the conduction velocity of action potentials (Nave and Werner, 2014). As a result, highly myelinated fibers show higher conduction velocity. Fiber's diameter also impacts the conduction velocity, as the conduction velocity of large fibers is higher than the conduction velocity of small ones (Waxman, 1980). Depending on these properties, sensory neurons have been classified into four types of neurons: Aα, Aβ, Aδ and C fibers (Kandel *et al.*, 2012) (**Table 1**).

Fiber type	Fiber diameter (µm)	Fiber myelination	Conduction velocity (m/s)
Aα	12-20	Large	72-120
Aβ	6-12	Intermediate	36-72
Aδ	1-6	Small	4-36
C	0.2-1.5	Non-myelinated	0.4-2.0

Table 1. Groups of DRG sensory neuron afferents in human. Adapted from (Kandel *et al.*, 2012).

These four types of sensory neurons carry different sensory information (**Table 1**). Cutaneous mechanoreceptors in the skin act as exteroceptive receptors sensing touch and vibration from the outside. Cutaneous low threshold thermoreceptors sense changes in skin temperature, playing a role in body thermoregulation and object identification with touch. Proprioceptive neurons, called proprioceptors, are interoceptive mechanoreceptors providing information about body position by detecting muscle contractions through the muscle spindles, but also tensions in the tendons and joint movements. Nociceptive neurons, called nociceptors, are polymodal neurons sensing both interoceptive and exteroceptive thermal, mechanical and chemical noxious stimuli in different organs such as skin, muscles, tendons or internal organs. Depending on their roles, DRG sensory neurons show different physiological and molecular properties that will be described in the following text.

1.2) Cutaneous mechanoreceptors of touch

Cutaneous mechanoreceptors, located in the skin throughout the body, detect and convert skin mechanical stimuli into electrical signals. DRG mechanical sensory neurons can be classified depending on the nature of the mechanical stimuli they detect as well as the

force threshold for spike initiation. ‘Low-threshold mechanoreceptors’ (LTMRs) respond to light and innocuous tactile forces on the skin (Lewin and McMahon, 1991; Koltzenburg, Stucky and Lewin, 1997), while ‘high-threshold mechanoreceptors’ (HTMRs) detect higher mechanical forces and are the main receptors for noxious mechanical stimuli (Bessou and Perl, 1969; Ghitani *et al.*, 2017). LTMRs are associated with end-organ structures located in different zones in the skin and respond to different mechanical stimuli such as pressure, stretching or vibration of the skin. Different subtypes of LTMR endings are associated with glabrous (non-hairy) or hairy skin, carrying different firing adaptation properties. LTMRs are classified as slowly, intermediately, or rapidly adapting (SA, IA, or RA-LTMRs) according to their rates of adaptation to sustained mechanical stimuli (Burgess, Petit and Warren, 1968; Johnson and Hsiao, 1992). SA LTMRs are firing continuously during a sustained stimulus, whereas RA LTMRs respond only to the onset and offset of the stimulus.

Glabrous skin mechanoreceptors*.* Glabrous skin, found on fingertips, lips or hand and feet palms among others, possesses four different subtypes of Aβ afferents (**Figure 2**).

Slowly adapting (SA) Aβ afferent endings associate with Merkel cells in the basal layer of the epidermis to form Merkel cell–neurite complexes (Merkel, 1875; Halata, Grim and Bauman, 2003) in both glabrous and hairy skins. Merkel cell-neurite complex is thought to be responsible for tactile discrimination of shapes and textures (Iggo and Muir, 1969; Maksimovic, Baba and Lumpkin, 2013). At the molecular level, Merkel cells relay tactile stimuli by releasing neurotransmitters at the cell-neurite synapses, such as serotonin that activates Aβ afferents through ionotropic and metabotropic 5-hydroxytryptamine (5-HT) receptors (Chang *et al.*, 2016).

Ruffini corpuscles are also innervated by SA Aβ encapsulated afferents forming large receptive fields in the dermis of glabrous skin (Ruffini, 1894). Ruffini corpuscles respond to tension and stretch of the skin (Knibestöl, 1975).

Rapidly adapting (RA) Aβ encapsulated afferents innervate Meissner corpuscles in the dermis. RA in Meissner corpuscles are responsible for the detection of dynamic skin intermediate deformations (5-50Hz frequencies) (Johansson, Landström and Lundström, 1982).

RA afferents also innervate Pacinian corpuscles deeply in the dermis, forming large receptive fields with an ‘onion-like’ structure. These fibers respond to surface textures (Weber *et al.*, 2013) and vibrations transmitted through objects held in the hand (Brisben, Hsiao and Johnson, 1999).

Hairy skin mechanoreceptors. Hairy skin LTMR afferents are associated with hair follicles of different functions that are grouped in three distinct types: guard, zigzag and awl/auchene hair follicles innervated by Aβ-, Aδ- or C-LTMRs combinations (L. Li *et al.*, 2011) (**Figure 2**).

Slow adapting Aβ afferents innervate complex with Merkel cells on guard follicles, at the level of the epidermal/dermal junction, to form touch domes (Iggo and Muir, 1969). Guard hair follicles SA Aβ afferents show similar firing properties to glabrous skin ones (Woodbury and Koerber, 2007).

Rapidly adapting Aβ afferents form longitudinal lanceolate endings surrounding both guard and awl/auchene hair follicles at the basal level, while rapidly adapting Aδ-LMTRs form lanceolate endings on awl/auchene and zigzag hair follicles (L. Li *et al.*, 2011). RA Aβ and Aδ afferents are sensitive to hair follicle deflection (Brown and Iggo, 1967) and low-frequency vibrations.

C-LTMRs form longitudinal lanceolate endings on awl/auchene and zigzag hair follicles and are thought to be associated with pleasant touch by responding to intermediate brushing velocities, playing a role in social touch (Löken *et al.*, 2009; Liljencrantz and Olausson, 2014).

The three types of hair follicles are also innervated with circumferential endings, surrounding the other LTMR longitudinal lanceolate endings (Millard and Woolf, 1988). Recent evidence indicates that those circumferential endings are HTMRs responsible for mechanical pain detection of hair pulling (Ghitani *et al.*, 2017).

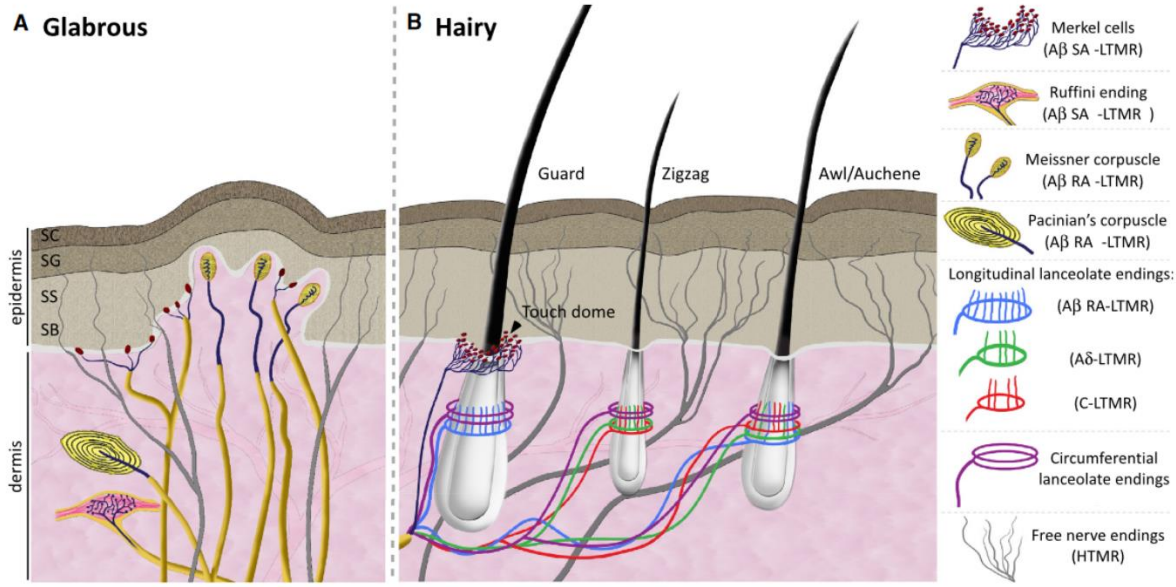

Figure 2. Cutaneous mechanoreceptors organization in skin. Innocuous touch information is processed by both glabrous hairless **(A)** and hairy **(B)** skin. **(A)** In glabrous skin, innocuous touch is mediated by four types of mechanoreceptors. The Merkel cell-neurite complex is in the basal layer of the epidermis and it consists of clusters of Merkel cells making synapse-like associations with enlarged nerve terminals branching from a single Aβ fiber. This complex and its associated SA-LTMR responses help us in reconstructing acute spatial images of tactile stimuli. Meissner corpuscles are localized in the dermal papillae and consist of horizontal lamellar cells embedded in connective tissue. Their characteristic RA-LTMR responses detect movement across the skin. Ruffini endings are localized deep in the dermis and are morphologically similar to the Golgi tendon organ, a large and thin spindle-shaped cylinder composed of layers of perineural tissue. Historically, Ruffini endings have been associated with SA-LTMR responses, which respond best to skin stretch, though such correlations remain highly controversial. Lastly, Pacinian corpuscles are located in the dermis of glabrous skin where their characteristic onion-shaped lamellar cells encapsulate a single Aβ ending. Their well-recognized RA-LTMR responses detect high-frequency vibration. **(B)** In hairy skin, tactile stimuli are transduced through three types of hair follicles, defined in the mouse as guard, awl/auchene, and zigzag. The longest hair type, guard hairs, is associated with touch domes at the apex and Aβ-LTMR longitudinal lanceolate endings at the base. Awl/auchene hairs are triply innervated by C- LTMR, Aδ-LTMR, and Aβ-LTMR longitudinal lanceolate endings. Zigzag hair follicles are the shortest and are innervated by both C- and Aδ-LTMR longitudinal lanceolate endings. In addition, all three hair follicle types are innervated by circumferential lanceolate endings. Noxious touch is detected by free nerve endings found in the epidermis of both glabrous and hairy skin and are characterized by both Ad- and C-HTMR responses. Abbreviations: SA, slowly adapting; RA, rapidly adapting; LTMR, low-threshold mechanoreceptor; HTMR, high-threshold mechanoreceptor; SC, stratum corneum; SG, stratum granulosum; SS, stratum spinosum; SB, stratum basalis. Adapted from (Abraira and Ginty, 2013).

Ascending pathway of cutaneous mechanoreceptors from the spinal cord to the brain. The dorsal column medial lemniscal (DCML) pathway (**Figure 3**) carries sensations of touch and vibration, as well as conscious proprioception. Mechanoreceptors enter in the dorsal horn of the spinal cord and project onto second-order neurons in the dorsal column nuclei in the lower medulla oblongata (Kandel *et al.*, 2012). Cuneate nuclei and gracile nuclei carry information from the upper trunk, and lower trunk respectively. The second-order neurons' axons decussate and form the medial lemniscus, a bundle of fibers that synapse in the ventral posterolateral (VPL) nucleus of the ventral nuclear group of the thalamus. These third-order neurons send axons to primary somatosensory cortex regions like the postcentral gyrus in the parietal lobe.

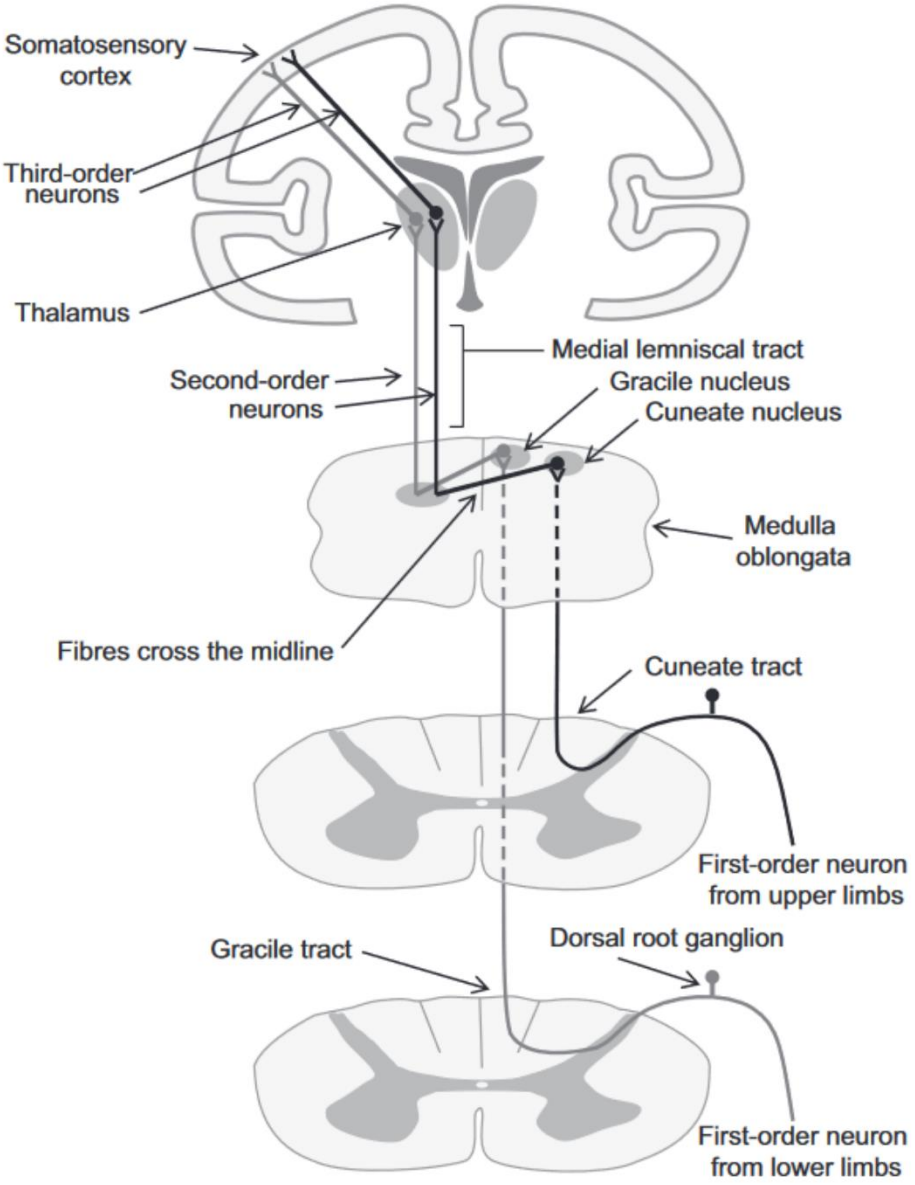

Figure 3. The dorsal column medial lemniscal (DCML) pathway, an ascending pathway of cutaneous mechanoreceptors. Adapted from (Chambers, Huang and Matthews, 2015)**.**

1.3) Cutaneous low threshold thermoreceptors

Low threshold thermoreceptors innervate the epidermis with free endings fibers to detect changes in skin temperature. Cold thermosensation is carried by both Aδ and C fibers (Campero *et al.*, 2001), while warm sensation is solely carried by C fibers (LaMotte and Campbell, 1978; Darian-Smith *et al.*, 1979). Thermosensation results from the detection by thermoreceptors of temperature differences between external air or of objects in contact with the skin, and the average temperature of the skin, which is approximately 32°C (Kandel *et al.*, 2012). Thus, thermoreceptors play a role in body thermoregulation as well as the identification of objects through touch (Schepers and Ringkamp, 2009).

1.4) Proprioceptive DRG neurons (proprioceptors)

The term proprioception has been passed out to us by Charles Sherrington (Sherrington, 1906) and is coming from the Latin *proprius*, meaning “one’s own”, so receiving signals from the organism itself. Proprioceptors are essential for our movements and perception of our environment as they convey critical information about body and limb position and movements to the CNS. Patients lacking proprioception show severe movement deficits (Sainburg *et al.*, 1995). Proprioceptors respond to muscle contraction, tendon tension and joint movement but not to light touch signals that are carried by cutaneous mechanoreceptors. Based on their peripheral organ target, proprioceptor afferents can be divided into three subclasses: muscle spindle afferents, Golgi tendons organs, and joint receptors.

Muscle spindle afferents*.* Muscle spindle afferents play the role of stretch sensors for skeletal muscles and are considered the most important proprioceptors (Proske and Gandevia, 2012). Muscle spindles consist of a bundle of specialized intrafusal muscle fibers lying in parallel with the surrounding extrafusal muscle fibers (**Figure 4**). To properly detect changes in muscle length and velocity, two types of DRG proprioceptor afferents innervate muscle spindles in humans, namely the primary group Ia (Aα) and secondary group II (Aβ) fibers, which show different morphological and physiological properties. Primary Ia fibers have a larger diameter compared to group II fibers (Eccles and Sherrington, 1930), and accordingly show faster conduction velocity as documented in cat (Hunt, 1954). Nevertheless, some species may not have group II fibers like in mice where they have not been described yet (Wilkinson, Kloefkorn and Hochman, 2012). Ia primary afferent distal endings coil around the central (or equatorial) part of the muscle spindle to form spirals (‘annulospiral endings’) in rodents (Schröder *et al.*, 1989; Sonner, Walters and Ladle, 2017).

However, Ia primary afferent distal endings in humans form irregular coils with branches and varicose swellings (Kennedy, Webster and Yoon, 1975). Ia afferents signal the rate or velocity of change in muscle length during a muscle stretch by responding immediately after the stretch.

Group II afferent fibers innervate, when they are present, nuclear chain intrafusal fibers of the muscle spindles with 'flower spray' shape endings. At contrary to group Ia afferents, several group II fibers can innervate the same muscle spindle (Banks *et al.*, 2009). Group II afferents respond less quickly than Ia, but discharge all along the muscle stretch (static response), and they signal about the muscle length changes essentially.

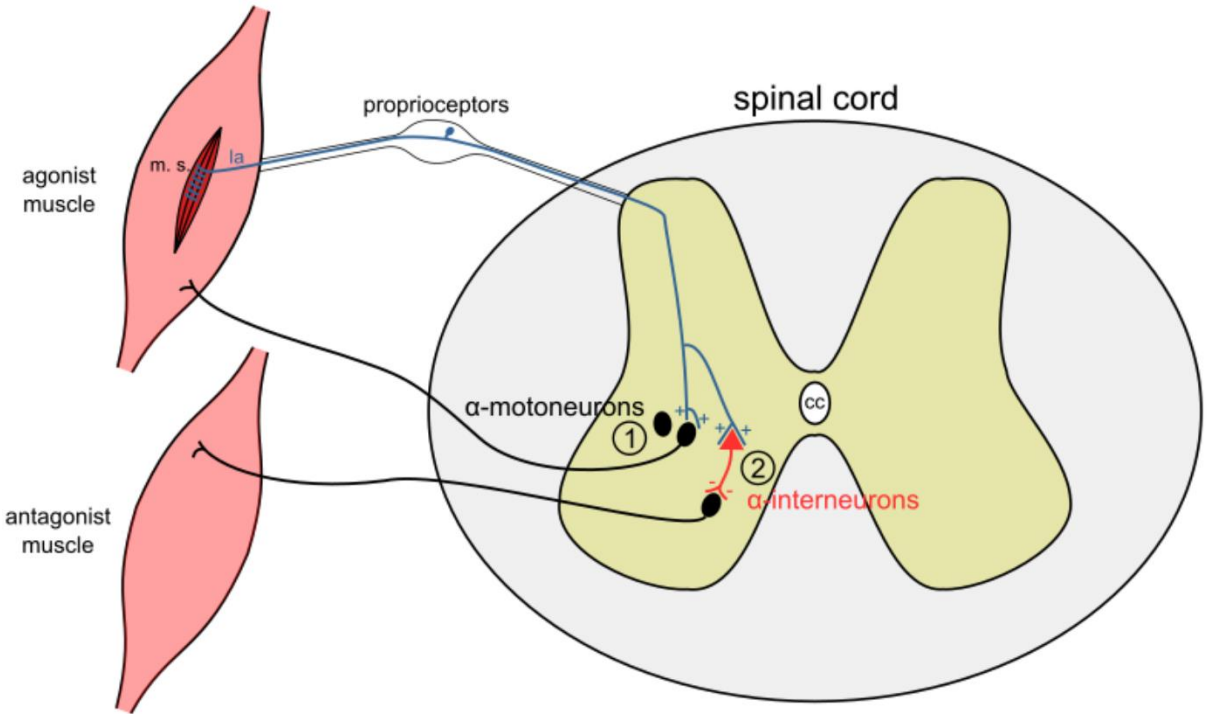

Figure 4. The spinal sensorimotor reflexes involving Ia afferents. (1) Myotatic reflex through monosynaptic connections of Ia afferents with α-motoneurons activating the agonist muscle. **(2)** Disynaptic inhibition of the reciprocal (antagonist) muscle through connections of Ia afferents with α-interneurons. cc: central canal. m.s.: muscle spindle.

The spinal sensorimotor reflexes involving muscle spindle afferents. Usually, each muscle spindle is innervated by only a single Ia primary afferent fiber (Boyd, 1962) involved in the monosynaptic reflex arc after muscle stretch, considered as the fastest reflex (**Figure 4**). Muscle length changes following a myotatic reflex are detected by deformations of Ia primary afferent endings, generating inputs in the form of action potentials of frequencies corresponding to the size and rate of the stretch (De-Doncker *et al.*, 2003). Ia primary afferents then penetrate the proximal spinal cord to form monosynaptic connections with ventral homonymous α-motoneurons, i.e., motoneurons projecting to the same muscle than

the primary afferent (Lloyd, 1943a, 1943b), leading to an increase of the homonymous muscle contraction in response to muscle elongation. In addition, primary afferent fibers can also establish connections with synergistic α-motoneurons, i.e., motoneurons projecting on another muscle as the primary afferent (David P C Lloyd, 1946; David P. C. Lloyd, 1946; Eccles, 1946), which may be playing a role in tonus and posture adjustment.
In parallel to excitation of α-motoneurons, Ia primary fibers also play a role in the disynaptic inhibition of the reciprocal muscle by connecting to inhibitory Ia interneurons that act as inhibitors of the antagonist of the stretched muscle (**Figure 4**) (Eccles and Lundberg, 1958; Hultborn, 1972). It is an important pathway for coordinating body movements.

Golgi tendon organ. Golgi tendon organ (GTO) is located at the myotendinous junction, at the interface between the muscle and its tendon. GTO is innervated with DRG group Ib (Aα) afferent fibers and is involved in inverse myotatic reflex or autogenic inhibitory reflex pathway after an increase of tendon tension (**Figure 5**). Ib afferents reach the spinal cord and connect to Ib inhibitory interneurons, leading to inhibition of α-motoneurons at rest. This is believed to prevent important muscle contraction leading to excessive tendon tension.
During locomotion, however, the autogenic inhibitory reflex was found to switch to another Ib afferent reflex pathway carrying the opposite effect of exciting α-motoneurons (Gossard *et al.*, 1994; Guertin *et al.*, 1995). This reflex may activate extensor muscles during the stance phase of locomotion (Guertin *et al.*, 1995), as well as play a role in the regulation of the stepping reflex during locomotion (Conwey, Hultborn and Kiehn, 1987).

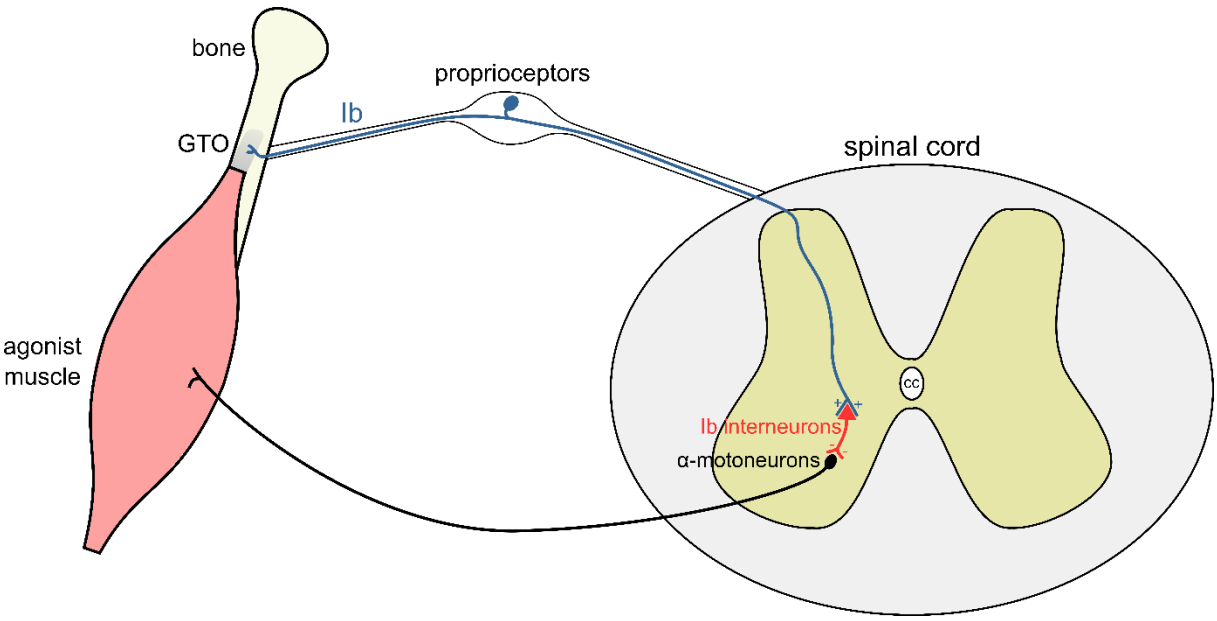

Figure 5. Inverse myotatic reflex involving Ib afferents in Golgi tendon organs. cc: central canal. GTO: Golgi tendon organ.

Joint receptors. Joint receptor afferents innervate receptors located at joint capsules and close to ligaments. Joint afferents are sensitive to joint movements at maximum flexion and extension (Ferrell, 1980) or contraction of muscle inside the joint capsule (Grigg and Greenspan, 1977). Three different types of encapsulated endings were described in joints: Ruffini-like endings in dogs (Sfameni, 1902), named Ruffini because they resembled endings previously described by Ruffini in the skin; Pacinian-like corpuscles (Hagen-Torn, 1882; Gardner, 1942) not located strictly but close to joint capsules and ligaments, in the fibrous periosteum; and Golgi organs that are located at the ligaments. In human (Burke, Gandevia and Macefield, 1988) and primate (Grigg and Greenspan, 1977), joint afferents mainly exhibit responses after joint rotations out of the physiological range - like hyperflexion or hyperextension - suggesting that these fibers are involved primarily in sensing potential joint damage.

Ascending pathway of proprioceptors from the spinal cord to the brain. In addition to sensory-motor loops allowing motoneuron modulation in the spinal cord, proprioceptors also transmit signals to the somatosensory cortex through ascending pathways such as the spinocerebellar tracts or the DCML described previously (**Figure 3**). The spinocerebellar tracts can be divided into dorsal and ventral tracts that run in parallel (**Figure 6**). The dorsal spinocerebellar tract conveys unconscious proprioceptive information from proprioceptors in the muscle spindles and GTO to the cerebellum. Proprioceptors connect to the posterior thoracic nucleus in the spinal cord, projecting onto the cerebellum through the inferior cerebellar peduncle. The ventral spinocerebellar tract proprioceptors connect to second-order neurons in the ventral border of the lateral funiculi in the spinal cord. These neurons project axons that cross into the opposite side of the body in the spinal cord and connect to the cerebellum via the superior cerebellar peduncle, where they cross a second time at the end of the cerebellum to finish ipsilaterally to the original location of the neurons in the spinal cord.

1.5) Nociceptive DRG neurons (nociceptors)

Appropriate detection of noxious stimuli is primordial for the survival of a living organism. Nociception, coming from the Latin *nocere*, meaning ‘to harm or hurt’, corresponds to the process involved in encoding and processing of intense noxious chemical, mechanical or thermal stimuli, and plays an important defensive role. A specialized population of sensory neurons is responsible for nociception, the nociceptors. Nociceptor nerve endings are found in multiple tissues such as the skin, muscle, tendon, joint or internal organs. Nociceptors are

high threshold receptors detecting intense noxious stimuli. Based on the physiological and molecular properties of these endings, nociceptors are characterized in two main different classes: Aδ myelinated afferents and unmyelinated C fibers.

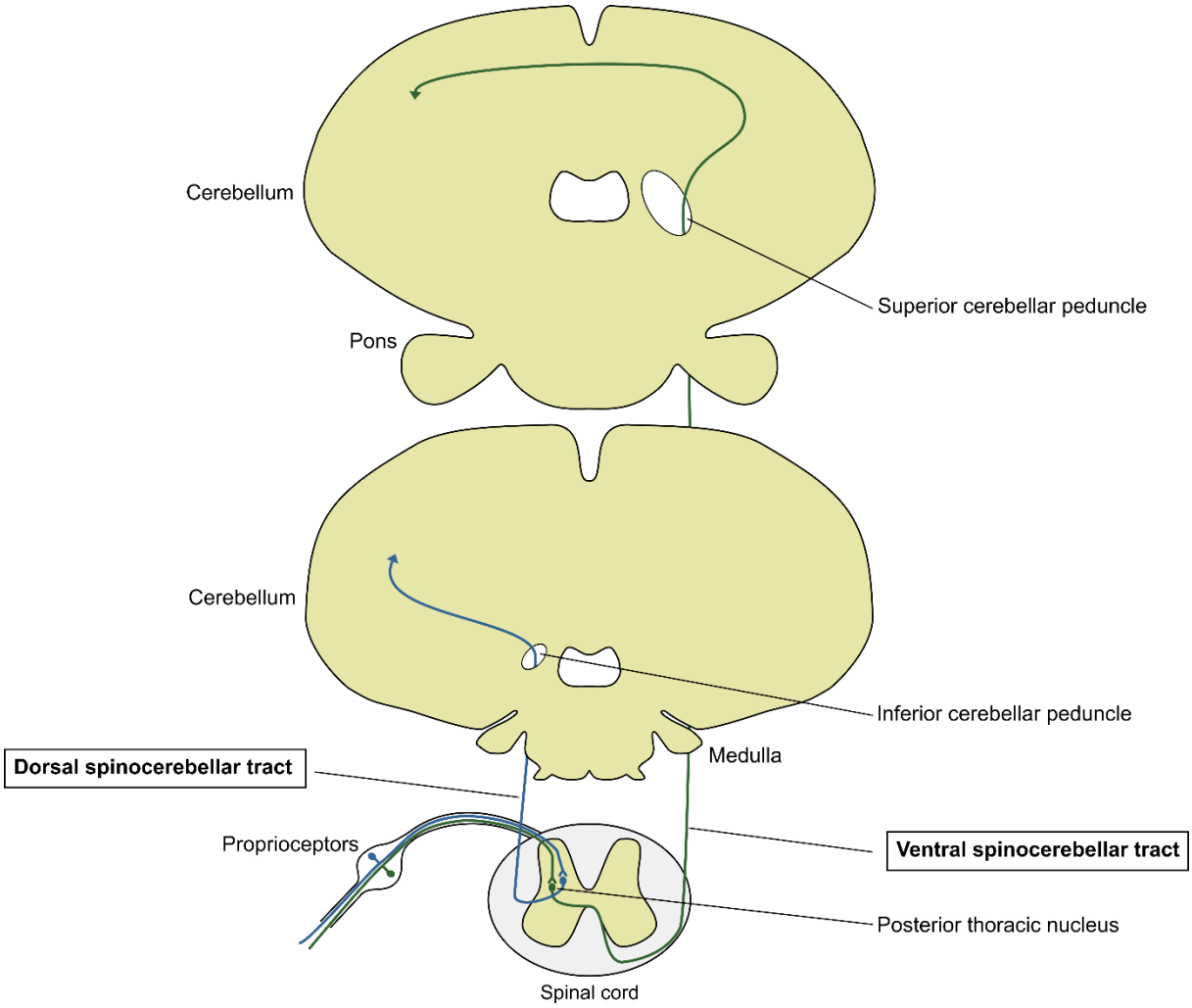

Figure 6. The spinocerebellar tracts, an ascending pathway for proprioceptors.

Nociceptor Aδ afferents. Nociceptor Aδ afferents are myelinated and show fast conduction velocity compared to nociceptor C fibers, and are involved in the "first" acute pain we feel. Based on their mechanical, chemical, and thermal modalities, different classifications of Aδ fibers exist. For example, after stimulation of cat's cornea afferents with mechanical, chemical and thermal stimuli, Aδ afferents have been classified as either polymodal (i.e. detecting all types of stimuli) (A-PM), mechano-heat (i.e., both thermo- and mechano-sensitive) (A-MH), or high-threshold mechanoreceptors (A-HTM) nociceptors (Belmonte *et al.*, 1991). In primates, A-MH nociceptors are divided into two subpopulations: type I A-MH with a high threshold for thermal stimuli (>53°C) but a low threshold for mechanical stimuli and type II A-MH responding to lower thermal stimuli (>47°C) but higher mechanical stimuli

(Treede, Meyer and Campbell, 1998). Mechano-cold Aδ nociceptors (A-MC) respond to both mechanical and cold noxious stimuli. Then, Aδ fibers can sense combinations of thermal, mechanical and chemical stimuli. This diversity is essential for acute pain mediation as it allows detection of diverse noxious stimuli involving specific subtypes of afferents depending on the nature of the stimuli. At the proximal level, Aδ projects to the dorsal horn of the spinal cord that has a precise laminar organization from superficial lamina I to deep lamina V. Aδ fibers mainly project to laminae I and V.

Nociceptor C fibers*.* C fibers are unmyelinated fibers of small diameter responsible for slow pain, the "second" poorly localized pain. Comparably to Aδ afferents, C fibers are mainly polymodal, with classifications based on the nature of the stimuli detected or the molecular properties of the fibers. C fiber recordings in human skin revealed fibers sensitive to both mechanical and heat stimuli (CMH), as well as heat- (CH) or mechanical-sensitive (CM) only fibers, and fibers insensitive to both mechanical and heat stimuli (CM_iH_i) (Schmidt *et al.*, 1995).

C fibers are also heterogeneous at the molecular level. The so-called 'peptidergic' C fibers contain substance P or somatostatin (Hökfelt *et al.*, 1976) and express calcitonin-gene related peptide (CGRP) in rats (Eftekhari *et al.*, 2013). Peptidergic C fibers also express receptors for peptides like tyrosine kinase A (TrkA) neurotrophin receptor in rats (Fang *et al.*, 2005), responding to nerve growth factor (NGF). The "non-peptidergic" C fibers lack peptides but contain fluoride-resistant acid phosphatase activity (FRAP) (Nagy and Hunt, 1982) and bind the plant lectin isolectin B_4 (IB_4) in rat (Silverman and Kruger, 1990). At the proximal level, C fibers project to superficial laminae I and II.

Ascending pathway of nociceptors and thermoreceptors from the spinal cord to the brain. The thermoceptive and nociceptive output from the dorsal horn of the spinal cord to the brain is coming from laminae I to V in the dorsal horn of the spinal cord. These cells are second-order neurons at the origin of ascending pathways such as the spinothalamic and spinoreticular tracts. The spinothalamic tract is an ascending pathway reaching the thalamus (**Figure 7**). It can be divided into two paths, the lateral spinothalamic tract that transmits pain and thermal signals, and the anterior spinothalamic tract that transmits crude touch and firm pressure. Second-order neurons' fibers decussate via the anterior white commissure and project onto the ventral posterolateral (VPL) nucleus, relaying the sensory signal to the primary sensory cortex.

The spinoreticular tract is close to the spinothalamic tract and reaches the brainstem. Second-order neurons in the dorsal horn laminae project onto the medullary-pontine reticular formation in the brainstem. These third-order neurons connect to the thalamic intralaminar

nuclei, that project to the entire cerebral cortex. The spinoreticular tract relays information of slow and diffuse pain.

This large range of nociception modalities described above allows the detection of multiple noxious stimuli, such as thermal, mechanical, or chemical stimuli. To sense each type of sensory stimuli, different ion channels are involved to generate action potentials and transduce the signal to the CNS via the dorsal horn of the spinal cord.

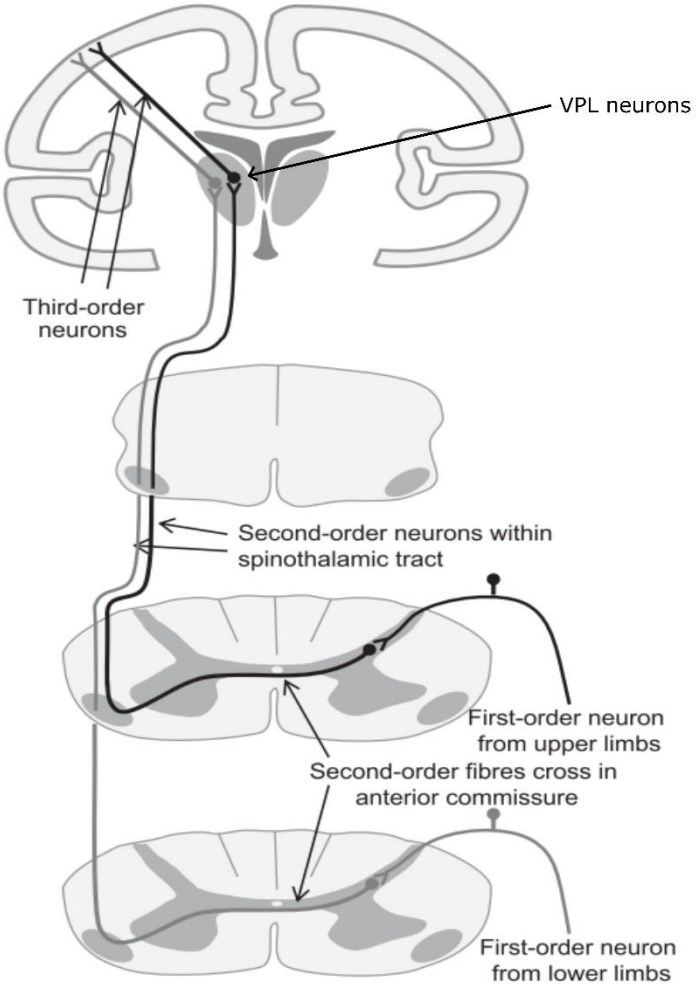

Figure 7. The spinothalamic tracts, an ascending pathway of nociceptors. VPL: ventral posterolateral. Adapted from (Chambers, Huang and Matthews, 2015)**.**

Heat transduction by nociceptors. Thermal transduction in mammals is mainly carried by polymodal transient receptor potential (TRPs) ion channels (see summary in **Table 2**), a family of six transmembrane domain receptors (Vriens, Nilius and Voets, 2014). To better understand how intense heat is detected by the different TRPs, capsaicin (an active

component of the chili plant) was of great help as it depolarizes specific nociceptors to cause heat-burning sensation (Caterina *et al.*, 1997).

Channel	Temperature of activation	Role in heat nociception (KO mutants)	References
TRPV1	> 42°C	Decrease of sensitivity to capsaicin and noxious heat	(Caterina *et al.*, 1997, 2000; Tominaga *et al.*, 1998; Davis *et al.*, 2000)
TRPV2	> 52°C	Normal thermal nociception	(Caterina *et al.*, 1999; Park *et al.*, 2011)
TRPV3	> 33°C	1) No effect on thermal sensitivity 2) Deficit on noxious heat detection	(Smith *et al.*, 2002; Moqrich *et al.*, 2005; Huang *et al.*, 2011)
TRPV4	> 27°C	1) No effect on thermal sensitivity 2) Diminution of thermal hyperalgesia in inflammation context	(Güler *et al.*, 2002; Todaka *et al.*, 2004; Huang *et al.*, 2011)
TRPM2	34-42°C	Deficit in sensation of non-noxious heat (38°C)	(Tan and McNaughton, 2016)
TRPM3	> 40°C	Deficiency in noxious heat detection (> 45°C)	(Vriens *et al.*, 2011)

Table 2. Channels implicated in heat thermotransduction of nociception.

The TRP cationic channel subfamily V (vanilloid) member 1 (TRPV1) is a non-selective cationic TRP channel activated by capsaicin or noxious temperature greater than 43°C (Caterina *et al.*, 1997). Considering its function in noxious heat detection and its expression in a majority of heat-sensitive nociceptors (Caterina *et al.*, 1997), TRPV1 has been hypothesized as the main transducer of intense and noxious heat. In support, it has been shown that protons (acidic pH) decrease the temperature threshold for TRPV1 response from 43 to 22°C (Tominaga *et al.*, 1998). Therefore, in the context of inflammation when physiological pH is decreased *in vivo*, TRPV1 activation could be enhanced leading to hypersensitivity to heat. To further investigate the physiological role of TRPV1 in heat detection, TRPV1 KO mutant mice have been generated and exhibited a large decrease of sensitivity to capsaicin and noxious heat (>43°C) (Caterina *et al.*, 2000; Davis *et al.*, 2000). According to this evidence, TRPV1 appears to be a main contributor to noxious heat detection.

Is there evidence for TRPV1-independent heat detectors? Other members of the TRPV family, such as TRPV2, TRPV3 and TRPV4 shown to be thermosensitive *in vitro,* could be putative heat sensors and participate in noxious heat detection.

TRPV3 is activated by temperatures above 33°C but not by capsaicin *in vitro* (Smith *et al.*, 2002), while TRPV4 is also activated *in vitro* by lower temperatures than TRPV1, between 27 and 35°C (Güler *et al.*, 2002). Considering their responses to lower temperatures (<40°C), TRPV3 and 4 could be dedicated to innocuous thermal stimuli detection rather than noxious stimuli. To decipher the physiological role in heat detection of these channels *in vivo*, TRPV3 and TRPV4 KO mutant mice were generated and placed on a surface of graded temperature and did not display any altered thermal preference, reacting the same way as wild type mice (Huang *et al.*, 2011), suggesting that these two channels may not be of first importance for heat sensation, or that other thermal receptors detect the heat stimuli. However, another study in mice found that KO mice for TRPV3 showed strong deficits in response to innocuous and noxious heat, suggesting a role of TRPV3 in thermosensation (Moqrich *et al.*, 2005). Another TRPV4 KO study also revealed that mutant mice showed a longer latency to escape from a 35-45°C hot surface in a context of an inflammation causing hyperalgesia, suggesting a role in thermal hyperalgesia (Todaka *et al.*, 2004).

TRPV2 is a non-specific cationic channel expressed in medium and large DRG neurons and responds to a higher temperature than TRPV1 (greater than 52°C) *in vitro* (Caterina *et al.*, 1999). Thus, the TRPV2 high heat threshold suggests that it could be involved in acute pain detection through Aδ fibers. However, TRPV2 KO mice displayed normal thermal nociception, suggesting that TRPV2 is not essential for noxious heat detection (Park *et al.*, 2011).

Other TRP ion channels, the TRP subfamily M (melastatin) (TRPM) members, have also recently been found to be involved in heat detection. TRPM2 responds to heat and mice KO mutant for this channel showed a striking deficit in their sensation of non-noxious warm temperature (38°C) (Tan and McNaughton, 2016), suggesting a role in warmth detection, but not in noxious stimuli detection. TRPM3 is also activated by heat (40°C) and KO mutant mice for TRPV3 elicit impaired detection of noxious heat (>45°C) (Vriens *et al.*, 2011).

Cold transduction by nociceptors*.* As for capsaicin with heat-sensing, cooling agents such as menthol (a component of mints) have been useful to investigate the cool detection by nociceptors. Channels for cold transduction in nociception are summarized in **Table 3**.

Channel	Temperature of activation	Role in cold nociception (KO mutants)	References
TRPM8	< 26°C	Loss of response to menthol and cold temperature (< 26°C) Partial insensitivity to cold in behavior (still avoid surface < 10°C)	(McKemy, Neuhausser and Julius, 2002; Peier *et al.*, 2002; Bautista *et al.*, 2007; Colburn *et al.*, 2007; Dhaka *et al.*, 2007)
TRPA1	< 20°C	1) Normal cold sensitivity 2) Not sensing correctly cold pain sensation	(Story *et al.*, 2003; Bautista *et al.*, 2006; Karashima *et al.*, 2009)

Table 3. Channels implicated in cold thermotransduction of nociception.

Transient receptor potential cation channel subfamily M (melastatin) member 8 (TRPM8), a Na^+ and Ca^{2+} permeable channel, was found to be activated by menthol, as well as temperatures below 26°C *in vitro* (McKemy, Neuhausser and Julius, 2002; Peier *et al.*, 2002). To further investigate the physiological role of TRPM8 in cold detection *in vivo*, mutants have been generated and TRPM8-deficient mice exhibit an important loss of response to low temperatures (below 26°C) and menthol (Bautista *et al.*, 2007; Colburn *et al.*, 2007; Dhaka *et al.*, 2007). However, behavior experiments on TRPM8 mutant mice showed only partial insensitivity to cold as they still avoid contact to surfaces below 10°C (Bautista *et al.*, 2007), suggesting that other sensors may be involved in cold sensing or the modulation of temperature threshold for detection of noxious cold stimuli.

Transient receptor potential cation channel, subfamily A (ankyrin), member 1 (TRPA1) was also suggested to be a potential cold sensor, particularly for low temperatures (<20°C) (Story *et al.*, 2003). TRPA1 has been shown to respond to menthol at higher concentrations than TRPM8 (Bandell *et al.*, 2004; Karashima *et al.*, 2007). However, the role of TRPA1 in cold sensation is debated, as behavioral assays in TRPA1 KO mutant mice showed normal cold sensitivity in cold-plate cooling assays (Bautista *et al.*, 2006). Another study showed that TRPA1 KO mutant mice displayed reduced pain-related behavior: while wild type mice started to jump when dropped on 0°C cold plates indicating that the cold plate induced significant pain, almost all the mutant mice did not jump meaning that they are not sensing correctly the pain sensation (Karashima *et al.*, 2009). Then, a hypothesis is that TRPA1 is not recruited for normal acute cold sensitivity, but rather for cold sensitivity in the setting of tissue injury.

Mechanical transduction by nociceptors. Transduction channels mediating noxious mechanical stimuli have remained elusive, but several candidates emerged as potential pain mechanotransducers (**Table 4**).

Channel	Species	Role in mechanical nociception (KO mutants)	References
MEC-10	*C. elegans*	Not responding to hard touch	(Chatzigeorgiou *et al.*, 2010)
ASIC2	Mouse	1) No touch defect 2) Reduction in mechanosensation	(Price *et al.*, 2000; Drew *et al.*, 2004)
ASIC3	Mouse	1) No touch defect 2) Increase of sensitivity to mechanical pain	(Chen *et al.*, 2002; Drew *et al.*, 2004)
TRP-4	*C. elegans*	Loss of response to hard touch stimuli	(W. Li *et al.*, 2011)
painless	*Drosophila*	Defective at detecting mechanical and thermal noxious stimuli	(Tracey *et al.*, 2003)
TRPV2	Mouse	No mutant available	(Muraki *et al.*, 2003)
TRPA1	Mouse	Unclear (controversial results)	(Bautista *et al.*, 2006; Kwan *et al.*, 2006)

Table 4. Channels implicated in mechanical transduction of nociception.

Mechanosensory abnormality 4 (*mec4*) (Driscoll and Chalfie, 1991) and *mec-10* (Huang and Chalfie, 1994) genes encode for degenerin/epithelial Na^+ channel (DeG/enaC) transmembrane proteins, MEC-4 and MEC-10. MEC-4 and MEC-10 channels were identified in *Caenorhabditis elegans* (*C. elegans*) as mechanotransducers involved in body touch, as mutants lead to touch-insensitive animals (Chalfie and Sulston, 1981). In *C. elegans*, MEC-10 is expressed in PVD multi-dendritic neurons involved in mechanical nociception (Albeg *et al.*, 2011), and the *mec-10(tm1552)* deletion mutants do not respond to hard touch stimulations, suggesting that MEC-10 is required for PVD mechanical nociception (Chatzigeorgiou *et al.*, 2010).

For other organisms, the mammalian orthologues of MEC-4 and MEC-10, acid-sensing ion channel (ASIC) 2 and 3, respectively, have been proposed as putative candidates. Investigations on ASIC2- and ASIC3-deficient mice produced modest or no-touch defects (Drew *et al.*, 2004), failing to support a role for these channels in cutaneous mechanotransduction. However, another ASIC2 KO mutant mice study found that loss of ASIC2 led to a reduction of mechanosensation (Price *et al.*, 2000). ASIC3 has been found

involved in the detection of mechanical pain, as ASIC3 KO mutant showed an augmentation of mechanical sensitivity to pain stimuli (Chen *et al.*, 2002). Thus, the physiological role of ASICs channels in nociception is complex and remains incompletely understood.

Some TRP ion channels, that play a role in thermotransduction, have also been proposed to transduce noxious mechanical stimuli. In invertebrates, the TRP ion channel TRP-4 expressed in the PDE neurons of *C. elegans* has been found involved in mechanical nociception, as *trp-4* mutants lost response to harsh touch mechanical stimuli (W. Li *et al.*, 2011). painless, a TRP channel in drosophila is required for both thermal and mechanical nociception (Tracey *et al.*, 2003), and could be involved in nociception, maybe as a polymodal channel.

In mammals, TRPV2 is activated by osmotic stimuli in aortic myocytes in mice (Muraki *et al.*, 2003). Nonetheless, the mechanosensitivity of TRPV2 needs to be tested *in vivo* and further characterized. A study using knock-out mice showed that the TRPA1 ion channel is involved in mechanical stimuli detection (Kwan *et al.*, 2006), but another research group found the opposite (Bautista *et al.*, 2006). Consequently, the role of TRPA1 in mechanical mediation is still unclear. In summary, there are multiple potential mechanical transducers of nociception but more investigations are needed to better understand their role and function in nociception.

Chemical transduction by nociceptors. Nociception of chemical noxious stimuli is important for sensing changes after physiological stress or tissue injury. As TRP channels respond to plant-derived irritants like capsaicin or menthol, they probably play a major role in the detection of chemicals. Among them, TRPA1 appears to be an interesting candidate as it responds to pungent natural compounds (Bandell *et al.*, 2004) and allyl isothiocyanate (Jordt *et al.*, 2004), the pungent responsible for mustard taste. An example of TRPA1 relevance as a chemo-nociceptor transducer is 2-propenal (acrolein) which is a toxic component of smokes like vehicle exhaust. 2-propenal is able to activate eye and airway innervating sensory neurons to produce pain and inflammation (Bautista *et al.*, 2006), a response that is reduced in TRPA1 KO mutant mice (Caceres *et al.*, 2009), suggesting that TRPA1 may be a sensor for toxic smokes components. TRPA1 is also activated by general anesthetics like isofluorane, inducing pain-related responses in mice (Matta *et al.*, 2008). These responses are abolished in TRPA1-null mice (Matta *et al.*, 2008), showing that TRPA1 is important for sensing noxious general anesthetics. In conclusion, if the role of TRPA1 in thermal and mechanical sensation is debated, it is a main detector of chemical irritants.

At the peripheral level, nociceptors are also sensitive to their chemical environment. Tissue damage may be associated with an accumulation of chemical factors released by the cells that reside or infiltrated the injured area, such as macrophages or neutrophils. All these

factors at the site of inflammation are referred to as the 'inflammatory soup' and include neurotransmitters, peptides like substance P or CGRP, neurotrophins, or cytokines (Kandel *et al.*, 2012). What can be the targets of these chemical molecules? ASIC channels are activated by acidification, so they are essential for detecting protons produced as a consequence of tissue inflammation. Particularly, the ASIC 3 channel subtype is expressed in nociceptors innervating skeletal and cardiac muscles. In cardiac ischemia, anaerobic metabolism leads to the production of lactic acid inducing acidification, and it has been found that such acidification activates nociceptors leading to pain (Immke and McCleskey, 2001). ASIC 3 channel investigations in sensory neurons innervating the rat heat showed that they respond to a range of pH (6.7 to 7.3) corresponding to pH changes observed during cardiac muscle ischemia (Yagi *et al.*, 2006). Thus, ASIC channels are of first importance for the detection of protons in the inflammatory soup.

Nerve growth factor (NGF) is a neurotrophic factor important for the survival and development of neurons, but it is also produced during tissue injury and is part of the inflammatory soup. After a first response to capsaicin, several minutes (~10 minutes) of exposure of DRG neurons in culture to NGF led to facilitation of a second capsaicin-evoked response, meaning that NGF acutely conditions the response to capsaicin through direct action on DRG neurons (Shu and Mendell, 1999). NGF binds to TrkA tyrosine kinase receptors expressed by peptidergic nociceptors in order to activate mitogen-activated protein (MAP) kinase and phospholipase C (PLC) - γ signaling pathways (Ganju *et al.*, 1998).

Voltage-gated sodium channels, an important component of nociception transduction.

Voltage-gated sodium channels are expressed in a large variety of nociceptors, with some of them of particular interest for nociception (**Table 5**). For example, the channel $Na_v1.7$ is interesting as a variety of pain troubles occur when it is degraded (Cox *et al.*, 2006; Dib-Hajj, Yang and Waxman, 2008). In contrast, gain-of-function mutations of $Na_v1.7$ lead to intense burning sensations due to hyperexcitability of the channel (Fertleman *et al.*, 2006; Estacion *et al.*, 2008). This observation suggests that $Na_v1.7$ plays an important role in the transduction of pain sensation.

Most nociceptors also express the $Na_v1.8$ sodium channel. It has been shown that $Na_v1.8$-deficient mice showed pronounced analgesia to noxious mechanical stimuli (Akopian *et al.*, 1999). Moreover, $Na_v1.8$ is also involved in cold pain sensation, the mutant for the channel also showing cold resistance (Zimmermann *et al.*, 2007). These results highlight a polymodal role for this channel in the transduction of noxious pain stimuli.

Other sodium channels are expressed in somatosensory neurons like $Na_v1.1$ or $Na_v1.9$. $Na_v1.1$ has been recently found functionally upregulated in chronic visceral hypersensitivity and $Na_v1.1$ inhibition can reduce pain hypersensitivity in this context (Salvatierra *et al.*,

2018). $Na_v1.9$ channel has been subjected to a regain of interest as it has been linked to human pain disorders (Leipold *et al.*, 2013; Zhang *et al.*, 2013; Huang *et al.*, 2014). Overall, voltage-gated sodium channels seem to be critical for the transduction of noxious sensory stimuli, with some of them being polymodal and involved in various types of noxious stimuli sensing.

Channel	Role in nociception	References
$Na_v1.1$	Reduce pain hypersensitivity when inhibited	(Salvatierra *et al.*, 2018)
$Na_v1.7$	Responsible of pain troubles when degraded Gain of function: intense burning sensations	(Cox *et al.*, 2006; Fertleman *et al.*, 2006; Dib-Hajj, Yang and Waxman, 2008; Estacion *et al.*, 2008)
$Na_v1.8$	KO mutant: pronounced analgesia to noxious mechanical stimuli KO mutant: noxious cold resistance (< 20°C)	(Akopian *et al.*, 1999; Zimmermann *et al.*, 2007)
$Na_v1.9$	Linked to human pain disorders	(Leipold *et al.*, 2013; Zhang *et al.*, 2013; Huang *et al.*, 2014)

Table 5. Voltage-gated sodium channels implicated nociception transduction.

Recent findings: bacterial infection detection by nociceptors. Recently, nociceptors have been described as sensors of bacterial infection at the skin level (Chiu *et al.*, 2013). Bacterial infection in mice paw leads to pain hypersensitivity. The activity of nociceptors has been investigated and TRPV1 positive nociceptors respond to heat-killed bacterial strains *in vitro*. To further understand the mechanisms under pain hypersensitivity and nociceptor detection of bacteria, nociceptor responses were recorded upon stimulation by bacterial compounds. Heat-stable bacterial formyl peptides, N-Formylmethionyl-leucyl-phenylalanine (fMLF) and N-Formyl-Met-Ile-Phe-Leu (fMILF) activate TRPV1-positive nociceptors and contribute to mechanical hypersensitivity. α-haemolysin (αHL) is a pore-forming toxin (PFT) secreted by nearly all *S. aureus* strains, induces tissue damage and promotes bacterial spread and inflammation. TRPV1 nociceptors were also activated after stimulation with this toxin, showing that nociceptors are able to sense different bacterial molecules. Altogether, these data show that bacterial pathogens are triggering pain in mice by directly activating nociceptors.

More recently, it has been shown that *Salmonella enterica*serovar Typhimurium (STm) activates gut-innervating nociceptors (Lai *et al.*, 2020). In response to the bacterial pathogen,

nociceptors release CGRP in order to regulate microfold cell (M cells) homeostatic level. M cells are epithelial cells of the gastrointestinal tract used as entry points by the pathogen to invade the gut. Therefore, regulation of M cells density by nociceptors allows controlling the pathogen infection. Moreover, nociceptors also maintain the level of segmented filamentous bacteria (SFB), a gut microbe mediating the pathogen infection. In conclusion, nociceptors also play a role in sensing and combating enteric bacterial pathogens in the gut. These recent findings indicate that nociceptors can be crucial to detect pathogens all over the body and to, in turn, activate defensive mechanisms.

In summary, DRG sensory neurons of the peripheral nervous system (PNS) have been extensively investigated and represent a heterogeneous population of neurons located in different body organs where they detect diverse sensory modalities to relay the information to the CNS. However, the position of the spine in the trunk is not mediated by the DRG sensory neurons. Thus, are there other cells detecting spine position?

2/ A recent discovery: the cerebrospinal fluid-contacting neurons form an interoceptive system in the spinal cord

The cerebrospinal fluid (CSF) is a physiological fluid circulating throughout the different brain ventricles, the subarachnoid space and the central canal of the spinal cord, and is secreted by the choroid plexuses in brain ventricles (**Figure 8**). Classically, CSF has been known to hydro-mechanically protect the brain, as well as to maintain brain homeostasis. The CSF contains molecules crucial for central nervous system development (Gato *et al.*, 2005; Lehtinen *et al.*, 2011), and plays a role in metabolites clearance during sleep in mice (Xie *et al.*, 2013).

CSF also contains a large variety of active neuromodulators: neurotransmitters like acetylcholine (Welch, Markham and Jenden, 1976), dopamine, noradrenaline and serotonin (Strittmatter *et al.*, 1997); neuropeptides like somatostatin, neuropeptide Y (Nilsson *et al.*, 2001), vasopressin and oxytocin (Martin *et al.*, 2014); but also neurosteroids (Kim, Creekmore and Vezina, 2003; Meletti *et al.*, 2017), purines (Schmidt *et al.*, 2015), and endocannabinoids (Romigi *et al.*, 2010). Besides its passive role, CSF could also have an active role in signaling different neurons of the central nervous system. Then, we can ask about the potential targets for CSF active molecules, which cells detect and respond to these molecules?

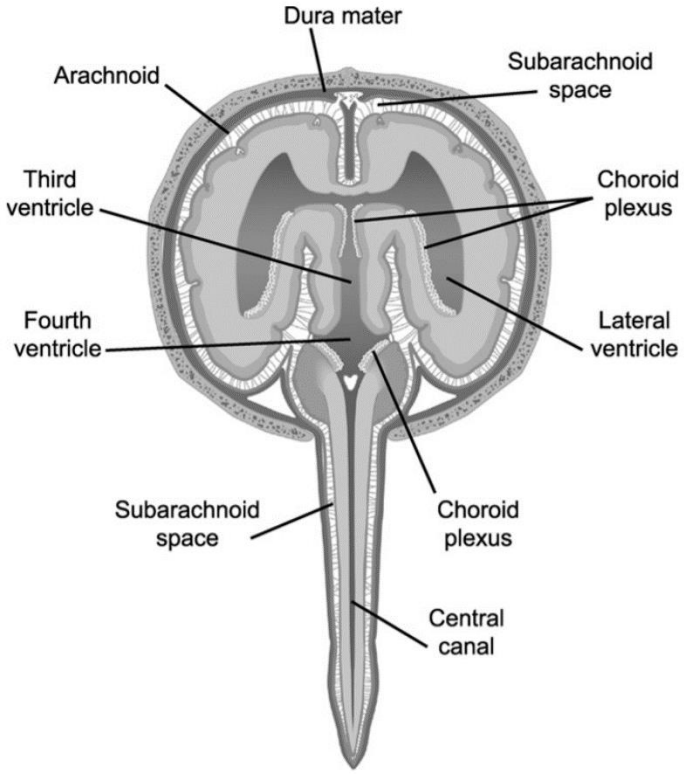

Figure 8. The cerebrospinal fluid circulates through the brain and the central canal of the spinal cord. Reprinted from (Di Terlizzi and Platt, 2006).

2.1) Definition of the cerebrospinal fluid-contacting neurons

Kolmer (Kolmer, 1921, 1931) and Agduhr (Agduhr, 1922) described a century ago, in over a hundred vertebrates, neurons in contact with the cerebrospinal fluid that they called cerebrospinal fluid-contacting neurons (CSF-cNs, also known as Kolmer-Agduhr “KA” cells) (**Figure 9A**). Based on their location at the interface between the central nervous system and the CSF (**Figure 9**), CSF-cNs could sense the active molecules of the CSF. In their description, Kolmer and Agduhr hypothesized that CSF-cNs may be sensory cells forming a sensory organ detecting changes in the CSF. Since their discovery, CSF-cNs have been extensively studied to investigate this question, with the help of recent technological progress in genetics or optical tools notably.

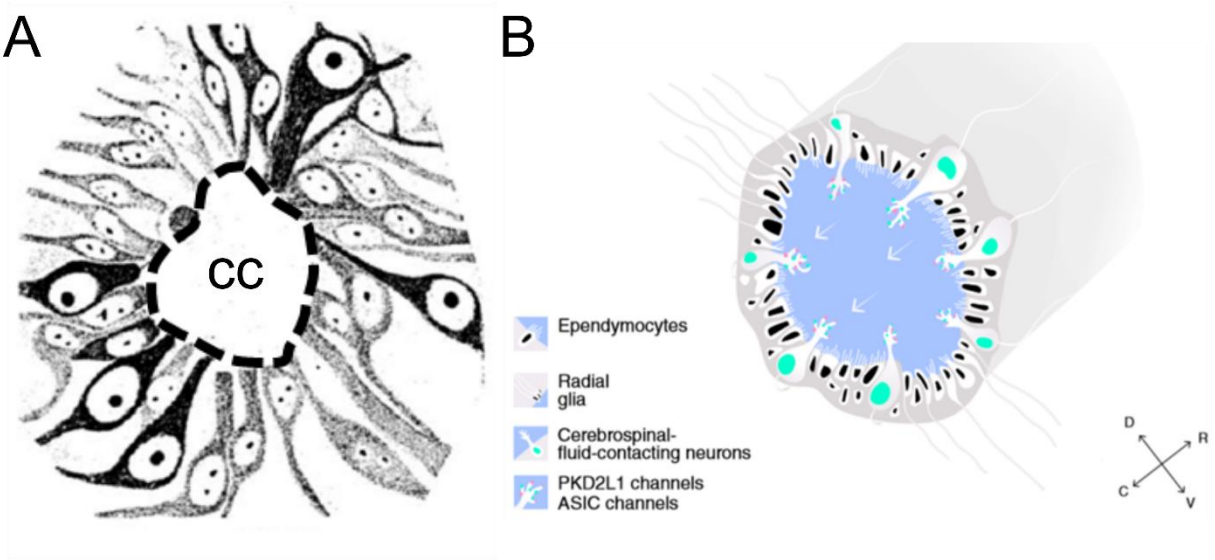

Figure 9. The cerebrospinal fluid-contacting neurons in the spinal cord. (A) Cerebrospinal fluid-contacting neurons in black, described in (Agduhr, 1922). **(B)** Section of the spinal cord shows the organization of cells surrounding the CSF in the central canal: radial glia, ependymocytes and CSF-cNs, which possess on their apical extension bathing in the CSF the ASIC and PKD2L1 channels that detect changes in CSF pH and osmolarity. R, rostral; C, caudal, V, ventral; D, dorsal. Reprinted from (Orts-Del'Immagine and Wyart, 2017).

CSF-cNs are located in the spinal cord, and different structures of the brain, like the subcomissural organ (SCO), the hypophysis, the retina, the paraventricular organ or the pineal gland for examples (Vigh and Vigh-Teichmann, 1981, 1998; Vígh *et al.*, 2004). Depending on the location, CSF-cNs display different morphologies and express different markers, suggesting that they might carry different functions. For example, the rat CSF-cNs of the brain mesencephalon have been found to express the TRPM8 receptor channel involved in cold sensation (Du *et al.*, 2009), and so could be involved in cold detection. The CSF-cNs, described as forming a novel interoceptive sensory system, are the ones located in the spinal cord and will be called spinal CSF-cNs.

Spinal CSF-cN somata ultrastructure. The spinal CSF-cN soma is located in the intra or the sub-ependymal layers of the area around and including the central canal, called the central gelatinosa (Vigh and Vigh-Teichmann, 1973, 1998; Nagatsu *et al.*, 1988). Spinal CSF-cN soma can exhibit a round or ovoid shape (Barber, Vaughn and Roberts, 1982; Jaeger *et al.*, 1983; Shimosegawa *et al.*, 1986; Dale *et al.*, 1987; Stoeckel *et al.*, 2003), as well as a triangular and fusiform shape (Barber, Vaughn and Roberts, 1982; Jaeger *et al.*, 1983; Shimosegawa *et al.*, 1986; Stoeckel *et al.*, 2003). Compared to their neighboring cells in the central gelatinosa, spinal CSF-cNs are less-electron dense and possess a round to oval nucleus (Schueren and DeSantis, 1985; Alibardi, 1990; Marichal *et al.*, 2009; Alfaro-

Cervello *et al.*, 2012). The soma of spinal CSF-cNs is commonly small with a diameter of around 10µm (Barber, Vaughn and Roberts, 1982; Nagatsu *et al.*, 1988; Stoeckel *et al.*, 2003; Orts-Del'Immagine *et al.*, 2014), however larger spinal CSF-cN soma was described in rat with diameters of 13 to 28µm (Shimosegawa *et al.*, 1986). In rat, fusiform spinal CSF-cNs with a diameter of 22µm were also described (Barber, Vaughn and Roberts, 1982). In the cytoplasm of spinal CSF-cNs, the presence of a rough endoplasmic reticulum (RER) (Barber, Vaughn and Roberts, 1982; Schueren and DeSantis, 1985; Alfaro-Cervello *et al.*, 2012), as well as free ribosomes (Barber, Vaughn and Roberts, 1982; Alibardi, 1990; Marichal *et al.*, 2009; Alfaro-Cervello *et al.*, 2012) suggests a high level of protein synthesis. In the central canal, rat spinal CSF-cNs form apical zonulae adhaerens to link to ependymal cells (Stoeckel *et al.*, 2003).

Spinal CSF-cN dendritic extension. Electron microscopy revealed that spinal CSF-cNs bear a dendritic apical extension protruding into the CSF in the central canal. This apical extension expresses the dendritic marker microtubule-associated protein2 (MAP2) (Djenoune *et al.*, 2014; Orts-Del'Immagine *et al.*, 2014). Spinal CSF-cNs apical extension slightly differs depending on the species, exhibiting or not multiple microvilli at the dendritic extension (Vigh and Vigh-Teichmann, 1973), as well as a cilium for some species like *Xenopus* (Dale *et al.*, 1987), mice (Alfaro-Cervello *et al.*, 2012) and zebrafish for example (Djenoune *et al.*, 2017). Ultrastructure analysis in zebrafish showed that this brush of actin-based microvilli at the apical extension extends in the central canal and encircle a single cilium with a "9 + 2" microtubule organization, typical of a kinocilium. Further analysis in vitro and in vivo in zebrafish showed that this kinocilium is motile (Hubbard *et al.*, 2016; Sternberg *et al.*, 2018).

Spinal CSF-cN axonal projections. Spinal CSF-cNs project a single axon from the basal part of the cell body. In some species like lamprey or Xenopus, spinal CSF-cNs project axons into the ventrolateral margin of the spinal cord (Vigh, Vigh-Teichmann and Aros, 1977; Megías, Álvarez-Otero and Pombal, 2003), forming neurohormonal nerve endings attached by hemidesmosomes to the basal lamina of the spinal cord, allowing possible direct contact with the facing subarachnoid space CSF. In lamprey, spinal CSF-cNs also project into the lateral margin of the spinal cord where they can connect with intraspinal stretch receptors called the Edge cells (Christenson *et al.*, 1991; Jalalvand *et al.*, 2014), that can play a role of intraspinal mechanoreceptor (Grillner, Williams and Lagerbäck, 1984). In zebrafish, spinal CSF-cNs ventrally project ipsilateral ascending axons (Djenoune *et al.*, 2014, 2017).

Molecular markers to label spinal CSF-cNs. Spinal CSF-cNs are gamma-aminobutyric acid (GABA)-ergic neurons, as it has been shown in multiple species like the rat (Barber, Vaughn and Roberts, 1982; Stoeckel *et al.*, 2003), African clawed frog (Dale *et al.*, 1987; Binor and Heathcote, 2001), lamprey (Christenson *et al.*, 1991; Jalalvand, Robertson, Tostivint, *et al.*, 2016), eel and trout (Roberts *et al.*, 1995), dogfish (Sueiro *et al.*, 2004), turtle (Reali *et al.*, 2011) zebrafish (Bernhardt *et al.*, 1992; Higashijima, Mandel and Fetcho, 2004; Higashijima, Schaefer and Fetcho, 2004; Wyart *et al.*, 2009; Yang, Rastegar and Strähle, 2010; Djenoune *et al.*, 2014), mouse and primate (Djenoune *et al.*, 2014) (**Figure 10**). GABA expression is consistent in all spinal CSF-cNs and, coupled with their peculiar morphology, constituted for a long time the best way to identify the spinal CSF-cNs.

However, to facilitate further investigation of spinal CSF-cNs, specific genetic markers were needed to specifically label all spinal CSF-cNs in the spinal cord. The marker of choice appeared to be the polycystic kidney disease 2-like 1 (PKD2L1) channel, a non-selective cationic channel that was found expressed in spinal CSF-cNs (Huang *et al.*, 2006). Later on, PKD2L1 was also found expressed in spinal CSF-cNs in other species such as non-human primates (macaques, Djenoune *et al.*, 2014) or zebrafish (Djenoune *et al.*, 2014; Sternberg *et al.*, 2018; Orts-Del'Immagine *et al.*, 2020), and Pkd2l1 is co-expressed with Pkd1l2 protein (England *et al.*, 2017) (**Figure 10**). Spinal CSF-cNs also express molecular markers of "immature" neurons, such as polysialylated neural cell adhesion molecule (PSA-NCAM), HuC/D, NKX6.1 and doublecortin (DCX) (Stoeckel *et al.*, 2003; Russo *et al.*, 2004; Marichal *et al.*, 2009; Reali *et al.*, 2011; Kútna *et al.*, 2014; Orts-Del'Immagine *et al.*, 2014). The specific marker PKD2L1 rapidly became the best way to label spinal CSF-cNs, allowing the generation of transgenic lines targeting spinal CSF-cNs that became essential for dissecting the functional roles of CSF-cNs, as well as their developmental origin.

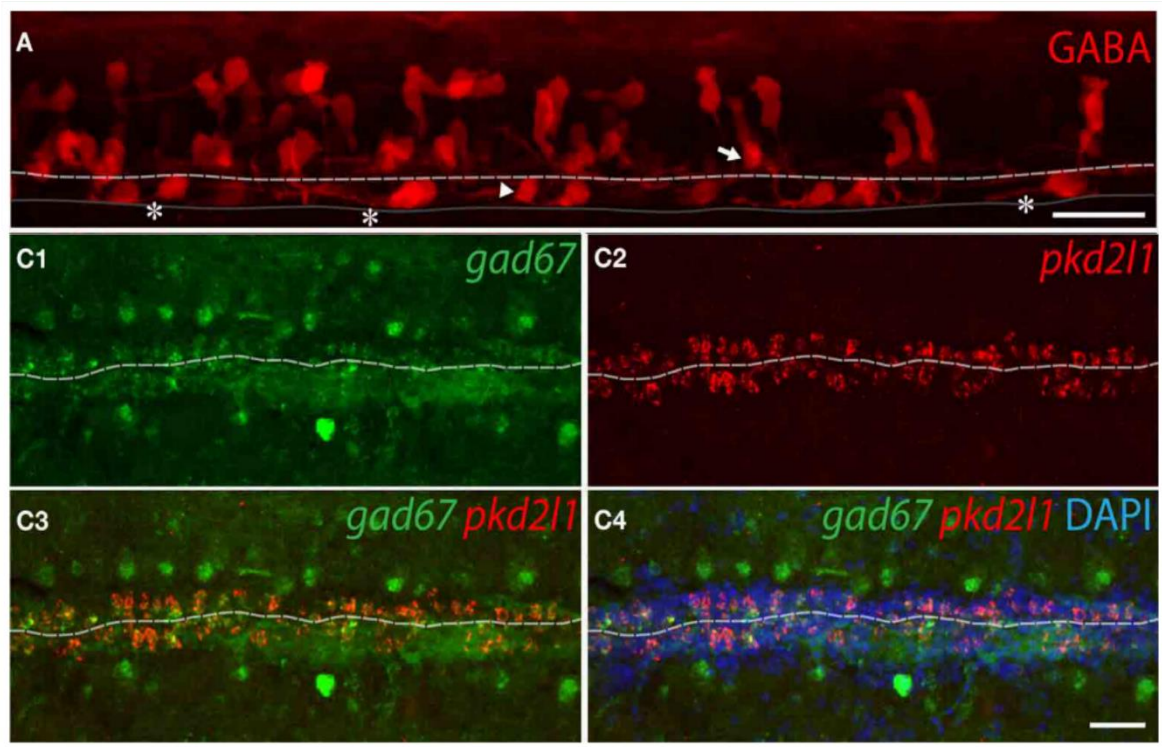

Figure 10. GABA and PKD2L1 are molecular markers for spinal CSF-cNs. (A) GABA IHC on WT 30-somite embryos shows ventral (arrowhead) and dorsal (arrow) spinal CSF-cNs and their ascending axon (asterisks). **(C1–C4)** In the adult, pkd2l1+ spinal CSF-cNs are gad67+ as shown by FISH for gad67 **(C1, C3, C4)** and pkd2l1 **(C2–C4)** on sections of WT spinal cord. The white dash line indicates the central canal, the dark line the ventral limit of the spinal cord. **(A)** is a projection from the lateral view of a whole-mount embryo immunostained for GABA while **(C1–C4)** correspond to frontal sections. DAPI staining appears in blue. Scale bars = 30µm. Adapted from (Djenoune *et al.*, 2014).

Spinal CSF-cNs dual developmental origin. Spinal CSF-cNs are organized in two rows of cells in the spinal cord, one is dorsolateral and the second is ventral. Developmental origin of spinal CSF-cNs was investigated in zebrafish to show that they derive from two different spinal cord progenitor domains: the p3 progenitor domain for the dorsolateral spinal CSF-cNs and pMN domain for the ventral ones (Park, Shin and Appel, 2004; Yang, Rastegar and Strähle, 2010; Huang *et al.*, 2012; Djenoune *et al.*, 2014). This dual origin was also confirmed in mice with the p2/pOL (for dorsolateral spinal CSF-cNs or CSF-cNs') and cells adjacent to the floor plate in the p3 progenitor domains (for ventral spinal CSF-cNs or CSF-cNs'') (Petracca *et al.*, 2016a; Di Bella *et al.*, 2019).

Morphological investigations in zebrafish showed that dorsolateral and ventral spinal CSF-cNs display distinct axonal projections and apical extensions. Dorsolateral spinal CSF-cNs apical extension is more extended along the border of the central canal, compared to the ventral one that is more compact (Djenoune *et al.*, 2017; Desban *et al.*, 2019). Conversely,

ventral spinal CSF-cNs have axons of larger length, with more branches and wider arborization than dorsolateral ones (Djenoune *et al.*, 2017).

Electrophysiological properties of spinal CSF-cNs. Spinal CSF-cNs expressing markers of immature neurons such as PSA-NCAM or HuC/D, it was investigated in different species, such as juvenile turtle (Russo *et al.*, 2004) or neonatal rat (Marichal *et al.*, 2009), whether these cells are neurons possessing neuronal electrophysiological properties such as firing.

Spinal CSF-cNs firing properties were investigated by monitoring their responses to depolarizing current pulses, and subpopulations of spinal CSF-cNs carrying different electrophysiological properties have been distinguished (**Figure 11**). It was described in slices *in vitro* in the juvenile turtle (Russo *et al.*, 2004) and neonatal rat (P0-P5) (Marichal *et al.*, 2009) that one population of spinal CSF-cNs exhibit phasic firing (generation of a unique action potential in response to current injection) (**Figure 11A, C**), while other spinal CSF-cNs exhibit tonic firing (train of action potentials in response to current injection) (**Figure 11B, D**). These two populations of cells show similar high input resistances (from ~4 to ~6 GΩ, see **Table 6**), characteristic of the small spinal CSF-cNs. In juvenile turtle, the resting potential of single-spiking cells was significantly lower than repetitive-spiking cells (Russo *et al.*, 2004) (see **Table 6**), but this difference between populations was not observed in neonatal rat (Marichal *et al.*, 2009). However, spike amplitudes of single-spiking cells and repetitive-spiking cells were significantly different in both turtle and rat, with lower amplitudes in single-spiking cells (32-41 mV) compared to repetitive-spiking cells (54-72 mV) (**Table 6**). Both single and train of action potentials were blocked by the toxin Tetrodotoxin, a sodium (Na^+) channel blocker, suggesting that these subpopulations of spinal CSF-cNs fire Na^+ fast action potentials. In addition, slow after-hyperpolarization (sAHP) was observed in the repetitive-spiking population in juvenile turtle, as well as in neonatal rat in cells exhibiting the more robust repetitive spiking. Such sAHP was not observed in single-spiking spinal CSF-cNs. In neonatal rat, another population of spinal CSF-cNs showed a slow depolarizing potential blocked by manganese (Mn^{2+}), suggesting a calcium conductance mediation (Marichal *et al.*, 2009). It was proposed that these different electrophysiological properties in neuronal subpopulations of spinal CSF-cNs were due to different stages of maturation (Russo *et al.*, 2004; Marichal *et al.*, 2009). As it has been shown with the development of *Xenopus* spinal neurons *in vitro* (Spitzer and Lamborghini, 1976), the most immature spinal CSF-cNs would exhibit slow calcium-mediated depolarizing potential, and as spinal CSF-cNs differentiate they would shift from slow Ca^{2+} potentials to fast Na^+ action potentials corresponding to the single-spiking population of spinal CSF-cNs. The ability to fire train of action potentials would appear at more advanced stages of maturation, coupled with the development of calcium-

dependent potassium (K^+) channels that would generate sAHP to remove Na^+ channel inactivation, as it was described in *Xenopus* spinal neurons (Spitzer, Vincent and Lautermilch, 2000).

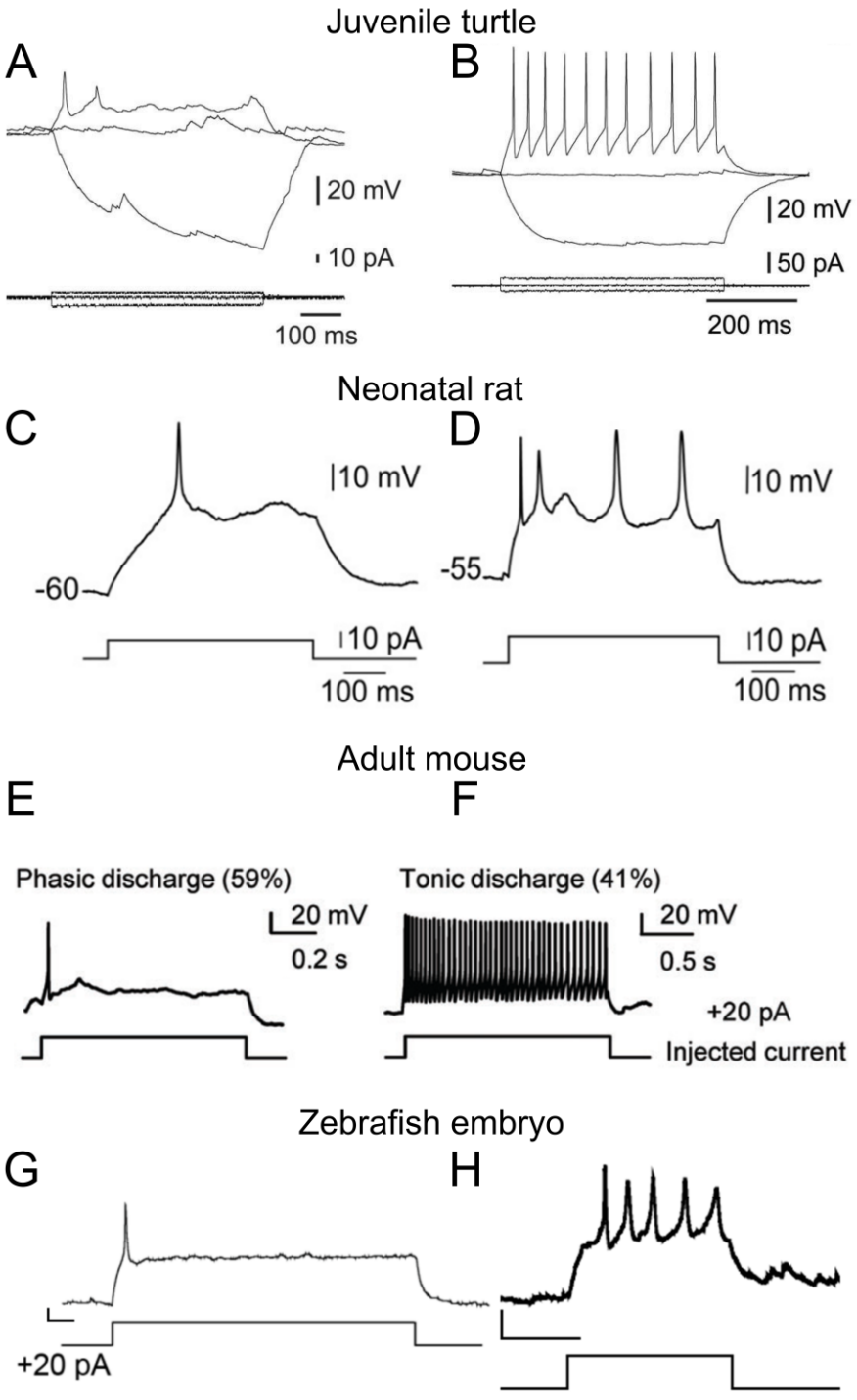

Figure 11. Firing properties of CSF-cNs in diverse species. (A) In juvenile turtle, electrophysiological properties of a cell fired a single full spike in response to sustained depolarization. **(B)** In juvenile turtle, electrical properties of a repetitive spiking cell. **(C)** In neonatal rat, electrophysiological properties of a cell that fired a single full spike in response to sustained

depolarization. **(D)** In neonatal rat, electrical properties of a repetitive spiking cell. **(E-F)** In adult mice, two representatives CSF-cNs recorded in current-clamp mode at −60 mV (current injected to maintain the membrane potential at −60 mV: −12 pA in **E**; −18 pA in **F**) exhibiting either phasic **(E)** or tonic **(F)** action potential discharge in response to depolarizing current injection (+20 pA). **(G)** In zebrafish embryo, current-clamp recording of a spinal CSF-cN. CSF-cN fires single action potential in response to a small depolarizing current step (+20pA). Vertical scale: 20mV, horizontal scale: 100ms. **(H)** In zebrafish embryo, a representative firing of a CSF-cN at 28 hpf. 10–20 pA of injected current. Scale: 100 ms, 20 mV. Adapted from (Russo *et al.*, 2004), (Marichal *et al.*, 2009), (Orts-Del'Immagine *et al.*, 2012), (Thesis Sternberg, 2016) and (Sternberg *et al.*, 2018).

In adult mice, electrophysiological properties of brainstem CSF-cNs were investigated on slices *in vitro* (Orts-Del'Immagine *et al.*, 2012). The two single-spiking and repetitive-spiking populations of CSF-cNs were also found in adult mice brainstem (**Figure 11E-F**), showing similar high membrane resistance and membrane resting potential (see **Table 6**) (Orts-Del'Immagine *et al.*, 2012). Recently, the electrophysiological properties of spinal CSF-cNs were also investigated in zebrafish embryo (24 hours post fertilization) *in vivo*. As described in turtle, rat and mice, spinal CSF-cNs in zebrafish embryo can be divided into two subpopulations (**Figure 11G-H**): single-spiking cells and repetitive-spiking cells that are highly resistive (3-6 GΩ) (Sternberg thesis, 2016; Sternberg *et al.*, 2018).

Another hallmark of the spinal CSF-cNs is their spontaneous channel activity (**Figure 12**). Voltage-clamp recordings in mice (Orts-Del'Immagine *et al.*, 2012, 2016), lamprey (Jalalvand, Robertson, Tostivint, *et al.*, 2016) and zebrafish (Sternberg *et al.*, 2018) showed that the CSF-cN high input resistance enabled spontaneous single-channel openings (-10 to -20 pA) (**Figure 12**). Investigations in mice brainstem CSF-cNs showed that this channel activity is abolished in PKD2L1 KO mutants (Orts-Del'Immagine *et al.*, 2016) (**Figure 12B1-B2**), suggesting that these single-channel openings correspond to functional PKD2L1 channels expressed in CSF-cNs. In addition, it was shown that PKD2L1 channels are able, at a single-channel level, to generate a depolarization large enough to trigger action potentials in CSF-cNs in mice (Orts-Del'Immagine *et al.*, 2016). A Pkd2l1 KO mutant, generated in zebrafish, showed a similar loss of channel activity in spinal CSF-cNs compared to wild-type zebrafish (Sternberg *et al.*, 2018) (**Figure 12C1-C2**), reinforcing the evidence that spontaneous channel opening in spinal CSF-cNs corresponds to Pkd2l1.

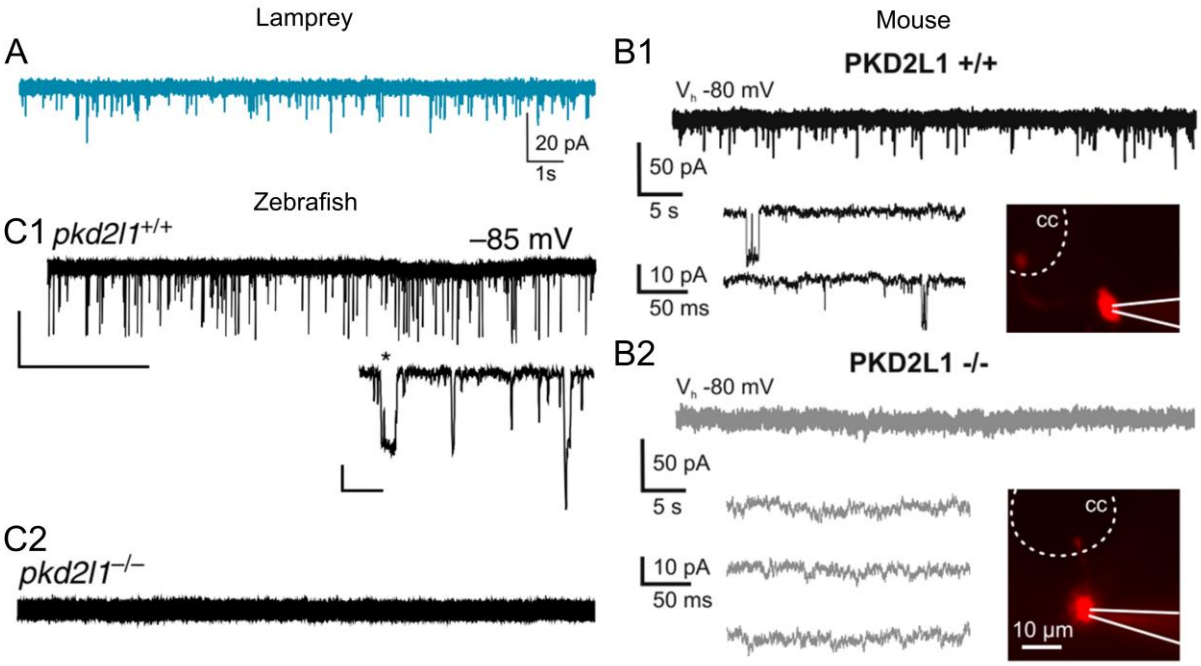

Figure 12. Spinal CSF-cNs exhibit spontaneous channel opening. (A) In voltage-clamp mode, spontaneous channel opening in lamprey. **(B1-B2)** Representative voltage-clamp recordings (V_h= -80 mV) showing current traces in identified CSF-cNs in acute brainstem slices from PKD2L1$^{+/+}$ **(B1)** and PKD2L1$^{-/-}$ **(B2)** animals. In **B1** and **B2**, bottom Left: current traces at a slower timescale showing that unitary currents are only observed in PKD2L1$^{+/+}$ animals; bottom right: micrographs illustrating the recorded cells dialyzed in whole-cell configuration with Alexa 594 (10 mM) to ensure that recordings were made from CSF-cNs (white lines delineate the recording electrode). **(C1-C2)** Gap-free voltage-clamp (VC) recordings from CSF-cNs show extensive single-channel opening exclusively in *pkd2l1*$^{+/+}$ embryos. Scale: top: 10 s, 20 pA; bottom: 20 ms, 10 pA. Adapted from (Jalalvand, Robertson, Tostivint, *et al.*, 2016), (Orts-Del'Immagine *et al.*, 2016) and (Sternberg *et al.*, 2018).

	Firing	Input resistance (GΩ)	Membrane potential (mV)	Spike amplitude (mV)	Reference
Juvenile turtle	Phasic firing	5.5 ± 0.7	−50 ± 2.4	36.7 ± 4	(Russo *et al.*, 2004)
	Tonic firing	6.0 ± 0.3	−57 ± 1.1	69.5 ± 2.2	
Neonatal rat	Phasic firing	3.95 ± 0.29	−61.4 ± 1.49	38.27 ± 1.52	(Marichal *et al.*, 2009)
	Tonic firing	4.25 ± 0.3	−71.11 ± 2.0	56.38 ± 2.1	
Adult mice	Phasic firing	2.0 ± 0.4	−43 ± 2	/	(Orts-Del'Immagine *et al.*, 2012)
	Tonic firing	2.5 ± 0.8	−42 ± 2	/	

Table 6. Spinal CSF-cN electrophysiological properties in diverse species.

Spinal CSF-cNs as potential neurosecretors? Electron microscopy investigations revealed clear vesicles (containing neurotransmitters) and dense core granules (containing neuropeptides and secreted proteins) at both apical extension and axonal projections (Vigh, Vigh-Teichmann and Aros, 1977; Djenoune *et al.*, 2017) (**Figure 13**). Thus, we can hypothesize that spinal CSF-cNs could play a neurosecretory role in the spinal cord, and potentially secrete into the CSF to modify its composition. In line with this hypothesis, spinal CSF-cNs express many other neuromodulators than GABA. For example, monoamines such as dopamine are found expressed in CSF-cNs of pigeon (Acerbo, Hellmann and Güntürkün, 2003) and lamprey (McPherson and Kemnitz, 1994), and serotonin in various species like salamander (Sims, 1977), hagfish or lamprey (Ochi, Yamamoto and Hosoya, 1979). In zebrafish, serotonin expression was found transient and restricted to ventral spinal CSF-cNs (Djenoune *et al.*, 2017), showing that the two subpopulations of spinal CSF-cNs also carry different molecular identities.

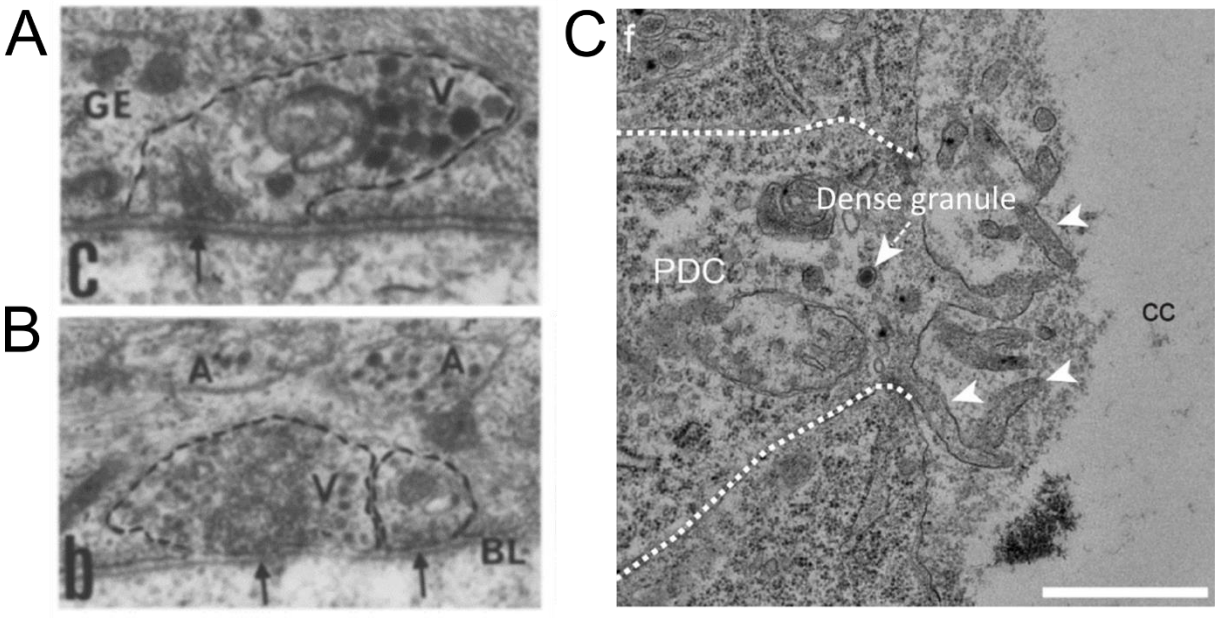

Figure 13. Clear vesicles and dense granules at synaptic and dendritic extensions of spinal CSF-cNs. (A-B) Axons (A) and terminals (dotted) containing granular vesicles (V) of 800 or 1400/~ in diameter and synaptic vesicles (at arrows) in the caudal spinal cord of the carp. BL basal lamina; GE glial endfoot, x 25,500. **(C)** Putative dorsal spinal CSF-cN referred to as PDC extending microvilli (arrowheads) in contact with the central canal (cc). Scale bar: 1 µm. Adapted from (Vigh, Vigh-Teichmann and Aros, 1977) and (Djenoune *et al.*, 2017).

Neuropeptides were also found enriched in spinal CSF-cNs. Somatostatin is expressed in spinal CSF-cNs from lamprey (Buchanan *et al.*, 1987; Christenson *et al.*, 1991), coho salmon (Yulis and Lederis, 1988) and the Somatostatin1.1 paralog in dorsal spinal CSF-cNs in zebrafish (Wyart *et al.*, 2009; Djenoune *et al.*, 2017). URP1 and URP2, neuropeptides of the urotensin II family playing different roles like regulation of endocrine and cardiovascular functions among others (Vaudry *et al.*, 2010), have been found expressed specifically in ventral spinal CSF-cNs in zebrafish (Quan *et al.*, 2015). Vasointestinal peptide (VIP) was found expressed in rat and macaque spinal CSF-cNs (Lamotte, 1987).

In conclusion, spinal CSF-cNs express a large variety of molecules, with some restricted to one subpopulation or the other, showing that in addition to a role of a sensor, spinal CSF-cNs could also secrete various compounds in response to sensory stimuli.

2.2) Spinal CSF-cNs are mechanosensory cells

The spinal CSF-cNs extend a motile kinocilium into the CSF suggesting a mechanosensory function, as hypothesized by Kolmer a century ago. A first evidence of mechanosensory function in mice was whole-cell recordings showing that hypo-osmotic shocks increase the single-channel activity of the spinal CSF-cNs (Orts-Del'Immagine *et al.*, 2012). In lamprey, spinal CSF-cNs respond to direct fluid pressure application (Jalalvand, Robertson, Wallén, *et al.*, 2016). This mechanical detection is dependent on the ASIC3 channel, as APETx2 (an ASIC3 channel inhibitor) inhibits mechanosensory response to fluid pressure application (Jalalvand, Robertson, Wallén, *et al.*, 2016). These data suggest a potential mechanical activation of spinal CSF-cNs by fluid pressure, maybe to detect changes in the CSF flow.

In zebrafish, spinal CSF-cNs were found to detect both passive and active spinal bending (Böhm *et al.*, 2016; Hubbard *et al.*, 2016). Spinal CSF-cNs are activated on the concave side of the tail bending, meaning that the cells respond to the mechanical compression applied with the bending, not the stretch (**Figure 14A**). Dorsal spinal CSF-cNs respond to lateral tail bending (Böhm *et al.*, 2016), while ventral ones respond to longitudinal bending (Hubbard *et al.*, 2016) (**Figure 14A**). These results are concordant with the evidence that spinal CSF-cNs *in vitro* respond to mechanical stimulation with a glass probe directly on the plasma membrane of the cell (Sternberg *et al.*, 2018). Detection of mechanical cues in zebrafish is dependent on the PKD2L1 channel (Böhm *et al.*, 2016; Sternberg *et al.*, 2018), as PKD2L1 KO abolishes spinal CSF-cN responses to both lateral tail bending (Böhm *et al.*, 2016) and glass probe mechanical stimulation (Sternberg *et al.*, 2018).

As spinal CSF-cNs respond to fluid pressure application (Jalalvand, Robertson, Wallén, *et al.*, 2016), and that embryonic activity of spinal CSF-cNs *in vivo* correlates with the integrity of CSF flow (Sternberg *et al.*, 2018), it was hypothesized that lateral tail bending induces a change in CSF flow that is detected by spinal CSF-cNs leading to their activation through PKD2L1 or ASIC3 ion channels. Recently, a study showed that spinal CSF-cNs mechanosensory functions rely on the Reissner fiber (RF) (Orts-Del'Immagine *et al.*, 2020). The Reissner fiber is an agglomeration of the SCO-spondin glycoprotein, extending from the SCO in the third brain ventricle (where SCO-spondin is secreted) to the end of the spinal cord in the central canal.

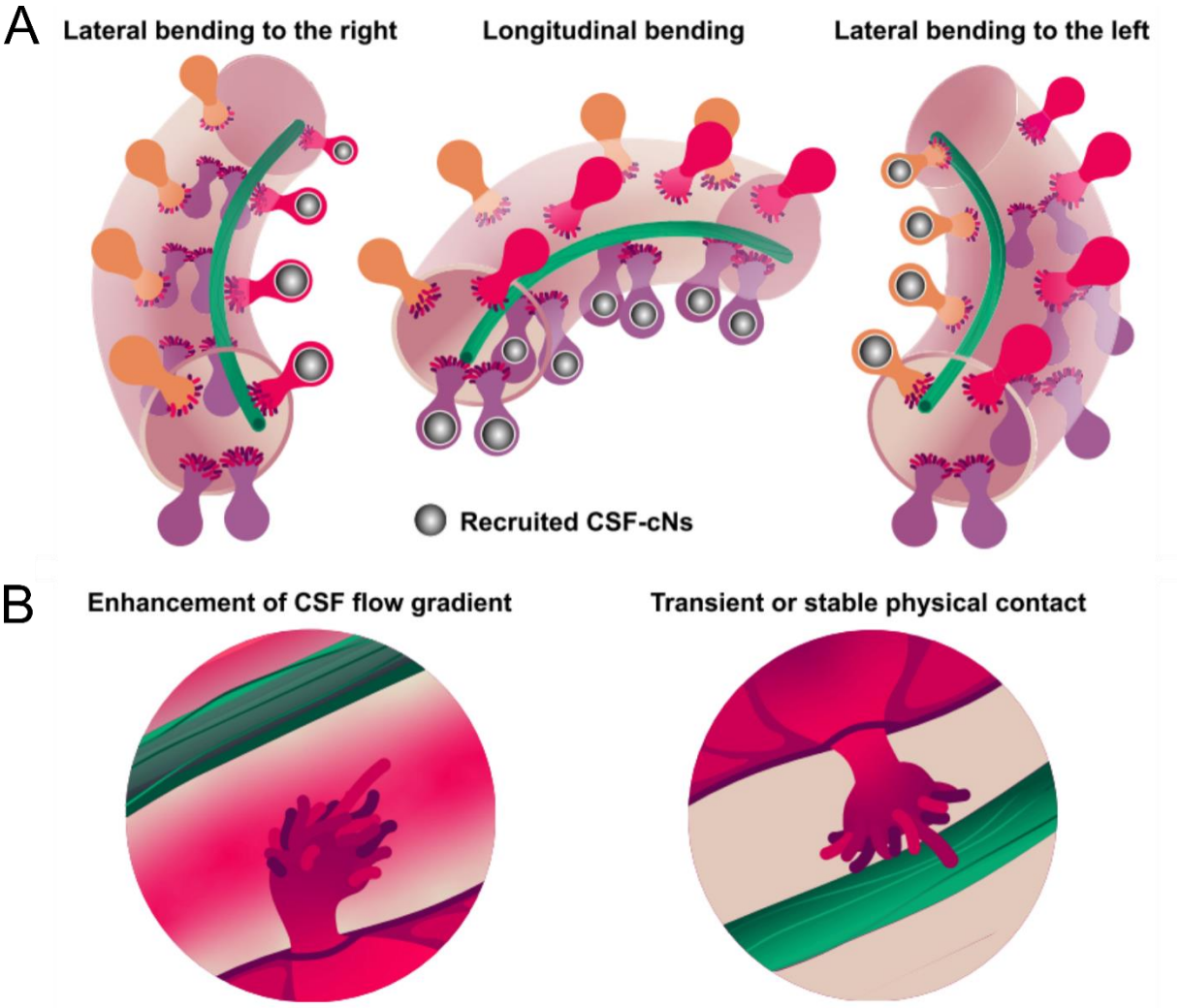

Figure 14. Spinal CSF-cNs are mechanosensory cells that detect spinal bending requiring the Reissner fiber. (A) Spinal CSF-cNs detect mechanical stimuli from lateral and longitudinal tail bendings and are activated ipsilaterally to the side of the bending. **(B)** Spinal bending detection requires the Reissner fiber. Two hypotheses emerged for Reissner fiber implication: either the Reissner fiber enhances the cerebrospinal fluid (CSF) flow during the bending, or the Reissner

fiber directly interacts with the apical extension of the spinal CSF-cNs to activate them. Reprinted from (Orts-Del'Immagine *et al.*, 2020).

As the RF is under tension in the central canal at rest, a spinal bending could lead to a RF closer to the side of the curvature, so the concave side where spinal CSF-cNs are activated during tail bending, inducing an asymmetry. Loss of RF formation in a zebrafish *scospondin* mutant was shown to impair spinal CSF-cN mechanosensitivity, as spinal CSF-cNs were not responding to lateral binding anymore (Orts-Del'Immagine *et al.*, 2020). Kolmer and Agduhr already noticed a century ago that the RF was in close vicinity to the spinal CSF-cNs, and Kolmer hypothesized a potential functional interaction between spinal CSF-cNs and RF (Kolmer, 1921), a theory not shared by Agduhr (Agduhr, 1922). Recent electron microscopy ultrastructure analysis in the central canal confirmed a close vicinity between the RF and the apical extension of the spinal CSF-cNs (Orts-Del'Immagine *et al.*, 2020). Then, two hypotheses emerged: either the RF directly interacts with the apical extension of spinal CSF-cNs, or the RF induces a change in the CSF flow inside the central canal activating in turn spinal CSF-cNs (Orts-Del'Immagine *et al.*, 2020) (**Figure 14B**). Further analysis is required to understand the functional role of the RF related to the apical extension of spinal CSF-cNs.

2.3) The role of spinal CSF-cNs in the modulation of locomotion and posture in response to mechanical stimuli

In response to spinal mechanical stimuli, spinal CSF-cNs modulate locomotion and posture through the release of neurotransmitters such as GABA or somatostatin (**Figure 15**). The first evidence for spinal CSF-cN modulation of locomotion was the discovery that optogenetic activation of these neurons induces slow swim bouts in zebrafish (Wyart *et al.*, 2009). Later on, it was discovered by combining *pkd2l1* transgenic line, electrophysiology and optogenetics that dorsolateral spinal CSF-cNs form GABAergic synapses onto V0-v interneurons in zebrafish, an essential component of the slow locomotion (Fidelin *et al.*, 2015; Djenoune *et al.*, 2017) (**Figure 15B**). Through these connections, spinal CSF-cNs modulate slow locomotion in a state-dependent manner through the release of GABA (Fidelin *et al.*, 2015). At rest, optogenetic activation of spinal CSF-cNs triggered delayed slow locomotion, such a delay let think that the locomotor response followed a long period of inhibition leading to a rebound swimming activity (Fidelin *et al.*, 2015). During ongoing fictive locomotion, spinal CSF-cNs activation silenced locomotor activity through V0-v interneurons (Fidelin *et al.*, 2015). In addition to GABA, a recent study showed that *somatostatin 1.1*

zebrafish KO mutant showed longer spontaneous swims, meaning that Somatostatin1.1 is also involved in slow locomotion inhibition (Quan *et al.*, 2020).

Zebrafish spinal CSF-cNs also project GABAergic synapses onto fast motor neurons and excitatory sensory interneurons of the escape circuit, namely the caudal primary (CaP) motoneurons and the commissural primary ascending (CoPa) interneurons respectively (**Figure 15A**) (Hubbard *et al.*, 2016; Djenoune *et al.*, 2017). Activation of ventral spinal CSF-cNs was shown to directly silence the CaP motoneurons that innervate fast skeletal muscles (Hubbard *et al.*, 2016). Silencing of neurotransmission in spinal CSF-cNs using botulinum toxin-induced postural defects during fast locomotion (Hubbard *et al.*, 2016).

Recently, a study showed that rostralmost spinal CSF-cNs synapse onto occipital motor neurons in the caudal hindbrain, responsible for the control of head position (Wu *et al.*, 2021) (**Figure 15**). Spinal rostralmost CSF-cNs also form axo-axonic synapses onto reticulospinal neurons located in the brain stem, that send descending information to the spinal cord, particularly to central pattern generators to control voluntary movements (Wu *et al.*, 2021). Ablation of the hindbrain-projecting rostralmost spinal CSF-cNs induced defect of postural control, with more rolling events during acousto-vestibular (A-V) induced escapes (Wu *et al.*, 2021). This result suggests that rostralmost spinal CSF-cNs send information to occipital motor neurons controlling head position, as well as to spinal motor neurons to maintain the stability of the fish during the initiation of the escape.

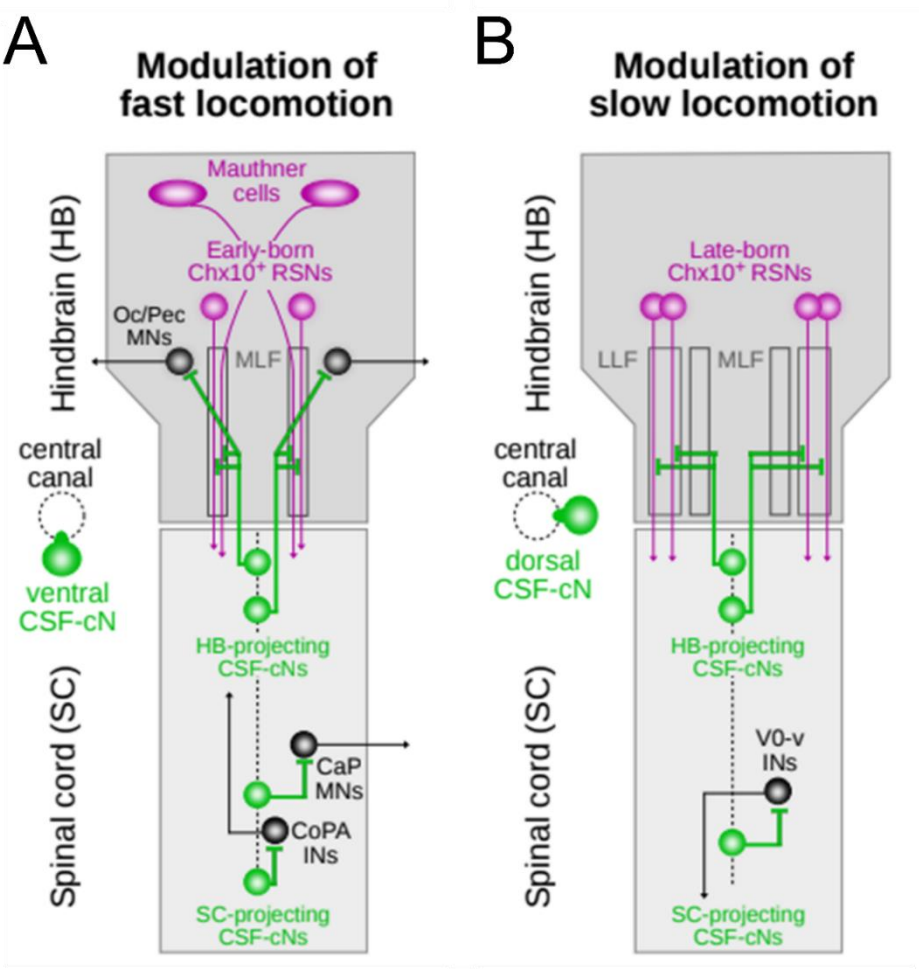

Figure 15. Spinal CSF-cNs modulate locomotion and posture in response to mechanical stimulation from spinal cord bending. (A) Modulation of fast locomotion. **(B)** Modulation of slow locomotion. Adapted from (Wu *et al.*, 2021).

Altogether, these data show that spinal CSF-cNs detect spinal mechanical stimuli, and in turn modulate locomotion and posture via the release of neurotransmitters. However, little is known about the chemosensory functions of spinal CSF-cNs. As it has been described in DRG neurons, are spinal CSF-cNs polymodal and able to detect mechanical and chemical stimuli? The spinal CSF-cNs could play a role in the CNS in detecting the CSF chemical content, being a new chemosensory system in zebrafish.

3/ Chemosensory systems in fish

The detection of chemicals from the external environment is of first importance for living organisms. Indeed, chemosensation enables avoiding predators and finding mating partners through detection of pheromones, or locating nutritious food or escaping toxic

substances in the environment. Chemosensation relies on different sensory systems allowing detection of a large variety of chemical substances: the olfactory system, the gustatory system, as well as the solitary chemosensory cells. These systems will be described in the following text.

3.1) The olfactory system

In zebrafish, the olfactory system allows the detection of water-soluble odorants and is of first importance to detect pheromones or food odors from the external environment. Various chemical odorants classes are detected by the olfactory system, such as amines, nucleotides, amino acids, steroids, bile acids or prostaglandins (Friedrich and Korsching, 1998). While odorants are detected and processed through two anatomically segregated neural pathways in mice, namely the main olfactory system and the vomeronasal (accessory olfactory) system (Buck, 2000), teleost fish lack independent olfactory organs and possess only a single main olfactory epithelium (Eisthen, 1992) that will be described in the following text.

Olfactory organ anatomy. The olfactory organ of zebrafish is composed of a pair of nasal cavities located on the dorsal side of the head, between the eyes (Hansen and Zeiske, 1998) (**Figure 16**). Each cavity comprises two nostrils: an anterior nostril allowing entry of water and a posterior one for water to exit. The olfactory epithelium (OE) lies between these two nostrils and is arranged in several lamellae that converge in a central raphe to form a cup-shaped structure known as the rosette (Hansen and Zeiske, 1998) (**Figure 16**). Each rosette lamella is composed of a sensory region surrounded by a non-sensory epithelium of basal and supporting cells (Byrd and Brunjes, 1995; Hansen and Zeiske, 1998). The sensory region of the lamellae contains olfactory sensory neurons (OSNs), bipolar sensory neurons that are receptor cells detecting water-soluble odorants. These neurons project their axons through the olfactory nerve to the olfactory bulbs (**Figure 16**), that are conveying olfactory stimuli to brain regions such as the telencephalon and the diencephalon (Fuller, Yettaw and Byrd, 2006; Miyasaka *et al.*, 2009).

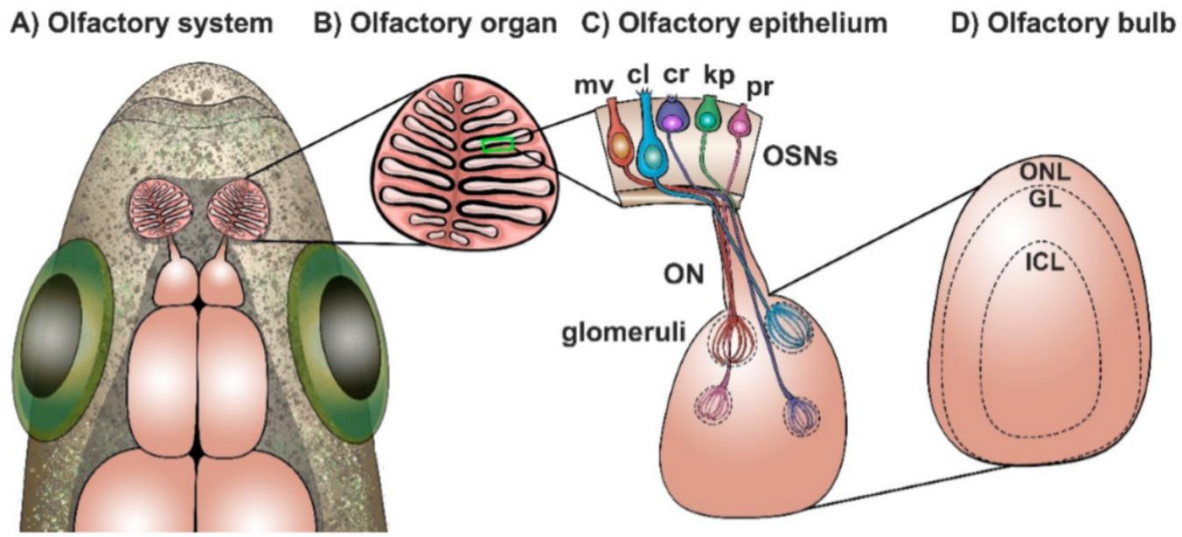

Figure 16. Anatomical and morphological organization of the zebrafish olfactory system. **(A)** Localization of the olfactory system in zebrafish. Dorsal side is shown; rostral side is located upwards; **(B)** Olfactory organ morphology. Olfactory sensory epithelium arranged in lamellae is shown in black; **(C)** Olfactory epithelium (OE) composed of the following olfactory sensory neurons (OSNs): microvillous (mv); ciliated (cl); crypt (cr); kappe (kp); and pear (pr) OSNs. OSNs extend their axons to the olfactory bulb via the olfactory nerve (ON) to form discrete glomeruli; **(D)** Olfactory bulb organization in three laminae: olfactory nerve layer (ONL); glomerular layer (GL); and intracellular layer (ICL). Reprinted from (Calvo-Ochoa and Byrd-Jacobs, 2019).

Olfactory sensory neurons and their sensory receptors. Detection of odorants by OSNs is mediated by families of G-protein coupled receptors (GPCRs) expressed in these neurons. The role of GPCRs in OSNs is to transduce odorant chemical signals into odor-evoked electrical signals by the regulation of intracellular cascades of second messengers. As described in mammals, it has been shown in fish that most OSNs follow the 'one neuron-one receptor' configuration (Sato, Miyasaka and Yoshihara, 2007) and that axons from OSNs expressing the same GPCR converge to a single spherical structure in the olfactory bulb called glomerulus (Sato, Miyasaka and Yoshihara, 2007; Braubach, Fine and Croll, 2012). Three types of GPCRs are expressed in OSNs: olfactory receptors (ORs), trace amine-associated receptors (TAARs) and vomeronasal receptors (V1Rs, V2Rs). In addition, olfactory sensory neurons are divided into five types that carry different morphology and express different types of GPCRs: ciliated, microvillous, crypt, kappe and pear neurons (**Figure 16**).

Ciliated OSNs are elongated neurons located in the deep layer of the OE and exhibiting long apical dendrites containing cilia (Morita and Finger, 1998; Sato, Miyasaka and Yoshihara, 2005). Ciliated OSNs express both OR and TAAR receptors and respond preferentially to

bile acids (Michel and Derbidge, 1997; Sato, Miyasaka and Yoshihara, 2005), suggesting a role in alarm substance detection. Patch-clamp recordings on isolated neurons from channel catfish showed that ciliated neurons respond also to amino acids and urine extracts containing bile acid (Sato and Suzuki, 2001).

Microvillous OSNs are located at intermediate depths of the OE and exhibit thick dendrites with apical microvilli (Morita and Finger, 1998; Sato, Miyasaka and Yoshihara, 2005). Microvillous OSNs detect amino acids by expressing V1 receptors coupled to the Gαi protein (DeMaria *et al.*, 2013), and it was suggested that they also express V2 receptor to recognize pheromones such as 4-hydroxyphenylacetic acid (Pfister and Rodriguez, 2005; Behrens *et al.*, 2014; Ahuja *et al.*, 2015). Microvillous neurons in catfish are also activated by ATP nucleotide (Hansen *et al.*, 2003).

Crypt neurons are found only in fish (Hansen *et al.*, 1999; Vielma *et al.*, 2008) and show spherical cell bodies bearing microvilli and few cilia (Hansen and Zielinski, 2005). Crypt neurons have been shown to express a single V1R-like receptor gene in zebrafish, *ora4*, although crypt neuron ligands are unclear (Oka, Saraiva and Korsching, 2012). Indeed, subsets of crypt cells respond to either amino acids, bile acids, or reproductive pheromones in mackerel (Schmachtenberg, 2006; Vielma *et al.*, 2008) and juvenile trout (Bazáes and Schmachtenberg, 2012). However, mature trout crypt neurons respond preferentially to gonadal extract and hormones from the opposite sex (Bazáes and Schmachtenberg, 2012), suggesting a role of crypt cells in reproduction-related odorant detection in adult fish.

More recently, the kappe neurons have been described as positive for G_o-immunoreactivity neurons characterized by an apical microvilli-bearing cap (Ahuja *et al.*, 2015). However, kappe neurons' receptors and corresponding ligands are still unknown.

Finally, pear neurons present a pear-shaped morphology and exhibit very short apical dendrites (Wakisaka *et al.*, 2017). Pear neurons express the A2c receptor, which is a novel receptor activated by adenine nucleotides and adenosine and could be involved in the detection of nucleotides released from food sources into environmental water (Wakisaka *et al.*, 2017).

Chemosensory transduction of olfactory signals. A canonical pathway for OSNs transduction through GPCRs was described in mammals (**Figure 17**). When a ligand binds to an olfactory GPCR, the receptor changes its conformation and its associated heterotrimeric olfactory specific G_{olf} protein (α, β and γ subunits) is activated by exchanging the GDP bound to the G protein for a GTP (**Figure 17**). Then, the Gα subunit linked to GTP

dissociates from β and γ subunits and activates the adenylyl cyclase III (ACIII) to catalyze the conversion of ATP to the second messenger cAMP (Firestein, Darrow and Shepherd, 1991). cAMP binds intracellularly to a cyclic nucleotide-gated cation channel allowing the increase of intracellular concentration of cations such as sodium and calcium (Firestein, Darrow and Shepherd, 1991) (**Figure 17**). This cationic influx results in the intracellular medium being less negative, generating eventually an action potential. In addition, the calcium influx through the activation of the cyclic nucleotide-gated cation channel also leads to the activation of another ion channel permeable to chloride anions (Kleene and Gesteland, 1991). Usually, chlorides channels mediate inhibitory responses by allowing chloride entrance into the cells, but OSNs have been shown to maintain a high intracellular chloride concentration. Thus, activation of ion chloride channels in an OSN leads to a chloride efflux (**Figure 17**), leading to a further depolarization of the neuron increasing the excitatory response magnitude.

Similar to mammals, it has been shown in zebrafish that OSNs express the olfactory-specific G_{olf} protein in ciliated (Koide *et al.*, 2009) and pear neurons (Wakisaka *et al.*, 2017). However, the teleost-specific whole-genome duplication (Hoegg *et al.*, 2004) led to a duplication of several G proteins including G_{olf}, but only the *Golf2* gene is expressed in OE (Oka and Korsching, 2011). As in mammals, it was also shown that ciliated and pear neurons in zebrafish express ACIII (Wakisaka *et al.*, 2017) and the cyclic nucleotide-gated cation channel (Sato, Miyasaka and Yoshihara, 2005; Wakisaka *et al.*, 2017). It is unknown in zebrafish whether calcium-activated chloride channels contribute to the OSN depolarization as it has been described in mammals.
However, G_0 protein has also been reported in the fish-specific kappe neurons (Ahuja *et al.*, 2015), as well as G_i protein in crypt neurons (Oka, Saraiva and Korsching, 2012) suggesting more diversity in chemosensory transduction in fish. The G_q protein immunoreactivity is also found in microvillous neurons in goldfish and catfish (Hansen and Zielinski, 2005), but is found only in the nose's non-sensory region in zebrafish (Oka, Saraiva and Korsching, 2012). Unlike the olfactory-specific G_{olf} protein, G_0 and G_q activate the phospholipase C/IP_3-mediated sensory transduction cascade, suggesting that another transduction cascade than cAMP is involved in fish. This supposition is concordant with the fact that an IP_3-channel blocker and a PLC inhibitor have been found to reduce in the zebrafish nose the response to amino acid stimuli (Ma and Michel, 1998). In addition, it has been found that microvillous neurons express the transient receptor potential cation channel, subfamily C, member 2 (TRPC2) (Sato, Miyasaka and Yoshihara, 2005; Koide *et al.*, 2009), an important channel in the cascade of transduction mediated by IP_3 as it allows an influx of cation, mainly sodium and calcium, leading to the generation of an action potential. TRPC2 has not been found in

kappe nor crypt neurons (Sato, Miyasaka and Yoshihara, 2005; Ahuja *et al.*, 2015). In summary, ciliated and pear neurons in zebrafish seem to possess the same transduction pathway as in mammals, as they express the specific G_{olf}protein as well as the main components of the cAMP transduction pathway. Unlike what was described in mammals, crypt and microvillous neurons exhibit evidence for another transduction pathway involving IP_3, as well as TRPC2 for the microvillous neurons.

In conclusion, the olfactory epithelium in zebrafish contains diverse subpopulations of olfactory sensory neurons expressing different types of receptors, allowing the detection of a large diversity of individual odorants from the external environment.

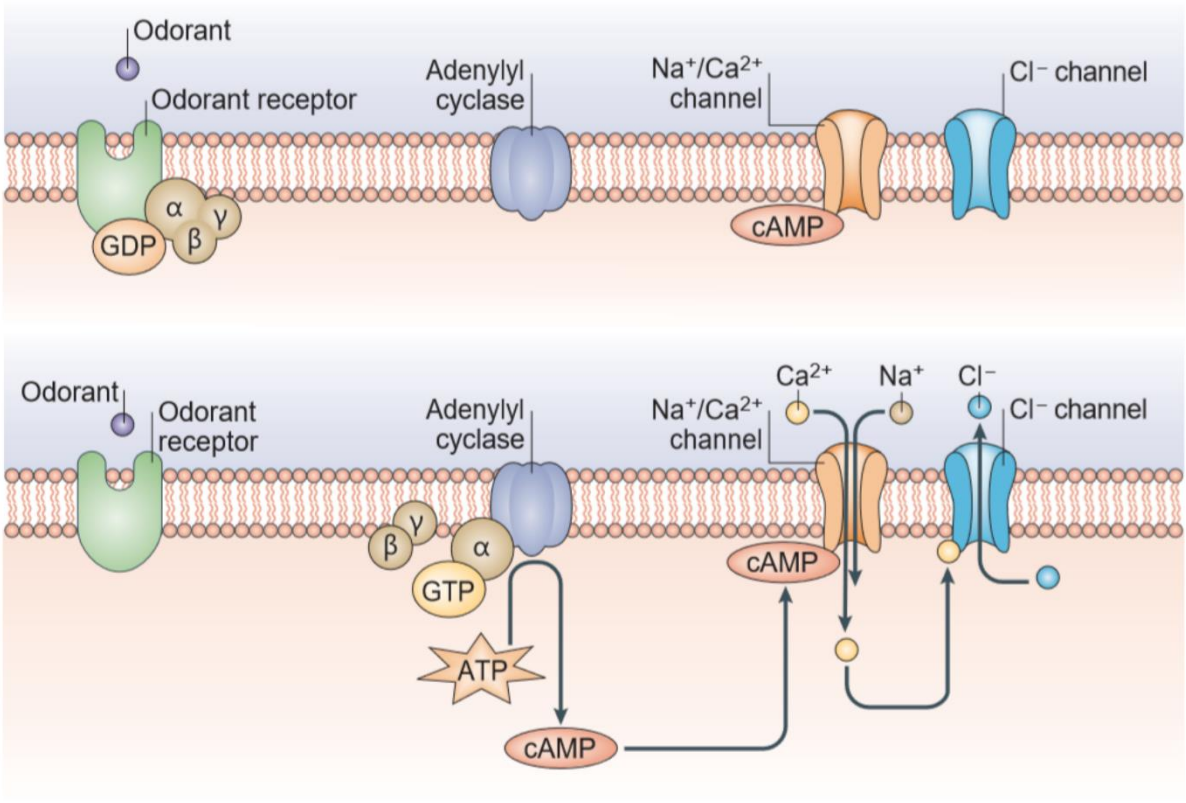

Figure 17. Canonical pathway of signal transduction in olfactory sensory neurons. The odorant receptor defines odorant responsiveness. The heterotrimeric G-protein, the adenylyl cyclase, the cyclic-nucleotide gated Na^+/Ca^{2+} channel and the Cl^- channel are thought to be common among olfactory sensory neurons. Reprinted from (Mombaerts, 2004).

3.2) The gustatory system

Taste is crucial in zebrafish for identifying water-soluble nutrients as well as avoiding toxins and indigestible materials from the external environment. In teleost, the taste receptor

cells are organized in structures called taste buds (Kirino *et al.*, 2013), with about a hundred elongated cells for each bud (Reutter, Boudriot and Witt, 2000). Three types of taste receptor cells were characterized in mammals: type I assumed to have a glial function; type II transducing taste signals through GPCRs; and type III transducing taste signals through ion channels. Similarly, an electron microscopy study allowed description of three types of taste receptor cells in zebrafish carrying different characteristics: dark cells with short and thin microvilli; light cells with a single large microvillus; and cells with intermediate electron density and microvilli of intermediate size (Hansen, Reutter and Zeiske, 2002). However, it is still unknown whether these cell types correspond to what was described functionally in mammals.

Gustatory system organization. Fish taste buds are located on the oral cavity but also gills, head, fins and body surface (Kasumyan, 2019). Taste receptor cells are innervated by neurons called gustatory neurons located in three ganglions: the geniculate ganglion of the facial cranial nerve, the petrosal of the glossopharyngeal cranial nerve, and the nodose ganglion of the vagal cranial nerve (Baker and Bronner-Fraser, 2001) (**Figure 18**). These neurons project via their respective cranial nerve to the facial, glossopharyngeal and vagal lobe in the brainstem. From these lobes, the signal is transmitted to the secondary gustatory nucleus sending ascending fibers to hypothalamic nuclei and tertiary gustatory nucleus (Rink and Wullimann, 1998; Folgueira, Anadón and Yañez, 2003) (**Figure 18**). Hypothalamic nuclei as well as tertiary gustatory nucleus send descending fibers to the facial and vagal lobes (Folgueira, Anadón and Yañez, 2003). Tertiary gustatory centers also project to the medial region of the dorsal telencephalic area and the ventral nucleus of the ventral telencephalon (Folgueira, Anadón and Yañez, 2003) (**Figure 18**).

Taste receptor cells and their sensory receptors. In mammals, type I receptor cells express a glutamate-aspartate transporter (GLAST) (Maxwell Lawton *et al.*, 2000), as well as the plasma membrane-bound nucleotidase NTPDase2, hydrolyzing extracellular ATP (Bartel *et al.*, 2006). As ATP plays a role of a neurotransmitter in taste buds (Finger *et al.*, 2005), and that glutamate is also a possible neurotransmitter, it was suggested that type I receptor cells could be involved in terminating synaptic transmission and restricting the spread of transmitters. One study in mice found that amiloride-sensitive epithelial sodium channels (ENaCs) are expressed in taste receptor cells that could correspond to type I cells (Vandenbeuch, Clapp and Kinnamon, 2008). In conclusion, type I cells are described as playing a support role in taste buds but could be involved in salt detection.

Type II receptor cells express GPCRs and bind sweet, bitter, or umami compounds in mammals. A given type II receptor cell express taste GPCRs specific for one taste quality such as sweet or bitter (Nelson *et al.*, 2001). Distinct groups of type II cells express two families of taste receptors: type receptor 1 (T1R) and type receptor 2 (T2R) (Chandrashekar *et al.*, 2006; Matsumoto, Ohmoto and Abe, 2013). T1R2/T1R3 heterodimers of T1Rs have been shown to be responsible for sweet-tasting (Nelson *et al.*, 2001; Zhao *et al.*, 2003), while T1R1/T1R3 heterodimers are responsible for umami taste (Nelson *et al.*, 2001; Zhao *et al.*, 2003). T2Rs have been described as bitter taste receptors detecting bitter tastants (Chandrashekar *et al.*, 2000).

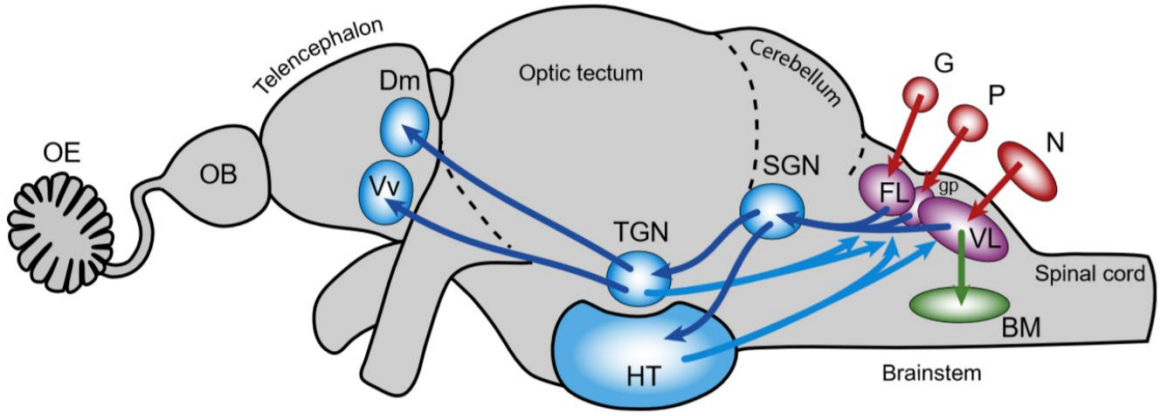

Figure 18. Neuronal circuits for taste in the zebrafish brain. Schematic representation of a fish brain with gustatory processing pathways. Red, sensory neurons; magenta, primary gustatory centers (facial, glossopharyngeal, and vagal lobes); cyan, secondary and tertiary gustatory centers and telencephalic areas; green, motor nuclei. Sensory ganglia and brain areas indicated by abbreviation: G, geniculate ganglion; P, petrosal ganglion; N, nodose ganglion; FL, facial lobe; gp, glossopharyngeal lobe; VL, vagal lobe; BM, branchiomotor neurons; SGN, secondary gustatory nucleus; HT, hypothalamus; TGN, tertiary gustatory centers including the tertiary gustatory nucleus; Dm, medial region of the dorsal telencephalic area; Vv, ventral nucleus of ventral telencephalon. Reprinted from (Korsching, 2020).

In mammals, type III receptor cells express neuronal-like genes including neural cell adhesion molecule (NCAM), as well as enzymes for the synthesis of at least two neurotransmitters (glutamic acid decarboxylase and aromatic amino acid decarboxylase), and calcium voltage-gated channels associated with neurotransmitter release (DeFazio *et al.*, 2006; Dvoryanchikov, Tomchik and Chaudhari, 2007). As they express synaptic proteins and they show depolarization-dependent calcium transients typical of synapses, type III cells have been called as ‘presynaptic cells’ (DeFazio *et al.*, 2006). In addition, type III presynaptic cells have been described as responding to sour taste stimuli (Tomchik *et al.*, 2007; Huang

et al., 2008) and carbonated solutions (Chandrashekar *et al.*, 2009), but receptors involved in the detection of such stimuli are unknown.

In fish, T1Rs and T2Rs were also described, showing significant identity to mammalian T1Rs and T2Rs respectively (Ishimaru *et al.*, 2005). It has been found recently that zebrafish possesses seven T2Rs (Shiriagin and Korsching, 2018). However, the only T2R receptor that has been deorphanized in zebrafish so far is T2R1, which responds to denatonium benzoate in heterologous expression assays (Oike *et al.*, 2007). Among the three T1Rs described in mammals, zebrafish show one-on-one orthologues of mammalian T1R1 and T1R3 genes but have expanded their T1R2 clade with two genes in zebrafish for one in mammals (Ishimaru *et al.*, 2005). Zebrafish T1R2/T1R3 co-expression studies showed responses to amino acids such as alanine, proline, serine or tyrosine, but no responses to glucose nor sucrose (Oike *et al.*, 2007). Other heterodimers were tested, such as T1R1/T1R3 responsible for sweet-tasting in mammals, and showed no response for glucose, sucrose or amino acids (Oike *et al.*, 2007). However, it has been shown that sucrose-containing food is strongly preferred by zebrafish (Kasumyan and Døving, 2003), suggesting that sucrose and glucose detection involves different receptors in zebrafish compared to mammals.

Chemosensory transduction of gustatory signals. In mammals, the gustatory GPCRs functions with a G protein called gustducin, which activates the phospholipase C β2 (PLCβ2) secondary messenger, leading to the opening of the transient receptor potential channel TRPM5 (Zhang *et al.*, 2003). Opening of TRPM5 allows the release of the ATP neurotransmitter in type II and III mammalian taste receptor cells (Finger *et al.*, 2005), which excites afferent of the gustatory neurons innervating the taste receptor cells. It has been shown that mice lacking the *PLCB2* gene lose both avoidance to denatonium benzoate and attraction to amino acids (Zhang *et al.*, 2003), suggesting that the PLCβ2-mediated transduction pathway is involved in different natures of taste stimuli. In zebrafish, *PLCβ2* has been found co-expressed with *T1R* and *T2R* in taste buds (Yasuoka *et al.*, 2004; Yoshida *et al.*, 2007), but the specialized gustducin G protein is lost in teleost fish and amphibians (Oka and Korsching, 2011) suggesting that other G proteins are involved in PLCβ2-mediated transduction in zebrafish. An analysis of the complete *Gα* gene repertoire of zebrafish has been performed and showed that only *Gi1b* and *G14a* are expressed in taste buds (Ohmoto *et al.*, 2011; Oka and Korsching, 2011). *T1R* and *T2R* genes are only co-expressed with *Gi1b* but not *G14a* (Ohmoto *et al.*, 2011), suggesting that G14a could function with other unidentified GPCRs. Finally, *PLCβ2* has also been found co-expressed with *TRPM5* in

zebrafish taste buds (Yoshida *et al.*, 2007), suggesting that TRPM5 plays a similar role to that has been described in mammals.

In conclusion, the zebrafish gustatory system seems to share chemosensory properties with the one described in mammals, with different taste receptor cells expressing GPC taste receptors, allowing detection of chemical molecules such as amino acids.

3.3) The solitary chemosensory cells system

The solitary chemosensory cells (SCCs) are isolated receptors cells distributed over the whole body surface within the epidermis (Kotrschal, 1996; Finger, 1997; Kotrschal, Krautgartner and Hansen, 1997). In zebrafish, SCCs have been detected from 3 days post fertilization (Kotrschal, Krautgartner and Hansen, 1997) and possess several small villi. Adult zebrafish possess 1-2 millions of SCCs exhibiting a single larger villus (Kotrschal, Krautgartner and Hansen, 1997). While in mammals SCCs are innervated by trigeminal neurons (Finger *et al.*, 2003; Ohmoto *et al.*, 2008), the innervating neurons in zebrafish are not known.

SCCs have been a cell population of interest in mammals considering their potential role in the detection of noxious stimuli in airway epitheliums, such as the nasal and respiratory epithelia. In mice, SCCs have been found in the nasal respiratory mucosa (Finger *et al.*, 2003), the entrance of the vomeronasal ducts (Ogura *et al.*, 2010) and the laryngeal and tracheal epithelium (Tizzano *et al.*, 2010). In terrestrial animals such as alligator or rodents, SCCs express both T1R and T2R genes (Ohmoto *et al.*, 2008; Lee *et al.*, 2017) and in human, the SCCs express the taste receptors TAS2R4, TAS2R14 and TAS2R46 (Barham *et al.*, 2013). SCCs also express diverse important components of the taste transduction pathway in mammals, such as gustducin, PLCβ2 and TRPM5 (Gulbransen *et al.*, 2008; Tizzano *et al.*, 2011). Mammalian A study in human airway epithelium showed that T2Rs sensitive to bitter substances are expressed in SCCs' motile cilia and that stimulations with bitter compounds such as the denatonium benzoate lead to an increase of intracellular calcium concentration as well as an increase in cilia beat frequency (Shah *et al.*, 2009), suggesting that SCCs could sense noxious substances in the airway and eliminate them by increasing cilia beating frequency. In the last decade, it has been shown that SCCs in mammals are involved in microbial metabolites detection in the airway epithelia. Indeed, SCCs respond to acyl-homoserine lactones serving as quorum-sensing molecules for Gram-negative pathogenic bacteria and evoke changes in respiration indicative of trigeminal

activation (Tizzano *et al.*, 2010). In addition, genetic ablation of Gα-gustducin or TRPM5, described previously as important components of the taste receptor transduction, eliminates the trigeminal response, suggesting that the bacterial detection is mediated by T2Rs (Tizzano *et al.*, 2010). Another study in mice showed that SCCs in the nasal cavity produced nitric oxide after stimulation with acyl-homoserine lactone leading to an increase of mucociliary clearance, a response requiring PLCβ2 and TRPM5 but not Gα-gustducin (R. J. Lee, Chen, *et al.*, 2014). These results are concordant with the role of SCCs in the detection and clearance of Gram-negative bacteria. Nasal SCCs have also been found to cause inflammatory responses in mice after stimulation with denatonium benzoate, a mechanism involving the T2R transduction pathway and the trigeminal fibers innervating the SCCs (Saunders *et al.*, 2014).

In zebrafish, the G alpha proteins Gi1b and G14, which were found in taste buds, as well as PLCβ2, have not been found in zebrafish SCCs (Ohmoto *et al.*, 2011), suggesting another transduction pathway and possibly other receptors than what has been described in mammals. So far, the biological function of SCCs and the receptors involved are not known in zebrafish.

3.4) Are spinal CSF-cNs chemosensory cells forming a novel chemosensory system in the CNS?

The first evidence for a chemosensory role in spinal CSF-cNs came from the observation that pH stimulation of mice spinal CSF-cNs triggered action potentials (Huang *et al.*, 2006). Further analysis in mice showed that spinal CSF-cNs detect both acidic and alkaline pH, through ASICs and PKD2L1 channels, respectively (Orts-Del'Immagine *et al.*, 2012, 2016). Because their apical extensions directly bath into the CSF, we can hypothesize that spinal CSF-cNs can sense pH variations of the CSF itself. Recent evidence in rodents showed that spinal CSF-cNs can also respond to the neuromodulators acetylcholine (Corns *et al.*, 2015; Johnson *et al.*, 2020) and adenosine triphosphate (ATP) (Stoeckel *et al.*, 2003; Johnson *et al.*, 2020), but there is no evidence yet for a physiological relevance.
In other species, lamprey spinal CSF-cNs responded to pH acidification and alkalinization through ASICs and PKD2L1 channels (Jalalvand, Robertson, Tostivint, *et al.*, 2016; Jalalvand, Robertson, Wallén, *et al.*, 2016), confirming what was established in mice. Spinal CSF-cNs also detect acidic pH when protons are directly uncaged in the central canal of zebrafish (unpublished data, Böhm thesis, 2017).

In conclusion, spinal CSF-cNs can sense pH, potentially to detect CSF pH variations. Despite some evidence for detection by spinal CSF-cNs of neuromodulators, the chemosensory role of these neurons remains poorly understood. More investigations are required to decipher the role of spinal CSF-cNs in chemical detection from the CSF.

Aim of the thesis

In summary, in addition to the classical DRG sensory neurons that carry multiple exteroceptive and interoceptive stimuli, spinal CSF-cNs have emerged as a novel interoceptive system in contact with the cerebrospinal fluid in the spinal cord. Spinal CSF-cNs extend an apical extension directly into the central canal, with a motile kinocilium bathing into the CSF, suggesting a sensory role for these cells. Recently, these neurons were found to sense mechanical cues in the spinal cord through ionic channels, and in turn release neuromodulators such as GABA and Somatostatin1.1 to modulate locomotion and posture.
However, little is known about the chemosensory functions of spinal CSF-cNs. While DRG neurons are known to detect various chemical stimuli like irritant or pungent molecules but also bacterial metabolites, spinal CSF-cNs' chemosensory relevance is unclear. Spinal CSF-cNs detect pH variations and neuromodulators like acetylcholine and ATP, suggesting that these neurons could sense other chemical molecules, potentially directly from the CSF. These molecules could be neurotransmitters and neuropeptides as it is known that CSF contains many bioactive molecules, but it could also be pathogens infecting the CSF (like in meningitis) since such detection has been described in skin and gut for the DRG neurons.
Therefore, I tackled the following questions during my PhD: What are the chemical cues that spinal CSF-cNs sense in the CSF? And what is the physiological relevance of chemosensation in CSF-cNs? To answer these questions, I needed to test the response of spinal CSF-cNs to different chemical molecules. However, testing chemical cues on spinal CSF-cNs *in vivo* is challenging due to the location of spinal CSF-cNs deep in the spinal cord tissue. It is therefore difficult to ensure that a molecule reaches the central canal to be in contact with the spinal CSF-cNs, and to monitor the exact concentration of molecules sensed by spinal CSF-cNs. To tackle the question of chemosensory properties of spinal CSF-cNs, my aims during my PhD were the following:

1) To develop primary cell cultures of spinal CSF-cNs to overcome the technical difficulties of investigations *in vivo*
2) To analyze the transcriptome of CSF-cNs to find receptors for chemical cues

3) To test the responses *in vitro* of spinal CSF-cNs to chemical cues that are agonists to the receptors found in transcriptomic analysis

4) To investigate if spinal CSF-cNs can also respond to chemical cues released by bacterial pathogens, as it was recently reported in DRG nociceptors

Chapter I: Development of a novel protocol for primary cell cultures of spinal CSF-cNs

As explained in the introduction, our team and others have shown in the last decade that spinal CSF-cNs form an interoceptive system in the spinal cord detecting mechanical stimuli to modulate locomotion. Chemosensory functions of these cells have been proposed early on by noticing the expression of the receptor PKD2L1 and exploring the responses of CSF-cNs to changes in pH and osmolarity (Huang *et al.*, 2006; Orts-Del'Immagine *et al.*, 2012; Jalalvand *et al.*, 2018). However, the extent and physiological roles of such chemosensory functions in CSF-cNs remain poorly understood. I developed a protocol of primary cultures together with chemical stimulation in order to investigate this question in controlled conditions.

Spinal CSF-cNs sense acidic and basic pH in mice (Orts-Del'Immagine *et al.*, 2012, 2016), lamprey (Jalalvand, Robertson, Tostivint, *et al.*, 2016; Jalalvand, Robertson, Wallén, *et al.*, 2016) and zebrafish (unpublished data, Böhm, 2017), as well as acetylcholine (Corns *et al.*, 2015; Johnson *et al.*, 2020) and ATP (Stoeckel *et al.*, 2003; Johnson *et al.*, 2020) in mice, but more investigations are required to decipher the chemosensory physiological role of spinal CSF-cNs. Considering their apical extension directly bathing into the CSF, we can hypothesize that spinal CSF-cNs chemosensory role consists in sensing the CSF content and that in turn release biomolecules directly in the CSF or at their axonal synapses.
In vivo, it is difficult to reach the spinal CSF-cNs as they are located deep in the spinal cord tissue and it is never clear whether a cell responds to the chemical cue directly or to the subsequent release of chemical cues from other cells. For example, the calcium activity of ventral spinal CSF-cNs has been reported to be restored *in vivo* in *scospondin* mutants defective for the Reissner fiber after CSF injections of the monoamines epinephrine and norepinephrine (Cantaut-Belarif *et al.*, 2020), but what was the concentration of the cues onto the CSF-cNs? And do these cells respond directly to the monoamines or indirectly via other cells? In the study by (Cantaut-Belarif *et al.*, 2020), chemical molecules were injected into the hindbrain ventricle using a thin pipette, and spinal CSF-cNs were image 20 to 60 minutes after hindbrain ventricle injection (Cantaut-Belarif *et al.*, 2020). As chemical molecules reach spinal CSF-cNs through the CSF circulation from the brain ventricles to the central canal of the spinal cord, one technical challenge with this technique is the control of the concentration of molecules sensed by the spinal CSF-cNs. The concentration of chemical

molecules inside the injection pipette does not correspond to the final concentration sensed by the spinal CSF-cNs, the molecule being diluted and transported into the CSF before reaching the spinal CSF-cNs. Another major problem is the specificity of the response to the stimulus. Spinal CSF-cNs activation observed after CSF injection of monoamines could be indirect and come from the effect of the monoamines on other targets than CSF-cNs in the spinal cord.

To investigate the chemosensory properties of spinal CSF-cNs, I developed an approach enabling the direct stimulation of spinal CSF-cNs with chemical cues and the observation of subsequent calcium responses in zebrafish. Primary sensory cultures of spinal CSF-cNs allow overcoming these issues by stimulating directly the spinal CSF-cNs with a pipette close to the cells. It allows controlling the concentration of chemicals sensed by the spinal CSF-cNs, as well as to observe spinal CSF-cNs responses to direct activation. In a first attempt, (Böhm *et al.*, 2016) developed a primary cell culture protocol of CSF-cNs by euthanizing 4 days post fertilization (dpf) *Tg(pkd2l1:GCaMP5G ; pkd2l1:TagRFP)* larvae and dissociating zebrafish cells with a solution of papain according to an existing protocol for goldfish retinal bipolar cells isolation (Joselevitch and Zenisek, 2009). Larval dissociated cells were plated in artificial CSF (aCSF) solution onto plastic petri dishes, the spinal CSF-cNs were identified based on their GCaMP5G/TagRFP fluorescence and imaged three hours after plating. This protocol was first developed to investigate the cilia beating of spinal CSF-cNs *in vitro* but is not suited for calcium imaging after chemical stimulation. Cells were plated in aCSF solution, a buffer solution that is not optimized for neuron survival, and therefore spinal CSF-cNs could be imaged only a few hours after plating. This period is too short to allow a proper differentiation of spinal CSF-cNs, in particular with the regrowth of their axonal extensions. In addition, in this protocol, spinal CSF-cNs were plated on a plastic surface that was not pre-coated with molecules such as Poly-L-lysine or Laminin, facilitating cell adherence to the surface.

Recently, (Sternberg *et al.*, 2018) developed in collaboration with Patrick Delmas' lab in Marseille a primary cell culture protocol of spinal CSF-cNs to investigate their response to direct mechanical stimulation on the plasma membrane. Here the chorion, yolk, head and caudal tail of embryos were removed and cells were dissociated in collagenase type IA solution for 45 minutes and plated on glass coverslips pre-coated with Laminin and Poly-Lysine in complemented Dulbecco's modified Eagle's medium (DMEM). *Tg(pkd2l1:TagRFP)* dissociated cells were plated on top of a feeder layer of spinal cord cells from 2 dpf embryos to improve adherence of the spinal CSF-cNs. Whole-cell recording of spinal *Tg(pkd2l1:TagRFP)* CSF-cNs was made after one day of plating, allowing proper differentiation for the cells. However, this original protocol is highly prone to biological contaminations by bacteria or yeasts, among others, as there is no decontamination of

embryos. Zebrafish eggs are fertilized externally, thus they are exposed to contaminants from the water, such as dejections from the parents, leading to potential contaminations when embryos are dissociated and plated in culture medium. In addition, the collagenase type IA dissociation lasts for 45 minutes, a long time required for dissociating all the tissues, but too-long dissociation can cause unwanted cell death. We therefore decided to use another dissociating enzyme preserving the proper dissociation of tissues, but with a shorter time of incubation to reduce potential cell death. DMEM used for cell plating of the two layers of cells is a general medium supporting the growth of different types of cells such as primary fibroblasts, neurons, glial cells or smooth muscle cells (according to Invitrogen information). This medium is ideal for the feeder layer to allow every type of cell to grow, but not specialized for the growing of neuronal cells for the plating of the second layer of cells. Thus, a medium specialized in neuronal growth such as the Neurobasal could be used instead of the general DMEM medium for the second layer of *Tg(pkd2l1:TagRFP)* cells, for which we want to promote the development of spinal CSF-cNs.

Thus, I adapted the primary cell culture protocol from (Böhm *et al.*, 2016) and (Sternberg *et al.*, 2018) to develop a novel two layers primary cell culture protocol avoiding contamination and optimizing culture medium and digestion enzyme to obtain spinal CSF-cNs ready for stimulation and calcium imaging (**Figure 1A**).

1) Optimization of a new primary cell culture protocol of spinal CSF-cNs

1.1) Preparations prior to cell culture

Pre-coating with Laminin and Poly-L-Lysine. Pre-coating was essential to ensure proper fixation of spinal CSF-cNs on the glass surface. (Sternberg *et al.*, 2018) used directly pre-coated glass coverslips (Dutscher, 354087). In our protocol, pre-coating was done manually by incubation of glass coverslips with a pre-coating solution composed of Laminin and Poly-L-Lysine for 24 hours, the pre-coating solution being removed prior to cell culture.

Bleaching of the embryos. Implementation of a decontamination step was critical to avoid contaminations. Bleaching of embryos consisted of 5 minutes incubation of 1 dpf embryos into diluted bleach (0.003% in reverse osmosis water) followed by 5 minutes of incubation into reverse osmosis water to rinse the bleach. These two 5 minutes' incubations were repeated two times. Then, bleached embryos were placed into plastic petri dishes filled with

sterile water complemented with methylene blue at 0.00005% (an antiseptic playing a fungicide and antibacterial role) to maintain the embryo's sterility.

Dechorionation of embryos. Dechorionation of 2 dpf embryos occurred prior to cell culture, to ensure that embryos are accessible for proper enzymatic tissue digestion. Incubation in pronase enzyme is commonly used for dechorionation, as it makes chorions brittle and easier to remove with gentle swishing (Westerfield, 2000). However, a too-long exposition of embryos to pronase enzyme can lead to embryonic tissue degradation. To ensure proper embryonic tissue integrity, we dechorionated manually the embryos using fine forceps under a hood to maintain embryos sterility.

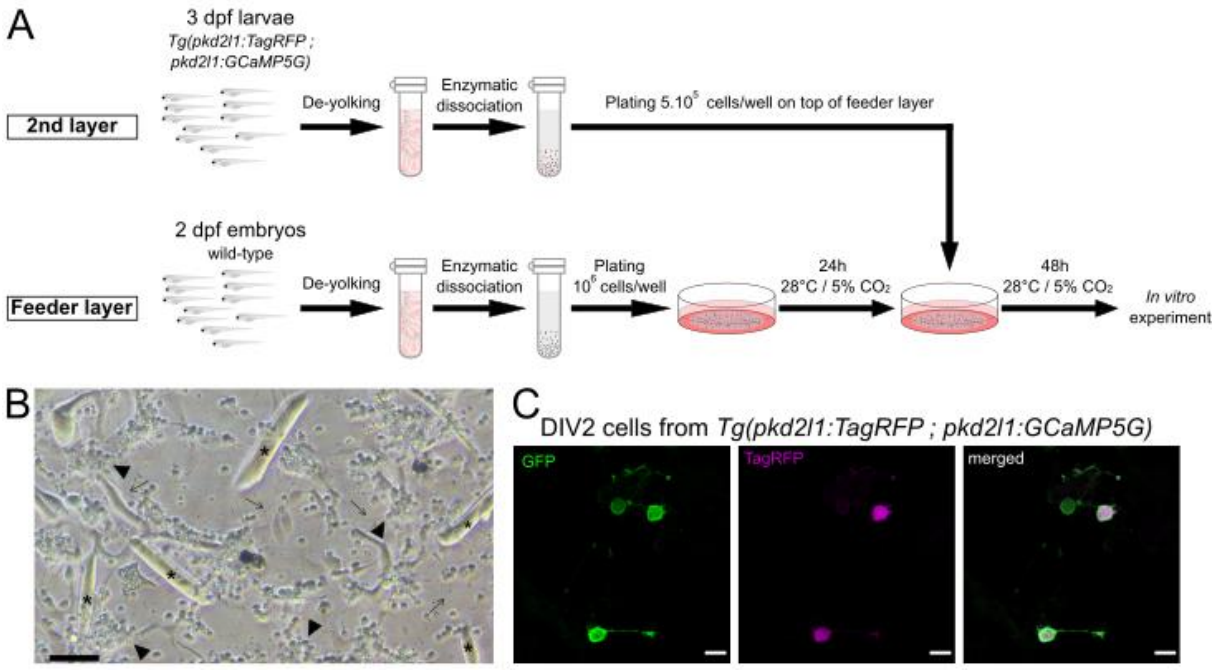

Figure 1. Primary cell culture protocol of spinal CSF-cNs. (A) General protocol of primary cell culture protocol of spinal CSF-cNs. Bottom: feeder layer of cells from wild-type embryos; Top: the second layer of cells from *Tg(pkd2l1:GCaMP5G ; pkd2l1:TagRFP)*. Cells are used at day *in vitro* 2 after second layer plating for *in vitro* experiments. **(B)** Light transmitted image of DIV2 primary cell culture of spinal CSF-cNs. *: striated myocytes, arrowheads: clusters of cells extending processes, arrows: visible processes. **(C)** Immunocytochemistry of spinal CSF-cNs in vitro from *Tg(pkd2l1:GCaMP5G ; pkd2l1:TagRFP*), extending processes. The top left cell is GFP positive only.

1.2) Initial feeder layer of wild-type zebrafish cells

After dechorionation, 2 dpf wild-type (WT) embryos were de-yolked by gentle trituration in de-yolking buffer (55 mM NaCl, 1.8 mM KCl, 1.25 mM $NaHCO_3$ in sterile water). De-yolked

embryos were dissociated in papain at 20U/mL in Hanks' Balanced Salt Solution (HBSS) 1X solution, complemented with 0.2 mg/mL cysteine, 1.25 µM $CaCl_2$, 0.5 µM EDTA and 2 µM NaOH at 37º for 20 minutes. Compared to collagenase type IA (Sternberg *et al.*, 2018), papain enzyme from (Böhm *et al.*, 2016) allowed a proper dissociation of embryonic tissues in a reduced amount of time (20 minutes for papain vs. 45 minutes for collagenase type IA) to not induce unwanted cell death. Dissociated cells were rinsed with HBSS 1X and filtrated using 30 µm filters to remove not dissociated cells and aggregates. Cells were counted and plated overnight at 28°C / 5% CO_2 at a concentration of 1.10^6 cells/well in DMEM medium complemented with 2mM L-Glutamine, 50U/mL penicillin/streptomycin, 25ng/mL NGF, 4ng/mL GDNF, 25mM glucose and 10% FBS, to promote the growth of all types of cells (**Figure 1A**).

1.3) Second layer of fluorescently labeled spinal CSF-cNs

3 dpf *Tg(pkd2l1:GCaMP5G ; pkd2l1:TagRFP)* larvae (Böhm *et al.*, 2016) were used for the second layer of cells, allowing identification of the spinal CSF-cNs among other cells through TagRFP and GCaMP5 fluorescence. The same protocol than feeder layer was used for dissociating transgenic larvae (**Figure 1A**), except:

- 20 minutes papain tissue dissociation of 3 dpf larvae can be less efficient compared to 2 dpf embryos, particularly for the eye tissue. To bypass this issue, dissociation can be extended to 25 minutes to completely dissociate the eyes. Filtering of the cells after dissociation ensures to get rid of all the potential not dissociated eyes that would remain. However, 20 minutes of papain incubation is sufficient to dissociate the entire trunk of the larvae, where the spinal CSF-cNs reside.

- Culture medium was changed from basal DMEM used in (Sternberg *et al.*, 2018) for a medium specialized in growth and maintenance of neuronal cells, the Neurobasal medium, complemented with 1X B27 supplement, 1X N2 supplement, 2 mM L-glutamine, 10 U/mL penicillin/streptomycin, decomplemented FBS and 1 mM sodium pyruvate.

- Cells were plated overnight at 28°C / 5% CO_2 at a concentration of 5.10^5 cells/well on top of the feeder layer, for not to end up with too many cells on the coverslips.

One day *in vitro* (DIV-1) after second layer plating, the culture medium was renewed by replacing 1/3 of the volume of culture medium with fresh Neurobasal complemented medium.

To allow spinal CSF-cNs to grow and develop, coverslips were used at DIV2 after second layer plating for calcium imaging, electrophysiology and immunostaining.

At DIV-2, primary cultures were composed of cells from the entire zebrafish organism (**Figure 1B**), in which we can recognize striated myocytes, as well as clusters of cells extending processes (**Figure 1B**). Spinal CSF-cNs were identified through their GCaMP5G and TagRFP fluorescence (**Figure 1C**). After two days of maturation, spinal CSF-cNs were able to extend processes (**Figure 1C**), suggesting that Neurobasal complemented medium was efficient to promote neuronal growth.

2) Electrophysiological properties of spinal CSF-cNs *in vitro*

To determine whether spinal CSF-cNs conserved their electrophysiological properties *in vitro* after dissociation, we compared whole-cell patch-clamp recording of spinal CSF-cNs *in vitro*, versus *in vivo* using *Tg(pkd2l1:GAL4 ; UAS:GFP)* or *Tg(pkd2l1:GAL4 ; UAS:mCherry)* transgenic fish to identify the spinal CSF-cNs. This work was done in collaboration with the electrophysiologist Dr. Adeline Orts-Del'Immagine in the lab.

2.1) *In vitro* spinal CSF-cNs exhibit characteristic high membrane resistance

Investigating the passive properties of spinal CSF-cNs in culture, we found that spinal CSF-cNs conserved a high membrane resistance (> 1 GΩ) similar than *in vivo* (**Figure 2A**) (12.5 ± 4.8 GΩ *in vitro* versus 8.2 ± 1.4 GΩ *in vivo*, $p > 0.05$). High membrane resistance is characteristic of spinal CSF-cNs in zebrafish (Sternberg *et al.*, 2018; Orts-Del'Immagine *et al.*, 2020), mice (Orts-Del'Immagine *et al.*, 2012; Corns *et al.*, 2015) and turtle (Russo *et al.*, 2004; Reali *et al.*, 2011). However, spinal CSF-cNs in culture showed higher membrane capacitance compared to *in vivo* (**Figure 2B**) (3.3 ± 0.5 pF *in vitro* versus 1.6 ± 0.2 pF *in vivo*, $p = 0.0063$), suggesting that spinal CSF-cNs *in vitro* are larger than *in vivo* as total membrane capacitance is directly proportional to the membrane surface area. A larger size could be due to less mechanical constraints in culture compared to *in vivo*, as spinal CSF-cNs *in vivo* are located into the ependymal radial glial cells in zebrafish. Further investigations are required to estimate the spinal CSF-cNs size and morphology *in vitro*.

2.2) Spinal CSF-cNs showed phasic and tonic firing *in vitro*

Two physiological types of spinal CSF-cNs have been observed in fish (Orts-Del'Immagine *et al.*, 2020), turtle (Russo *et al.*, 2004; Reali *et al.*, 2011) and rodents (Orts-Del'Immagine *et al.*, 2012, 2016; Petracca *et al.*, 2016b): one displayed tonic firing while the other showed phasic firing. Upon current injection, we found that recorded spinal CSF-cNs *in vitro* exhibited phasic firing (**Figure 2C top**) as well as tonic firing (**Figure 2C bottom**). Thus, we found that the firing properties of spinal CSF-cNs in culture are conserved.

2.3) Spinal CSF-cNs conserved their channel opening properties *in vitro*

One of the main functional properties of CSF-cNs is the presence of unitary currents due to single PKD2L1 channel openings that is observable in whole-cell patch-clamp recording (Orts-Del'Immagine *et al.*, 2012; Jalalvand *et al.*, 2018; Sternberg *et al.*, 2018). We found that *in vitro* spinal CSF-cNs exhibit spontaneous channel openings with similar mean channel opening probability (0.015 ± 0.004 *in vitro* versus 0.025 ± 0.015 *in vivo*, $p > 0.05$) and mean unitary current amplitude (-17.0 ± 1.7 pA *in vitro* versus -13.7 ± 0.2 pA *in vivo*, $p > 0.05$) than *in vivo* (**Figure 2D-F**). It is important to notice that we used different internal and external solutions for *in vitro* and *in vivo* recordings affecting the driving force of ions which does not allow a real comparison of current amplitude. However, the main ion affected is the chloride (E_{cl} = -53.9 *in vitro* versus E_{cl} = -0.8 *in vivo*), which is not involved in PKD2L1 channel current, and explains that we found a comparable mean current amplitude *in vitro* and *in vivo*. Similar mean current amplitude (-18.6 ± 0.3 pA in CSF-cNs from control siblings) has been found in a study investigating channel opening properties of spinal CSF-cNs *in vivo* that used a similar internal solution as we used in our experiment in culture (Orts-Del'Immagine *et al.*, 2020). Altogether, these results showed that PKD2L1 channel opening and amplitude of spinal CSF-cNs are comparable *in vivo* and in culture. The mean duration of a single opening is significantly longer *in vitro* compared to *in vivo* (3.2 ± 0.3 ms *in vitro* versus 0.7 ± 0.1 ms *in vivo*, $p = 0.0013$) (**Figure 2G**). In the study investigating channel opening properties of spinal CSF-cNs *in vivo*, they found a mean duration of a single opening of 3.7 ± 0.5 ms (Orts-Del'Immagine *et al.*, 2020), which was similar to what we found *in vitro*. In mice slice preparations, spinal CSF-cNs single-channel analysis showed channel opening properties of the same range as *in vitro* zebrafish spinal CSF-cNs, with a mean channel opening probability of 0.028 ± 0.004 and a mean unitary current amplitude of -11.6 ± 0.4 pA (Orts-Del'Immagine *et al.*, 2012). Altogether, our results suggested that spinal CSF-cNs *in vitro*

conserved functional channels. More recordings are necessary to know if the longer mean duration of single openings *in vitro* is real and significant.

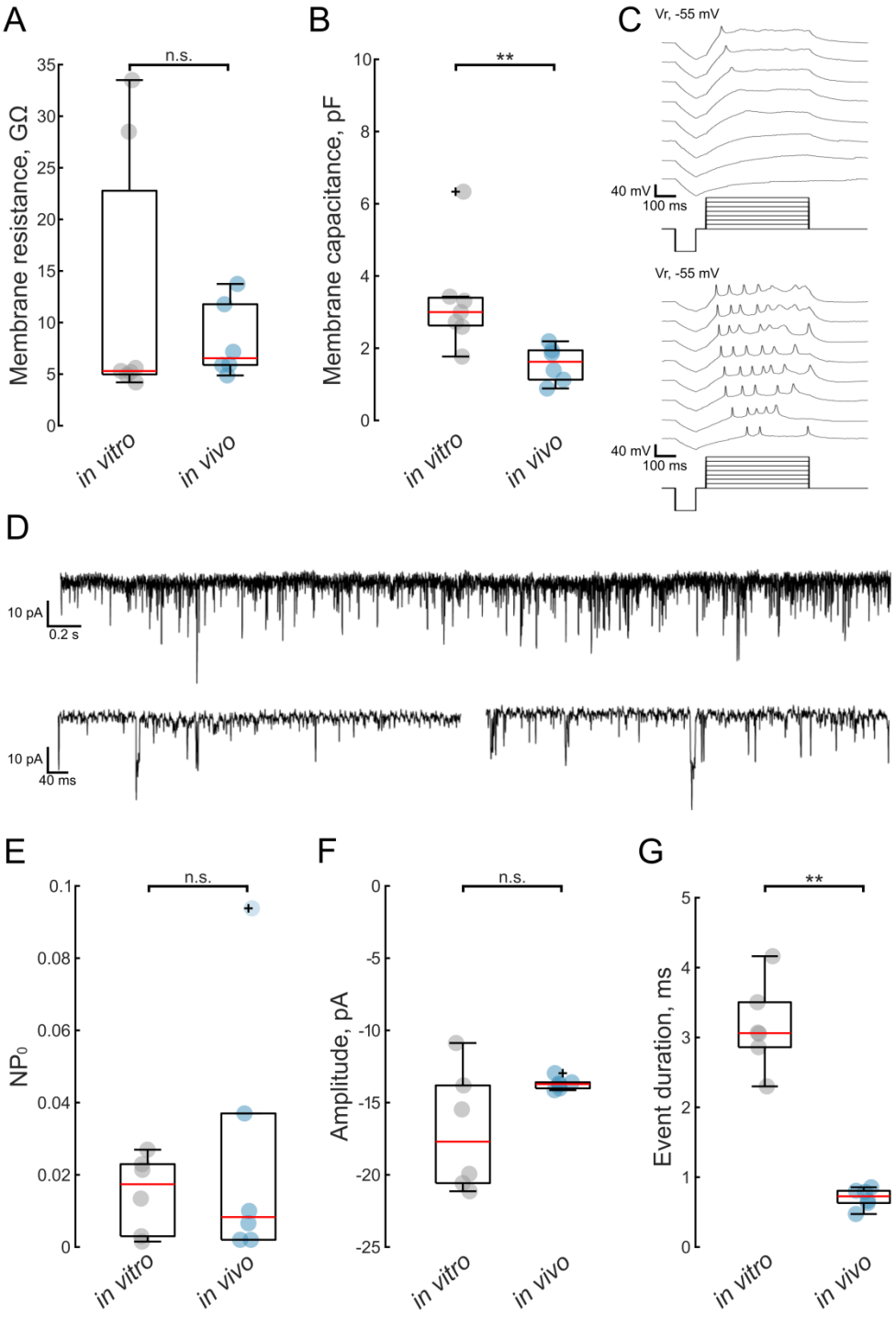

Figure 2. Spinal CSF-cNs *in vitro* conserved their electrophysiological properties. (A-B) Quantification of spinal CSF-cN basic intrinsic electrophysiological properties *in vitro* and *in vivo*. **(A)** Spinal CSF-cN membrane resistance is similar *in vitro* compared to *in vivo* (mean membrane resistance = 12,5 ± 4,8 GΩ *in vitro* versus 8,2 ± 1,4 GΩ *in vitro*; two-sample Kolmogorov-Smirnov test;

p > 0.05; ks2stat = 0.548; n = 7 cells *in vitro*; n = 6 cells *in vivo*). **(B)** Spinal CSF-cN membrane capacitance is higher *in vitro* compared to *in vivo* (mean membrane capacitance = 3,3 ± 0,5 pF, n = 7 cells *in vitro* versus 1,6 ± 0,2 pF, n = 6 cells *in vivo*; two-sample Kolmogorov-Smirnov test; p = 0.0063; ks2stat = 0.857). **(C)** Discharge of action potential in spinal CSF-cNs recorded *in vitro* in CC-mode in response to successive current steps. Top: single action potential (phasic firing) (500-ms-long pulses from 0 pA to 14 pA in 2-pA increments). Bottom: repetitive action potentials (tonic firing) (500-ms-long pulses from 0 pA to 14 pA in 2-pA increments) **(D)** *In vitro* whole-cell patch-clamp recording of spinal CSF-cNs in voltage clamp (VC) mode targeted for TagRFP in cells from *Tg(pkd2l1:GCaMP5G ; pkd2l1:TagRFP*) exhibits single channel opening. Bottom traces represent a higher magnification from the top trace. **(E-G)** Unitary currents reflecting spontaneous channel opening properties. **(E-F)** Channel opening probability and amplitude of spinal CSF-cNs *in vitro* are similar to *in vivo* (mean NP0 = 0,015 ± 0,004 *in vitro* versus 0,025 ± 0,015 *in vivo*; two-sample Kolmogorov-Smirnov test, p > 0.05, ks2stat = 0.333; mean unitary current amplitude = -17,0 ± 1,7 pA *in vitro* versus -13,7 ± 0,2 pA *in vivo*, p > 0.05, ks2stat = 0.667). **(G)** Mean duration of single opening is higher in spinal CSF-cNs *in vitro* compared to *in vivo* (mean duration of single opening = 3,2 ± 0,3 ms *in vitro* versus 0,7 ± 0,1 ms *in vivo*, p = 0.0122, ks2stat = 0.833). n = 6 cells *in vitro* and *in vivo*. Each data point represents one recording from one cell; plots use median as measure of central tendency (central mark on the boxplot in red), and the bottom and top edges of the box indicate the 25th and 75th percentiles. The whiskers extend to the most extreme data points without considering outliers, and the outlier is identified with a + symbol.

3) Molecular characterization of spinal CSF-cNs *in vitro*

After validating electrophysiological properties of spinal CSF-cNs *in vitro*, we investigated their molecular identity. Immunohistochemistry (IHC) studies showed that spinal CSF-cNs are GABAergic in species such as turtle (Reali *et al.*, 2011), eel and trout (Roberts *et al.*, 1995), African clawed frog (Dale *et al.*, 1987; Binor and Heathcote, 2001), rat (Barber, Vaughn and Roberts, 1982; Stoeckel *et al.*, 2003), dogfish (Sueiro *et al.*, 2004), lamprey (Christenson *et al.*, 1991; Jalalvand, Robertson, Tostivint, *et al.*, 2016), macaque and mice (Djenoune *et al.*, 2014), and zebrafish (Bernhardt *et al.*, 1992; Higashijima, Mandel and Fetcho, 2004; Higashijima, Schaefer and Fetcho, 2004; Wyart *et al.*, 2009; Yang, Rastegar and Strähle, 2010; Djenoune *et al.*, 2014). Thus, we tested if spinal CSF-cNs *in vitro* conserved their GABAergic identity by conducting immunocytochemistry (ICC) on cells from *Tg(pkd2l1:GCaMP5G ; pkd2l1:TagRFP)* larvae. We looked at co-labeling of GCaMP5G with GABA, and found that GABA is still enriched in spinal CSF-cNs soma and extended processes (**Figure 3A**).

In addition, PKD2L1 has been described as a specific marker of spinal CSF-cNs in mice (Huang *et al.*, 2006; Djenoune *et al.*, 2014; Orts-Del'Immagine *et al.*, 2016), macaque (Djenoune *et al.*, 2014), or zebrafish (Djenoune *et al.*, 2014; Sternberg *et al.*, 2018; Orts-Del'Immagine *et al.*, 2020). In these studies, PKD2L1 was found enriched in the apical extension of spinal CSF-cNs. ICC co-labeling of GCaMP5G and Pkd2l1 revealed that spinal CSF-cNs *in vitro* also express Pkd2l1 in the soma (**Figure 3B**). A better resolution for Pkd2l1 staining is required to decipher its cellular pattern of expression.

Altogether, our results showed that spinal CSF-cNs conserved their molecular identity and express GABA and Pkd2l1 molecular markers. More investigations are required to determine whether spinal CSF-cNs *in vitro* express other molecular markers, such as PKD1L2 (England *et al.*, 2017) or markers of immure neurons like NKX6.1, HuC/D, PSA or DCX (Stoeckel *et al.*, 2003; Russo *et al.*, 2004; Marichal *et al.*, 2009; Reali *et al.*, 2011; Kútna *et al.*, 2014; Orts-Del'Immagine *et al.*, 2014).

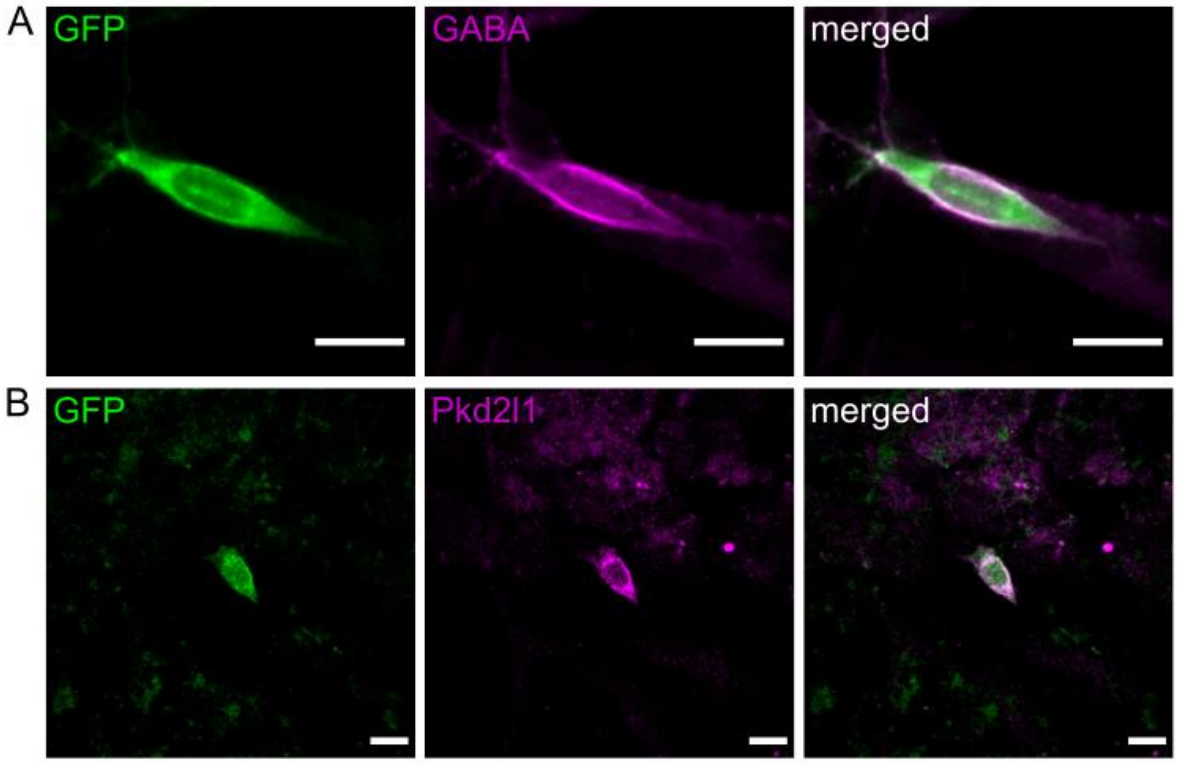

Figure 3. Spinal CSF-cNs *in vitro* conserve their molecular identity. (A) Immunocytochemistry for GFP and GABA in DIV2 cells from *Tg(pkd2l1:GCaMP5G ; pkd2l1:TagRFP*) larvae shows that GABA neurotransmitter is localized in CSF-cN cell body and extend processes. **(B)** Immunocytochemistry for GFP and Pkd2l1 in DIV2 cells from *Tg(pkd2l1:GCaMP5G ; pkd2l1:TagRFP*) larvae shows that Pkd2l1 protein is localized in CSF-cN cytoplasm. Scale bars: 10 µm.

Conclusion and perspectives

Altogether, I succeeded in adapting an existing spinal CSF-cNs primary cell culture protocols (Böhm *et al.*, 2016; Sternberg *et al.*, 2018) to develop a novel protocol to investigate the chemosensory properties of mature spinal CSF-cNs. Notably, prior to cell culture, I incorporated a crucial step of embryos bleaching avoiding contamination issues. I reduced the dissociation duration using the papain enzyme to ensure a proper dissociation in a reduced amount of time to maintain cell viability. DMEM medium was replaced by Neurobasal complemented medium promoting neuronal cell growth and maintenance, allowing spinal CSF-cNs to extend processes within two days after plating. Spinal CSF-cNs *in vitro* are extremely resistive and conserved their electrophysiological properties, except for membrane capacitance that was higher, suggesting larger spinal CSF-cNs *in vitro*. Spinal CSF-cNs exhibited both tonic and phasic firing, as it has been described in zebrafish, rodents or turtle. Finally, we confirmed with immunocytochemistry that spinal CSF-cNs expressed PKD2L1 and GABA *in vitro* recapitulating what has been found in various species, suggesting that they conserved their molecular identity.

In the future, more cell recordings will be required *in vitro* and *in vivo* to consolidate our results on electrophysiological properties of spinal CSF-cNs, in particular for channel opening duration and amplitude as well as firing properties, as we did not manage to record spinal CSF-cNs with phasic firing *in vitro* yet. Using immunostaining, we could look for other markers of spinal CSF-cNs such as PKD1L2, which is co-expressed with PKD2L1 in zebrafish (England *et al.*, 2017), or markers of immature neurons that have been found expressed in spinal CSF-cNs. In addition, it would be of first interest to dig into the morphology of spinal CSF-cNs *in vitro*, to assess if they conserved an apical extension, and a motile cilia as was the case with (Böhm *et al.*, 2016) protocol; or to investigate their size as membrane capacitance analysis suggested that spinal CSF-cNs are larger *in vitro*. To do so, we could use a cell membrane marker, such as the BODIPY, to label and image spinal CSF-cNs cell membranes.

In summary, my novel primary cell culture protocol succeeded to form functional spinal CSF-cNs that can be stimulated to decipher their chemosensory properties. This primary cell culture protocol is essential for the chemosensory investigations on spinal CSF-cNs presented in Chapters II and III.

Methods

Cell culture protocol

Embryos preparation prior to cell culture. Eggs from wild-type (WT) and *Tg(pkd2l1:GCaMP5G ; pkd2l1:TagRFP)* incrosses were collected in clean petri dishes using fresh blue water (reverse osmosis water with methylene blue at 0.00005%). To avoid contamination, we ensure that embryos density never exceeds 75 embryos per petri dish, the ideal density being around 50 embryos. Before decontamination, positive embryos as well as WT embryos were rinsed one time with fresh blue water. To sterilize the embryos and avoid contamination, eggs were bleached at room temperature under a laminar flow hood. To do so, eggs were collected in a strainer and dipped in a beaker filled with a bleach solution (0.003% bleach in reverse osmosis water sterilized at 121°C for 20 minutes) for five minutes, immediately followed by five minutes in another beaker filled with reverse osmosis water (sterilized at 121°C for 20 minutes) to rinse eggs. Those two steps were performed two times in a row for a total bleaching protocol of 20 minutes. After bleaching, embryos were placed into sterile blue water (sterilized at 121°C for 20 minutes) and raised at 28.5°C.

Pre-coating of glass coverslips. The day prior to cell culture, 12 mm glass coverslips (Karl Hecht™, 41001112) were pre-coated to enhance cell attachment on the coverslips. Coverslips were incubated into a coating solution composed of a mix of Poly-L-lysine hydrobromide (Sigma, P2636-25MG) at 20µg/mL, and laminin (SIGMA, L2020-1MG) at 40µg/mL, for 24 hours at 28°C / 5% CO_2.

Initial feeder layer of cells. Prior to cell culture, WT embryos were manually dechorionated at 2 dpf under a hood using fine forceps (Dumont #5 Fine tips forceps, #11254-20 Fine Science Tools). WT dechorionated embryos were euthanized at 2 dpf by an overdose of 0.2 % (w/v) tricaine (MS-222; Sigma, A5040), and immediately placed in ice. Yolks of the larvae were removed by short incubation into a de-yolking buffer (NaCl 55 mM, KCl 1.8mM, $NaHCO_3$ 1.25mM, in sterile water), followed by gentle mechanical trituration to completely remove the yolk. After one rinse with HBSS 1X (Fisher Scientific, 14170088), enzymatic dissociation was performed using papain at 20 U/mL (Serlabo Technologies, LS003124) in HBSS 1X solution complemented with 0.2 mg/mL cysteine (Sigma, 30089), 1.25 µM $CaCl_2$ (Sigma, C3306), 0.5 µM EDTA (Sigma, E5134), and 2 µM NaOH (Sigma, 71687), at 37ºC for 20 minutes, followed by 20 gentle mechanical triturations using a P1000 pipette to complete the dissociation. Dissociated cells were centrifuged for ten minutes at 1000 rotations per minute (rpm) and papain mix supernatant was removed. Cell pellets were rinsed one time with HBSS 1X followed by a filtration using 30 µM filters (MACS SmartStrainers, 130-098-458) in order to

remove the not dissociated aggregates. Then, HBSS 1X supernatant was removed by centrifuging ten minutes at 1000 rpm, and DMEM medium (ThermoFisher, 10938025) complemented with 2mM L-Glutamine (Thermo Fisher Scientific, 25030024), 50U/mL penicillin/streptomycin (Thermo Fisher Scientific, 15140122), 25ng/mL NGF (Merckmillipore, 01-125), 4ng/mL GDNF (Fisher Scientific, 10679963), 25mM glucose (SIGMA, G8769-100ML), 10% FBS (Thermo Fisher Scientific, 10270106) was added. Cells were plated on pre-coated 12mm glass coverslips at a concentration of 1.10^6 cells per well and put at 28°C / 5% CO_2 overnight.

Second layer of cells from transgenic larvae. Euthanasia, de-yolking, enzymatic dissociation and filtration are identical to what was previously described in the initial feeder layer of cells, except that dissociation duration can be extended to 25 minutes to fully dissociate larvae. Filtrated cells were centrifuged for ten minutes at 1000 rpm to remove the HBSS 1X supernatant, and Neurobasal medium (Thermo Fisher Scientific, 10888022) complemented with 1X B27 (Thermo Fisher Scientific, 17504044), 1X N2 (Thermo Fisher Scientific, 17502001), 2mM L-glutamine (Thermo Fisher Scientific, 25030024), 10U/mL penicillin/streptomycin (Thermo Fisher Scientific, 15140122), 5% FBS (Thermo Fisher Scientific, 10270106) and 1X sodium pyruvate (Thermo Fisher Scientific, 11360039) was added. DMEM complemented medium from the initial layer of cells was carefully removed, and the cells in Neurobasal complemented medium were immediately plated on top of the feeder layer of cells, at 5.10^5 cells per well concentration, and put at 28°C / 5% CO_2 overnight. One day after the second layer plating, 1/3 of the culture medium was renewed with fresh Neurobasal complemented. Cells were used two days after the second layer plating.

Use of transgenic lines

Allele name	Transgenic	Reference	Identifier
icm17	*Tg(pkd2l1:tagRFP)*	(Böhm *et al.*, 2016)	ZFIN: ZDB-ALT-160119-8
icm07	*Tg(pkd2l1:GCaMP5G)*	(Böhm *et al.*, 2016)	ZFIN: ZDB-ALT-160119-4
icm10	*Tg(pkd2l1:GAL4)*	(Fidelin *et al.*, 2015)	ZFIN: ZBD-ALT-150324-1
/	*Tg(UAS:mCherry)*	(Robles, Laurell and Baier, 2014)	ZFIN: ZDB-ALT-130702-1

***In vitro* patch-clamp recording**

Whole-cell recordings were performed in aCSF (NaCl 140mM (Sigma, S7653), KCl 1mM (Sigma, P9333), $CaCl_2$ 2.5mM (Sigma, 223506), $MgCl_2$ 1mM (Sigma, M2670), HEPES 10mM (Sigma, H3375), D-(+)-Glucose 10mM (Sigma, G8270), diluted in MilliQ water; pH was adjusted at 7.4, 290 $mOsm.kg^{-1}$ on DIV2 spinal CSF-cNs from *Tg(pkd2l1:TagRFP ; pkd2l1:GCaMP5G)* transgenic larvae for second layer. A Multi-Clamp 700B amplifier, a Digidata series 1440 A Digitizer, and pClamp 10.3 software (Axon Instruments, Molecular Devices, San Jose, California, USA) were used for acquisition. Raw signals were acquired at 50 kHz and low-pass filtered at 10 kHz. Patch pipettes (1B150F-4, WPI) with a tip resistance of 5–8MΩ were filled with internal solution (concentrations in mM: K-gluconate 115, KCl 15, $MgCl_2$ 2, Mg-ATP 4, HEPES-free acid 10, EGTA 5, 290 mOsm/L, pH adjusted to 7.4 with KOH; Alexa 488 40 mM). Holding potential was -85 mV, away from the calculated chloride reversal potential (E_{Cl} = - 53.9 mV).

***In vivo* patch-clamp recording**

Whole-cell patch-clamp recordings were performed in aCSF (NaCl 134mM, KCl 2.9mM, $MgCl_2$ 1.2mM, HEPES 10mM, glucose 10mM and $CaCl_2$ 2.1mM; 290 mOsm.kg-1, adjusted to pH 7.7–7.8 with NaOH) on *Tg(pkd2l1:GAL4;UAS:mCherry)* and *Tg(pkd2l1:GAL4;UAS:GFP)*. Larvae were pinned through the notochord with 0.025mm diameter tungsten pins. Skin and muscle from two to three segments around segment 10 were dissected out using a glass suction pipette. A Multi-Clamp 700B amplifier, a Digidata series 1440 A Digitizer, and pClamp 10.3 software (Axon Instruments, Molecular Devices, San Jose, California, USA) were used for acquisition. Raw signals were acquired at 50 kHz and low-pass filtered at 10 kHz. Patch pipettes (1B150F-4, WPI) with a tip resistance of 5–8MU were filled with internal solution (concentrations in mM: KCl 125, $MgCl_2$ 2, Mg-ATP 4, HEPES-free acid 10, EGTA 5, 290 mOsm/L, pH adjusted to 7.2 with KOH with Alexa 488 at 40 mM final concentration). Holding potential was -85 mV, away from the calculated chloride reversal potential (E_{Cl} = - 0.8 mV).

Analysis of electrophysiological data

Analysis of electrophysiological data was performed offline using Clampex 10 software (Molecular Devices, San Jose, California, USA). Single-channel events were identified using single-channel search in Clampfit (Molecular Devices, San Jose, California, USA), with a first-level set at -15 pA from the baseline (level 0). A 20 s window was used to identify channel events from a gap-free voltage-clamp recording from the first 1 to 3 min of recording. Passive properties were determined, in voltage-clamp mode at -85 mV, from the cell current response to a 10 mV hyperpolarization step (V step). Membrane resistance (R_m) was

estimated from the amplitude of the sustained current at the end of the 100 ms voltage step (R_m = V step / Im). Membrane capacitance (C_m) was estimated as the ratio between the cell decay time constant (t), obtained from the exponential fit of the current decay an R_S (C_m ~t/ R_S). Action potential discharge was monitored in current-clamp mode in response to successive depolarizing current steps of 100 ms from – 2 pA to + 28 pA steps *in vivo*, and 500 ms from 0 pA to + 14 pA steps *in vitro*; and with a 2 pA increment after a fixed prepulse with -10 pA for 20 ms while holding the cell membrane potential at - 50 mV *in vivo* and – 65 mV *in vitro*.

Immunocytochemistry

DIV2 spinal CSF-cNs in vitro were3 dpf larva were fixed 20 minutes in phosphate-buffered saline (PBS) containing 4% paraformaldehyde (PFA) and 0.1% glutaraldehyde at room temperature. Cells were stored at 4°C for one week maximum if needed. Samples were incubated for 8 minutes in PBS containing 0.1% Triton for cell permeabilization and blocked for 1 hour in PBS containing 10% NGS. Primary antibodies were incubated 24 hours at 4°C in a blocking buffer containing 1% NGS. All secondary antibodies were from Molecular Probes (Invitrogen, Life Technologies, Carlsbad, California, USA) and used at 1:1000 in blocking buffer, and incubated 45 minutes at room temperature. The following primary antibodies were used: rabbit anti-Pkd2l1 (1:1000, custom-made) (Sternberg *et al.*, 2018), chicken anti-GFP (1:1000, ab13970, Abcam, Cambridge, England) mice anti-TagRFP (1:1000, MA515257, Thermo Fischer Scientific, Waltham, Massachusetts, USA) and rabbit anti-GABA (Sigma, A2052). The following secondary antibodies were used at 1:1000: Alexa Fluor-488 goat anti-chicken IgG A11039, Alexa Fluor-568 goat anti-mouse A11004 and Alexa Fluor-647 goat anti-rabbit IgG A21244 (Thermo Fischer Scientific, Waltham, Massachusetts, USA). Coverslips were mounted in 6 µL drops of Vectashield Anti-fade Mounting Medium (Vector Laboratories, Inc., Burlingame, California, USA and imaged on an inverted SP8 confocal microscope equipped with a 40X NA = 1.3 oil immersion objective. Images were then processed using FIJI (Schindelin *et al.*, 2012).

Quantification and statistical analysis

All values are mean ± standard error of the mean (SEM) and represented as a boxplot where the central mark indicates the median (in red), the bottom and top edges of the box indicate the 25th and 75th percentiles. The whiskers extend to the most extreme data points that are not considered outliers, outliers are identified with a ‘‘+’’ symbol.

Chapter II: Transcriptome analysis of spinal CSF-cNs reveals numerous receptors to chemical cues

CSF plays a key role in the neurogenesis process (Sawamoto *et al.*, 2006; Zappaterra and Lehtinen, 2012) and for brain and spine development (Sawamoto *et al.*, 2006; Lehtinen *et al.*, 2011). Analysis of nascent CSF from embryonic mice showed that the CSF contains the proteins Sonic hedgehog (Shh), Bone morphogenetic proteins (Bmps) and retinoic acid (RA) (Chau *et al.*, 2015). Other studies on embryonic CSF in different species, such as chick, mice or zebrafish, confirmed the presence of signaling molecules for development, such as fibroblast growth factor 2 (FGF2) (Martín *et al.*, 2006), Shh (Huang *et al.*, 2010), RA (Chang, Lehtinen and Sive, 2016), leukemia inhibitory factor (Hatta *et al.*, 2006) and the semaphorin3B (Arbeille *et al.*, 2015). Choroid plexus epithelial cells produce and secrete factors into the CSF (Damkier, Brown and Praetorius, 2013). Choroid plexi transcriptomic investigation showed a spatial heterogeneity of gene expression between the lateral ventricle (telencephalic) and the fourth ventricle (hindbrain) (Lun *et al.*, 2015). Proteomic analyses demonstrate that ~200 proteins are differentially expressed by the telencephalic and hindbrain choroid plexi (Lun *et al.*, 2015). Furthermore, the CSF protein content varies in an age-dependent manner during the development (Lehtinen *et al.*, 2011; Chau *et al.*, 2015; Lun *et al.*, 2015). Altogether, these results show that the CSF content could be tightly regulated and thus ensuring the delivery of important signaling factors promoting the development of the central nervous system. In addition to developmental factors, the CSF contains active neuromodulators such as acetylcholine (Welch, Markham and Jenden, 1976), dopamine, noradrenaline and serotonin (Strittmatter *et al.*, 1997), as well as neuropeptides such as somatostatin, neuropeptide Y (Nilsson *et al.*, 2001), vasopressin and oxytocin (Martin *et al.*, 2014), but also neurosteroids (pregnenolone sulfate, dehydroepiandros-terone sulfate) (Kim, Creekmore and Vezina, 2003; Meletti *et al.*, 2017), purines (adenosine, ATP) (Schmidt *et al.*, 2015) and endocannabinoids (anandamide) (Romigi *et al.*, 2010). The CSF content depends on the physiological states (Chalermkitpanit *et al.*, 2017; Albayar *et al.*, 2019), thus CSF is analyzed for classic diagnostic of diseases of the nervous system (Deisenhammer *et al.*, 2006). Altogether, these results show the CSF chemical cues act on neuronal physiology (Bjorefeldt *et al.*, 2018) and reflect physiological states.

Previously described as a passive fluid, the recent effort of research investigation on CSF provides evidence that CSF acts more actively on brain and spine homeostasis (Matsumae *et al.*, 2016). The remaining question is: are there specific cells receiving and integrating CSF

chemical cues? Due to their sensory function and their close relation with CSF, spinal CSF-cNs appear to be the best candidate to achieve this function. To test this hypothesis, I first investigated which receptors for chemical cues are expressed by spinal CSF-cNs.

To identify the chemical biomolecules activating spinal CSF-cNs in zebrafish, we were required to know more about receptors expressed by spinal CSF-cNs. I took advantage of the transcriptomic analysis of spinal CSF-cNs performed by Dr. Laura Desban and Dr. Andrew Prendergast in the lab to investigate the receptors expressed in spinal CSF-cNs (Prendergast *et al.*, 2019). To identify transcriptomic specificity in CSF-cNs, Prendergast and Desban used fluorescence-activated cell sorting (FACS) of GFP-positive cells to isolate spinal CSF-cNs from decapitated 3 dpf *Tg(pkd2l1:Gal4;UAS:GFP)* zebrafish larvae and compared GFP-positive spinal CSF-cNs to other darks cells of the trunk (**Figure 1A-C**).
This transcriptomic analysis identified more than 18,000 transcripts expressed in spinal CSF-cNs, of which 202 were enriched (Prendergast *et al.*, 2019). In these transcripts, we found as expected enrichment for TRP channel *pkd2l1*, but also enrichment for previously described spinal CSF-cNs markers such as the transcription factors of the *nkx* and *gata* families (Yang, Rastegar and Strähle, 2010; Petracca *et al.*, 2016b; Andrzejczuk *et al.*, 2018), as well as secreted peptides involved in arching spinal curvature (*urp1*, *urp2*) (Quan *et al.*, 2015; Zhang *et al.*, 2018a; Cantaut-Belarif *et al.*, 2020) or *somatostatin1.1* (*sst1.1*) (Christenson *et al.*, 1991; Djenoune *et al.*, 2017) involved in locomotion in zebrafish (Quan *et al.*, 2020) (see **Figure 2**). In addition, we found expression (but no enrichment) of transcripts of ASIC channels that were found involved in acidic pH detection in spinal CSF-cNs (Orts-Del'Immagine *et al.*, 2012; Jalalvand, Robertson, Tostivint, *et al.*, 2016; Thesis Böhm, 2017), as well as enzymes involved in the GABA synthesis (*gad1a*, *gad1b*, *gad2*) (Djenoune *et al.*, 2014) (see **Figure 2**). Furthermore, we found enrichment for transcripts of peptides such as *nppc* or *scg2a* (**Figure 2**) that have been investigated in the publication in Chapter III.

To validate our transcriptome, we combined labeling of spinal CSF-cNs with GFP antibody in 1 and 3 dpf *Tg(pkd2l1:GCaMP5G)* transgenic larvae with fluorescent *in situ* hybridization (FISH) for 47 enriched transcripts. We confirmed that 40 over 47 genes (85%) were expressed selectively in spinal CSF-cNs (Prendergast *et al.*, 2019) (see Chapter III for more details). The remaining 7 genes not expressed in spinal CSF-cNs could correspond either to genes expressed at a low level, or to rare contamination from floor plate or motor neurons in close vicinity with spinal CSF-cNs (Prendergast *et al.*, 2019). To avoid contamination of spinal CSF-cNs with other cell populations, we could use single-cell RNA-sequencing allowing the dissection of gene expression at single-cell resolution. Using this technique, we gain in specificity for spinal CSF-cNs as we can control for expression of genes encoding for

markers of spinal CSF-cNs such as PKD2L1; and it could provide information about spinal CSF-cNs gene expression heterogeneity, maybe highlighting receptors expressed specifically in CSF-cNs subpopulations (Chen, Ning and Shi, 2019). However, receptors show typically low levels of expression making them difficult to identify. Thus, single-cell RNA-sequencing is not adapted as we lose in sensitivity by analyzing single cells, leading to the under-detection of lowly expressed genes. Here, bulk RNA-sequencing technology, combining gene expression of pools of spinal CSF-cNs, was more adapted to identify lowly-expressed genes such as receptors. I therefore choose to dig into the > 18,000 transcripts to investigate which receptors for chemical cues were expressed by spinal CSF-cNs.

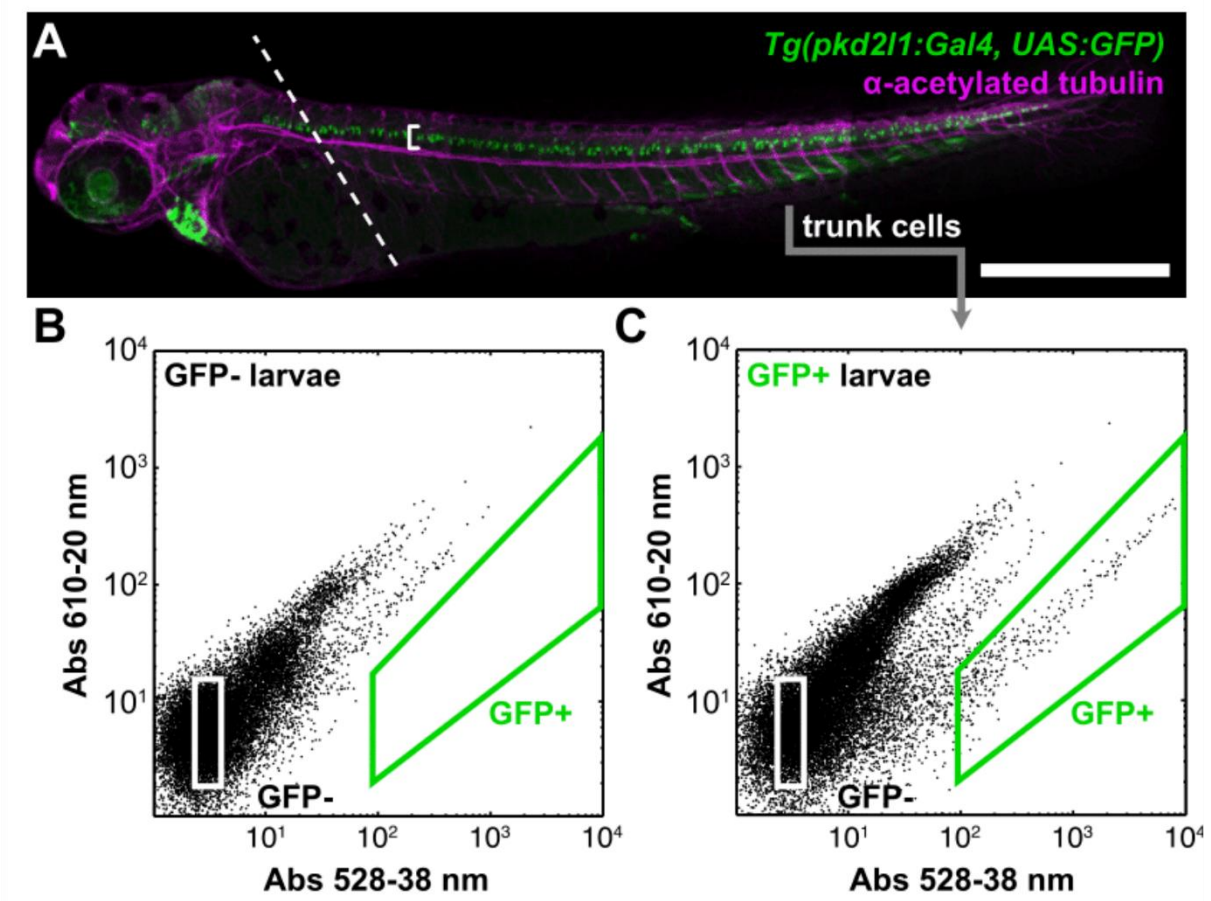

Figure 1. Transcriptome of spinal CSF-CNs from 3 dpf larva. (A) 3 dpf zebrafish *Tg(pkd2l1:GAL4, UAS:GFP)* larva immunostained for GFP (green) and acetylated tubulin (magenta). Dashed line indicates plane of decapitation prior to dissociation (anterior tissues were discarded to exclude labeled cells in brain and heart); bracket indicates CSF-cN domain. Scale bar: 500 µm. **(B)** Calibration FACS plot from non-transgenic siblings. **(C)** FACS plot from a typical dissociation of cells from transgenic larvae. A small fraction (~0.2% of input) of cells is green-shifted. Adapted from (Prendergast *et al.*, 2019).

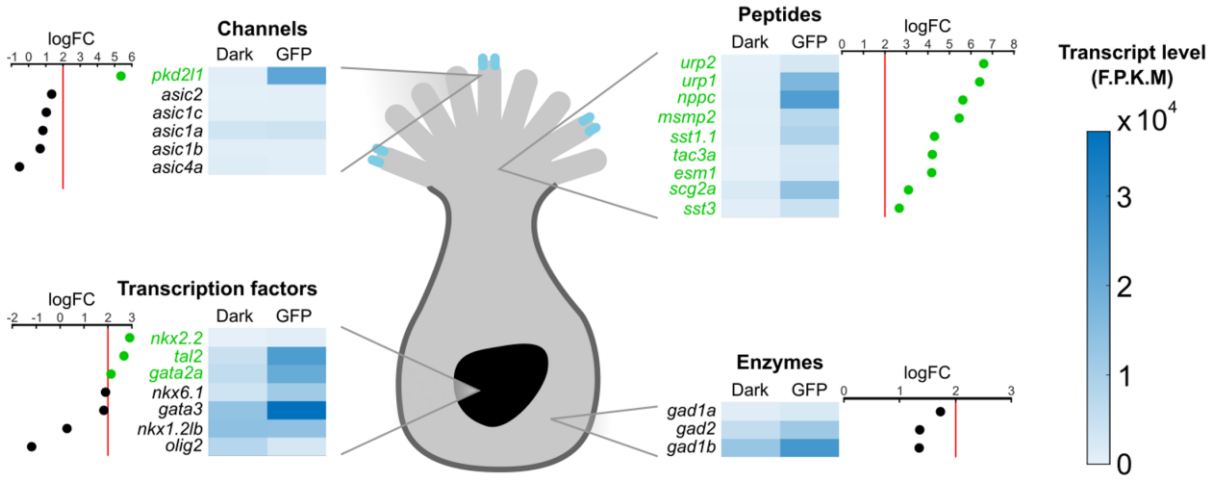

Figure 2. Transcripts present and enriched in spinal CSF-cNs. Log fold change (logFC)> 2 (vertical red lines) was used as a threshold for enrichment in spinal CSF-cNs; enriched transcripts are represented in green.

1) Transcriptome analysis of spinal CSF-cNs

Analysis of the transcriptomic data highlighted a large variety of transcripts expressed in spinal CSF-cNs, which were grouped into the following families of genes.

1.1) Receptors for neurotransmitters and neuromodulators

We found that spinal CSF-cNs express diverse receptors for the classical GABA and glutamate neurotransmitters (**Table 1**). However, a majority of these receptors are expressed at really low levels, and we only found three glutamatergic receptors enriched in spinal CSF-cNs (metabotropic: *grm3*, *grm2a*; ionotropic: *grin2bb*) (**Figure 3**). Thus, the receptors lowly expressed and not enriched receptors may not be functional in spinal CSF-cNs.

In addition, we found expression of receptors for other neurotransmitters and neuromodulators, such as purinergic, serotoninergic, cholinergic and adrenergic receptors (**Table 2**). Purinergic and cholinergic receptors expression is concordant with previous studies showing that spinal CSF-cNs respond to acetylcholine (Corns *et al.*, 2015; Johnson *et al.*, 2020) and ATP (Stoeckel *et al.*, 2003; Johnson *et al.*, 2020). However, spinal CSF-cNs were shown to express the $P2X_2$ receptor in rat spinal cord (Stoeckel *et al.*, 2003), a receptor that was not expressed in our transcriptome, maybe due to a level of transcripts too low to be detected, or differences of receptor expression among species. In addition, none of these neurotransmitter and neuromodulator receptors found in spinal CSF-cNs were enriched nor

highly expressed (**Figure 4**), suggesting that these receptors may not be functional receptors important for the physiology of the spinal CSF-cNs in zebrafish larva.

The CSF contains a large variety of active neuromodulators and neurotransmitters such as acetylcholine (Welch, Markham and Jenden, 1976), dopamine, noradrenaline and serotonin (Strittmatter *et al.*, 1997) and purines (Schmidt *et al.*, 2015) which could act on spinal CSF-cNs. Thus, it would be interesting first to investigate whether these receptors we found lowly expressed and not enriched in spinal CSF-cNs are functional receptors by testing receptor agonists in spinal CSF-cNs *in vitro*.

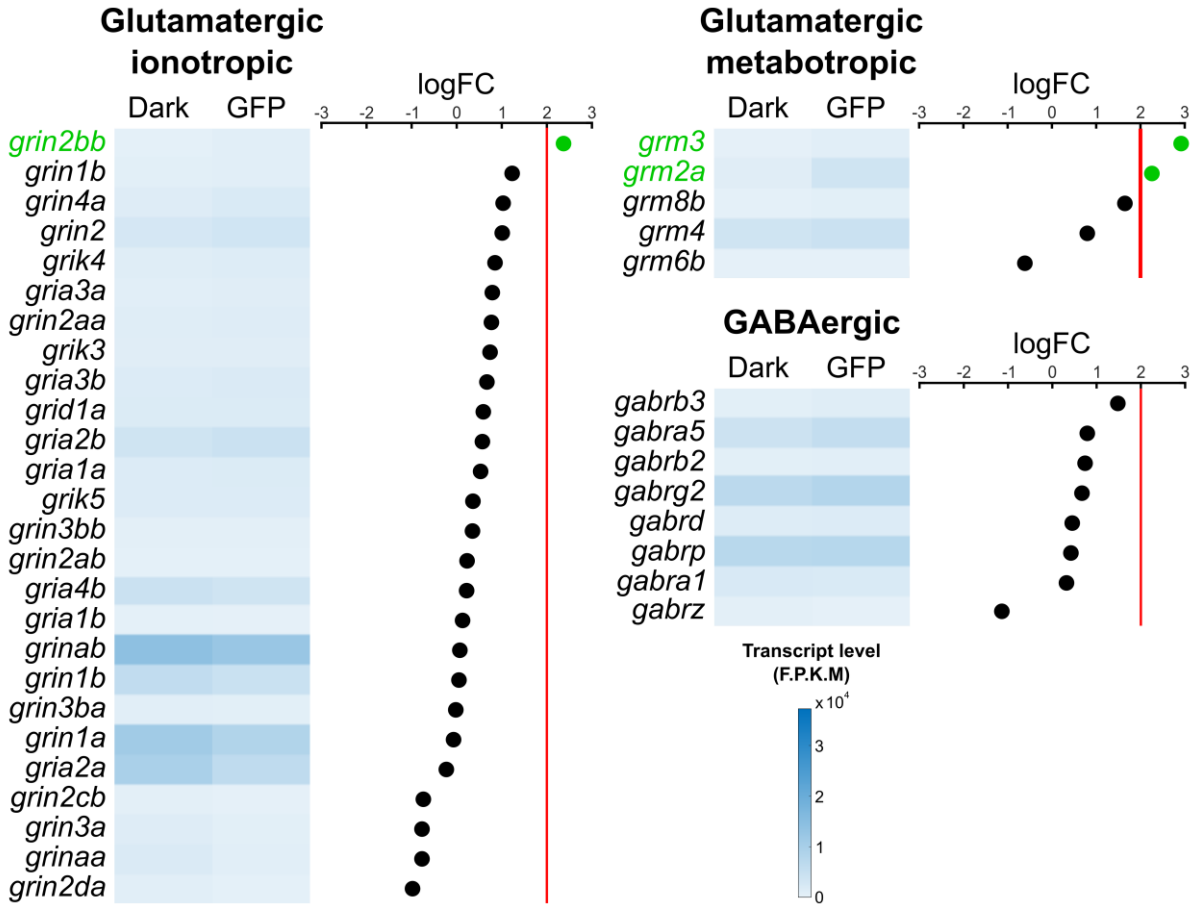

Figure 3. Summary of GABAergic and glutamatergic receptors expressed in spinal CSF-cNs. Log fold change (logFC) > 2 (vertical red lines) was used as a threshold for enrichment in spinal CSF-cNs; enriched transcripts are represented in green.

1.2) Hormones receptors

Interestingly, we found transcripts of receptors for different hormones (**Table 3**), in particular receptors for hormones involved in reproduction, such as the luteinizing hormone (LH), the

estrogen or the prolactin, suggesting a role of spinal CSF-cNs in reproduction. Particularly, the *lhcgr* receptor for LH hormone is of first interest as it is enriched specifically in spinal CSF-cNs (**Figure 5**). Another transcript found enriched in this transcriptome was *tac3a* (**Figure 2**), a gene encoding for the precursor of two peptides: the Neurokinins Ba (NKBa) and NKB-Related Peptide a (NKB-RPa, also named NKF). Tac3a has been found expressed in the optic tectum, thalamus, hypothalamus, pituitary, and ovary in zebrafish (Zhou *et al.*, 2012). A study in adult zebrafish females showed that a single intraperitoneal injection of NKBa and NKBRPa peptides significantly increased luteinizing hormone levels (Biran *et al.*, 2012). We found transcripts for a Tac receptor, *tacr1a*, in our transcriptome (**Table 4**) but this receptor is not enriched in spinal CSF-cNs (**Figure 6**). Moreover, estrogen treatment of pre-pubertal fish elicited increases of Tac3a and Tacr3a/b in the brain (Biran *et al.*, 2012). Altogether, the results suggest that spinal CSF-cNs could detect sexual hormones through the enriched LH receptor, but also potentially tachykinin and estrogen receptors, and in turn potentially release NKBa and NKB-RPa peptides.

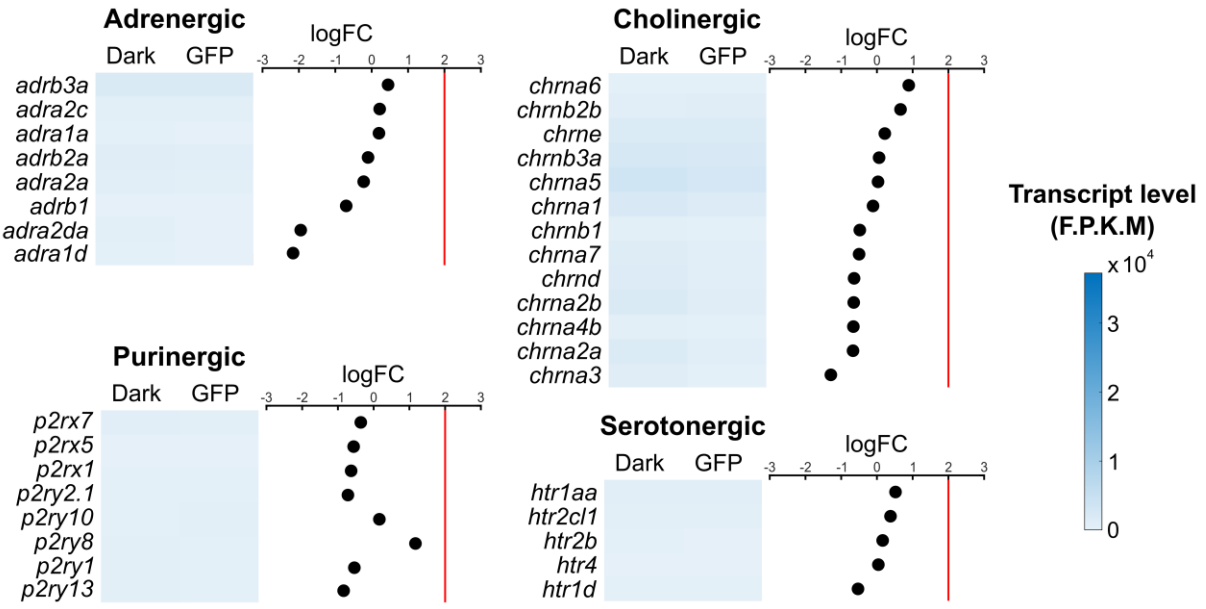

Figure 4. Summary of neurotransmitter and neuromodulator receptors expressed in spinal CSF-cNs. Log fold change (logFC) > 2 (vertical red lines) was used as a threshold for enrichment in spinal CSF-cNs.

	Receptor	Full name (ZFIN)	Mean dark (F.P.K.M.)	Mean GFP (F.P.K.M.)
GABA receptors	*gabrb3*	gamma-aminobutyric acid type A receptor subunit beta3	469,6	1026
	gabra5	gamma-aminobutyric acid type A receptor subunit alpha5	4121	5544
	gabrb2	gamma-aminobutyric acid type A receptor subunit beta2	537,4	686
	gabrg2	gamma-aminobutyric acid type A receptor subunit gamma2	6885,8	8089
	gabrd	gamma-aminobutyric acid type A receptor subunit delta	1422,6	1488
	gabrp	gamma-aminobutyric acid type A receptor subunit pi	7344,4	7657
	gabra1	gamma-aminobutyric acid type A receptor subunit alpha1	2084,6	1941
	gabrz	gamma-aminobutyric acid type A receptor subunit zeta	333,6	122
Glutamatergic metabotropic receptors	*grm3*	glutamate receptor, metabotropic 3	95,4	595
	grm2a	glutamate receptor, metabotropic 2a	1007,8	3771
	grm8b	glutamate receptor, metabotropic 8b	262,2	562
	grm4	glutamate receptor, metabotropic 4	3749,8	4384
	grm6b	glutamate receptor, metabotropic 6b	124,8	63
Glutamatergic ionotropic receptors	*grin2bb*	glutamate receptor, ionotropic, N-methyl D-aspartate 2B, genome duplicate b	164,6	633
	grid1b	glutamate receptor, ionotropic, delta 1b	489,2	733
	gria4a	glutamate receptor, ionotropic, AMPA 4a	1279,8	1909
	grid2	glutamate receptor, ionotropic, delta 2	2667,6	3428
	grik4	glutamate receptor, ionotropic, kainate 4	1051,4	1369
	gria3a	glutamate receptor, ionotropic, AMPA 3a	819,6	990
	grin2aa	glutamate receptor, ionotropic, N-methyl D-aspartate 2A, a	1128,8	1272
	grik3	glutamate receptor, ionotropic, kainate 3	885,8	991
	gria3b	glutamate receptor, ionotropic, AMPA 3b	1597	1847
	grid1a	glutamate receptor, ionotropic, delta 1a	1715,4	1667
	gria2b	glutamate receptor, ionotropic, AMPA 2b	3667	4442
	gria1a	glutamate receptor, ionotropic, AMPA 1a	1507	1608
	grik5	glutamate receptor, ionotropic, kainate 5	1597,2	1530
	grin3bb	glutamate receptor, ionotropic, N-methyl D-aspartate 3B, genome duplicate b	358,4	305
	grin2ab	glutamate receptor, ionotropic, N-methyl D-aspartate 2A, b	270,2	290
	gria4b	glutamate receptor, ionotropic, AMPA 4b	4427	3668
	gria1b	glutamate receptor, ionotropic, AMPA 1b	199,2	143
	grinab	glutamate receptor, ionotropic, N-methyl D-aspartate-associated protein 1b	14185	12484
	grin1b	glutamate receptor, ionotropic, N-methyl D-aspartate 1b	5856,8	4633
	grin3ba	glutamate receptor, ionotropic, N-methyl-D-aspartate 3Ba	664,4	462
	grin1a	glutamate receptor, ionotropic, N-methyl D-aspartate 1a	11125,2	8491
	gria2a	glutamate receptor, ionotropic, AMPA 2a	9661,4	6226
	grin2cb	glutamate receptor, ionotropic, N-methyl D-aspartate 2Cb	310,2	130
	grin3a	glutamate receptor, ionotropic, N-methyl-D-aspartate 3A	1265	559
	grinaa	glutamate receptor, ionotropic, N-methyl D-aspartate-associated protein 1a	1765,6	801
	grin2da	glutamate receptor, ionotropic, N-methyl D-aspartate 2D, a	763	278

Table 1. Summary of classical neurotransmitter receptors expressed in spinal CSF-cNs. Hits are grouped by families and then ranked by log fold change (logFC) between GFP- reference and GFP+ CSF-cN RNA pools. In blue: genes found enriched in spinal CSF-cNs.

	Receptor	Full name (ZFIN)	Mean dark (F.P.K.M.)	Mean GFP (F.P.K.M.)
Adrenoceptors	*adrb3a*	adrenoceptor beta 3a	1972	1917
	adra2c	adrenoceptor alpha 2C	552,4	477
	adra1a	adrenoceptor alpha 1Aa	153,2	118
	adrb2a	adrenoceptor beta 2, surface a	984,8	718
	adra2a	adrenoceptor alpha 2A	624,6	438
	adrb1	adrenoceptor beta 1	126,4	59
	adra2da	adrenergic, alpha-2D-, receptor a	524	106
	adra1d	adrenoceptor alpha 1D	288,2	55
Serotonergic receptors	*htr1aa*	5-hydroxytryptamine (serotonin) receptor 1A a	631,4	741
	htr2cl1	5-hydroxytryptamine (serotonin) receptor 2C, G protein-coupled-like 1	431,6	400
	htr2b	5-hydroxytryptamine (serotonin) receptor 2B, G protein-coupled	161	119
	htr4	5-hydroxytryptamine receptor 4	122,4	88
	htr1d	5-hydroxytryptamine (serotonin) receptor 1D, G protein-coupled	270,6	157,00
Purinergic receptors	*p2rx7*	purinergic receptor P2X, ligand-gated ion channel, 7	1138,4	700
	p2rx5	purinergic receptor P2X, ligand-gated ion channel, 5	546	283
	p2rx1	purinergic receptor P2X, ligand-gated ion channel, 1	830,6	418
	p2ry2.1	purinergic receptor P2Y2, tandem duplicate 1	106,6	55
	p2ry10	P2Y receptor family member 10	200,2	171
	p2ry8	P2Y receptor family member 8	224,8	381
	p2ry1	purinergic receptor P2Y1	435,2	242
	p2ry13	purinergic receptor P2Y13	362,8	154
Cholinergic receptors	*chrna6*	cholinergic receptor, nicotinic, alpha 6	173,6	275
	chrnb2b	cholinergic receptor, nicotinic, beta 2b like	736	942
	chrne	cholinergic receptor, nicotinic, epsilon	1707,6	1732
	chrnb3a	cholinergic receptor nicotinic beta 3 subunit a	2579,2	2172
	chrna5	cholinergic receptor, nicotinic, alpha 5	3359,2	2737
	chrna1	cholinergic receptor, nicotinic, alpha 1	2088,4	1597
	chrnb1	cholinergic receptor, nicotinic, beta 1	474,2	282
	chrna7	cholinergic receptor, nicotinic, alpha 7a	1218,4	622
	chrnd	cholinergic receptor, nicotinic, delta	1502,6	738
	chrna2b	cholinergic receptor, nicotinic, alpha 2b	1897,6	906
	chrna4b	cholinergic receptor, nicotinic, alpha 4b	392,2	193
	chrna2a	cholinergic receptor, nicotinic, alpha 2a	1636,4	842
	chrna3	cholinergic receptor, nicotinic, alpha 3	888,4	290

Table 2. Summary of neuromodulator and neurotransmitter receptors expressed in spinal CSF-cNs. Hits are grouped by families and then ranked by log fold change (logFC) between GFP- reference and GFP+ CSF-cN RNA pools.

	Receptor	Full name (ZFIN)	Mean dark (F.P.K.M.)	Mean GFP (F.P.K.M.)
Estrogen receptors	*esr1*	estrogen receptor 1	219	452
	esr2b	estrogen receptor 2b	355	301
	esr2a	estrogen receptor 2a	167,2	128
Prolactin receptor	*prlra*	prolactin receptor a	925,2	477
Growth hormone releasing hormone receptor	*ghrhrb*	growth hormone releasing hormone receptor b	201,4	112
Luteinizing hormone/choriogonadotropin receptor	*lhcgr*	luteinizing hormone/choriogonadotropin receptor	127,2	646
Melanocortin receptor	*mc5rb*	melanocortin 5b receptor	84,6	101

Table 3. Summary of hormone receptors expressed in spinal CSF-cNs. Hits are grouped by families and then ranked by log fold change (logFC) between GFP- reference and GFP+ CSF-cN RNA pools. In blue: genes found enriched in spinal CSF-cNs.

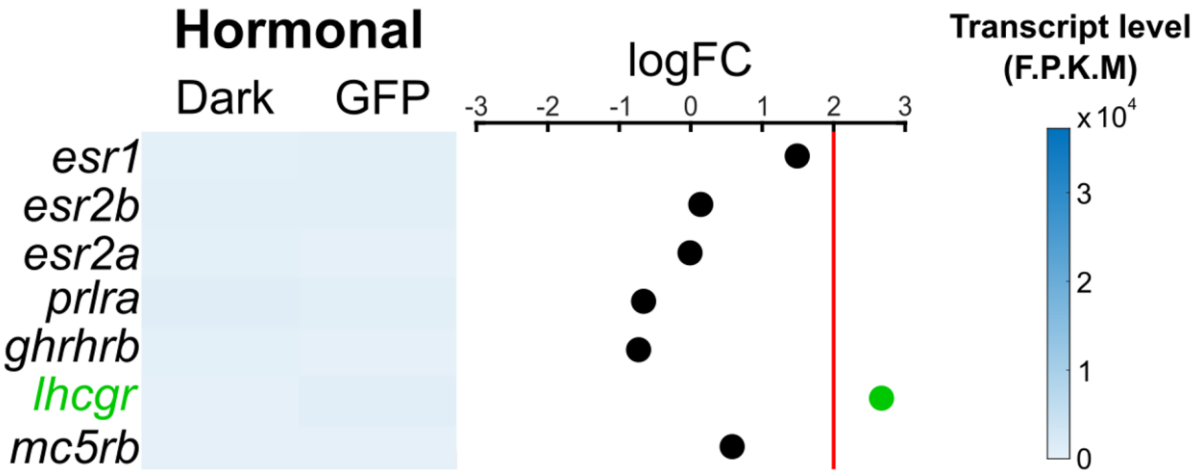

Figure 5. Summary of hormone receptors expressed in spinal CSF-cNs. Log fold change (logFC) > 2 (vertical red lines) was used as a threshold for enrichment in spinal CSF-cNs; enriched transcripts are represented in green.

1.3) Peptides receptors

In addition to the *tacr1a* receptor discussed previously, we found several receptors for peptides (**Table 4**). However, only the *natriuretic peptide receptor 3* (*npr3*) was found enriched in spinal CSF-cNs. As for neuromodulators/neurotransmitters, the CSF contains neuropeptides such as somatostatin, neuropeptide Y (Nilsson *et al.*, 2001), vasopressin and oxytocin (Martin *et al.*, 2014). We found low expression of receptors for neuropeptide Y,

vasopressin and somatostatin, but none of them were enriched in spinal CSF-cNs, thus these receptors may not be functional to detect these peptides in the CSF. The natriuretic peptide C (NPC) is highly enriched in spinal CSF-cNs (**Figure 2**) (Prendergast *et al.*, 2019), suggesting that spinal CSF-cNs could sense the extracellular concentration of NPC through the enriched *npr3* receptor to in turn modulate their release in an autocrine manner.

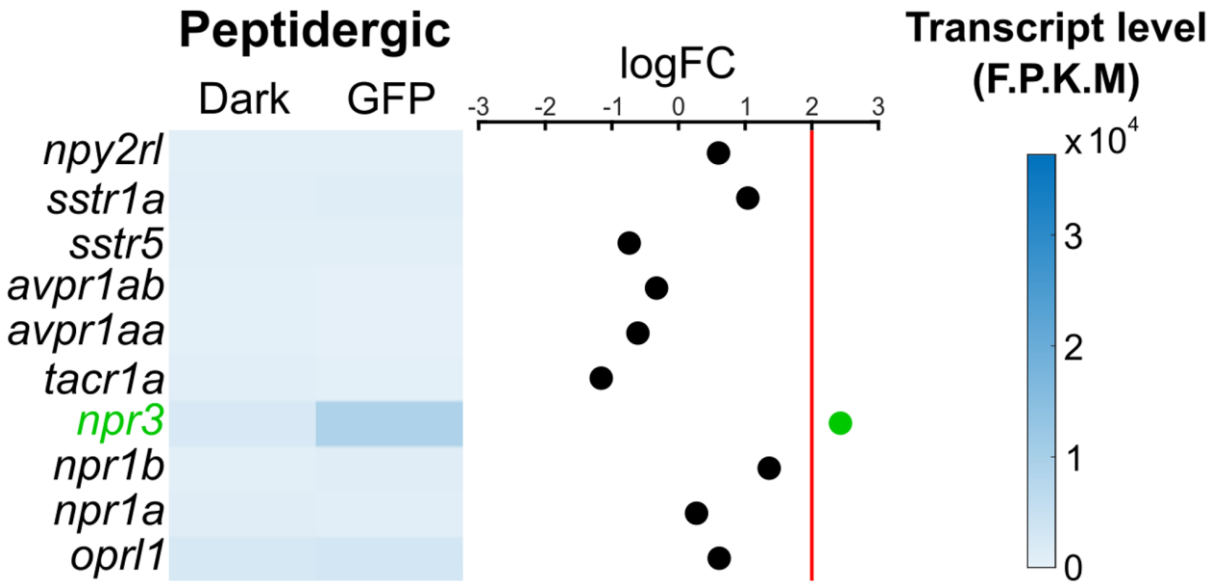

Figure 6. Summary of peptide receptors expressed in spinal CSF-cNs. Log fold change (logFC) > 2 (vertical red lines) was used as a threshold for enrichment in spinal CSF-cNs; enriched transcripts are represented in green.

1.4) Taste receptors

We found two orphan taste receptor transcripts, *tas2r3a/b*, highly enriched in spinal CSF-cNs (logFC = 8.73, mean dark = 2 F.P.K.M versus mean GFP = 728 F.P.K.M) (Prendergast *et al.*, 2019). Taste receptors of type 2 (T2Rs) are G protein-coupled receptors (GPCRs) responsible for the detection of bitterness (Li, 2013), firstly described in mammals (Adler *et al.*, 2000). T2Rs were also described to detect bacterial quorum-sensing metabolites such as acyl-homoserine lactone (AHL) (Lee *et al.*, 2012) or quinolones (Freund *et al.*, 2018) in ciliated cells of the upper airway. Activation of the T2R38 receptor in the upper airway leads to an increase in intracellular calcium concentration, which in turn activates the production of nitric oxide (NO) through the nitric oxide synthase (NOS) and increases mucociliary clearance (Lee *et al.*, 2012). Thus, we can hypothesize that spinal CSF-cNs can sense bacterial metabolites acting as bitter compounds during bacterial infection of the CSF, to in turn secrete molecules into the CSF to combat the pathogen. We will test this hypothesis in

Chapter III, by performing experiments in which spinal CSF-cNs are transiently exposed to microbial bitter metabolites.

	Receptor	Full name (ZFIN)	Mean dark (F.P.K.M.)	Mean GFP (F.P.K.M.)
NPY receptor	*npy2rl*	neuropeptide Y receptor Y2, like	549,2	529
Somatostatin receptors	*sstr1a*	somatostatin receptor 1a	638,6	1024
	sstr5	somatostatin receptor 5	559,6	299
Arginine vasopressin receptors	*avpr1ab*	arginine vasopressin receptor 1Ab	174,4	115
	avpr1aa	arginine vasopressin receptor 1Aa	175	94
Tachykinin receptor	*tacr1a*	tachykinin receptor 1a	696,6	229
Natriuretic peptide receptors	*npr3*	natriuretic peptide receptor 3	2115,8	9108
	npr1b	natriuretic peptide receptor 1b	496	942
	npr1a	natriuretic peptide receptor 1a	1009	862
Opioid receptor	*oprl1*	opiate receptor-like 1	2530,4	3010

Table 4. Summary of peptide receptors expressed in spinal CSF-cNs. Hits are grouped by families and then ranked by log fold change (logFC) between GFP- reference and GFP+ CSF-cN RNA pools. In blue: genes found enriched in spinal CSF-cNs.

1.5) Immune-related receptors

Surprisingly, we found in our transcriptome analysis multiple immune-related receptors (**Table 5**), suggesting that spinal CSF-cNs play a role in immunity. Toll-like receptors (TLRs) are proteins involved in innate immunity and expressed in the membrane of leukocytes, as well as non-immune cells such as epithelial cells, endothelial cells and fibroblasts (Delneste, Beauvillain and Jeannin, 2007). In particular, CSF-cNs express the Tlr5 receptor, involved in flagellin detection (Miao *et al.*, 2007). Expression of TLRs suggests that during CSF infection by a pathogen spinal CSF-cNs could contribute to innate immunity by detecting pro-inflammatory cues released by infected cells, such as the tumor necrosis factor-alpha (TNF-α), which is consistent with a role in bacterial detection for spinal CSF-cNs as proposed previously. In addition, spinal CSF-cNs express the cytokine receptors Crfb1 and Crfb2, activated by virus-induced interferons (IFNs) in zebrafish (Langevin *et al.*, 2013), suggesting that spinal CSF-cNs could detect viral pathogen as well in the CSF. However, none of these receptors were found enriched in spinal CSF-cNs (**Figure 7**), then a proper functional characterization of these receptors is needed using receptors agonists. More investigations on the role of spinal CSF-cNs in innate immunity will be presented in Chapter III.

	Receptor	Full name (ZFIN)	Mean dark (F.P.K.M.)	Mean GFP (F.P.K.M.)
Cytokine receptors	*crfb15*	cytokine receptor family member B15	92,8	160
	crfb4	cytokine receptor family member b4	1045,8	1060
	crfb1	cytokine receptor family member b1	1005,6	1015
	crfb2	cytokine receptor family member b2	286,6	148
Toll-like receptors	*tlr3*	toll-like receptor 3	200,2	390
	tlr22	toll-like receptor 22	160,4	119
	tlr5a	toll-like receptor 5a	161,6	78
	tlr18	toll-like receptor 18	477,2	120
	tlr21	toll-like receptor 21	121	34
	tlr5b	toll-like receptor 5b	1554,8	415
Tumor necrosis factor receptors	*tnfrsf1b*	tumor necrosis factor receptor superfamily, member 1B	191,6	203
	tnfrsf1a	tumor necrosis factor receptor superfamily, member 1a	1652,6	1535
	tnfrsf9a	tumor necrosis factor receptor superfamily, member 9a	197	184
	tnfrsf21	tumor necrosis factor receptor superfamily, member 21	5653,2	4042
	tnfrsf19	tumor necrosis factor receptor superfamily, member 19	1565,4	912
	tnfrsf11a	tumor necrosis factor receptor superfamily, member 11a	2733,6	1813
	tnfrsfa	tumor necrosis factor receptor superfamily, member a	1630,4	433
Interferon gamma receptor	*ifngr1*	interferon gamma receptor 1	595	268
Interleukin receptors	*ilr21.1*	interleukin 21 receptor, tandem duplicate 1	112,2	232
	il7r	interleukin 7 receptor	110	153
	il2rga	interleukin 2 receptor, gamma a	1639,8	2097
	il10ra	interleukin 10 receptor, alpha	674	730
	il20ra	interleukin 20 receptor, alpha	184,8	191
	il6r	interleukin 6 receptor	3282	2792
	il13ra1	interleukin 13 receptor, alpha 1	803,2	669
	il10rb	interleukin 10 receptor, beta	5285	3886
	il12rb2	interleukin 12 receptor, beta 2a	592	375
	il17rd	interleukin 17 receptor D	1233,2	848
	il4r.1	interleukin 4 receptor, tandem duplicate 1	233,2	132
	il13ra2	interleukin 13 receptor, alpha 2	409,2	220
	il2rb	interleukin 2 receptor, beta	383,8	144
	il17ra1a	interleukin 17 receptor A1a	291,4	64

Table 5. Summary of immune-related receptors expressed in spinal CSF-cNs. Hits are grouped by families and then ranked by log fold change (logFC) between GFP- reference and GFP+ CSF-cN RNA pools.

In summary, we analyzed transcriptomic data of spinal CSF-cNs and found that they express various receptors allowing detection of chemical cues in the CSF. The large variety of receptors suggests an implication of spinal CSF-cNs in different functions such as reproduction and innate immunity. However, a large amount of these receptors are lowly

expressed and not enriched in spinal CSF-cNs, then requiring functional characterization. Thus, I was interested in testing agonists of several receptors by performing calcium imaging experiments taking advantage of the cell culture protocol developed in Chapter I.

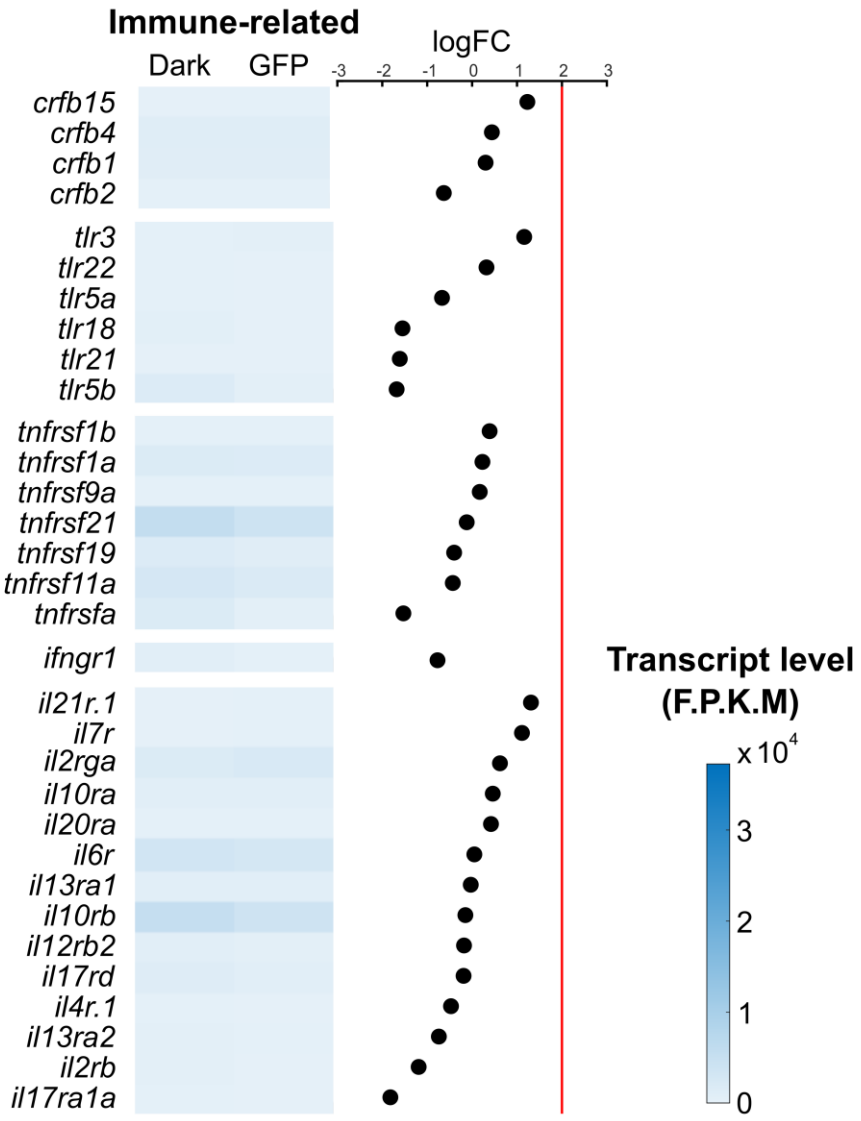

Figure 7. Summary of immune-related receptors expressed in spinal CSF-cNs. Log fold change (logFC) > 2 (vertical red lines) was used as a threshold for enrichment in spinal CSF-cNs.

2) Stimulation of spinal CSF-cNs with receptor agonists *in vitro*

To monitor the functionality of receptors for neurotransmitters and neuromodulators found lowly expressed but not enriched in spinal CSF-cNs (**Table 2**, **Figure 4**), I tested different neuromodulators and neurotransmitters that act as agonists of these receptors. I tested epinephrine 3mM, norepinephrine 3mM, ATP 500µM and serotonin 500µM.

ATP binds to ionotropic P2X receptors and metabotropic P2Y receptors. P2X receptors are a family of 7 ligand-gated cation-permeable ion channels (P2X1-7) (North, 2002) with two transmembrane domains, modulating the liberation of neurotransmitters at the presynaptic level (Khakh and North, 2012). P2X channel opening allows the entrance of cations such as Ca^{2+}, leading to cell membrane depolarization (Koshimizu *et al.*, 2000). P2Y metabotropic receptors are G protein-coupled receptors (GPCR) with 8 member families in human (Dubyak, 2003), that are also located at the presynaptic level and modulating neurotransmitters release. Activation of the $P2Y_I$ subfamily of P2Y receptors (comprising P2Y1, P2Y2, P2Y4, P2Y6 and P2Y11 receptors) leads to activation of the phospholipase C (PLC)-β (Harden *et al.*, 2010), leading to cleavage of phosphatidylinositol 4,5-bisphosphate (PIP_2) into inositol 1,4,5-trisphosphate (IP_3), which triggers the release of calcium from the endoplasmic reticulum into the cytosol. $P2Y_{12}$ subfamily of P2Y receptors (P2Y12, P2Y13 and P2Y14 receptors) are G_i-coupled and G_q-coupled receptors inhibiting the adenylyl cyclase that produce the second messenger cyclic AMP (cAMP) from ATP (Harden *et al.*, 2010), and thus playing an inhibitory role in cascade transduction of the signal.

Adrenergic receptors are GPCRs that can be divided into two types: α and β receptors (Perez, 2006). α receptors are also divided into two main classes: α1 and α2. As $P2Y_I$ purinergic receptors, α1 receptors lead to PLC activation through the G_q protein, inducing IP_3 production and release of calcium in the cytosol (Perez, 2006). α2 receptors are coupled with the G_i protein and lead to adenylyl cyclase inhibition (Perez, 2006). β receptors are coupled with G_s protein leading to adenylyl cyclase activation and production of cAMP that activates the proteinase K (PKA) and intracellular signaling (Perez, 2006). Some β receptors are also coupled to G_i, inhibiting the adenylyl cyclase.

Serotonergic receptors are composed of 6 GPCRs ($5\text{-}HT_1$, $5\text{-}HT_2$, $5\text{-}HT_{4\text{-}8}$) and one ligand-gated ion channel ($5\text{-}HT_3$) (Siegel *et al.*, 1999). $5\text{-}HT_1$ and $5\text{-}HT_5$ are inhibitory GPCRs coupled with G_i/G_o proteins decreasing the cellular level of the second messenger cAMP (Siegel *et al.*, 1999). $5\text{-}HT_{4,6\text{-}7}$ are GPCRs coupled with G_s protein, playing an excitatory role by increasing cellular level of cAMP through adenylyl cyclase (Siegel *et al.*, 1999). $5\text{-}HT_2$ is coupled with G_q/G_{11} proteins increasing IP_3 production and release of calcium in the cell (Siegel *et al.*, 1999). Finally, $5\text{-}HT_3$ is a ligand-gated ion channel permeable to sodium, potassium and calcium ions (Thompson and R. Lummis, 2006). Activation of the $5\text{-}HT_3$ receptors by serotonin ligand leads to channel opening, inducing an excitatory response in neurons carried by cations such as sodium or calcium (Thompson and R. Lummis, 2006).

In conclusion, P2X and $P2Y_1$ adrenergic receptors as well as α1 adrenergic and $5\text{-}HT_2$ serotonergic receptors trigger an increase of intracellular calcium when a ligand is bound, which can be observed with calcium imaging. All these different receptors were found expressed in our transcriptome of spinal CSF-cNs (P2Xs: *p2rx2*, *5* and *1*; $P2Y_1$s: *p2ry2.1* and *p2ry1*; α1s: *adra1a* and *adra1d*; $5\text{-}HT_2$: *htr2cl1* and *htr2b*; **Table 1**), suggesting that pressure-application of ATP, epinephrine, norepinephrine and serotonin should give rise to calcium responses in spinal CSF-cNs.

To monitor the concentration of molecule sensed by spinal CSF-cNs *in vitro* during pressure-application, we collaborated with Dr. Ludovic Keiser to conceive numerical simulations of the pressure-application system and estimated that during a 1-second pressure-application a CSF-cN *in vitro* is typically exposed to at most 50% of the initial concentration in the stimulation pipette, and thus independently of the coefficient of diffusion of the molecule that will only impact the decay of the chemical pulse (**Figure 8A-B**).

We used *in vitro* DIV2 cells from *Tg(pkd2l1:TagRFP ; pkd2l1:GCaMP5G)*, and spinal CSF-cNs were stimulated with 3 successive 1-second pressure-application of molecules, with 64 seconds between each pressure-application, using a thin pipette disposed at 100 µm (X-axis) from the neuron. Recordings without stimulation were performed to ensure that CSF-cN responses were due to the molecules applied and not to spontaneous activity (**Figure 8C-F**, left).

First, I performed control artificial CSF (aCSF) pressure-application to verify whether spinal CSF-cNs responses to chemical cues were specific to the molecule tested, and not due to mechanosensation. Interestingly, out of 31 CSF-cNs tested, none responded by a calcium transient to aCSF alone despite previous *in vitro* reports indicating that spinal CSF-cNs in lamprey respond to direct fluid pressure application (Jalalvand *et al.*, 2018) (**Figure 8C-F**, in light gray).

I also found that spinal CSF-cNs did not respond to pressure-application of epinephrine 3mM, norepinephrine 3mM, ATP 500µM and serotonin 500µM (**Figure 8C-D**). Spinal CSF-cNs express the ionotropic receptor $P2X_2$ in rat (Stoeckel *et al.*, 2003), which was not found expressed in our transcriptome. Spinal CSF-cNs respond to 300µM ATP pressure-application in CSF-cNs in mice, in spinal cord slice preparations (Johnson *et al.*, 2020).
Altogether, these results suggest that the receptors tested, which are lowly expressed and not enriched in spinal CSF-cNs, are not functional receptors involved in the detection of chemical neurotransmitters and neuromodulators in spinal CSF-cNs. The expression of

transcripts for these receptors could result from an artifact of picking motor neurons or floor plate cells.

However, other interpretations could explain these results: I) spinal CSF-cNs have different properties *in vitro* and *in vivo,* in particular in respect to the expression of receptors to chemical cues that may not match the expression of PKD2L1. We checked for molecular identity conservation of spinal CSF-cNs in Chapter I, but receptors for neuromodulators and neurotransmitters could not be verified easily using immunocytochemistry as they are weakly expressed. Thus, spinal CSF-cNs may not express these receptors *in vitro*. Another possibility is that spinal CSF-cNs *in vitro* required more time to develop in culture medium in order to start expressing the receptors; II) spinal CSF-cNs *in vitro* may express the receptors but missing key elements on the transduction path that lead to calcium entry; III) CSF-cN properties might differ across species (I focused in my PhD on zebrafish, while other studies involved mice, rat and lamprey); IV) as many receptors were described to not increase the level of intracellular calcium ($P2Y_{12}$ purinergic receptors, α2 and β adrenergic receptors, 5-HT_1 and 5-HT_{4-7} serotonergic receptors), responses of spinal CSF-cNs could be calcium-independent and not detectable with calcium imaging. Spinal CSF-cNs electrophysiological recordings coupled with pressure-application of the neuromodulators tested could inform about a possible calcium-independent response.

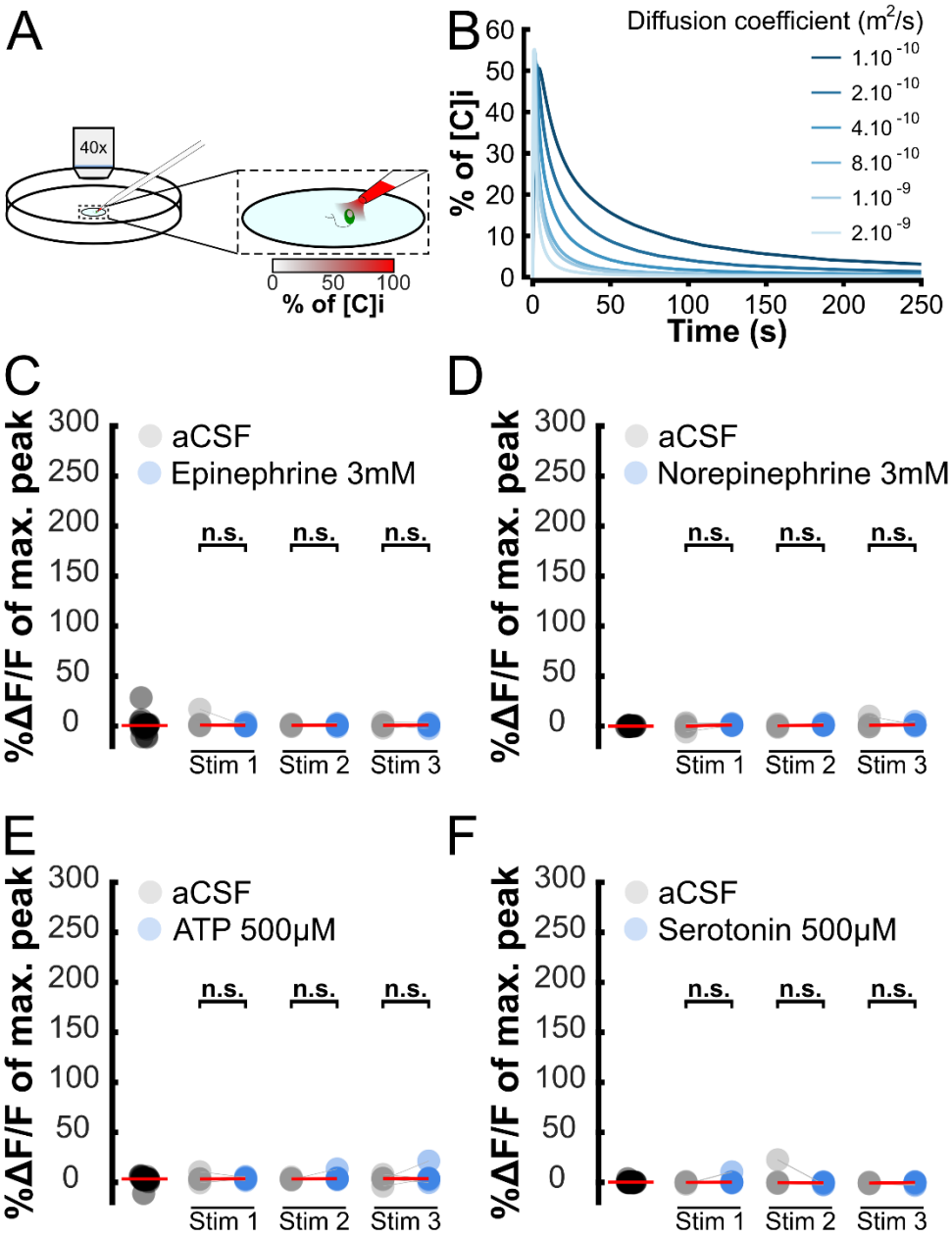

Figure 8. Spinal CSF-cNs do not respond to neuromodulators and neurotransmitter *in vitro*. **(A-B)** Simulations of chemical cues pressure-application *in vitro*. **(A)** Schematic view of the *in vitro* stimulation experimental set up combining calcium imaging at 40x, 5Hz and stimulation of spinal CSF-cN with a gradient of molecule. **(B)** Simulation of the concentration of molecule sensed by spinal CSF-cN for a range of coefficient of diffusions (from 1.10^{-10} to 2.10^{-9} m^2/s); [C]i corresponds to initial concentration in the stimulation pipette. **(C-F)** Quantification of calcium transients' amplitude after neuromodulators/neurotransmitters pressure-application. Paired line plots showing responses of individual cells to absence of stimulation (corresponding to spontaneous activity, on the left in black circle), or 3 successive 1-second stimuli of aCSF (grey circle) versus molecules (blue circle). **(C)** Epinephrine: 2-factor ANOVA, treatment factor F = 0.577, p = 0.45, Turkey HSD post-hoc testing, n.s. = not significant. Red bar: median ΔF/F (median spontaneous activity = -0.36%; median epinephrine = -0.04% and median aCSF = 0.45% for stimulation 1; median epinephrine = 0.10% and

median aCSF = -0.02% for stimulation 2; median epinephrine = 0.37% and median aCSF = -0.11% for stimulation 3), 0 responding cells out of 8. **(D)** Norepinephrine: 2-factor ANOVA, treatment factor F = 1.456, p = 0.24, Turkey HSD post-hoc testing, n.s. = not significant. Red bar: median ΔF/F (median spontaneous activity = 0.02%; median norepinephrine = 1.12% and median aCSF = -0.03% for stimulation 1; median norepinephrine = 0.94% and median aCSF = 0.29% for stimulation 2; median norepinephrine = 1.35% and median aCSF = 0.83% for stimulation 3), 0 responding cells out of 7. **(E)** ATP: 2-factor ANOVA, treatment factor F = 1.394, p = 0.24, Turkey HSD post-hoc testing, n.s. = not significant. Red bar: median ΔF/F (median spontaneous activity = -0.23%; median ATP = -0.09% and median aCSF = -0.27% for stimulation 1; median ATP = -0.04% and median aCSF = -0.24% for stimulation 2; median ATP = -0.05% and median aCSF = 0.14% for stimulation 3), 0 responding cells out of 8. **(F)** Serotonin: 2-factor ANOVA, treatment factor F = 0.226, p = 0.64, Turkey HSD post-hoc testing, n.s. = not significant. Red bar: median ΔF/F (median spontaneous activity = 0.19%; median serotonin = 0.13% and median aCSF = -0.15% for stimulation 1; median serotonin = -0.35% and median aCSF = -0.25% for stimulation 2; median serotonin = -0.12% and median aCSF = -0.79% for stimulation 3), 0 responding cells out of 8.

Conclusion and perspectives

The analysis of a transcriptome of spinal CSF-cNs performed by Dr. Desban and Dr. Prendergast showed that multiple receptors are expressed in spinal CSF-cNs. We found receptors for neuromodulators, neurotransmitters and neuropeptides present in the CSF, suggesting that spinal CSF-cNs could sense the CSF content *in vivo*. Some receptors were associated with sex hormones such as the LH hormone or the estrogen, suggesting a role for spinal CSF-cNs in reproduction. Surprisingly, we found numerous receptors involve in the detection of bacterial metabolites (Tas2r3 and Tlr5 receptors) and innate immunity, such as TLRs or cytokine receptors Crfb1/2, suggesting that spinal CSF-cNs could sense bacterial metabolites in the context of bacterial infection of the CSF and participate to immune defense. However, only a subset of these receptors expressed was found enriched in spinal CSF-cNs.

Stimulations *in vitro* with neurotransmitters and neuromodulators, which were agonists of receptors found lowly expressed but not enriched in the transcriptome, failed to activate spinal CSF-cNs, suggesting that these not enriched receptors are not functional in spinal CSF-cNs. These results could also be due to potential changes of spinal CSF-cNs molecular properties *in vitro*. Moreover, most of the transcripts code for receptors that do not directly increase intracellular concentration and cannot be identified here. To test their presence and functionality, other experimental approaches are needed such as patch-clamp recording.

However, I cannot exclude possible false-positive results from the transcriptome, which could provide from 'contamination' with cells that were not spinal CSF-cNs.

In perspective, it would be interesting to stimulate spinal CSF-cNs *in vitro* with neuromodulators/neurotransmitters after a longer maturation in cell culture medium, using DIV3/4 cells to decipher if the absence of responses is due to changes in the molecular identity of the cells. Other neuromodulators/neurotransmitters and neuropeptides contained in the CSF should be tested on spinal CSF-cNs *in vitro*, such as somatostatin, acetylcholine and dopamine, to have a better characterization of the spinal CSF-cNs receptors functionality.

To assess the question of transcriptome specificity, a new transcriptome could be performed using single-cell RNA-sequencing. As we do not pool hundreds of cells with this technique, we would lose sensitivity and some very weakly expressed receptors could be missed. However, we gain in specificity as we can check for specific markers of spinal CSF-cNs for each cell analyzed. A single-cell RNA-sequencing on spinal CSF-cNs is currently ongoing, with the help of Julian Roussel in the lab and collaborators from the lab of Jean-Pierre Levraud (Pasteur Institute). In Chapter III, we will investigate the role of spinal CSF-cNs in the detection of bacteria and innate immunity, a role that was suggested by the transcriptomic analysis of the spinal CSF-cNs receptors conducted in this chapter.

Methods

Primary cell cultures of spinal CSF-cNs

The complete primary cell culture protocol of spinal CSF-cNs was exposed in Chapter I.

Simulation of chemical cues pressure-application *in vitro*

In order to estimate the concentration of molecules at the surface of the CSF-cN during and after the 1-second stimulus, we carried out numerical simulations applying finite-element method (ComsolMultiphysics, Transport of Diluted Species & Laminar Flow modules). We here describe the model in more details. The concentration of molecules c obeys the advection-diffusion law:

$$\frac{\partial c}{\partial t} + \boldsymbol{v} \cdot \boldsymbol{\nabla} c - D\Delta c = 0$$

where D is the diffusion coefficient of the molecule, $\boldsymbol{\nabla}$ is the differential operator and Δ is the Laplacian operator. Here $\boldsymbol{v}$ is the fluid velocity vector obeying the incompressible Navier-Stokes equations:

$$\rho \boldsymbol{\nabla} \cdot (\boldsymbol{v}) = 0$$

$$\rho \frac{\partial \boldsymbol{v}}{\partial t} + \rho(\boldsymbol{v} \cdot \boldsymbol{\nabla})\boldsymbol{v} = -\boldsymbol{\nabla}.\boldsymbol{\sigma} + \mu \boldsymbol{\Delta v}$$

where $\rho = 10^3$ kg/m is the water density and $\boldsymbol{\sigma} = -p\boldsymbol{I} + \mu\boldsymbol{\nabla u} + \mu(\boldsymbol{\nabla u})^T$ is the total stress tensor, with $\mu = 10^{-3}$ Pa.s the water viscosity and $\boldsymbol{I}$ the identity matrix. Bold terms represent three dimensional vectors or tensors.

The flow is simulated in a cylindrical container of height 0.45 mm and diameter 2 mm. Note that the concentration distribution around the cell was found not to depend on the size of the container when the diameter exceeds 1.2 mm, which is smaller than the selected value. Inside this container, the initial concentration c_0 is set to 0. A flow of concentration c_{puff} passes through a spherical opening of diameter 3 µm, representing the stimulation pipette, with a flow rate of 3.6 nL/s during 1s, in the direction of the cell. The cell is represented by a portion of sphere of diameter 10 µm and of height above the floor plate 8 µm. The cell is located at a distance of 100 µm from the stimulation pipette.

Concerning the boundary conditions for the flow and the concentration, a no slip is imposed at the bottom wall and on the cell ($\boldsymbol{v} = \boldsymbol{0}$), and a complete impermeability is imposed against the passage of molecules ($\boldsymbol{n} \cdot (D\boldsymbol{\nabla c} + c\boldsymbol{v}) = 0$). The lateral walls as well as the upper wall of the cylindrical container are at imposed constant pressurep_0, and we impose the absence of concentration gradients $\boldsymbol{n} \cdot \boldsymbol{\nabla c} = 0$.

Numerically, the transition between the stimulus process (which lasts 1s) and the post-stimulus phase (t > 1s) is achieved via a smoothing function:

$$f(t) = \exp(-\left(\frac{t-1}{\tau}\right)^2), \text{ with } \tau = 17 \text{ ms}$$

The number of tetrahedral mesh elements varies between 685000 and 850000 in the simulations presented in this manuscript. All the simulations converged, and doubling the number of mesh elements led to similar results.

Calcium imaging in primary cell culture.

Calcium imaging on GCaMP5G-positive neurons from the *Tg(pkd2l1:TagRFP ; pkd2l1:GCaMP5G)* transgenic line was performed on an epifluorescence microscope equipped with a Lumen Dynamics XT600 Xenon lamp and a GFP filter cube. Acquisition was performed at 5 Hz using an EM-CCD Camera from Hamamatsu. Puffs stimuli were delivered using a 1 s long TTL pulse from a Digidata acquisition system (Axon Instruments) and repeated 3 times with an inter-trial interval of 64 seconds. Artificial CSF (aCSF) for recording and stimulations was composed of NaCl 140mM (Sigma, S7653), KCl 1mM (Sigma, P9333), $CaCl_2$ 2.5mM (Sigma, 223506), $MgCl_2$ 1mM (Sigma, M2670), HEPES 10mM (Sigma, H3375), D-(+)-Glucose 10mM (Sigma, G8270), diluted in MilliQ water; pH was adjusted at

7.4, 290 mOsm.kg^{-1}. For neuromodulators/neurotransmitters stimulation, I used epinephrine hydrochloride 3mM (Sigma, E4642), norepinephrine hydrochloride 3mM (Sigma, A7256), ATP 1mM (Sigma, A1852) and serotonin 1mM (Sigma, H9523); dilutions were done in aCSF.

In vitro calcium imaging analysis

Slow translational drifts of the image due to cell movements were corrected using image registration by taking as a reference image a frame of the original position of the CSF-cN. We identified CSF-cN calcium transients in response to 1-second stimuli by using a 100 ms-long flash of green light performed 12.74s before the stimulus. To determine the response of a given ROI to a 1-second stimulus, the $\Delta F/F$ amplitude of each peak response after each stimulus was calculated using a home-made MATLAB script available on the Wyart lab GitHub: the $\Delta F/F$ average of over six time points around the maximum $\Delta F/F$ of the peak was calculated, and was subtracted to this the $\Delta F/F$ average of six points before the stimulus. A cell was considered as a responding cell when we observed a response for at least one of the 3 1-second stimuli. Comparisons across conditions were made using 2-factor ANOVAs with Turkey HSD post-hoc tests on R.

Chapter III: Sensory neurons detect pneumococci and promote survival in central nervous system infection

Introduction

As explained in the introduction, a substantial body of work has described in the last decade that spinal CSF-cNs are mechanosensory cells detecting spinal tail bending and modulating in response locomotion and posture of zebrafish (Fidelin *et al.*, 2015; Hubbard *et al.*, 2016; Quan *et al.*, 2020; Wu *et al.*, 2021) and lamprey (Jalalvand, Robertson, Wallén, *et al.*, 2016). Spinal CSF-cNs act via the release of neurotransmitters such as GABA (Fidelin *et al.*, 2015) but also via neuropeptides such as Somatostatin1.1 (Christenson *et al.*, 1991; Wyart *et al.*, 2009; Jalalvand, Robertson, Wallén, *et al.*, 2016; Quan *et al.*, 2020). However, little is known about chemosensory functions of spinal CSF-cNs, especially *in vivo* where access to reach the center of the spinal cord is highly challenging.

The transcriptome analysis of spinal CSF-cNs performed by Andrew Prendergast and Laura Desban in the team shed light on receptors expressed in these cells that could contribute to detecting chemical cues in the CSF (Prendergast *et al.*, 2019). We found receptors for different neuromodulators and neurotransmitters such as adrenergic, serotonergic, purinergic, GABAergic, glutamatergic and cholinergic receptors (**Chapter II**). As the CSF contains active neuromodulators and neurotransmitters such as acetylcholine (Welch, Markham and Jenden, 1976), dopamine, noradrenaline and serotonin (Strittmatter *et al.*, 1997) and purines (Schmidt *et al.*, 2015), spinal CSF-cNs could sense the chemical cues from the CSF.

In addition, we surprisingly found that spinal CSF-cNs express numerous receptors related to immunity. Among them, the Tlr5 receptor is involved in the detection of flagellin allowing bacterial movements (Miao *et al.*, 2007), suggesting that spinal CSF-cNs could respond to the presence of bacteria in the CSF. We also found that CSF-cNs express the cytokine receptors Crfb1 and Crfb2, activated by virus-induced interferons (IFNs) in zebrafish (Langevin *et al.*, 2013). Thus, spinal CSF-cNs could detect viral pathogens during viral infection in the CSF. In addition to immune-related receptors, we found taste receptors that were highly enriched, the Tas2r3a/b receptors. The T2Rs are a family of GPC receptors that detect bitter metabolites (Li, 2013). Interestingly, T2Rs detect bacterial quorum-sensing metabolites such as quinolones (Freund *et al.*, 2018) and acyl-homoserine lactone (AHL)

(Lee *et al.*, 2012) in solitary chemosensory cells of the upper airway. Altogether, these observations suggested to us that spinal CSF-cNs could detect bacterial or viral pathogens in a context of pathogen infection of the CSF, such as meningitis that leads to meninges inflammation causing severe damages such as cognitive impairments (Hoogman *et al.*, 2007).

To tackle this question, Claire Wyart, Andrew Prendergast and Kin Ki Jim took advantage of a model of pneumococcal meningitis in zebrafish larvae (Jim *et al.*, 2016) to investigate whether infection by *Streptococcus pneumoniae* (*S. pneumoniae*) led to an activation of spinal CSF-cNs. After injection ~2000 colony forming units (CFU) in the hindbrain ventricles, spinal CSF-cNs showed large and long calcium responses to bacteria *in vivo*. To uncover the bacterial metabolites triggering activation of spinal CSF-cNs during infection, I took advantage of the primary cell culture protocol of spinal CSF-cNs developed during my PhD (**Chapter I**) to directly stimulate the neurons with bacterial metabolites. As spinal CSF-cNs transcriptome revealed a high enrichment for taste 2 receptors, we hypothesize that they could detect microbial volatile organic compounds (mVOCs) acting as bitter compounds, such as acetone, 2-butanone, 2-pentanone, 2-methylpropanal or dimethyl disulfide (DMDS) (Bos, Sterk and Schultz, 2013; Verbeurgt *et al.*, 2017). I found that DMDS and 2-pentanone induced large calcium responses in spinal CSF-cNs *in vitro*. We then investigated spinal CSF-cNs gene regulation during infection by performing a transcriptome analysis of spinal CSF-cNs in control versus infected zebrafish larvae. The transcriptome analysis highlighted the expression of cytokines and complement components involved in innate immunity that are up-regulated upon infection. To assess whether spinal CSF-cNs improve the host survival upon infection, we blocked the secretion of spinal CSF-cNs and found a significant reduction of host survival. Altogether, our results showed that spinal CSF-cNs carry interoceptive chemosensory functions to detect bacterial metabolites during infection, leading to up-regulation of genes involved in innate immunity and an improvement of host survival. Future investigations will be required to understand the mechanisms by which the activity of CSF-cNs upon infection promotes host survival.

Sensory neurons detect pneumococci and promote survival in central nervous system infection

AUTHORS

Andrew Prendergast[§1], Kin Ki Jim[§2,3], Hugo Marnas[§1], Laura Desban[1], Feng B. Quan[1], Lydia Djenoune[1], Julian Roussel[1], Ludovic Keiser[4], Yasmine Cantaut-Belarif[1], Francois-Xavier Lejeune[1], Mahalakshmi Dhanasekar[1], Pierre-Luc Bardet[1], Jean-Pierre Levraud[5], Diederik van de Beek[2], Christina Vandenbroucke-Grauls[*3], Claire Wyart[*1]

AFFILIATIONS

[1]Institut du Cerveau (ICM), Sorbonne Universités, UPMC Univ Paris 06, Inserm, CNRS, AP-HP, - Hôpital Pitié-Salpêtrière, Boulevard de l'hôpital, F-75013, Paris, France.
[2]Amsterdam University Medical Centers, University of Amsterdam and VU University Amsterdam, Neurology, Amsterdam Neuroscience, Meibergdreef 9, Amsterdam, Netherlands 1105 AZ.
[3]Amsterdam University Medical Centers, University of Amsterdam and VU University Amsterdam, Medical Microbiology and Infection Prevention, Amsterdam Institute for Infection and Immunity, De Boelelaan 1108, Amsterdam, Netherlands 1081 HV.
[4]Ecole Polytechnique Fédérale de Lausanne (EPFL) - Station 18, CH-1015, Lausanne, Switzerland.
[5]Macrophages and Development of Immunity Laboratory, Institut Pasteur (IP), UMR3738 CNRS, 75015, Paris, France.

*Correspondence to: claire.wyart@icm-institute.org & vandenbrouckegrauls@amsterdamumc.nl

§ Authors contributed to this manuscript equally.

KEYWORDS

Central nervous system infection; Sensory neurons; Interoception; Pathogen detection; Cerebrospinal fluid; Innate immunity; Host defense; Neurosecretion; Peptides; Cytolysins; Cytokines; Taste receptors; Bitter compounds; Bacterial meningitis.

eTOC

Prendergast, Jim, Marnas *et al.* discovered that central sensory neurons enhance innate immunity during pneumococcal infection by detecting bacterial metabolites and releasing peptides, complement factors and cytokines to increase host survival.

HIGHLIGHTS

- Sensory neurons contacting the cerebrospinal fluid (CSF) show vigorous and prolonged calcium responses to infection by *Streptococcus pneumoniae* invading the CSF *in vivo*
- Bitter compounds secreted by *S. pneumoniae* induce similar calcium responses in CSF-contacting neurons *in vitro*
- Accordingly, CSF-contacting neurons express orphan bitter taste receptors along with other receptors involved in innate immunity
- Upon infection, CSF-contacting neurons upregulate the expression of numerous cytokines and complement components involved in innate immunity
- Blocking the secretion of CSF-contacting neurons reduces host survival upon infection

GRAPHICAL ABSTRACT

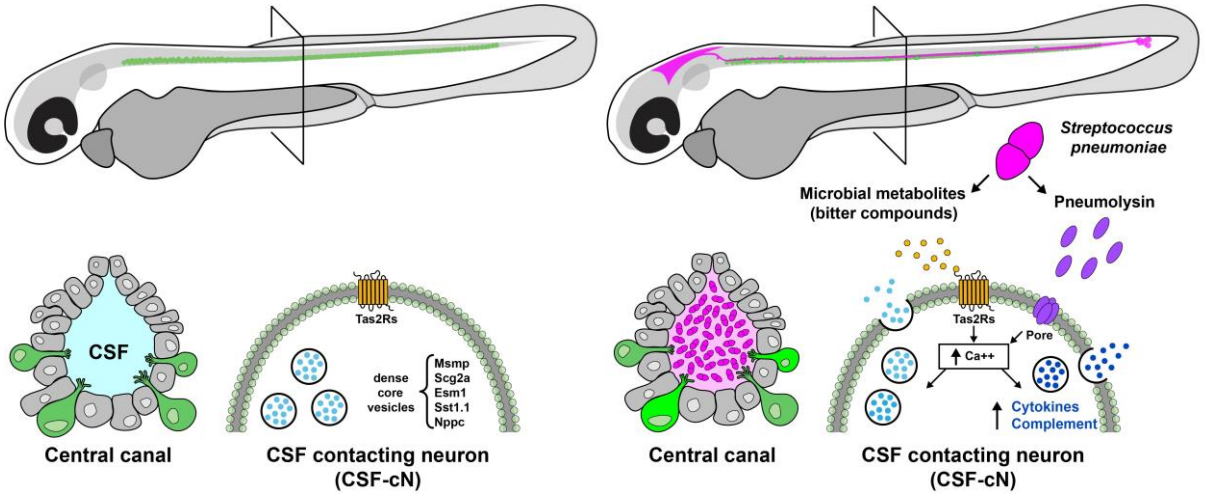

SUMMARY (144 out of 150 words)

Meningitis caused by Streptococcus pneumoniae can invade the cerebrospinal fluid (CSF) leading to bacterial meningitis with devastating consequences. Whether and how sensory cells in the central nervous system can detect pathogenic bacteria, as recently reported for the peripheral nervous system, is not known. We find that CSF infection by *S. pneumoniae* in larval zebrafish leads to phenotypes reminiscent of pneumococcal meningitis. We show that sensory neurons contacting the CSF ("CSF-cNs") exhibit massive calcium transients during infection. These neurons express multiple orphan type 2 taste receptors and respond accordingly to microbial metabolites secreted by *S. pneumoniae* and acting as bitter compounds. Upon infection, CSF-cNs upregulate expression for numerous cytokines and complement components. We find that CSF-cN neurosecretion enhances survival of the host. Our work reveals that central sensory neurons contribute to host survival by detecting pathogenic bacteria in the CSF and contributing to innate immunity.

INTRODUCTION

Streptococcus pneumoniae (the pneumococcus) is the most prevalent cause of community-acquired bacterial meningitis worldwide (van de Beek *et al.*, 2006, 2016; GBD 2016 Meningitis Collaborators, 2018) and is associated with high mortality and morbidity rates despite the introduction of conjugate vaccines (GBD 2016 Meningitis Collaborators, 2018). Reported case fatality rates for pneumococcal meningitis range from 12-30% in high-income countries and 50% or greater for low-income countries (Bijlsma *et al.*, 2016; GBD 2016 Meningitis Collaborators, 2018; Goldberg *et al.*, 2018). One third of surviving patients has neurological sequelae including cognitive impairment (Hoogman *et al.*, 2007; Bijlsma *et al.*, 2016).

Pathogenetic steps of pneumococcal meningitis involve mucosal colonization and invasion, survival and replication in the bloodstream, followed by traversal of the blood brain/cerebrospinal fluid (CSF) barrier (van de Beek *et al.*, 2016). During bacterial multiplication, pneumococci release immunogenic bacterial products that can trigger pattern recognition receptors (Kieser and Kagan, 2017) and thereby activate an immune response characterized by the production of inflammatory mediators such as chemokines and complement factors (Woehrl *et al.*, 2011; Kieser and Kagan, 2017). Such secreted chemotactic factors attract leukocytes, predominantly granulocytes in the initial response, to the CSF, as shown in a rabbit model of meningitis (Tuomanen *et al.*, 1985). Pneumococci grow within the CSF almost as efficiently as *in vitro* because of the weaknesses of the host's

immune system in this compartment (Koedel *et al.*, 2009). How the initial host immune response is orchestrated in the early phase of bacterial penetration in the CSF remains incompletely understood.

Macrophages, dendritic cells and mast cells are present in tissues surrounding the CSF and potentially could have a sentinel function against bacterial invasion. Data from animal studies are scarce and contradictory, especially in the early phase of CSF infection: while in a pneumococcal rat model, depletion of meningeal and perivascular macrophages led to increased bacterial titers and decreased CSF leukocyte counts (Polfliet *et al.*, 2001), macrophage depletion in a pneumococcal rabbit model did not influence CSF inflammation and neuronal injury (Trostdorf *et al.*, 1999).

In the peripheral nervous system, it has been shown that bacteria invading breaches in the skin produce peptides and pore-forming toxins that can directly activate nociceptor sensory neurons which then contribute to inflammation and innate immunity by releasing regulatory neuropeptides (Chiu *et al.*, 2013). A similar phenomenon occurs in the respiratory epithelium wherein ciliary epithelial cells detect bacterial metabolites and induce an inflammatory response (Shah *et al.*, 2009). Here, we therefore investigated whether pathogenic bacteria could be similarly detected in the central nervous system by interoceptive GABAergic sensory ciliated neurons contacting the CSF in the spinal cord, referred to as CSF-contacting neurons or “CSF-cNs” (Kolmer, 1921; Agduhr, 1922). CSF-cNs detect spinal curvature and modulate locomotion, posture and morphogenesis (Wyart *et al.*). We hypothesized that CSF-cNs, known to express a sour taste receptor (Huang *et al.*, 2006; Orts-Del’Immagine *et al.*, 2012; Djenoune *et al.*, 2014), may detect bacteria proliferating in the CSF and in return, modulate the inflammatory response in the CNS.

The recording of neuronal activity during bacterial meningitis *in vivo* is hampered by the difficulty in accessing deep neurons located in the vicinity of the ventricular cavities. We obviate this problem by taking advantage of a recently-developed model of pneumococcal meningitis in zebrafish larvae (Jim *et al.*, 2016) in order to establish a live calcium imaging approach to monitor the activation of CSF-cNs in larval zebrafish upon injection of *S. pneumoniae* in the brain ventricles. We discover that CSF-cNs respond to live pathogenic bacteria invading the CSF via large calcium transients and secrete immune-related factors. We show that such large calcium transients in CSF-cNs can be elicited *in vitro* by exposure to microbial metabolites acting as bitter compounds. Accordingly, we find that CSF-cNs specifically express orphan bitter taste receptors along with neuropeptides with antimicrobial or immunomodulatory functions. Upon infection, CSF-contacting neurons upregulate the expression of cytokines and complement components. Furthermore, blocking the

neurosecretion of CSF-cNs, or even more drastically, ablating these cells, diminishes host survival upon infection. Our study demonstrates that central sensory neurons respond to products of pathogenic bacteria during pneumococcal infection of the CNS and increase host defense via the secretion of factors involved in innate immunity.

RESULTS

Zebrafish larvae infected with *S. pneumoniae* exhibit phenotypes reminiscent of clinical symptoms of pneumococcal meningitis

Clinical features of pneumococcal meningitis include headache, fever, neck stiffness, and altered mental status (van de Beek *et al.*, 2004). Seizures occur in one out of five patients (Zoons *et al.*, 2008). An extreme form of neck stiffness is opisthotonos, an abnormal posture where the back becomes extremely arched (Hull, Parnes and Jankovic, 2021). To validate our zebrafish model, we monitored the behavior and posture of larval zebrafish after injection of the mCherry-labelled *S. pneumoniae* D39 HlpA-mCherry strain in the hindbrain ventricle (**Figure 1, STAR methods**). We observed that mCherry-positive pneumococci proliferate and migrate to colonize the brain ventricles and central canal over 24 hours (**Figure 1A, B**). Freely-swimming vehicle-injected control larvae at 5-6 dpf typically explored their environment via slow locomotor bouts (**Figure 1C-G**) occurring every second on average (Budick and O'Malley, 2000). In contrast, infected larvae swam less often (**Figure 1E**) as a possible reflection of motor fatigue associated with sickness behavior and neuroinflammation (Omdal, 2020). However, when they swam, ~25% of infected fish exhibited locomotor bouts which lasted longer (**Figure 1F**) and covered a much larger distance travelled (**Figure 1D,G**), consistent with epileptic-like seizures (Gawel *et al.*, 2020). Furthermore, their posture became also affected. While the body axis of vehicle-injected control larvae was reliably straight (**Figure 1H-L**), infected larvae developed pronounced dorsal curvature (**Figure 1M-Q**). The dorsal curvature scaled with the degree of bacterial colonization estimated by the red fluorescence of the larvae injected with the *S. pneumoniae* D39 HlpA-mCherry strain (**Figure 1R, S**). Taken together, the motor fatigue and abnormal posture in animals whose CSF is invaded by bacteria are reminiscent of clinical features of pneumococcal meningitis.

Sensory neurons contacting the cerebrospinal fluid respond *in vivo* to live *S. pneumoniae* invading the CSF

The overexpression of urotensin-related peptides (*urp1* and *urp2)* that are selectively expressed in CSF-cNs (Quan *et al.*, 2015) induces dorsal arching in embryonic zebrafish (Zhang *et al.*, 2018a; Cantaut-Belarif *et al.*, 2020). We therefore sought to investigate

whether pneumococcal infection of the CSF specifically activates CSF-cNs (**Figure 2A-D**). In 2 dpf transgenic larvae expressing GCaMP5G in CSF-cNs and injected with vehicle, CSF-cNs spontaneously exhibited unsynchronized and small calcium transients (rarely above 50% ΔF/F, see **Figure 2C, E**). In contrast, in infected larvae, a subset of CSF-cNs produced large and sustained calcium transients (mean maximum ΔF/F of 240%, mean duration of 13 seconds) (**Figure 2D, F, Supplemental Movie 1**). These massive calcium transients began as early as 12 hours post infection and continued within the same cells for several hours (**Figure 2D, F, G**). Concomitant with the unusual activation of CSF-cNs in infected larvae, we observed an overall decline in baseline calcium activity relative to controls (**Figure 2H**). We did not observe recruitment of neutrophils in the CSF at the level of the central canal before 24 hpi under the same conditions, (**Supplemental Figure 1**)**.** These observations are consistent with CSF-cNs responding to the invasion of the CSF by the pathogenic bacteria. In contrast to the results observed in CSF-cNs, we observed no calcium-mediated activation of ependymal radial glial cells that are also in contact with the CSF (**Figure 2I-L**). The observed response to a pneumococcal infection appears specific to neurons contacting the CSF and is not generalizable to all cells in contact with the CSF.

To determine whether active pathogenic bacteria are required to generate the observed neuronal activation during infection, we injected different bacterial preparations into the central canal. As before, the injection of vehicle did not trigger substantial CSF-cN activity, nor did injection of non-pathogenic *E. coli*, or heat-killed *S. pneumoniae* (**Figure 2M**). In this series of experiments, only infection with living pathogens generated CSF-cN transients (**Figure 2M, N** $p = 6.28E^{-16}$). Taken together, these results suggest that the observed effect in CSF-cNs is specific to infection by live pneumococci.

CSF-contacting neurons respond *in vitro* to cytolysins and bitter compounds secreted by *S. pneumoniae*

Several meningeal pathogens produce pore-forming toxins that are major virulence factors; an example of this is the production of pneumolysin by *S. pneumonia* (Kadioglu *et al.*, 2008). We tested the effects of pneumolysin on a primary culture of CSF-cNs expressing the genetically-encoded calcium indicator GCaMP5G together with tagRFP from the double transgenic larvae *Tg(pkd2l1:tagRFP; pkd2l1:GCaMP5G)* (Böhm *et al.*, 2016). We conceived numerical simulations (**STAR methods**) to estimate that during a 1-second pressure-application, a CSF-cN *in vitro* is typically exposed to at most 50% of the initial concentration in the stimulation pipette, independently of the molecule's coefficient of diffusion that will only impact the decay of the chemical pulse (**Figure 3A**). Thus, an initial concentration of 0.1 mg/mL pneumolysin diluted in artificial CSF (aCSF) leads to a chemical pulse of 0.05 mg/mL

onto the cultured neurons (**Figure 3A**). Pressure-application of aCSF alone did not induce a response in the CSF-cNs (**Figure 3B, C** middle panel and **Figure 3D**). In contrast, exposure to 0.05 mg/mL pneumolysin led to small and brief, stimulus-locked calcium increase in CSF-cNs (median = 17.49% ± 14.51% ΔF/F), see **Figure 3B right panel, 3D, Supplemental Movie S2**). We next tested whether CSF-cNs respond to microbial metabolites as shown in ciliated sensory cells in the mammalian airway epithelium (Shah *et al.*, 2009; Tizzano *et al.*, 2010; R. J. Lee, Chen, *et al.*, 2014; R. J. Lee, Kofonow, *et al.*, 2014; Saunders *et al.*, 2014; Freund *et al.*, 2018). These microbial metabolites include a number of microbial volatile organic compounds (mVOCs) that act as bitter compounds, such as acetone, 2-butanone, 2-pentanone, 2-methylpropanal, dimethyl disulfide (DMDS), methylmercaptan, γ-butyrolactone, isopentanol, formaldehyde, and trimethylamine (Bos, Sterk and Schultz, 2013; Verbeurgt *et al.*, 2017). *S. pneumoniae* has been shown to produce these compounds (Filipiak *et al.*, 2012), hence we reasoned that CSF-cNs might play a similar role in the central nervous system as peripheral sensory cells of the airways. Exposure to a mixture of 50 mM bitter compounds including acetone, 2-butanone, 2-pentanone, 2-methylpropanal, dimethyl disulfide (DMDS) elicited very large calcium transients in CSF-cNs (median ΔF/F = 101.25% ± 61%, **Figure 3C, E, F, G, Supplemental Movie S3, STAR methods**), an effect not observed with aCSF only (**Figure 3C, D, E**). CSF-cN responses were larger for bitter compounds than for pneumolysin, and mimicked more closely the response to live bacteria observed *in vivo*. When bitter compounds were tested individually 2-pentanone and DMDS, both induced responses (**Figure 3H, I, J**, **Supplemental Figure S2, Supplemental Movie S4, 5**), but only DMDS recapitulated, in a dose-dependent manner, the large responses observed with the mixture of compounds. This suggests that this compound is a major bitter metabolite activating CSF-cNs (**Figure 3H**). Taken together, these results show that CSF-cNs respond to at least two different bacterial products: a pore-forming cytolysin, and bitter mVOCs; the latter are especially effective in triggering massive calcium transients.

CSF-contacting neurons selectively express bitter taste receptors and numerous peptides involved in innate immunity

To determine how CSF-cNs could detect pneumococci and possibly promote host survival upon infection, we identified CSF-cN-enriched transcripts (**Figure 4**). At 3 dpf, larvae contain approximately 150 CSF-cNs per larva (see cell counts in the transgenic line *Tg(pkd2l1:GFP)* in which all CSF-cNs are GFP-positive, **Supplemental Figure S3**). We therefore used fluorescence-activated cell sorting (FACS) to isolate GFP-positive CSF-cNs from guillotined 3 dpf *Tg(pkd2l1:GAL4, UAS:GFP)* larvae (Fidelin *et al.*, 2015) (**Figure 4A-C**, see **STAR Methods**). Relative to the GFP-negative fraction, the GFP-positive fraction displayed

elevated expression of known CSF-cN markers, such as *pkd2l1* (Huang *et al.*, 2006; Djenoune *et al.*, 2014), *pkd1l2* (Petracca *et al.*, 2016b; England *et al.*, 2017), the GABAergic neuronal marker *gad67,* but as expected no hindbrain-specific markers (*raraa*, *rarab*) (**Supplemental Figure S4**).

We then performed RNA-seq on five biological replicates and identified 202 transcripts that were enriched in GFP-positive CSF-cNs relative to GFP-negative cells (**Figure 4D, E, Supplemental Table S1, STAR methods**). This set contained all previously identified CSF-cN-specific transcription factors for differentiation (members of the *nkx* and *gata* family, *tal2*, *olig2)* (Shin *et al.*, 2007; Yang, Rastegar and Strähle, 2010; Petracca *et al.*, 2016b; Andrzejczuk *et al.*, 2018; Desban *et al.*, 2019), enzymes involved in GABA synthesis (*gad65/67*) (Djenoune *et al.*, 2014), the transient receptor potential channel *pkd2l1* and associated protein *pkd1l2* (Huang *et al.*, 2006; Djenoune *et al.*, 2014; Petracca *et al.*, 2016b; England *et al.*, 2017), the secreted peptides involved in arching spinal curvature (*urp1, urp2)* (Quan *et al.*, 2015; Zhang *et al.*, 2018a; Cantaut-Belarif *et al.*, 2020) and somatostatin *sst1.1* (Christenson *et al.*, 1991; Schotland *et al.*, 1996; Djenoune *et al.*, 2017).

To validate our CSF-cN transcriptome, we combined fluorescent *in situ* hybridization (FISH) with GFP antibody staining in 1 and 3 dpf *Tg(pkd2l1:GCaMP5G)* transgenic larvae for 47 of the enriched transcripts, and found 40 (85%) where gene expression was confirmed and selective to CSF-cNs (**Figure 4F-J"**, **Supplemental Figures S5, S6**). The 7 out of 47 genes whose expression was not confirmed corresponded to genes expressed at low level or to contamination from floor plate or motor neurons (the close disposition of the latter can be seen in **Figure 4G**). In agreement with CSF-cN responses to mVOCs *in vitro* (**Figure 3C-E**), orphan taste receptors from the type 2 taste receptor family responding to bitter compounds *tas2r3a,tas2r3b* were the most enriched transcripts in CSF-cNs (**Figure D, E**). We generated a double knock-out zebrafish mutant for the taste 2 receptors *tas2r3a,tas2r3b* (**Supplemental Figure S7**). We found no effect *in vitro* on the calcium response of CSF-cNs to the bitter compound DMDS (**Supplemental Figure S7**), suggesting that compensation by other taste receptors expressed in CSF-cNs may occur.

The entry of *S. pneumoniae* in the brain triggers host cells to secrete proinflammatory cytokines (such as TNF-α, IL-1, and IL-6) and chemokines (such as monocyte chemoattractant protein 1, macrophage inflammatory protein 1 α, and IL-8). Interestingly, we found that CSF-cNs express several immune-related receptors including the TNF-α receptor (*tnfrsf1a*), interferon-gamma receptors (**Figure 4E**) and several inflammasome components (*asc*, *caspa/b*, *nod1* and*2*). Altogether, our transcriptome analysis indicates that CSF-cNs

can detect bacterial compounds such as pneumolysin and metabolites acting as bitter compounds, and can respond to proinflammatory cues and chemokines.

In terms of secreted peptides and proteins, CSF-cNs expressed, in addition to the well-known Somatostatin 1.1 (Djenoune *et al.*, 2017) and Urotensin related peptides (Quan *et al.*, 2015), numerous secreted factors implicated in immune responses: *esm1*, *nppc*, *msmp2, scg2a*, *sst3, ntn1b, and txn* (**Figure 4G, H**) some of which were expressed into adulthood (**Figure 4I-J"**). We generated zebrafish knock-out mutants for the peptides *scg2a, nppc, esm1* found specifically in CSF-cNs in the trunk; none of the individual homozygous mutants differed in survival compared to their control siblings (**Supplemental Figure S9**), possibly due to redundancy among peptides.

CSF-contacting neurons upregulate transcripts for secreted factors involved in innate immunity during pneumococcal infection

To investigate changes in CSF-cN expression upon infection, we used FACS to isolate GFP-positive CSF-cNs from *Tg(pkd2l1:GAL4, UAS:GFP)* larvae and performed RNA-seq on sorted CSF-cNs at 24 hours post injection of either vehicle or *S. pneumoniae* (**Figure 5**, see **STAR methods**). We validated that transcripts previously found to be CSF-cN specific were again enriched in this dataset (*pkd2l1, pkd1l2*) and found numerous taste 1 and 2 receptor families *tas2r200.1*, *tas1r2.2*, and *tas1r2.1*, (**Figure 5A, Supplemental Table S2**). Upon infection, transcripts for CSF-cN receptors remained stable in CSF-cNs (*pkd2l1*, *pkd1l2*, *tas1r2.1, tas2r200.1, tas1r2.2*, **Figure 5B**), in line with a selective sorting of CSF-cNs. In contrast, numerous transcripts encoding immune-related secretory compounds were upregulated in CSF-cNs upon infection (76 out of 231, 33%) (**Figure 5C, D, Supplemental Table S3**; **Supplemental Table S4**): a bar code of cytokines including IL-1β and IL-8/CXCL8 (**Figure 5D** *right*) and complement factor C3 and components of the terminal pathway (C4, C6) (**Figure 5D** *left*). Note that a lack of expression of components of the classical pathway is consistent with the activation of the complement system through the alternative pathway.

Secretion from CSF-contacting neurons contributes to host defense during pneumococcal infection

To test the role of CSF-cN in host defense, we ablated CSF-cNs at 2 dpf using the nitroreductase/metronidazole transgenic system (**Figure 6A,B,D**) (**Supplemental Figure S3**) (Marquart *et al.*, 2015) or selectively blocked their secretion using the botulinum toxin B light chain (BoTxBLC) (**Figure 6C,E,F**) (Sternberg *et al.*, 2016). After metronidazole treatment (**Figure 6A, B**), nitroreductase-expressing and non-expressing larvae were infected the following day and scored for survival every 24 hours. We observed that metronidazole in

itself conferred a survival benefit in control fish, (38% survival 96 hours post infection (**Figure 6D**)). Larvae in which CSF-cNs were ablated, however, exhibited a nearly threefold decrease in survival 96 hpi (13% survival 96 hours post infection, **Figure 6D**).

As large and sustained calcium transients observed in CSF-cNs during pneumococcal infection (**Figure 2**) enable the SNARE-dependent docking and release of dense core vesicles containing peptides (Moqbel and Coughlin, 2006; de Jong *et al.*, 2008; Murray and Stow, 2014; Cropper *et al.*, 2018), we tested the role of SNARE-dependent neurosecretion from CSF-cNs during infection. By cleaving VAMP2, BoTxBLC effectively prevents vesicular fusion and release (Sternberg *et al.*, 2016) (Brunger, Jin and Breidenbach, 2008). In *Tg(pkd2l1:GAL4, UAS:BoTxBLC-GFP)* transgenic larvae in which BoTxBLC was selectively expressed in CSF-cNs (**Figure 6C**), the survival following infection at 2 dpf was reduced compared to their control siblings (15% compared to 31.7% survival at 96 hpi, **Figure 6E**). Accordingly, more live bacteria were observed 24 hours after infection in transgenic larvae in which CSF-cN neurosecretion was altered compared to control siblings (**Figure 6F**). Altogether, our results suggest that CSF-cNs promote host defense in response to pneumococcal meningitis via extracellular secretion.

DISCUSSION

In a meningitis model in larval zebrafish, we show here that neurons in contact with the CSF respond vigorously to infection with *S. pneumoniae* and contribute to innate immunity.

Detection of pathogenic bacteria proliferating in the cerebrospinal fluid

We hypothesized that CSF-cNs could be directly or indirectly activated by chemical cues secreted by pathogenic bacteria. Our results are consistent with a direct detection by CSF-cNs of metabolites and virulence factors of *S. pneumoniae.* We found that CSF-cNs express orphan taste 2 receptors for bitter compounds and showed *in vitro* that these cells respond to microbial metabolites acting as bitter compounds, and to pneumolysin, a cytolysin released by pneumococci during growth. The CSF-cN response to bitter compounds was stronger than that to pneumolysin. These observations suggest that bacterial metabolites could directly trigger the response in sensory neurons we observed *in vivo*. Our multiple transcriptome analysis revealed other receptors (including the receptor to TNF-α, IL-13 and IL-14) that could also contribute to the activation of CSF-cNs based on proinflammatory cues and cytokines released by host cells during an infection. Remarkably, the response to

pathogenic bacteria occurs in a subset of CSF-cNs, manifesting as long and massive calcium transients. The only other cell type in contact with the CSF in the spinal cord, ependymal radial glia, do not respond similarly. This is presumably because (1) they lack the receptors for bitter compounds or (2) their substantially lower excitability makes them less responsive (less depolarization and potentially calcium entry) to membrane pore formation (input resistance in the 10 MΩ range vs. 1-15 GΩ for CSF-cNs) (Orts-Del'Immagine *et al.*, 2012, 2020; Sternberg *et al.*, 2018). These calcium transients unlikely reflect a pre-apoptotic calcium phenomenon, as they are recurrent in individual cells over many hours without apparent cell death. *In vivo*, heat-killed bacteria and non-virulent bacteria failed to elicit as strong of a response as we observed during live infection suggesting that metabolites released by living bacteria proliferating in the CSF, or proinflammatory cues from host cells infected by the pathogenic bacteria, are necessary to activate CSF-cNs. Secretion of bitter compounds by bacteria has been shown to activate chemosensory neurons in the lung epithelium via type 2 taste receptors (Allardyce *et al.*, 2006; Tizzano *et al.*, 2010; Filipiak *et al.*, 2012; R. J. Lee, Chen, *et al.*, 2014; R. J. Lee, Kofonow, *et al.*, 2014; Verbeurgt *et al.*, 2017; Freund *et al.*, 2018). We show here that at least two of these bitter compounds, DMDS and 2-pentanone, known to be secreted by *S. pneumoniae,* can strongly activate CSF-cNs in primary cultures. DMDS is also known to be secreted by *Neisseria meningitidis*, *Haemophilus influenzae* and *Listeria monocytogenes*, all major causes of community-acquired bacterial meningitis (Allardyce *et al.*, 2006; Filipiak *et al.*, 2012; Yu *et al.*, 2015; van de Beek *et al.*, 2016).

Promotion of host survival during a bacterial infection of the central nervous system

During an infection with *S. pneumoniae*, CSF-cNs confer a threefold survival benefit to the host, when survival of zebrafish larvae without CSF-cNs was compared to control siblings. Moreover, the selective blockage of neurosecretion in CSF-cNs also led to a reduction of survival in infected larvae. Accordingly, we found an elevated bacterial load in larvae where neurosecretion had been impaired. Although we did not monitor *in vivo* exocytosis at the CSF-cN membrane in the context of infection, our results from calcium imaging, transcriptome during infection and survival upon silencing of CSF-cN release are all consistent with the hypothesis that upon activation, CSF-cNs release compounds that promote survival of the host (see **Graphical Abstract**). CSF-cNs can release the neuropeptides that they largely express at baseline (*somatostatin 1.1*, *secretogranin 2a*, *nppc* among others, see **Figure 4**) together with the secreted compounds whose expression increased during an infection (**Supplemental Table S3, Supplemental Table S4**), including cytokines and complement factors (**Figure 5C, D**). The mechanisms by which CSF-cNs

promote host survival may involve the secretion of antimicrobial peptides such as secretogranin 2a (Shooshtarizadeh *et al.*, 2010) or the release of factors modulating inflammatory signaling (*msmp2*, *esm1, txn, nppc*, *sst3*, *ntn1b*) (Bertini *et al.*, 1999; Krantic, 2000; Dalm *et al.*, 2003; Ly *et al.*, 2005; Chen *et al.*, 2014; Pei *et al.*, 2014; W. Lee *et al.*, 2014; Tomasiuk *et al.*, 2016). Knocking out single peptides did not lead to a decrease in survival in our infection model, likely due to redundancy (Jakutis and Stainier, 2021). Combining knockouts of multiple peptides may be needed to observe an effect on survival rates, but is out of the scope of this study. Since large calcium transients such as those observed in CSF-cNs during pneumococcal infection are typically necessary for neurosecretory cells to release the content of dense core vesicles in which peptides and secreted proteins are loaded (Cropper *et al.*, 2018), we speculate that the large transients observed in CSF-cNs during the infection induce secretion. The reduced survival that we observed for zebrafish larvae with impaired CSF-cN secretion supports this hypothesis. Taken together, these data suggest that CSF-cNs play an important role in CNS defense by detecting the presence of bacteria and secreting factors that boost the innate immune responses.

Limitations of the Study

First, our observations that pneumolysin and bacterial metabolites elicit calcium transients in CSF-cNs *in vitro* suggest that these molecules may be involved in the detection of *S. pneumoniae* by CSF-cNs *in vivo*. Accordingly, we identified multiple orphan bitter taste receptors in CSF-cNs that could mediate the response to bacterial metabolites. However, CSF-cN response to bitter compounds in culture was not abolished in double taste receptor mutants. Therefore, we were not able to demonstrate whether the CSF-cN response during pneumococcal infection mainly relied on these pathways, neither could we identify all the chemical cues released by bacteria *in vivo* that could underlie CSF-cN activation.

Second, consistent with an induction of CSF-cN neurosecretion during infection, larval zebrafish exhibited a dorsal arching posture, in a similar manner that has been described upon injection of CSF-cN-specific peptides from the urotensin family (Zhang *et al.*, 2018a; Cantaut-Belarif *et al.*, 2020; Lu *et al.*, 2020). Upon pneumococcal infection of the CNS, we showed that CSF-cNs upregulated the expression of secreted factors (cytokines and complement factors). Together with the evidence that blocking secretion from CSF-cNs reduced host survival and increased bacterial loads, our results point towards an activation of secretion of CSF-cNs during infection to promote innate immunity. However, we did not monitor neurosecretion *in vivo*. Future studies will be needed to monitor vesicular fusion associated with CSF-cN neurosecretion *in vivo*.

Third, our results indicate that ciliated sensory neurons in contact with the CSF are diverse in their response to pathogenic bacteria *in vivo*, although they homogenously responded to pneumolysin and bitter compounds *in vitro*. This discrepancy suggests that the CSF in the central canal is a heterogeneous medium, where pneumococci may differ locally in terms of density or state during an infection. Although estimating the density and movements of bacteria is theoretically possible *in vivo* using confocal microscopy using mCherry-positive bacteria, monitoring two channels to collect the information of CSF-cN activation does lead to phototoxicity and subsequent, silencing of activity in CSF-cNs. This experiment could therefore not be achieved with the fluorescent sensors available for monitoring calcium and bacteria simultaneously *in vivo*.

Finally, our study does not address the diversity of pathogens that can cause CNS infection. In addition to response to pneumococcal infection, we have evidence that CSF-cNs also respond to *L. monocytogenes* (the third most common cause of community-acquired bacterial meningitis (van de Beek *et al.*, 2021)), as well as to cells infected by virus (data not shown). Future studies should address mechanisms by which CSF-cNs can respond to such diverse pathogens.

Similarity with peripheral sensory neurons involved in proprioception and pain

CSF-cNs are located in an ideal position to detect pathogenic bacteria invading the CSF, as well as to modulate immunity in the central nervous system by interacting with resident microglia and circulating leukocytes recruited in the ventricular space. Our discovery that *in vivo,* central sensory neurons are activated by live pathogens in the CSF and that they confer a survival benefit to the host recalls recent *in vitro* results on peripheral nociceptive sensory neurons activated by bacteria (Chiu *et al.*, 2013; Kashem *et al.*, 2015) or nodose ganglia (Talbot *et al.*, 2015). Dorsal root ganglia (DRG) are anatomically positioned to detect pathogens entering the body following injury. The similarity in sensory and secretory properties between nociceptive peripheral neurons and interoceptive CSF-cNs is important: (1) DRG, like CSF-cNs, are activated by bacterial toxins as well as other bacterial products (Chiu *et al.*, 2013); (2) upon activation, both DRG and CSF-cNs secrete immunomodulatory neuropeptides (Chiu *et al.*, 2013; Kashem *et al.*, 2015; Talbot *et al.*, 2015; Foster *et al.*, 2017). Our results therefore emphasize that sensory neurons are tuned throughout the nervous system (peripheral and central) to detect intruding pathogens and promote host survival. One specificity of CSF-cNs lies in their polymodal functions: these neurons are mechanosensory cells activated by spinal stretch (Böhm *et al.*, 2016; Sternberg *et al.*, 2018), influencing posture (Hubbard *et al.*, 2016; Wu *et al.*, 2021) and leading to dorsal arching by release of urotensin related peptides (Quan *et al.*, 2015; Sternberg *et al.*, 2016; Zhang *et al.*,

2018a; Cantaut-Belarif *et al.*, 2020). We show here that CSF-cN sensory role can be expanded to the chemical detection of pathogenic bacteria, and provide a potential mechanism by which CSF-cN activation could lead to postural defects associated with meningeal infection. Further investigations will be necessary to identify whether this effect is a result of direct antimicrobial action on CSF-cNs, increased recruitment of circulating leukocytes, or regulation of inflammatory signaling.

ACKNOWLEDGMENTS

We wish to thank Prof. Hitoshi Okamoto, Prof. David Lyons and Prof. Wilbert Bitter for fruitful discussions, Bethany Berry for her generous gift of *gfap* promoter construct (originally cloned by Brooke Gaynes), Prof. Jan-Willem Veening for providing the *S. pneumoniae* D39 hlpA-mCherry strain, Yannick Marie, Romain Daveau and Justine Guégan for their critical assistance in completing the transcriptomic analysis, as well as Cora Chadick, Jeroen Kole, Coen Kuijl and Theo Verboom for technical assistance. CW was a New York Stem Cell Foundation (NYSCF) Robertson Investigator (grant #NYSCF-R-NI39). This work was supported by the Fondation Schlumberger pour l'Education et la Recherche (FSER/2017), the ERC Starting Grants "Optoloco" #311673, ERC PoC 'ZebraZoom' #825273 and "MeninGene" #281156, the HFSP Program Grants #RGP0063/2014 and #RGP0063/2017 both coordinated by CW. DvdB was supported by a ZonMw VICI grant #391819627. AP was further supported by an EMBO long term fellowship (ALTF-549-2013) and a Research in Paris grant from the Marie de Paris. LDe was supported by the French Ministry of Higher Education and Research doctoral fellowship. MD was supported by a PhD fellowship from the Sorbonne Université Ecole Doctorale ED3C.

AUTHOR CONTRIBUTIONS

Project was conceived by CW, CV-G, AP, KKJ, and DvdB. AP, LDe, KKJ, JR performed FACS and transcriptome analysis with help of FXL for statistical analysis. AP, KKJ and CW combined bacterial infections with calcium imaging. HM received advice of YCB to perform primary culture experiments and collected the calcium imaging data *in vitro*. AP, KKJ, FQ and CW performed the behavioral experiments and postural analysis. AP, HM, FQ, LDe, and LDj performed histochemistry and *in situ* gene expression data. MD counted CSF-cNs. JPL and PLB provided advice on the transcriptome analysis. AP, KKJ, FQ and SS performed survival analysis. CW, AP, KKJ, HM, FQ generated figures. CW, AP, KKJ, CV-G, DvdB wrote the manuscript with the inputs of all authors.

Declaration of interests

The authors declare no competing interests.

FIGURE TITLES AND LEGENDS

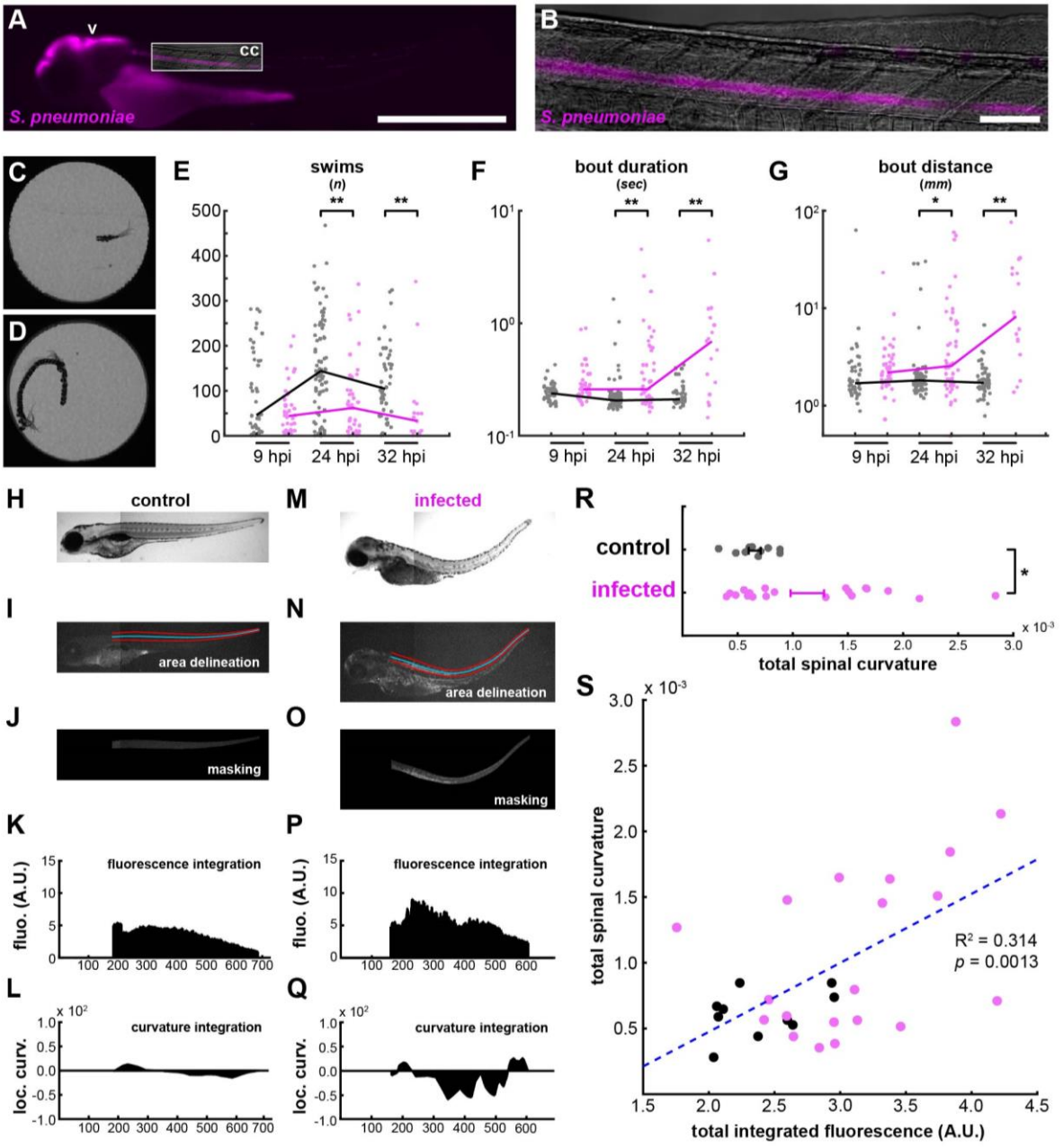

Figure 1. Infection induces behavioral changes and spinal curvature reminiscent of clinical symptoms of pneumococcal meningitis. (A) Fluorescence image of a larva infected with mCherry-labelled *S. pneumoniae* at 2 dpf and imaged at 24 hours post injection (hpi) showing colonization of the brain ventricle (v) and central canal (cc). Box indicates field of view for **(B)**. Scale: 500 µm. **(B)** Higher magnification image of the central canal colonized with mCherry-labelled *S. pneumoniae*. Scale: 50 µm. **(C)** Representative motion overlay of a detected swim bout from a larva injected with vehicle. Most bouts are short forward swims. **(D)** Representative motion overlay of a detected swim bout from a larva infected with *S. pneumoniae*. These swim bouts tend to be much longer in duration and distance. **(E)** Quantification of the overall number of bouts in PBS-injected (grey) and *S. pneumoniae*-infected (magenta) fish at three different time points post infection. At later

infection time points, infected fish swim substantially less often (** = $p < 0.01$). **(F)** Quantification of bout duration in control vs. infected fish. As infection progresses, swim bouts become substantially and progressively longer in infected fish while generally remaining stable in controls. **(G)** Quantification of bout distance in control vs. infected fish. Similar to **(E)**, infected fish swim substantially farther in a given bout than control fish (* = $p < 0.05$). **(H)** Brightfield image of a PBS-injected larva at 3 dpf. **(I)** Spinal cord area (here in the control larva from **I**) was defined by manual tracing (red lines), from which a smoothing spline curve was fit (blue line). **(J)** The resulting boundaries were used to isolate a masked portion of the red channel. Since this larva was not injected with fluorophores, this represents autofluorescence. **(K)** The resulting image patch was summed along the x-axis to derive a fluorescence plot. **(L)** Curvature was locally determined along the x-axis and plotted. Positive values indicate downward curvature, negative values indicate upward curvature. **(M)** Brightfield image of a larva injected with *S. pneumoniae* at 2 dpf and imaged at 32 hours post injection. Note the strong upward tail curvature. **(N)** Similar spinal cord delineation as in **(M)**, but applied to the larva in **(K)**. **(O)** Red channel fluorescence from the masked spinal cord of the infected larvae. Since this embryo was injected with mCherry-labeled *S. pneumoniae*, this plot provides a visual assessment of infection progression. **(P)** Similar fluorescence plot as in **(K)**. Note that fluorescence is overall higher than in **(K)**. **(Q)** Similar curvature plot as in **(L)**. The larva's strong upward spinal curvature is reflected in the large downward deflection of the curvature plot midway along the anterior/posterior axis. **(R)** The absolute value of the spinal curvature was summed over x for all control and infected fish. Infected fish exhibit greater spinal curvature ($p = 0.039$). **(S)** Spinal red channel fluorescence was summed over x for all fish and plotted against overall curvature. In infected fish, there is a positive correlation between spinal fluorescence (i.e. implied infection progression) and spinal curvature ($R^2 = 0.314$, $p = 0.0013$).

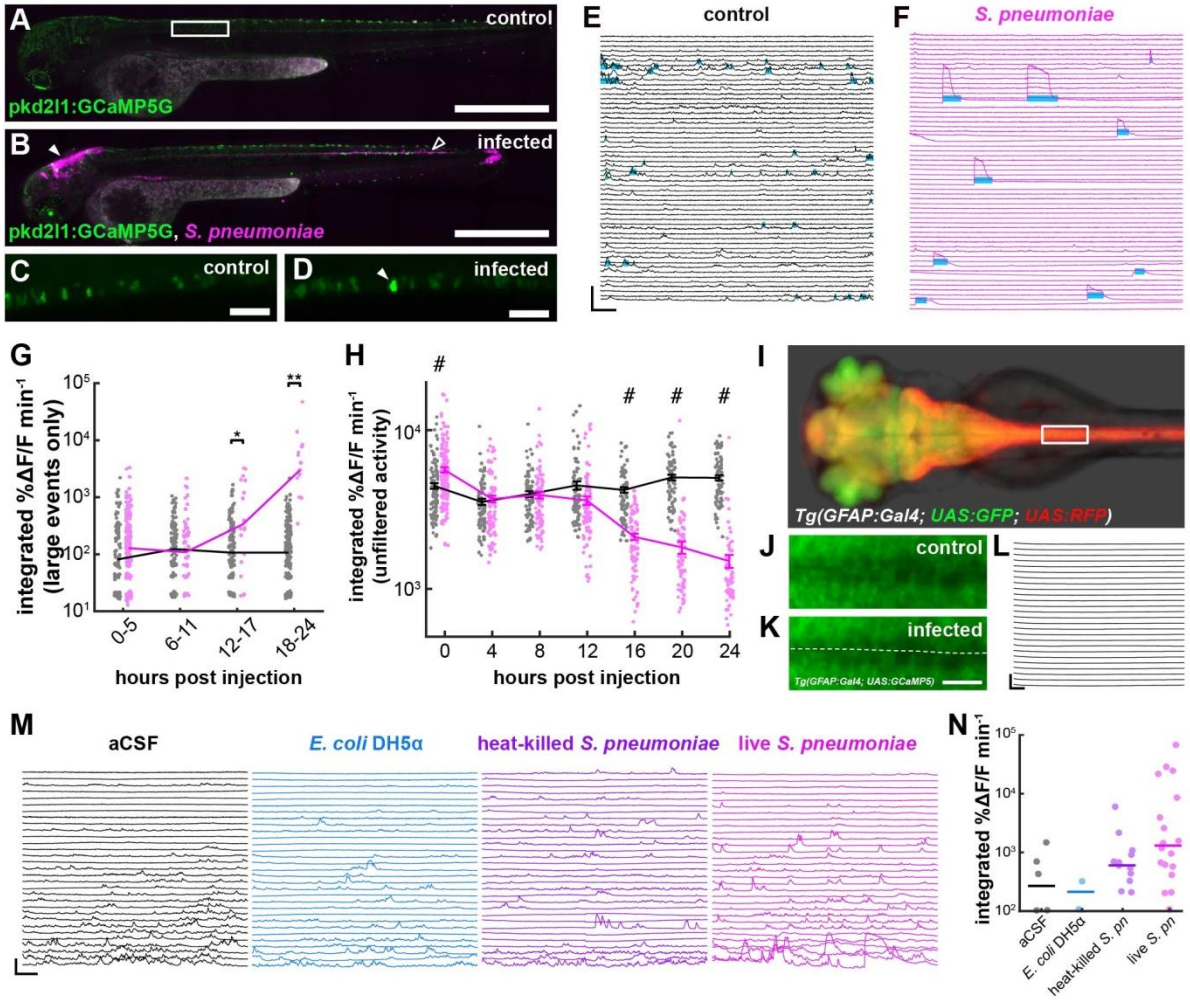

Figure 2. Activity of CSF-cNs drastically changes in response to the invasion of *Streptococcus pneumoniae* into the CSF. (A) Untreated 3 dpf *Tg(pkd2l1:GCaMP5G)* larva. Box indicates field of view for **(C, D)**. Scale: 500 µm. **(B)** Sibling larva, 24 hours after injection of fluorescently-labeled *S. pneumoniae* into the hindbrain ventricle (HBV, indicated by filled arrowhead); empty arrowhead indicates extent of bacterial proliferation. **(C)** Higher magnification image of control CSF-cN calcium imaging. Scale: 50 µm. **(D)** Comparable image from an infected larva with *S. pneumoniae*. Arrowhead indicates a CSF-cN undergoing a high-amplitude transient. **(E)** Ca^{2+} activity plots of uninfected CSF-cNs 21 hours after the beginning of the experiment. Cyan bars indicate detected long lasting high-amplitude events. Vertical scale: 500% ΔF/F, horizontal scale: 20 seconds. **(F)** Similar plots from CSF-cNs of infected larvae showing high-amplitude transients. **(G)** Quantification of software-detected high-amplitude transients in control (grey) and *S. pneumoniae*-infected (magenta) larvae. Large transients appear 12 hours after infection (Lines represent median values, Wilcoxon signed-rank test, * = $p< 0.0125$, ** = $p< 0.0063$). **(H)** Integrated Ca^{2+} activity in CSF-cNs in control (grey) and infected (magenta) larvae over 24 hours of infection. Overall activity undergoes a significant decline over the course of infection (2-factor ANOVA, injection factor F = 124.36, $p = 1.61 \times 10^{-27}$, Scheffé post-hoc testing, # = $p< 0.05$, data are represented as mean ± S.E.M.). **(I)** Dorsal view of 3dpf *Tg(gfap:GAL4, UAS:GFP, UAS:RFP)* larva. White box indicates orientation and position of

image in **(J)** and **(K)**. **(J)** Representative optical plane in vehicle-injected fish used for Ca^{2+} imaging. **(K)** Similar plane from infected fish. Dashed line, cc = central canal. Scale bar: 50 µm. **(L)** Ca^{2+} traces from single ROIs at 22 hours post-infection. Calcium transients, large or otherwise, are never observed using this transgenic line. Vertical scale: 250% ΔF/F, horizontal scale: 50 seconds. **(M)** Individual CSF-cN Ca^{2+} traces from 2 dpf zebrafish injected with aCSF, DH5α *Escherichia coli*, heat-killed *S. pneumoniae* and live *S. pneumoniae*. Injection with live *S. pneumoniae* elicits by far the largest transients. Vertical scale: 200% ΔF/F, horizontal scale: 25 seconds. **(N)** Quantification of software-detected large transients from the four conditions in **(M)**, lines represent median values. More transients are observed in live infected fish than the other three conditions (chi-square test, p = 6.28E-16).

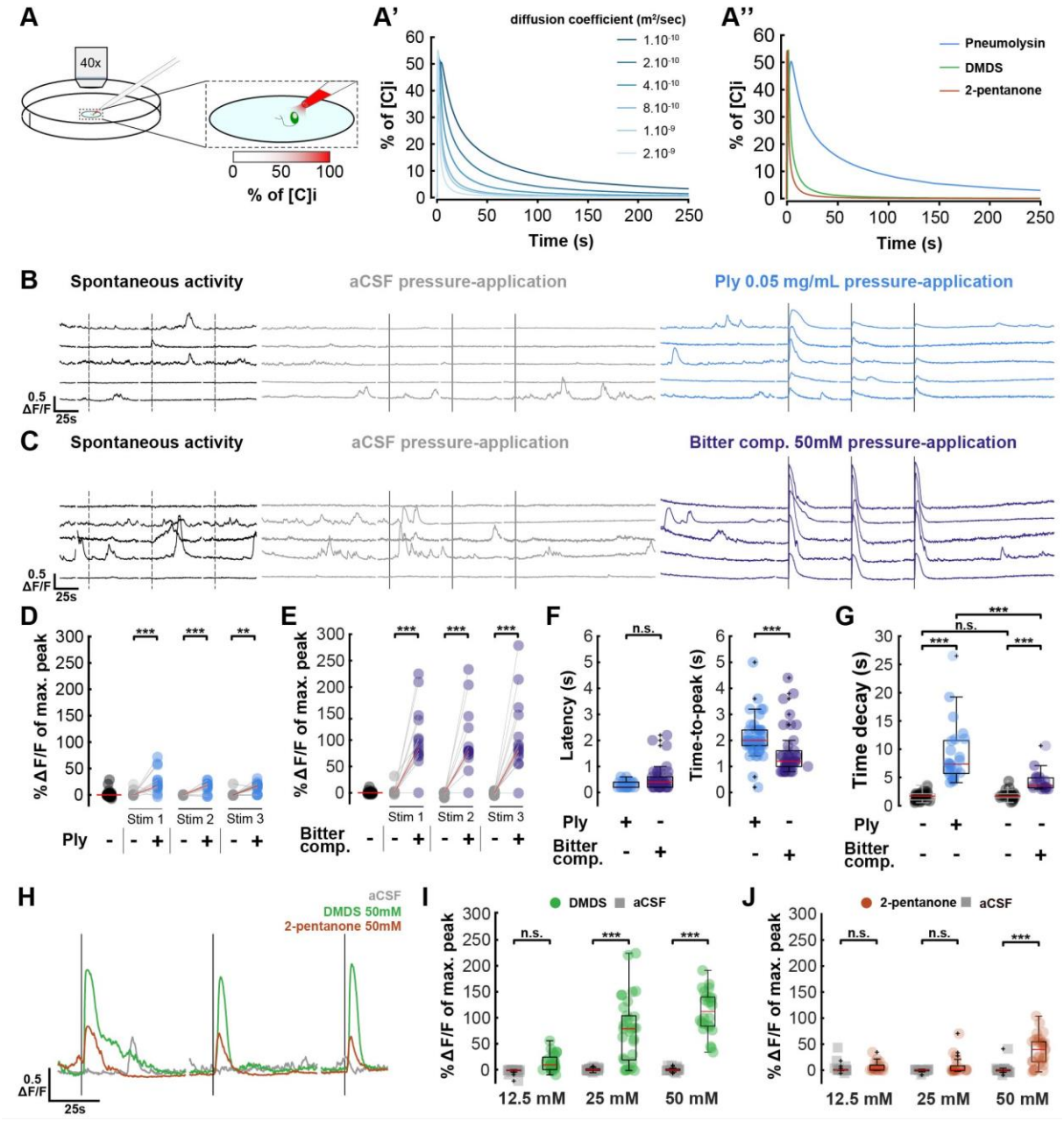

Figure 3. CSF-cNs respond *in vitro* to pneumolysin and bitter compounds. (A) Simulations of *in vitro* CSF-cN stimulation. **(A)** Schematic view of the *in vitro* stimulation experimental set up combining calcium imaging at 40x, 5Hz and stimulation of a CSF-cN with a gradient of molecule. **(A')** Simulation of the concentration of molecule sensed by a CSF-cN for a range of coefficient of diffusions (from 1.10^{-10} to 2.10^{-9} m^2/s); [C]i corresponds to initial concentration in the stimulation pipette. **(A'')** Simulation of the concentration of pneumolysin (Ply), dimethyl disulfide (DMDS) and 2-pentanone, coefficients of diffusion: 1.10^{-10}, 1.10^{-9} and 2.10^{-9} m^2/s respectively; [C]i corresponds to initial concentration in the stimulation pipette. **(B)** Representative individual *in vitro* CSF-cN Ca^{2+} traces from no stimulation control (left, dark), 3 successive 1-second stimulations of aCSF (middle, grey), and 3 successive 1-second stimulations of 0.05 mg/mL pneumolysin (Ply) (right, blue). Dark lines correspond to 1-second stimulations, dashed lines correspond to putative 1-second

stimulations during spontaneous activity. Vertical scale: 0.5 ΔF/F, horizontal scale: 25 seconds. **(C)** Representative individual *in vitro* CSF-cN Ca^{2+} traces from no stimulation control (left, dark), 3 successive 1-second stimulations of aCSF (middle, grey), and 3 successive 1-second stimulations of 50 mM bitter compounds mix (right, purple). Bitter compounds mix: acetone, 2-butanone, 2-pentanone, 2-methylpropanal, dimethyl disulfide (DMDS). Dark lines correspond to 1-second stimulations, dashed lines correspond to putative 1-second stimulations during spontaneous activity. Vertical scale: 0.5 ΔF/F, horizontal scale: 25 s. **(D)** Quantification of calcium transients' amplitude after pneumolysin pressure-application. Paired line plots showing responses of individual cells to absence of stimulation (corresponding to spontaneous activity, on the left in black circle), or 3 successive 1-second stimuli of aCSF (grey circle) versus 0.05 mg/mL pneumolysin (Ply, blue circle). 2-factor ANOVA, treatment factor F = 66.185, $p = 1.47 \times 10^{-12}$, Turkey HSD post-hoc testing, *** = $p < 0.001$. Red bar: median ΔF/F (median spontaneous activity = 0.03%; median Ply = 17.49% and median aCSF = 0.19% for stimulation 1; median Ply = 18.78% and median aCSF = 0.03% for stimulation 2; median Ply = 17.20% and median aCSF = -0.20% for stimulation 3), 16 responding cells out of 17. **(E)** Quantification of the amplitude and kinematics of calcium transients after pressure-application of bitter compounds. Paired line plots showing responses of individual cells to absence of stimulation (corresponding to spontaneous activity, on the left in black circle), or 3 successive 1-second stimuli of aCSF (grey circle) versus 50 mM bitter compounds mix (purple circle). 2-factor ANOVA, treatment factor F = 116.762, $p < 2.0 \times 10^{-16}$, Turkey HSD post-hoc testing, *** = $p < 0.001$. Red bar: median ΔF/F (median spontaneous activity = 0.10%; median bitter compounds = 87.26% and median aCSF = 0.05% for stimulation 1; median bitter compounds = 78.85% and median aCSF = -0.13% for stimulation 2; median bitter compounds = 83.64% and median aCSF = -0.50% for stimulation 3), 15 responding cells out of 15. **(F)** Quantification of latency and time-to-peak after pneumolysin (blue circle) or bitter compounds in mix (purple circle) stimuli. Red bar: median (for latency, median Ply = 0.2s and median bitter compounds = 0.4s, $p > 0.05$; for time-to-peak, median Ply = 2s and median bitter compounds = 1.2s, $p < 1 \times 10^{-6}$; Kolmogorov-Smirnov test). **(G)** Quantification of time decay for spontaneous activity (black circle) or after pneumolysin (blue circle) or bitter compounds in mix (purple circle) stimuli. Red bar: median (on the left, median Ply = 7.36s and median spontaneous activity = 1.71s, $p < 1 \times 10^{-11}$; on the right, median bitter compounds = 3.59s and median spontaneous activity = 1.69s, $p < 1 \times 10^{-6}$, Ply and bitter compounds decays are significantly different, $p < 1 \times 10^{-4}$; Kolmogorov-Smirnov test). Significant longer time decay for Ply compared to bitter compounds in mix is probably due to a smaller coefficient of diffusion as shown in panel **A''**. **(H)** Illustration of calcium transients after pressure-application of DMDS and 2-pentanone. Representative individual *in vitro* CSF-cN Ca^{2+} traces from 3 successive 1-second stimulations with either aCSF (grey), DMDS 50 mM (green) of 2-pentanone 50 mM (brown). Dark lines correspond to 1-second stimulations. Vertical scale: 0.5 ΔF/F, horizontal scale: 25 s. **(I)** Quantification of calcium transients after aCSF (grey circle) or dimethyl disulfide (DMDS, green circle) stimuli. 2-factor ANOVA, treatment factor F = 170.58, $p < 2.0 \times 10^{-16}$, concentration factor F = 29.43, $p = 1.66 \times 10^{-11}$, Turkey HSD post-hoc testing, *** = $p < 0.001$, n.s. = not significant. Red bar: median ΔF/F (median 12.5 mM DMDS = 9.44% and median aCSF = -1.20%, 6 responding cells out of 8; median 25 mM DMDS = 78.96% and median aCSF = -

0.26%, 8 responding cells out of 10; median 50 mM DMDS = 112.09% and median aCSF = -0.54%, 8 responding cells out of 8). **(J)** Quantification of calcium transients after aCSF (grey circle) or 2-pentanone (brown circle) stimuli. 2-factor ANOVA, treatment factor F = 53.48, p = 2.67 x 10^{-11}, concentration factor F = 13.89, p = 3.53 x 10^{-6}, Turkey HSD post-hoc testing, *** = p < 0.001, n.s. = not significant. Red bar: median $\Delta F/F$ (median 12.5 mM DMDS = 2.19% and median aCSF = 0.14%, 4 responding cells out of 6; median 25 mM DMDS = 0.63% and median aCSF = 0.04%, 3 responding cells out of 6; median 50mM DMDS = 39.72% and median aCSF = -0.39%, 9 responding cells out of 10).

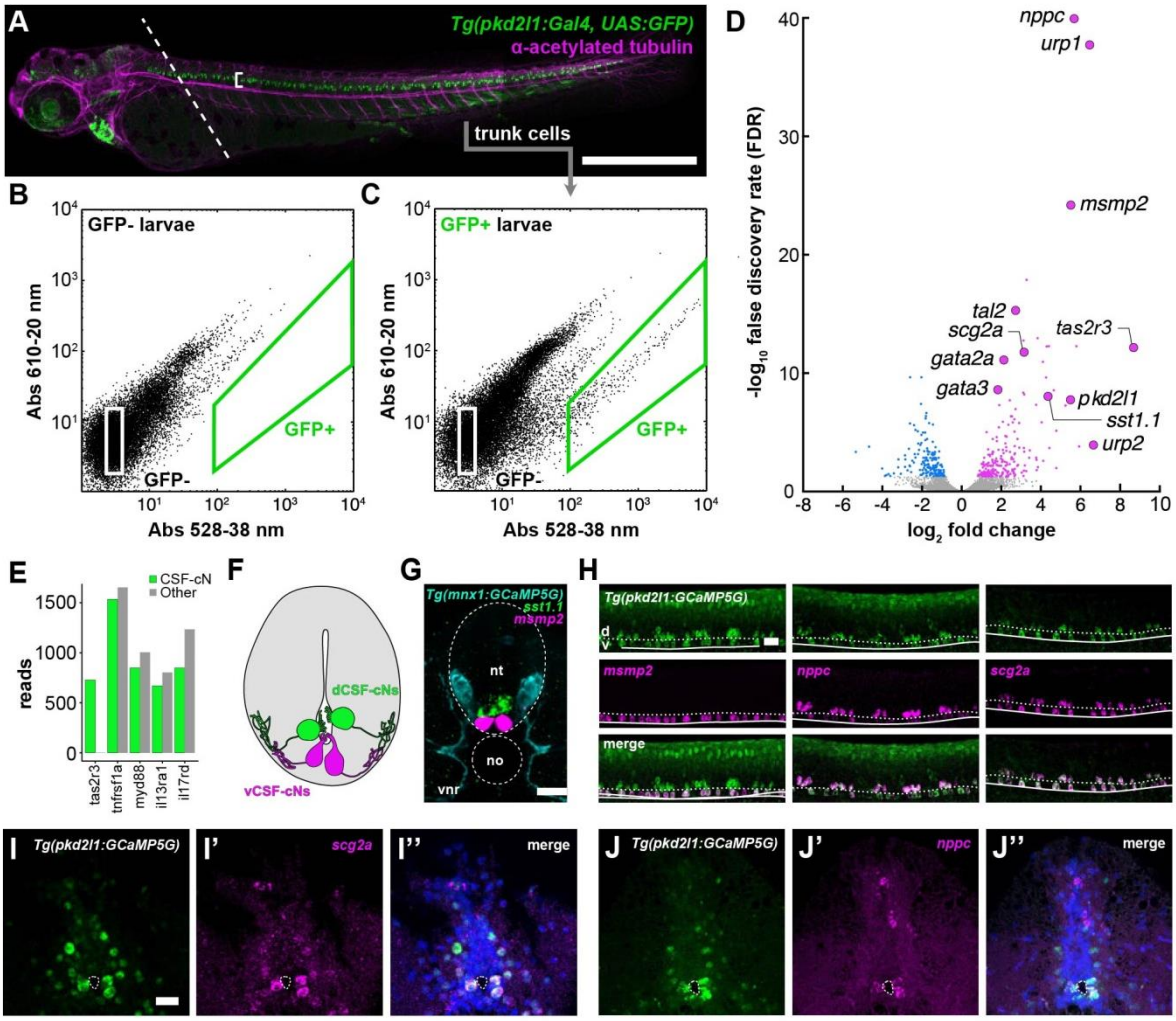

Figure 4. The CSF-cN transcriptome reveals the expression of taste receptors and immune-related secreted factors. **(A)** 3 dpf zebrafish *Tg(pkd2l1:GAL4, UAS:GFP)* larva immunostained for GFP (green) and acetylated tubulin (magenta). Dashed line indicates plane of decapitation prior to dissociation (anterior tissues were discarded to exclude labeled cells in brain and heart); bracket indicates CSF-cN domain. Scale: 500 µm. **(B)** Calibration FACS plot from non-transgenic siblings. **(C)** FACS plot from a typical dissociation of cells from transgenic larvae. A small fraction (~0.2% of input) of cells is green-shifted. **(D)** Volcano plot of all RNA-seq replicates: 202 transcripts were enriched in CSF-cNs. **(E)** Quantification of reads for selected immune-related receptors in both GFP+ CSF-cNs and GFP- (i.e., all other) cells. **(F)** Schematic representation of a transverse section of the spinal cord and central canal showing the disposition of dorsolateral CSF-cNs (dCSF-cNs, green) and ventromedial CSF-cNs (vCSF-cNs, magenta). **(G)** A mixed fluorescent *in situ* hybridization/immunofluorescent stain showing the disposition of motor neurons (cyan, *Tg(mnx1:GCaMP5)*), dCSF-cNs (green, *sst1.1*), and vCSF-cNs (magenta, *msmp2*). Scale: 50 µm. **(H)** Fluorescent *in situ* hybridization reveals that the putative immune-related secreted factors *msmp2*, *nppc*, and *scg2a* are expressed in CSF-cNs. Scale: 50 µm. **(I-I'')** Transverse section of adult *Tg(pkd2l1:GCaMP5G)* spinal cord; expression of *scg2a* is specific to CSF-cNs. Scale: 50 µm. **(J-J'')** Adults continue to express *nppc* and *scg2a* in CSF-cNs.

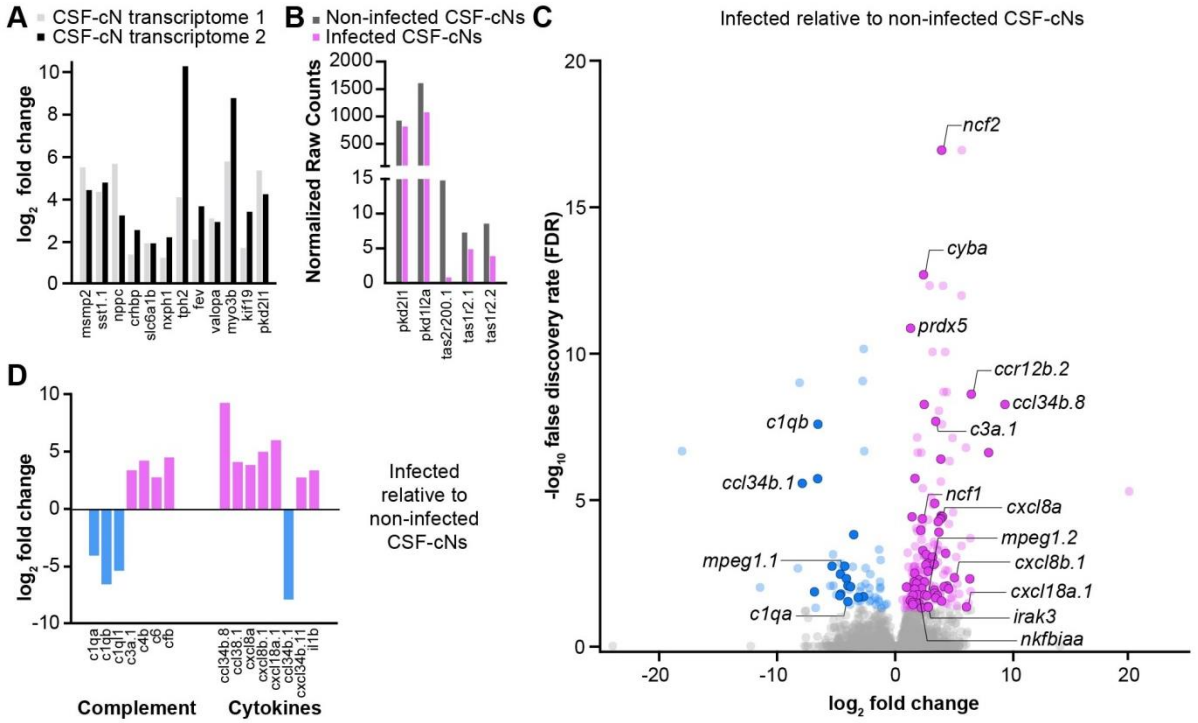

Figure 5. RNA-seq shows upregulation of complement system of the alternative and terminal pathway as well as cytokines in CSF-cNs during *S. pneumoniae* infection. (A) Log fold change bar plot comparing enrichment of known CSF-cN transcripts in the GFP+ fraction compared to control GFP- cells in the original differential transcriptome 1 (gray bars, see **Table S1**, **Figure 4**) and subsequent transcriptome 2 for non-infected larvae (black bars, see **Table S2**). **(B)** A plot of raw reads comparing selected receptors in non-infected (gray bars) and infected (pink bars) CSF-cNs showing that the expression of receptors that are specifically enriched in CSF-cNs (*pkd2l1, pk1l2* and *taste receptors*) remains stable. **(C)** Volcano plot comparing the expression of transcripts in infected CSF-cNs relative to uninfected CSF-cNs. Transcripts for several immune-related secretory compounds are differentially expressed. **(D)** Log fold change bar plot of selected immune-related transcripts corresponding to complement system and cytokines from the same data as in **(B)**. We observe significant upregulation of complement system of the alternative (C3) and terminal (C4, C6) pathway (left side) as well as cytokines (right side).

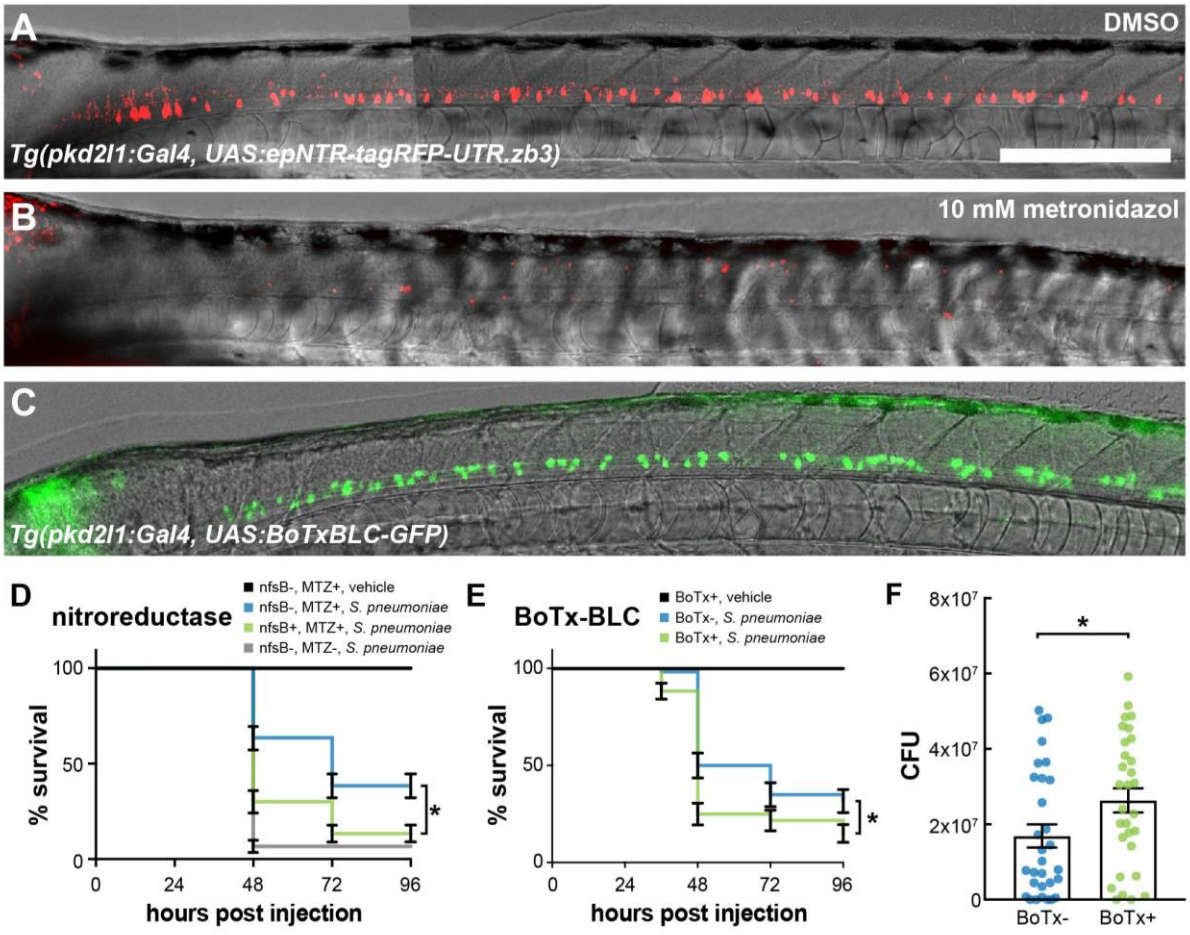

Figure 6. Secretory activity of CSF-cNs confers a survival benefit during pneumococcal meningitis. (A) *Tg(pkd2l1:GAL4; UAS:epNTR-tagRFPT-UTR.zb3)* larva at 3 dpf following 24 hours of incubation in 0.1% DMSO. Scale: 500 µm. **(B)** Sibling larva incubated for the same time period in 10 mM metronidazole (MTZ). All tagRFP^{+} CSF-cNs are lost. **(C)** Expression of BoTxBLC-GFP in the *Tg(pkd2l1:GAL4; UAS:BoTxBLC-GFP)* larva at 3 dpf. **(D)** Survival curves of *Tg(pkd2l1:GAL4, UAS:epNTR-tagRFPT-UTR.zb3)* (nfsB) larvae and their siblings when exposed to metronidazole or DMSO from 1 to 2 dpf, washed with fish facility water, and subsequently infected with 4000 CFU *S. pneumoniae*. Metronidazole alone slightly protects larvae against infection by *S. pneumoniae* (compare blue and grey lines, Log-rank test, p< 0.0001). However, metronidazole-mediated ablation of CSF-cNs confers a large survival deficit (compare blue and green lines, Log-rank test, p = 0.0002). The survival data represent the mean ± SEM of three individual experiments with n = 20 larvae per group (total n = 60 per group). **(E)** Survival curves of *Tg(pkd2l1:GAL4, UAS:BoTxBLC-GFP)* (BoTx) larvae (green line) and non-transgenic sibling controls (blue line) injected with ~300 CFU *S. pneumoniae* D39 wild-type strain into the hindbrain ventricle at 2 days post fertilization reveal that BoTx-expressing larvae exhibit higher mortality rates (Log-rank test, p = 0.0065). The survival data represent the mean ± SEM of three individual experiments with n = 20 larvae per group (total n = 60 per group). **(F)** *Tg(pkd2l1:GAL4, UAS:BoTxBLC-GFP)* (referred to as 'BoTx') larvae (green line) exhibit higher bacterial loads at 24 hours injection as compared to non-transgenic sibling controls. (unpaired

t-test, p = 0.0368). Each dot represents a single larva. Error bars = mean ± SEM of three individual experiments with n = 10 larvae per group (total n = 30 per group).

STAR METHODS

CONTACT FOR REAGENT AND RESOURCE SHARING

Further information and requests for resources and reagents should be directed to and will be fulfilled by the Lead Contact, Claire Wyart (claire.wyart@icm-institute.org).

EXPERIMENTAL MODEL AND SUBJECT DETAILS

Zebrafish handling and husbandry. Zebrafish adults were maintained on a 14h/10h light/dark cycle and fed using a combination of Gemma Micro 500 diet and cultured rotifers (Lawrence, 2011, 2016). All embryos and larvae described in this study were obtained by natural mating procedures. Animals were used for experiments until no later than 6 days post fertilization. All experimental procedures comply with European animal welfare regulations.

Bacterial strains and growth conditions. *Streptococcus pneumoniae* D39 serotype 2 wild-type strain or the isogenic red fluorescent *S. pneumoniae* D39 mutant strain, in which mCherry is fused to the histone-like protein HlpA, was grown on Columbia agar supplemented with 5% (v/v) defibrinated sheep blood (Biomerieux; 43049) at 37°C in a humidified atmosphere with 5% CO_2 (Avery, MacLeod and McCarty, 1979; Beilharz *et al.*, 2015; Slager, Aprianto and Veening, 2018). Before injection, *S. pneumoniae* was grown to mid log phase in C+Y medium (Martin *et al.*, 1995) at 37°C. Bacteria were subsequently harvested by centrifugation (6000 rpm, 10 min) and suspended in sterile 0.5% (w/v) phenol red solution in PBS (Sigma-Aldrich, P2090) to aid visualization of the injection process (Jim *et al.*, 2016). Note that at this concentration, the use of phenol red for injections did not affect bacterial growth during the pre-injection interval (**Supplemental Figure S10**).

Bacterial load and competitive index. We injected zebrafish larvae with *S. pneumoniae* D39 wild-type strain into the hindbrain ventricle (see **Table S5** for a summary of all conditions used in imaging and survival experiments) and determined the bacterial load in whole infected zebrafish larvae homogenates at 24 hours post injection (hpi). At 24 hpi, infected zebrafish larvae were anesthetized in 0.02 % Tricaine (Sigma-Aldrich A5040), transferred to a 1.5 ml screwcap tube (1 larva per tube) filled with 1.0 mm glass beads (Sigma-Aldrich; Z250473) to ~25% capacity of the tubes volume, placed in a microvial rack, and violently

shaken (3 times 10 sec, 10 sec interval) in a bead beater (Biospec Products; Mini Beadbeater) to disrupt the cells and tissues. Subsequently, serial dilution plating of the homogenates was performed on Columbia Blood Agar (Thermo Scientific, NLT018) plates supplemented with 5% defibrinated sheep blood (bioTRADING, BTSG10), 10 mg/ml colistinsulphate and 5 mg/ml oxolinic acid (COBA, Oxoid), to inhibit growth of commensal bacteria in zebrafish. The plates were incubated O/N at 37°C and quantified the next day. All experiments were performed in duplicate. To determine the competitive index, we co-injected similar number of *S. pneumoniae* D39 wild-type strain or *S. pneumoniae* D39 HlpA-mCherry strain into the hindbrain ventricle of 2 dpf zebrafish larvae. The number of colony-forming units (CFU) per strain was determined by quantitative plating of the injection suspension and the ratio between each strain was calculated. At 24 hpi the bacterial load was determined as described above and the ratio between each strain was calculated and compared to the ratio in the injection suspension. To distinguish the *S. pneumoniae* D39 wild-type strain from the *S. pneumoniae* D39 HlpA-mCherry mutant strain on the selective plates we used a Leica MZ16FA fluorescence microscope. Notably, the use of fluorescent tag does not affect bacterial virulence (see **Supplemental Figure S11**).

Primary cell culture of CSF-cNs. We improved a two-step culture protocol previously published involving the successive seeding of an initial feeder layer of cells, and a second layer of cells from *Tg(pkd2l1:GCaMP5G)*, *Tg(pkd2l1:tagRFP)* the following day (Sternberg *et al.*, 2018). Briefly, we made three critical changes: first, we bleached all embryos prior to dissociation in 0.003% NaClO (bleach) in reverse osmosis water. Second, we used papain at 20 U/mL (Serlabo Technologies, LS003124) in HBSS 1X solution (Fisher Scientific, 15630080) complemented with 0.2 mg/mL cysteine (Sigma, 30089), 1.25 µM $CaCl_2$ (Sigma, C3306), 0.5 µM EDTA (Sigma, E5134), and 2 µM NaOH at 37º for 20 minutes replacing the previous digestion of 2 mg/mL collagenase. Finally, for the second seeding, we used a culture medium optimized for neurons (Neurobasal, Thermo Fisher Scientific, 10888022), complemented with 1X B27 supplement (Thermo Fisher Scientific, 17504044), 1X N2 supplement (Thermo Fisher Scientific, 17502048), 2 mM L-glutamine (Thermo Fisher Scientific, 25030024), 10 U/mL penicillin/streptomycin (Thermo Fisher Scientific, 15140122), decomplemented fetal bovine serum (FBS) (Thermo Fisher Scientific, 10270106), and 1 mM sodium pyruvate (Thermo Fisher Scientific, 11360039). These culture conditions will be published in greater detail in a coming manuscript (Marnas *et al.*).

Simulations of in vitro CSF-cN stimulation. In order to estimate the concentration of molecules at the surface of the CSF-cN during and after the 1-second stimulus, we carried

out numerical simulations applying finite-element method (ComsolMultiphysics, Transport of Diluted Species & Laminar Flow modules). We here describe the model in more details. The concentration of molecules c obeys the advection-diffusion law:

$$\frac{\partial c}{\partial t} + \boldsymbol{v} \cdot \boldsymbol{\nabla} c - D\Delta c = 0$$

where D is the diffusion coefficient of the molecule, $\boldsymbol{\nabla}$ is the differential operator and Δ is the Laplacian operator. Here $\boldsymbol{v}$ is the fluid velocity vector obeying the incompressible Navier-Stokes equations:

$$\rho \boldsymbol{\nabla} \cdot (\boldsymbol{v}) = 0$$

$$\rho \frac{\partial \boldsymbol{v}}{\partial t} + \rho(\boldsymbol{v} \cdot \boldsymbol{\nabla})\boldsymbol{v} = -\boldsymbol{\nabla}.\boldsymbol{\sigma} + \mu \boldsymbol{\Delta v}$$

where $\rho = 10^3$ kg/m is the water density and $\boldsymbol{\sigma} = -p\boldsymbol{I} + \mu\boldsymbol{\nabla u} + \mu(\boldsymbol{\nabla u})^T$ is the total stress tensor, with $\mu = 10^{-3}$ Pa.s the water viscosity and $\boldsymbol{I}$ the identity matrix. Bold terms represent three dimensional vectors or tensors.

The flow is simulated in a cylindrical container of height 0.45 mm and diameter 2 mm. Note that the concentration distribution around the cell was found not to depend on the size of the container when the diameter exceeds 1.2 mm, which is smaller than the selected value. Inside this container, the initial concentration c_0 is set to 0. A flow of concentration c_{puff} passes through a spherical opening of diameter 3 µm, representing the stimulation pipette, with a flow rate of 3.6 nL/s during 1s, in the direction of the cell. The cell is represented by a portion of sphere of diameter 10 µm and of height above the floor plate 8 µm. The cell is located at a distance of 100 µm from the stimulation pipette.

Concerning the boundary conditions for the flow and the concentration, a no slip is imposed at the bottom wall and on the cell ($\boldsymbol{v} = \boldsymbol{0}$), and a complete impermeability is imposed against the passage of molecules ($\boldsymbol{n} \cdot (D\boldsymbol{\nabla c} + c\boldsymbol{v}) = 0$). The lateral walls as well as the upper wall of the cylindrical container are at imposed constant pressurep_0, and we impose the absence of concentration gradients $\boldsymbol{n} \cdot \boldsymbol{\nabla c} = 0$.

Numerically, the transition between the stimulus process (which lasts 1s) and the post-stimulus phase (t > 1s) is achieved via a smoothing function:

$$f(t) = \exp(-\left(\frac{t-1}{\tau}\right)^2), \text{ with } \tau = 17 \text{ ms}$$

The number of tetrahedral mesh elements varies between 685000 and 850000 in the simulations presented in this manuscript. All the simulations converged, and doubling the number of mesh elements led to similar results.

METHOD DETAILS

Confocal imaging. All widefield confocal imaging was either performed live and mounted in 1.5% agarose on a Nikon ECLIPSE Ti2 inverted microscope (**Figure 1**), a Nikon AIR confocal microscope system (**Figure 2**), a 3i VIVO spinning disk microscope (**Figure 6**), or fixed and mounted in 50% glycerol on a Zeiss LSM5 Pascal confocal microscope (**Figure 4**).

Fluorescence activated cell sorting of CSF-cNs and validation. 50 to 300 *Tg(pkd2l1:GAL4, UAS:GFP)* zebrafish larvae expressing green fluorescent protein (GFP) in cerebrospinal fluid-contacting neurons (CSF-cNs) were collected at 3 days post fertilization (dpf), anaesthetized in 0.02 % (w/v) buffered 3-aminobenzoic acid methyl ester (pH 7.0) (Tricaine; Sigma-Aldrich, A5040) and decapitated at the level of the hindbrain. The remaining trunk tissue was immediately de-yolked (in de-yolking buffer: 55 mM NaCl, 1.8 mM KCl, 1.25 mM $NaHCO_3$) and manually dissociated in FACSMax buffer (AMS Biotechnology, T200100) through a 30 µm sterile filter as described previously (Manoli and Driever, 2012). The resulting suspension was re-filtered and then sorted on a BD Biosciences FACS Jazz sorter to isolate CSF-cNs (between 3,000-15,000 cells/run, ~0.2% of total input). Cells were sorted directly into lysis buffer (Qiagen, 74004; Clontech, 634894) for both qRT-PCR validation and RNA-seq library preparation; sorting runs were either entirely diverted to validation or library preparation as cell yield was insufficient to perform both analyses on the same sample. In each sorting run, we isolated separate populations of putative CSF-cNs and an assortment of other, GFP- cell types as a reference population (referred to as “green” and “dark” cells, respectively throughout this manuscript). To verify that a highly enriched population of CSF-cNs was being isolated prior to library preparation, several sorting runs were diverted to qRT-PCR analysis. These cells were converted to cDNA using the RNeasy Micro kit (Qiagen, 74004) followed by the VILO RT kit (Thermo Fisher, 11756500). qRT-PCR was performed comparing the relative expression of a panel of diagnostic transcripts including known CSF-cN-specific genes between “green” and “dark” cDNA pools using SYBR Green chemistry (Thermo Fisher, K0991). Previously known CSF-cN markers, such as *pkd2l1* (Huang *et al.*, 2006; Djenoune *et al.*, 2014) and *pkd1l2* (Petracca *et al.*, 2016b; England *et al.*, 2017), were massively upregulated while markers of hindbrain cells (*raraa*, *rarab*) were not.

Library preparation and RNAseq (differential CSF-cN RNAseq). Following validation by qPCR, five additional RNA pools were generated from both “dark” and “green” cells isolated by sorting on five different experimental days (since RNA yield was too low to split the pool for validation and sequencing). The SMART-Seq v4 Ultra Low Input kit (Clontech, 634888) was used to generate double-stranded cDNA from each sorting replicate; these pools were fragmented and tagged for sequencing using the Nextera DNA Library Preparation Kit

(Illumina). Finally, the prepared library was sequenced on an Illumina NextSeq 500 (SY-415-1001).

Fluorescent *in situ* hybridization and immunohistochemistry. cDNA was generated from 3 dpf AB larvae using the RNeasy Mini Kit (Qiagen, 74104) and SuperScript IV reverse transcriptase (Thermo Fisher, 18091050). DNA fragments from a subset of ~40 candidate genes derived from the RNA-seq hitlist were amplified from this cDNA by PCR and cloned into TOPO vectors (Thermo Fisher, 451641). Antisense digoxigenin-incorporating probes were transcribed from these clones and hydrolyzed to ~300 bp as previously described (Thisse and Thisse, 2008; Morris, Benson and White-Cooper, 2009; Vize, McCoy and Zhou, 2009). To verify that these transcripts were enriched in CSF-cNs, we combined fluorescent *in situ* hybridization and immunohistochemistry for GFP in *Tg(pkd2l1:GCaMP5G)* or *Tg(mnx1:GCaMP5)* transgenic animals at 24 hours post fertilization (hpf) and adult stages as previously described (Thisse and Thisse, 2008; Vize, McCoy and Zhou, 2009; Djenoune *et al.*, 2014, 2017).

Generation of transgenic zebrafish lines. To generate a Tol2 vector driving GAL4 under the control of GFAP regulatory elements, we used Gateway recombination-based cloning (Thermo Fisher, 11791020) using p5E-GFAP, which contains 7.4 Kb of GFAP intron 1 and exon 1 (Bernardos and Raymond, 2006; Johnson *et al.*, 2016), pME-GAL4, and p3E-poly(A) into pDestpA2. The resulting vector was injected into *Tg(UAS:RFP; cryAA:Venus)* at 30 ng/µL with 35 ng/µL Tol2 transposase to generate germline transgenics as previously described (Fisher *et al.*, 2006; Kwan *et al.*, 2007).

Generation of*tas2r3* mutants. Site-specific crRNAs were designed targeting the *tas2r3* coding sequence using the CRISPOR web tool (Concordet and Haeussler, 2018) (IDT). These were then annealed to a common tracRNA component to form an RNA duplex stock (33 µM) which was then complexed with 10 µg/µL Alt-R-S.p. Cas9 Nuclease V3 (IDT) in Cas9 buffer (20 mM HEPES, 150 mM KCl, pH 7.5) at a 1:1 molar ratio according to the manufacturer's instructions. Zebrafish embryos were obtained at the 1-2 cell stage and 1nL of the described mixture was injected into each embryo. Embryos were allowed to recover in E3 medium. ~10 embryos were collected at 1-3 days post fertilization (dpf) and their DNA was harvested by proteinase K digest and gRNAs were validated using an *EaeI* restriction cleavage site present in the crRNA binding region that would be disrupted by indel mutations caused by CRISPR/Cas9 modification. As noted in **Supplemental Figure S7**, we would later find that *tas2r3* is present in our wild type background as at least two different paralogous

alleles, which we were able to independently mutate and segregate in genotyping assays using paralog-specific PCR.

Generation of mutants of CSF-cN neuropeptides. To generate *scg2a*, *nppc*, *esm1* null mutant line, we used the CRISPR/Cas9-mediated genome editing method. crRNA were designed by using online CRISPOR program (crispor.tefor.net/). crRNA and tracRNA were ordered from Integrated DNA Technology. The guiding RNA (**Supplemental Table 6**) complex is prepared by Duplex buffer, and mixed with Cas9 protein provided by Dr. Jean-Paul Concordet (MNHN, Paris, France). The mixed complex was injected into one-cell stage wild type eggs. The editing efficiency was tested after injection at 2 dpf by performing genotyping on 3 pools of 20 embryos. Genomic DNA was extracted in lysis buffer (10 mM Tris pH 8.2 mM EDTA, 0.2% Triton X-100, 200 µg/mL Proteinase K) at 55°C for 2 h followed by 10 min of deactivation at 99°C. Then the target region was amplified by performing PCR with specific primers (**Supplemental Table 7**). The F0 generation which contains high efficiency mutations was raised to sexual maturity. The best transmitters were selected by screening the rate of mutation in F1 embryos. The mutations of F1 adult fish have been analyzed by sequencing the subcloned PCR product. The F1 fish that carried the best type of the mutation has been chosen and raised by crossing with AB wild type fish to generate the F2 fish. Analyzing the enzymatic restriction (**Supplemental Table 7**) in the targeted site has screened the homozygote, heterozygote, and wild type of F2 fish.

scg2a encodes a precursor of 540 amino acids in a single exon. The beginning of this exon was targeted by two gRNAs. To generate the *scg2a*^{icm42} mutant allele, sequence analysis revealed that 10 nucleotides were deleted by the gRNA1/Cas9 complex, leading to a frameshift and a premature STOP codon leading to a truncated amino acid sequence deprived of the mature peptide precursor sequence. The Nppc precursor is encoded by 3 exons and the mature peptide sequence is contained in the second exon. To generate the *nppc*^{icm36} mutant allele, we targeted the beginning of the first exon in order to disrupt the signal peptide sequence. The gRNA/Cas9 complex we used mediated a 3 nucleotide deletion that led to a mutation on the start codon (from ATG to ATT), hindering the translation of first exon. The *esm1* gene is composed of 3 exons and encodes a 139 amino acids protein whose binding domain is encoded by exon1. The gRNA1/Cas9 complex we used induced an insertion of 13 nucleotides, which led to frame shift and premature STOP codon forming a truncated protein of 29 amino acids devoid of the binding domain in the *esm1*^{icm34} mutant allele.

Calcium imaging of zebrafish larvae after injections in the hindbrain ventricle. Transgenic zebrafish larvae expressing GCaMP in a cell-type specific manner— *Tg(pkd2l1:GCaMP5G)* transgenic larvae for CSF-cNs and *Tg(GFAP:GAL4, UAS:GCaMP5G)* for ependymal radial glia— were anesthetized in tricaine and paralyzed with α-bungarotoxin (1mM, 1nL, Tocris Biosciences, 2133) i.m. or i.v. for imaging. Subsequently, the larvae were embedded in 1.5% low-melting point agarose dissolved in egg water (60 µg/mL sea salts (Sigma-Aldrich, S9883), in MilliQ) in an open uncoated 8-well chamber slide (ibidi, 80826) and kept at 28°C in a temperature-controlled chamber (Okolab). Larvae were imaged on a Nikon AIR confocal microscope system. FIJI/MATLAB was used for image analysis. Imaging involved several experimental conditions, unless otherwise noted, all solutions were injected into the hindbrain ventricle of 2 dpf larvae—

- Pneumococcal meningitis. ~2000 colony forming units (CFU) of red fluorescent S. pneumoniae D39 HlpA-mCherry or vehicle-injected with sterile 0.5% (w/v) phenol red solution in PBS were injected into the hindbrain ventricle after anesthesia of zebrafish larvae with tricaine followed by paralysis with α-bungarotoxin injection, before being embedded in low-melting point agarose as described previously.
- Heat-killed *S. pneumoniae*. Bacteria were prepared as above, except the culture was incubated for 20 minutes at 80ºC prior to injection.
- *E. coli.* A culture of DH5α *E. coli* (ATCC) was grown to OD_{600} 0.6. 1nL of this culture was injected into the hindbrain ventricle as above.

Primary cell culture of CSF-cNs. We adapted a two-step culture protocol previously published comprising an initial feeder layer of cells on which were plated a second layer of fluorescent positives CSF-cNs cells (Sternberg *et al.*, 2018). Briefly, all embryos were bleached prior to dissociation in 0.003% bleach in reverse osmosis water in order to avoid contaminations. To perform the initial feeder layer of cells, we dissociated 2 dpf AB WT embryos using papain at 20U/mL (Serlabo Technologies, LS003124) in HBSS 1X solution (Fisher Scientific, 15630080) complemented with 0.2 mg/mL cysteine (Sigma, 30089), 1.25 µM $CaCl_2$ (Sigma, C3306), 0.5 µM EDTA (Sigma, E5134), and 2 µM NaOH at 37º for 20 minutes. Dissociated cells were rinsed using HBSS 1X and plated overnight at a concentration of 1.10^6 cells/well in DMEM medium (ThermoFisher, 10938025) complemented with 2mM L-Glutamine (Thermo Fisher Scientific, 25030024), 50U/mL penicillin/streptomycin (Thermo Fisher Scientific, 15140122), 25ng/mL NGF (Merckmillipore, 01-125), 4ng/mL GDNF (Fisher Scientific, 10679963), 25mM glucose (SIGMA, G8769-100ML), and 10% FBS (Thermo Fisher Scientific, 10270106). 24 hours after the initial feeder layer plating, we dissociated 3 dpf *Tg(pkd2l1:tagRFP, pkd2l1:GCaMP5G)* double transgenic embryos using

the same 20u/mL papain complemented solution used for the initial layer. Dissociated cells were rinsed using HBSS 1X and plated overnight at a concentration of 5.10^5 cells/well in Neurobasal medium (Thermo Fisher Scientific, 10888022), complemented with 1X B27 supplement (Thermo Fisher Scientific, 17504044), 1X N2 supplement (Thermo Fisher Scientific, 17502048), 2 mM L-glutamine (Thermo Fisher Scientific, 25030024), 10 U/mL penicillin/streptomycin (Thermo Fisher Scientific, 15140122), decomplemented FBS (Thermo Fisher Scientific, 10270106), and 1 mM sodium pyruvate (Thermo Fisher Scientific, 11360039). Cells were used 48 hours after the plating of the second layer.

Calcium imaging in primary cell culture. Calcium imaging on GCaMP5G-expressing neurons from the *Tg(pkd2l1:GCaMP5G)* transgenic line was performed on an epifluorescence microscope equipped with a Lumen Dynamics XT600 Xenon lamp and a GFP filter cube. Acquisition was performed at 5 Hz using an EM-CCD Camera from Hamamatsu. Puffs stimuli were delivered using a 1 s long TTL pulse from a Digidata acquisition system (Axon Instruments) and repeated 3 times with an inter trial interval of 64 seconds—

- *aCSF.* Artificial CSF (aCSF) was composed of NaCl 140mM (Sigma, S7653), KCl 1mM (Sigma, P9333), $CaCl_2$ 2.5mM (Sigma, 223506), $MgCl_2$ 1mM (Sigma, M2670), HEPES 10mM (Sigma, H3375), D-(+)-Glucose 10mM (Sigma, G8270), diluted in MilliQ water; pH was adjusted at 7.4.
- *Pneumolysin.* Recombinant serotype 4 pneumolysin purified from *E. coli* (MyBioSource, MBS1141054) was reconstituted in aCSF at a concentration of 0.1 mg/mL. In our *in vitro* experiments, the concentration of pneumolysin applied onto the cultured CSF-cNs was 50 µg/mL, which exceeds the threshold for 100% hemolytic activity more than threefold (**Figure 3, Supplemental Figure S12**).
- *Mix of bitter compounds.* Acetone (Sigma, 534064), 2-butanone (Sigma, W217012), 2-pentanone (Sigma, W284220), dimethyl disulfide (Sigma, W353604), 2-methylpropanal (Sigma, W222003) were diluted as a mix of bitter compounds in aCSF at a concentration of 100mM each. In our *in vitro* experiments, the concentration of each bitter compound applied onto the cultured CSF-cNs was 50 mM according to *in silico* simulations (**Figure 3**).
- *Dimethyl disulfide (DMDS) and 2-pentanone.* DMDS (Sigma, W353604) and 2-pentanone (Sigma, W284220) were diluted in aCSF at 25, 50 and 100mM concentrations. In our *in vitro* experiments, the concentrations of DMDS and 2-pentanone applied onto the cultured CSF-cNs were 12.5, 25 and 50 mM according to *in silico* simulations (**Figure 3**).

- *Acetone, 2-butanone and 2-methylpropanal.* Acetone (Sigma, 534064), 2-butanone (Sigma, W217012) and 2-methylpropanal (Sigma, W222003) were diluted in aCSF at 100 mM concentration. In our *in vitro* experiments, the concentration of acetone, 2-butanone and 2-methylpropanal applied onto the cultured CSF-cNs was 50 mM according to *in silico* simulations (**Figure 3, Supplemental Figure S2**).

FACS sorting of infected larvae. Larvae were injected with 2000 CFU *S. pneumoniae* D39 wild-type strain as described above, collected at 24 hours post infection, and a single-cell suspension was generated using the same protocol as for prior rounds of FACS. Analysis and isolation were performed using a BD InFlux cell sorter controlled by BD FACS Sortware v1.2.0.142 software. Infected neurons were identified by eGFP reporter protein which was excited by a 488nm, 200mW laser and detected through a 530/40 bp filter. Cell auto-fluorescence was also excited by the 488nm laser and detected through a 692/40 bp filter. Live and intact cells were identified by DAPI staining and excited by a 405nm, 100mW laser. For gating and trigger thresholds, background particulate was identified by running cell suspension buffer alone and standard FSC vs. SSC gating was applied to select whole, intact events of similar scatter properties. Live cells were then gated according to low DAPI signal events within a distinct event cluster and, from there, 2 separate auto-fluorescent populations were sorted from the eGFP positive events. eGFP gating edges were set with no-color and eGFP FMO controls. Compensation was not applied to any parameters.

Library preparation and RNAseq (uninfected vs. infected CSF-cNs). Three RNA pools were generated from both “dark” and “green” cells isolated in control and infected conditions by sorting. The SMART-Seq v4 Ultra Low Input kit (Clontech, 634888) was used to generate double-stranded cDNA from each sorting replicate; these pools were fragmented and tagged for sequencing using the Nextera XT DNA Library Preparation Kit (Illumina). Finally, the prepared library was sequenced on an Illumina NovaSeq 6000 SP (200 cycles, up to 800 million reads, Illumina).

RNA-seq (uninfected vs. infected CSF-cNs) analysis using DESeq2. Differential expression (DE) analysis of uninfected vs. infected CSF-cNs RNA-seq data was conducted in R version 3.6.1 (R Development Core Team, 2019) using the DESeq2 Bioconductor package (v1.26.0). From the raw count data, the DESEeq function performs all the processing steps from the normalization of the counts with the calculation of size factors (accounting for differences in library sizes) and dispersion factors to the differential analysis itself. DE genes between infected and control cells were explored separately within each

population of green and dark cells, and also for the difference of variation observed in the two populations (testing the “ratio of ratios”: i.e. the Infected/Control ratio in the green cells divided by the Infected/Control ratio in the dark cells). Significant DE genes were determined by fitting Negative Binomial Generalized Linear Models (one model per gene), followed by a Wald test on the model coefficients for significance testing. To control for the false discovery rate (FDR), all pvalues were adjusted using the Benjamini-Hochberg (BH) procedure, and all DE genes with a BH-adjusted p-value < 0.05 were considered statistically significant. Within each population of green and dark cells, the directional change of the DE gene expression level was indicated by the sign of the log fold: either positive when the average expression level in the infected cells was significantly higher than that in the control cells (“up in infected”); or negative when expression level was decreased in the infected cells (“down in infected”).

Survival assays. Survival (defined as larvae that do not respond to tail touches nor have a beating heart) was assessed every 24 hours. Curves were generated with GraphPad Prism 7.0 and survival data were analyzed with the log rank (Mantel-Cox) test.

Survival experiments in CSF-cN compromised transgenic larvae. Zebrafish larvae were infected as described previously by injecting 2000 colony forming units (CFU) wild-type *S. pneumoniae* D39 into the hindbrain ventricle and kept in 6-well plates at 28°C with 20 larvae in each group per well (Jim *et al.*, 2016). The mortality rate was scored by monitoring live and dead embryos at 24 hours intervals post-injection; mortality was determined by heartbeat and response mechanical stimuli. All experiments were performed in triplicate. Survival analyses were performed and involved the following experimental conditions—

- *Nitroreductase. Tg(pkd2l1:GAL4, UAS:epNTR-tagRFPT-UTR.zb3)* zebrafish embryos (Marquart *et al.*, 2015) and control sibling embryos were treated with 10mM metronidazole (Sigma-Aldrich, M3761) in 0.1% DMSO (Sigma-Aldrich, D8418) for at least 16 hours to induce nitroreductase-mediated ablation of *pkd2l1*+ cells after mechanical dechorionation. At 2 dpf the larvae were washed 3 times with egg water and subsequently infected.
- *Botulinum toxin B Light Chain. Tg(pkd2l1:GAL4, UAS:BoTxBLC-GFP)* zebrafish embryos (Auer *et al.*, 2015; Böhm *et al.*, 2016; Sternberg *et al.*, 2016) and control wild-type embryos were infected at 2 dpf.

Survival experiments in mutant larvae. Adult heterozygous zebrafish mutants (*pkd2l1*^{icm02}, *sgc2a*^{icm42}, *esm1*^{icm34}, *nppc*^{icm36}) were incrossed in order to compare survival between

homozygous mutants and control siblings within the same clutches. Injection of *S. pneumoniae* targeted the hindbrain ventricle of 2 dpf zebrafish mutants and their control siblings (**Supplemental Figure S9**) at different doses (200cfu, 1000cfu, 2000cfu per larva). We injected ~25 larvae for each CFU for each group in each experiment. The survival rate was evaluated every 12h until 72 hours post-infection (hpi) prior to genotyping after euthanasia of all larvae.

Analysis of calcium transients *in vivo*. To determine the overall activity of a given ROI, the integrated ΔF/F was calculated; comparisons across conditions were made using multifactorial ANOVAs with Scheffé post-hoc tests. To compare isolated large-amplitude transients (as in **Figure 2E, F, G,** and **N**), a MATLAB script was written to identify features of the Ca^{2+} trace where a prolonged high-amplitude (i.e. > 100% ΔF/F) interval was followed by a sharp onset (i.e. differential of ΔF/F trace > 30). Statistical testing was performed on these isolated events using the Wilcoxon rank sum test with Bonferroni correction for multiple comparisons.

Analysis of calcium transients *in vitro*. Slow translational drifts of the image due to cell movements were corrected using image registration by taking as a reference image a frame of the original position of the CSF-cN. We identified CSF-cN calcium transients in response to 1-second stimulus by using a 100 ms-long flash of green light performed 12.74s before the stimulus. Frames corresponding to flashes stimuli were removed from the representative traces (see **Figure 3B, 3C**). To determine the response of a given ROI to a 1-second stimulus (as in **Figure 3D, 3E**), the ΔF/F amplitude of each peak response after stimulus was calculated using a home-made MATLAB script available on the Wyart lab github: the ΔF/F average of over six time points around the maximum ΔF/F of the peak was calculated, and was subtracted to this the ΔF/F average of six points before the stimulus. A cell was considered as a responding cell when we observed a response for at least one of the 3 1-second stimuli. Latency was calculated as time between the 1s-stimulus and the beginning of the peak response. Time-to-peak was calculated as the time between the beginning of the peak response and the maximum of the peak. Time decay was calculated by applying an exponential fit of model 'a*exp(-b*x)+c' and extracting the time decay as follow: decay = 1/b. As control for no-stimulus (see **Figure 3G**, black circles), we measured the time decay of transients corresponding to spontaneous activity with no stimulus (see **Figure 3B-C**, left). Comparisons across conditions (as in **Figure 3D**, **3E**) were made using 2-factor ANOVAs with Turkey HSD post-hoc tests on R. Comparisons for latency, time-to-peak and time decay were made using two-sample Kolmogorov-Smirnov non-parametric test on MATLAB.

Analysis of neutrophil infiltration to the central canal after infection. *Tg(mpo:GFP)* transgenic larvae (Renshaw *et al.*, 2006) expressing green fluorescent neutrophils were anesthetized and infected with 2000 CFU mCherry+ *S. pneumoniae* as described above or injected with 1 nL Alexa 647 Dextran (Thermo Scientific, D22914) in the hindbrain ventricle. After embedding the larvae in low-melting point agarose, time-lapse imaging was performed at 28°C on a Nikon AIR confocal microscope system equipped with a temperature-controlled chamber. Images were obtained at 20 min. intervals for 12-24 hours.

Pneumolysin hemolytic assay. The hemolytic activity of recombinant pneumolysin (MyBioSource, MBS1141054) was determined using sheep erythrocytes (bioTRADING, BTSG100). Serial two-fold dilutions of pneumolysin in PBS was prepared and mixed with an equal volume of a solution with 1% (v/v) sheep erythrocytes in PBS in a 96-well plate (Corning, CLS3598), incubated at 37°C for 1 h and centrifuged for 5 minutes at 3000 g. As a positive control a 10% saponin (w/v) solution was used, in which 100% of the erythrocytes will be lysed. The absorbance was then measured at 405 nm and the percentage of lysed erythrocytes was calculated and plotted for each pneumolysin concentration.

Phenol red killing assay. *S. pneumoniae* D39 cells were grown to mid-log phase and harvested by centrifugation (6000 RPM, 10 min.). After removal of the supernatant, the cells were suspended in different concentrations of phenol red in PBS (0.125%, 0.25% and 0.5%) or PBS alone, and incubated at room-temperature. Subsequently, serial quantitative plating was performed to determine the CFU at each time-point post incubation.

Behavioral analysis. Zebrafish larvae were either infected with 6000 CFU *S. pneumoniae* or injected with PBS at 5 dpf. Larvae were rested until 9, 24, or 32 hours post injection and plated individually in a 32 wells (80 mm x 140 mm) made from 3 mm acrylic sheets (Plexiglas) plate (BFP CINDAR, Champigny-sur-Marne, France) cut by a laser cutter into 1.5 cm diameter wells holding a volume of 500 µL. Larvae were then recorded freely for 5 minutes at 160 fps after 10 min of acclimation. Behavioral parameters were extracted using ZebraZoom (Mirat *et al.*, 2013).

Analysis of spinal curvature. Zebrafish larvae were infected with 2000 CFU mCherry+ *S. pneumoniae* bacteria and then imaged using a 3i VIVO spinning disk microscope. The spinal cord was manually delineated using MATLAB (“curvature.m, linecurvature2D.m,” (Sternberg *et al.*, 2018)). This produced an imaging area from which curvature was calculated from a smoothing spline curve fit to the x-axis boundaries and total 568 nm fluorescence was integrated across the x-axis.

DATA AND SOFTWARE AVAILABILITY

All MATLAB scripts used herein (e.g. for calcium imaging analysis) are available at https://github.com/wyartlab.

SUPPLEMENTARY FIGURE TITLES AND LEGENDS

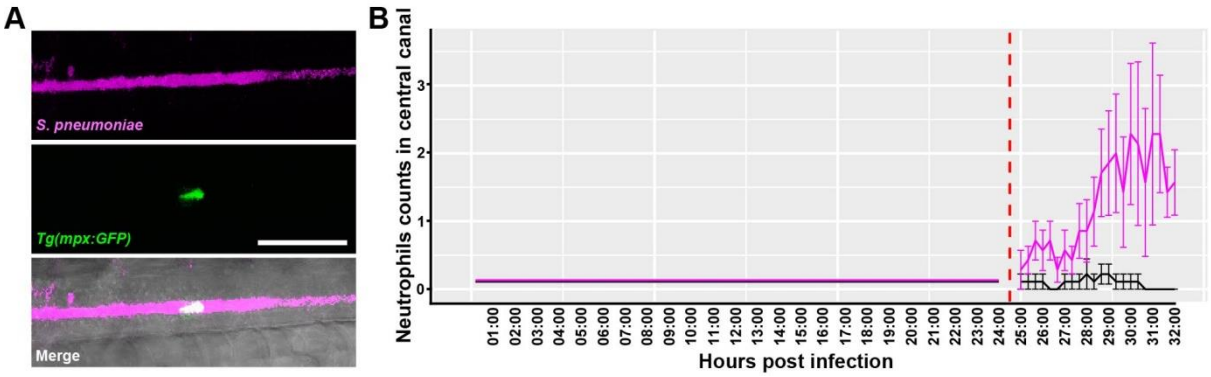

Supplemental Figure S1. Neutrophil infiltration following our pneumococcal infection protocol with 2000 CFU in 2 dpf *Tg(mpo:GFP)* larvae does not occur before 24 hpi. (A-C) Only from 24 hours post infection onwards did we observe increased infiltration of neutrophils to the central canal as compared to control larvae. The number of neutrophils present in the central canal was significantly higher as compared to control larvae injected with an Alexa647 dextran. Two-way ANOVA, $p<0.0001$. Error bars = mean ± SEM of two individual experiments with n = 3 - 4 larvae per group in the 0 – 24 hpi experiment and n = 7 - 9 larvae per group in the 25 - 32 hpi per experiment.

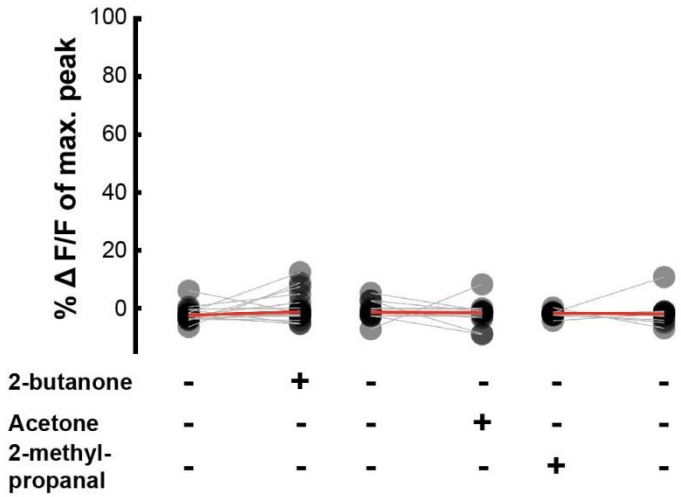

Supplemental Figure S2. Cultured CSF-cNs respond to individual bacterial metabolites acting as bitter compounds. Paired line plots showing responses of individual cells to 3 successive 1-second stimuli of aCSF versus individual bitter compounds (2-butanone, acetone and 2-methylpropanal) at 50mM, n.s. = not significant. Red bar: median ΔF/F (median 2-butanone = 1.12% versus median aCSF = -0.26%, 2 cells responding out of 6 ; median acetone = 0.81% versus median aCSF = 0.94%, 0 cell responding out of 4 ; median 2-methylpropanal = 0.18% versus median aCSF = 0.55%, 1 cell responding out of 4).

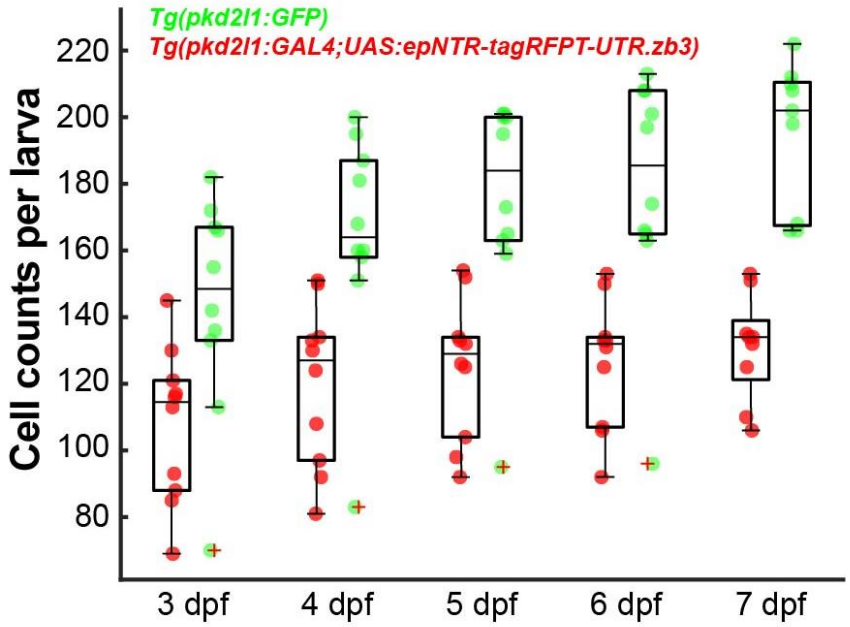

Supplemental Figure S3. CSF-cN total cell counts in the *Tg(pkd2l1:GCaMP5G)* and the fraction expressing NTR in the *Tg(pkd2l1:GAL4, UAS:epNTR-tagRFPT-UTR.zb3)* larvae. GFP+ and NTR-tagRFP+ cells were counted per larvae daily between 3 and 7 dpf. At the larval stages, all CSF-cNs are labeled in the direct line *Tg(pkd2l1:GCaMP5G)* while only a fraction express NTR due to the varigation of the UAS/GAL4 system. The same phenomenon of varigation applies to the *UAS:BotxLCB-GFP*.

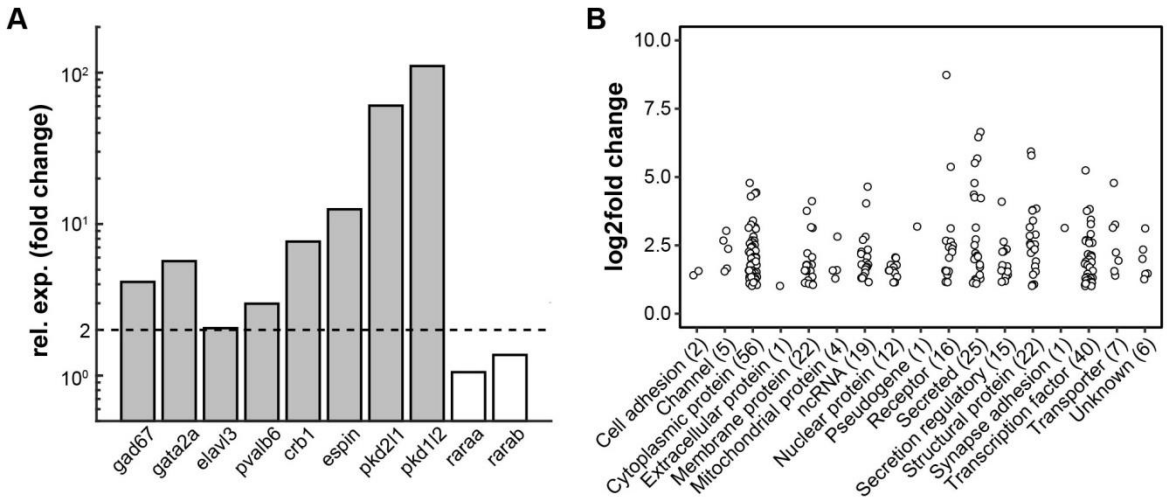

Supplemental Figure S4. qPCR validation of FACS sorting and categorization of differentially-expressed transcripts. (A) Validation and comparison of known marker genes expression between GFP- and GFP+ cells by RT-qPCR. Gray bars: CSF-cN marker genes *crb1* (Desban *et al.*, 2019), *espin* (Desban *et al.*, 2019), *pkd1l2* (England *et al.*, 2017), and *pkd2l1* (Huang *et al.*, 2006; Djenoune *et al.*, 2014; England *et al.*, 2017); these are enriched in the GFP+ RNA pool. White bars: *raraa* and *rarab* hindbrain markers; these show that RNA pools are not contaminated by non-CSF-cN GFP+ cells. **(B)** Categorical breakdown of selected RNA-seq hits.

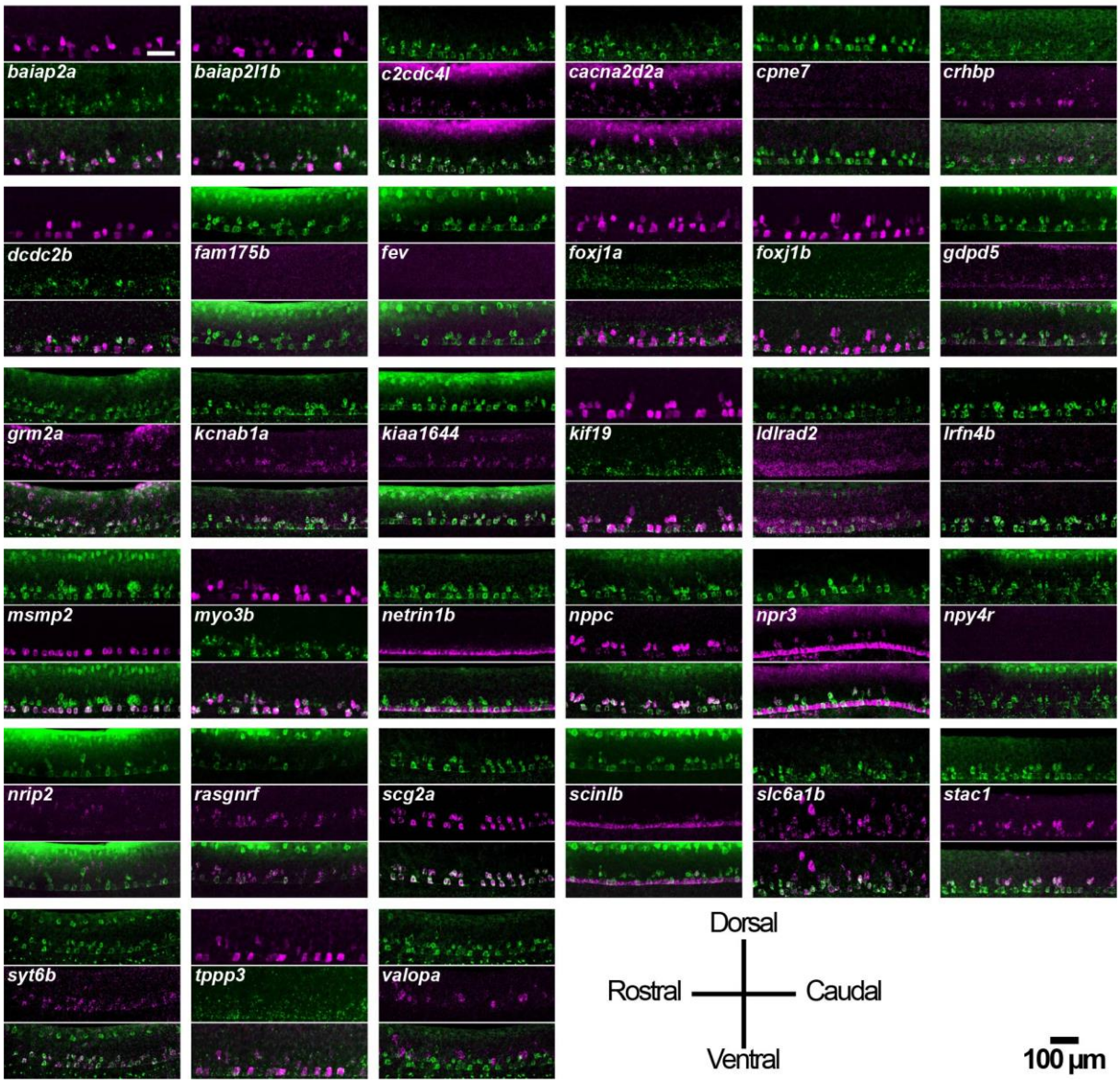

Supplemental Figure S5. Fluorescent *in situ* hybridization of hits from differential RNA-seq at 24 hpf. 24 hpf embryos were subjected to fluorescent *in situ* hybridization using either *Tg(pkd2l1:GCaMP5G)* or *Tg(pkd2l1:GAL4, UAS:tagRFP)* as a marker of CSF-cNs. The vast majority (85%) of RNA-seq hits were confirmed by *in situ* hybridization to be expressed in CSF-cNs.

Figure S6

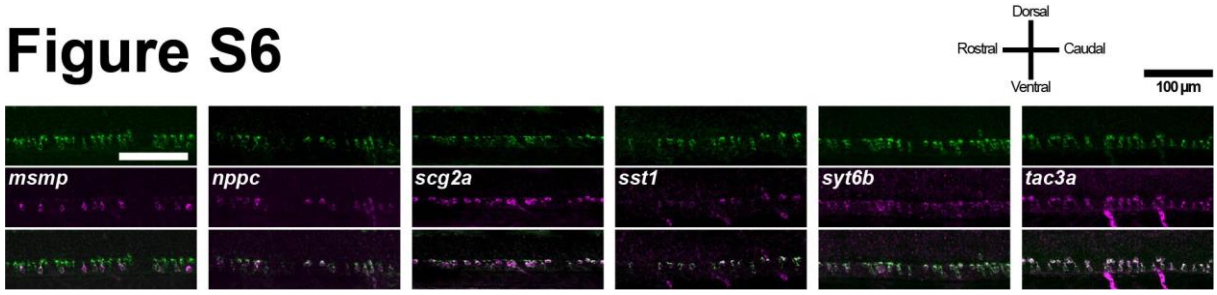

Supplemental Figure S6. Fluorescent *in situ* hybridization of hits from differential RNA-seq at 3 dpf. A subset of hits were assessed as above at 3 dpf (the stage at which RNA-seq was performed). These continued to be expressed at later stages.

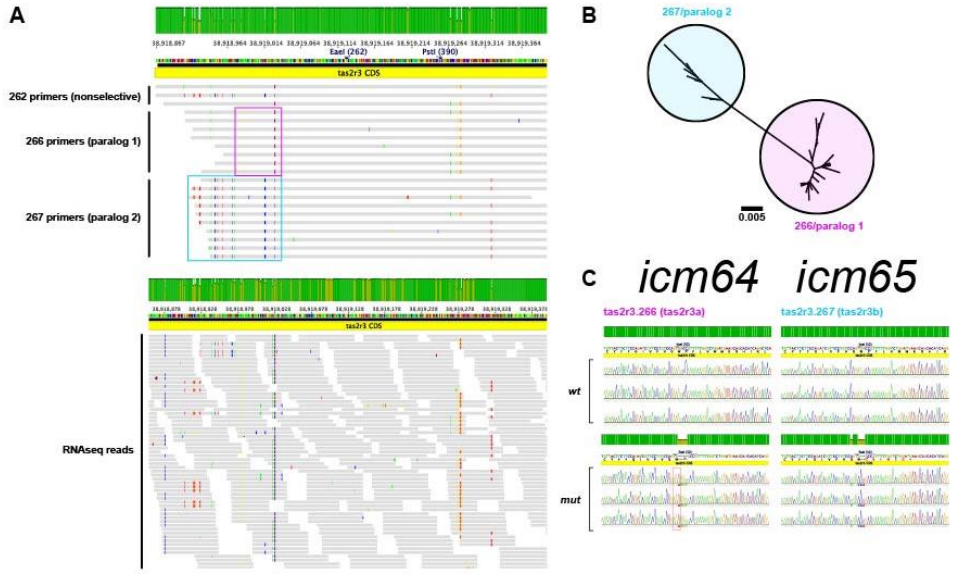

Supplemental Figure S7. *tas2r3* exists as at least two paralogs in our wild type population. (A) Local alignment of individual *tas2r3* TOPO clones. We identify a signature region differing between two paralogs that can be discriminated using paralog-specific primers (266, 267, see magenta and cyan boxes). These paralog-specific marks are also evident in RNA-seq alignments suggesting both are expressed. **(B)** Dendrogram of individual TOPO clone sequences showing that *tas2r3* sequences cluster in two major families, paralog 1 (primer set 266/*tas2r3a*) and paralog 2 (primer set 267/*tas2r3b*). **(C)** We are able to generate identifiable mutants in both paralogs that segregate somewhat independently (*icm64* is an allele of *tas2r3a* and *icm65* is an allele of *tas2r3b*).

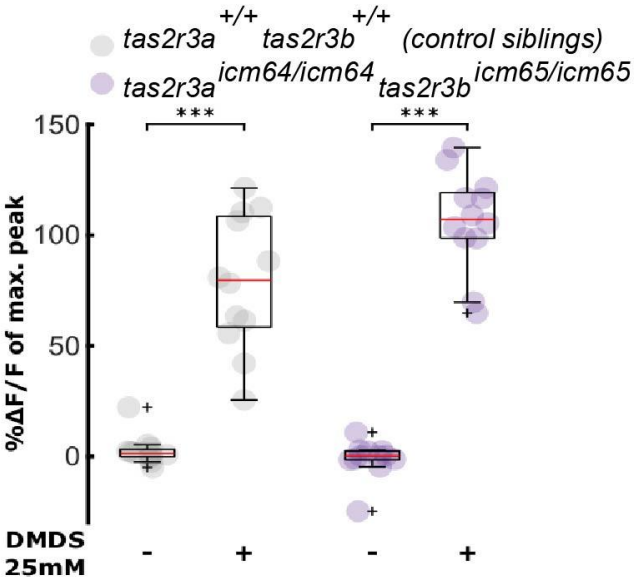

Supplemental Figure S8. In double knockout for *tas2r3* receptors, CSF-cNs are responding *in vitro* to DMDS. Quantification of calcium transients of *tas2r3a*$^{+/+}$ *tas2r3b*$^{+/+}$ (in grey) or *tas2r3*$^{icm64/icm64}$ *tas2r3*$^{icm65/icm65}$ (in purple) CSF-cNs after control (DMDS "-") or 25mM dimethyl disulfide (DMDS "+") stimuli. 2-factor ANOVA performed, nature of stimulation factor F = 265.179, $p < 2.0 \times 10^{-16}$; Turkey HSD post-hoc testing, *** = $p < 0.001$. Red bar: median ΔF/F (control siblings: median 25mM DMDS on 79.65% and aCSF 1.31%, N = 4 cells; *tas2r3*$^{icm64/icm64}$ *tas2r3*$^{icm65/icm65}$: median 25mM DMDS 107.15% and aCSF 0.22%, N = 4 cells).

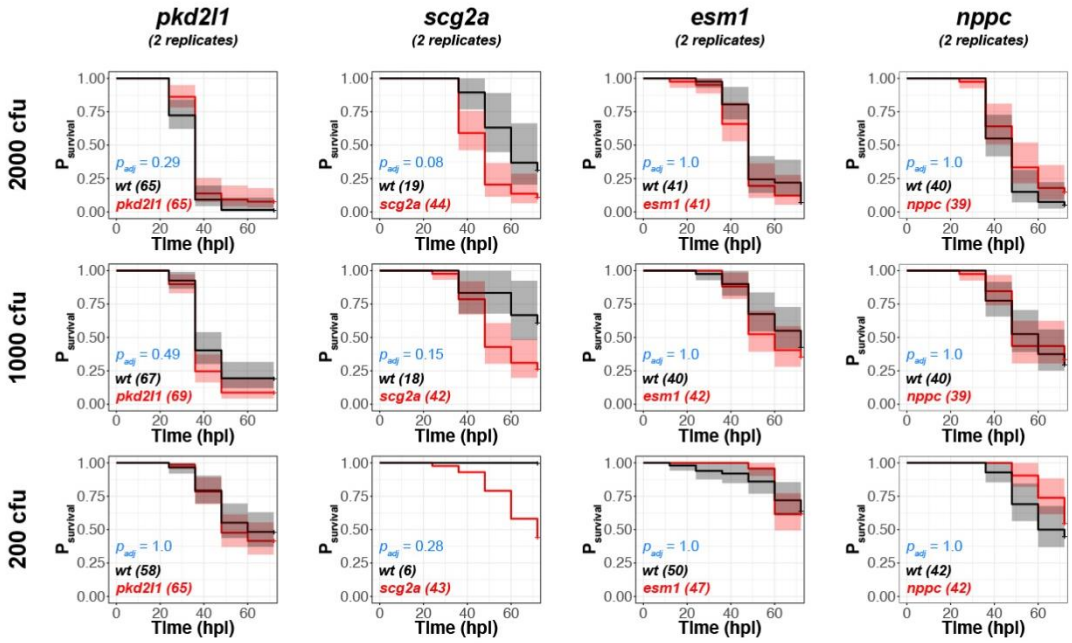

Supplemental Figure S9. Host survival was not altered in mutants for CSF-cN peptides receptor *pkd2l1* as well as *scg2a*^{icm42}, *esm1*^{icm34} and *nppc* ^{icm36}. Survival curves of 2 dpf *scg2a*, *nppc*, *esm1* and *pkd2l1* null mutants larvae injected in the hindbrain ventricle with either 200, 1000 or 2000 colony forming units (CFU) of *S. pneumoniae* showed no difference compared to control siblings. Survival rate was evaluated every 12h until 72 hours post-infection (hpi). Number of animals per condition is indicated between brackets.

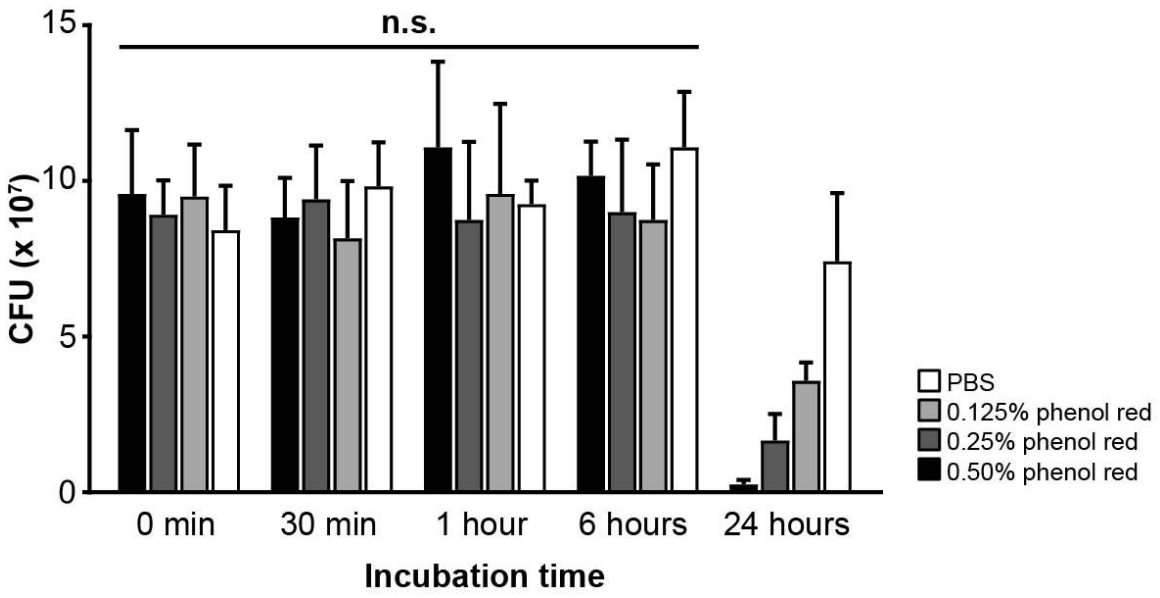

Supplemental Figure S10. Pneumococci incubated in phenol red remain viable for at least 6 hours. Bar plots of total CFU count of *S. pneumoniae* D39 wild-type strain over time after incubation in different concentrations of phenol red. The CFU count was comparable between incubation with 0.5% phenol red, 0.25% phenol red, 0.125% phenol red or PBS up to 6 hours post incubation (two-way ANOVA, $p = 0.3520$). Dose-dependent killing of wild-type *S. pneumoniae* D39 by phenol red was observed at 24 hours after incubation.

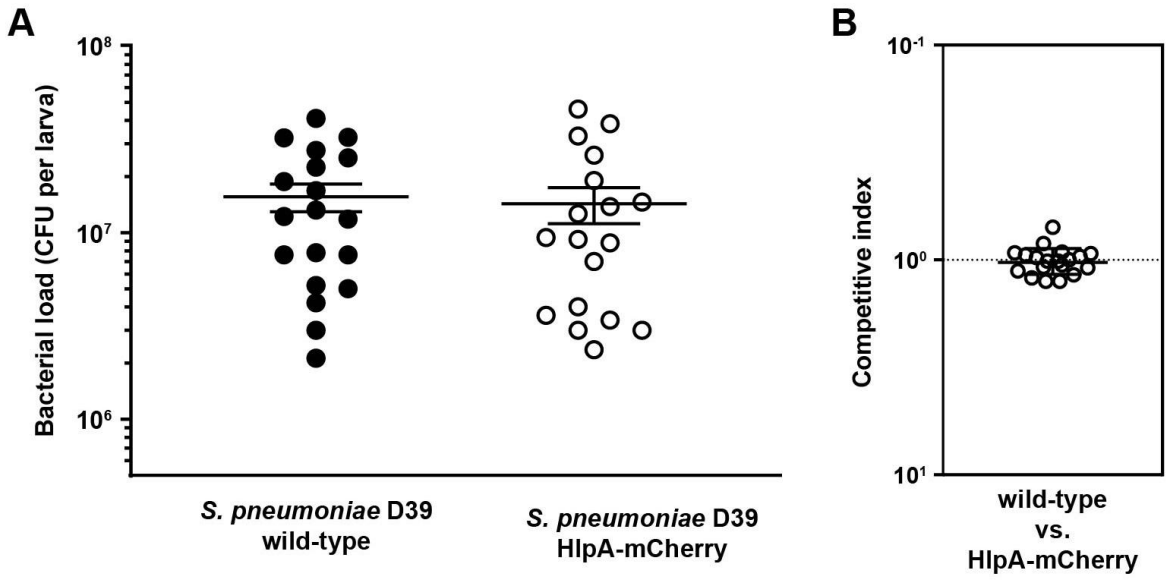

Supplemental Figure S11. Red fluorescently-labeled *S. pneumoniae* D39 HlpA-mCherry mutant strain retains its virulence compared to *S. pneumoniae* D39 wild-type strain. (A) Bacterial load at 24 hours post injection was comparable between zebrafish larvae infected at 2 dpf into the hindbrain ventricle with *S. pneumoniae* D39 HlpA-mCherry mutant strain or *S. pneumoniae* D39 wild-type strain (unpaired t-test, p = 0.7520). Each dot represents a single larva. Error bars = mean ± SEM of two individual experiments with n = 9-10 larvae per group per experiment (total n = 19-20 per group). **(B)** Competitive index of 2 dpf larvae co-injected with similar number of *S. pneumoniae* D39 HlpA-mCherry mutant strain and *S. pneumoniae* wild-type strain (total CFU = ~400). Each dot represents a single larva. Error bars = mean ± SEM of two individual experiments with n = 9-10 larvae per experiment (total n = 19).

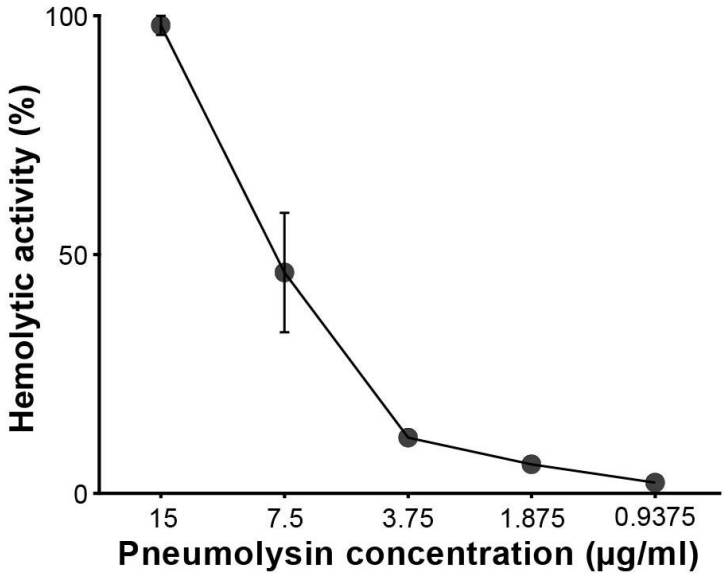

Supplemental Figure S12. Hemolytic activity of recombinant pneumolysin. Hemolytic activity of recombinant pneumolysin in serial 2-fold dilutions of 15 µg/ml recombinant pneumolysin against 1% (v/v) defibrinated sheep blood in PBS at 37°C for 1 hour. Error bars = mean ± SEM of three individual experiments.

Supplemental Movie 1.Calcium imaging of control and infected larvae 21 hours post injection. Representative time-lapse movie of CSF-cN activity in control larvae (top) and *S. pneumoniae*-infected larvae (bottom). 4 Hz imaging, 15X playback.

Supplemental Movie 2. *In vitro* imaging of cultured CSF-cN exposed to pneumolysin. Representative time-lapse movie of a CSF-cN activity *in vitro* during three successive 1-second 0.05 mg/mL pneumolysin stimulations. 5 Hz imaging, speeded up 20X. The three 1-second stimulations occur at 6.48, 9.68 and 12.88 seconds. Scale bar, 10 µm.

Supplemental Movie 3. *In vitro* imaging of cultured CSF-cN exposed to mixture of bitter compounds. Representative time-lapse movie of a CSF-cN activity *in vitro* during three successive 1-second 50 mM bitter compounds stimulations. 5 Hz imaging, speeded up 20X. The three 1-second stimulations occur at 6.48, 9.68 and 12.88 seconds. Scale bar, 10 µm.

Supplemental Movie 4. *In vitro* imaging of cultured CSF-cN exposed to DMDS. Representative time-lapse movie of a CSF-cN activity *in vitro* during three successive 1-second 50 mM DMDS stimulations. 5 Hz imaging, speeded up 20X. The three 1-second stimulations occur at 6.48, 9.68 and 12.88 seconds. Scale bar, 10 µm.

Supplemental Movie 5. *In vitro* imaging of cultured CSF-cN exposed to 2-pentanone. Representative time-lapse movie of a CSF-cN activity *in vitro* during three successive 1-second 50 mM 2-pentanone stimulations. 5 Hz imaging, speeded up 20X. The three 1-second stimulations occur at 6.48, 9.68 and 12.88 seconds. Scale bar, 10 µm.

Supplemental Movie 6. *In vitro* imaging of cultured CSF-cN exposed to aCSF. Representative time-lapse movie of a CSF-cN activity *in vitro* during three successive 1-second aCSF stimulations. 5 Hz imaging, speeded up 20X. The three 1-second stimulations occur at 6.48, 9.68 and 12.88 seconds. Scale bar, 10 µm.

Supplemental Table 1. Summary of initial differential RNA-seq replicates. Hits are grouped broadly by statistical significance, then ranked by log fold change between GFP- reference and GFP+ CSF-cN RNA pools.

Supplemental Table 2. Summary of subsequent RNA-seq replicates. Differential RNA-seq was performed again with improved technology. Results generally were in agreement with initial set.

Supplemental Table 3. Summary of differentially regulated genes in infected vs. uninfected CSF-cNs. Hits are ranked by statistical significance.

Supplemental Table 4. Functional enrichment analysis of GO terms from infected vs. uninfected CSF-cN RNA-seq dataset. We observe enrichment of several immune-related categories.

Supplemental Table 5. Inoculum used for each type of experiments (CFU per larva). Note that in order to test the effect of genetic manipulations, the experiments of calcium imaging and transcriptome relied on 2000 CFU while the survival experiments relied typically on smaller inoculum in order to reach close to 50% survival in controls.

Supplemental Table 6. crRNA used for target the interest region in DNA.

Supplemental Table 7. Primers and restriction enzymes used for genotyping.

REFERENCES

Abraira, V. E. and Ginty, D. D. (2013) 'The sensory neurons of touch', *Neuron*. Elsevier Inc., 79(4), pp. 618–639. doi: 10.1016/j.neuron.2013.07.051.

Acerbo, M. J., Hellmann, B. and Güntürkün, O. (2003) 'Catecholaminergic and dopamine-containing neurons in the spinal cord of pigeons: an immunohistochemical study', *Journal of Chemical Neuroanatomy*, 25, pp. 19–27. doi: 10.1016/S0891-0618(02)00072-8.

Adler, E. *et al.* (2000) 'A novel family of mammalian taste receptors', *Cell*, 100(6), pp. 693–702. doi: 10.1016/S0092-8674(00)80705-9.

Agduhr, E. (1922) 'Über ein zentrales Sinnesorgan (?) bei den Vertebraten.', *Zeitschrift für Anatomie und Entwicklungsgeschichte*, 66(3), pp. 223–360.

Ahuja, G. *et al.* (2015) 'Kappe neurons, a novel population of olfactory sensory neurons', *Scientific Reports*, 4, pp. 1–8. doi: 10.1038/srep04037.

Akopian, A. N. *et al.* (1999) 'The tetrodotoxin-resistant sodium channel SNS has a specialized function in pain pathways', *Nature Neuroscience*, 2(6), pp. 541–548. doi: 10.1038/9195.

Albayar, A. A. *et al.* (2019) 'Biomarkers in spinal cord injury: Prognostic insights and future potentials', *Frontiers in Neurology*, 10(JAN). doi: 10.3389/fneur.2019.00027.

Albeg, A. *et al.* (2011) 'C. elegans multi-dendritic sensory neurons: Morphology and function', *Molecular and Cellular Neuroscience*, 46(1), pp. 308–317. doi: 10.1016/j.mcn.2010.10.001.

Alfaro-Cervello, C. *et al.* (2012) 'Biciliated ependymal cell proliferation contributes to spinal cord growth', *Journal of Comparative Neurology*, 520(15), pp. 3528–3552. doi: 10.1002/cne.23104.

Alibardi, L. (1990) 'Cerebrospinal fluid contacting neurons inside the regenerating caudal spinal cord of xenopus tadpoles', *Bolletino di zoologia*, 57(4), pp. 309–315. doi: 10.1080/11250009009355713.

Allardyce, R. A. *et al.* (2006) 'Detection of volatile metabolites produced by bacterial growth in blood culture media by selected ion flow tube mass spectrometry (SIFT-MS)', *Journal of Microbiological Methods*, 65(2), pp. 361–365. doi: 10.1016/j.mimet.2005.09.003.

Andrzejczuk, L. A. *et al.* (2018) 'Tal1, Gata2a, and Gata3 have distinct functions in the development of V2b and cerebrospinal fluid-contacting KA spinal neurons', *Frontiers in Neuroscience*, 12(MAR), pp. 1–24. doi: 10.3389/fnins.2018.00170.

Arbeille, E. *et al.* (2015) 'Cerebrospinal fluid-derived Semaphorin3B orients neuroepithelial cell divisions in the apicobasal axis', *Nature Communications*, 6. doi: 10.1038/ncomms7366.

Auer, T. O. *et al.* (2015) 'Deletion of a kinesin I motor unmasks a mechanism of homeostatic branching control by neurotrophin-3', *eLife*, 4(JUNE), pp. 1–26. doi: 10.7554/eLife.05061.

Avery, O. T., MacLeod, C. M. and McCarty, M. (1979) 'Studies Nature Inducing of on of the the Chemical Transformation Types', *Journal of Experimental Medicine*, 149, pp. 297–326.

Baker, C. V. H. and Bronner-Fraser, M. (2001) ‘Vertebrate cranial placodes. I. Embryonic induction’, *Developmental Biology*, 232(1), pp. 1–61. doi: 10.1006/dbio.2001.0156.

Bandell, M. *et al.* (2004) ‘Noxious Cold Ion Channel TRPA1 Is Activated by Pungent Compounds and Bradykinin’, *Neuron*, 41, pp. 849–857. doi: 10.1016/s0896-6273(04)00150-3.

Banks, R. W. *et al.* (2009) ‘A comparative analysis of the encapsulated end-organs of mammalian skeletal muscles and of their sensory nerve endings’, *Journal of Anatomy*, 214(6), pp. 859–887. doi: 10.1111/j.1469-7580.2009.01072.x.

Barber, R. P., Vaughn, J. E. and Roberts, E. (1982) ‘The cytoarchitecture of GABAergic neurons in rat spinal cord’, *Brain Research*, 238, pp. 305–328. doi: 10.1016/0006-8993(82)90107-X.

Barham, H. P. *et al.* (2013) ‘Solitary chemosensory cells and bitter taste receptor signaling in human sinonasal mucosa’, *International Forum of Allergy & Rhinology*, 3(6), pp. 450–457. doi: 10.1002/alr.21149.

Bartel, D. L. *et al.* (2006) ‘Nucleoside triphosphate diphosphohydrolase-2 is the ecto-ATPase of type I cells in taste buds’, *The Journal of Comparative Neurology*, 497(1), pp. 1–12. doi: 10.1002/cne.20954.

Bautista, D. M. *et al.* (2006) ‘TRPA1 Mediates the Inflammatory Actions of Environmental Irritants and Proalgesic Agents’, *Cell*, 124(6), pp. 1269–1282. doi: 10.1016/j.cell.2006.02.023.

Bautista, D. M. *et al.* (2007) ‘The menthol receptor TRPM8 is the principal detector of environmental cold’, *Nature*, 448(7150), pp. 204–208. doi: 10.1038/nature05910.

Bazáes, A. and Schmachtenberg, O. (2012) ‘Odorant tuning of olfactory crypt cells from juvenile and adult rainbow trout’, *Journal of Experimental Biology*, 215(10), pp. 1740–1748. doi: 10.1242/jeb.067264.

van de Beek, D. *et al.* (2004) ‘Clinical Features and Prognostic Factors in Adults with Bacterial Meningitis’, *New England Journal of Medicine*, 351(18), pp. 1849–1859. doi: 10.1056/nejmoa040845.

van de Beek, D. *et al.* (2006) ‘Community-Acquired Bacterial Meningitis in Adults’, *New England Journal of Medicine*, 354(1), pp. 44–53. doi: 10.1056/NEJMra052116.

van de Beek, D. *et al.* (2016) ‘Community-acquired bacterial meningitis’, *Nature Reviews Disease Primers*. Macmillan Publishers Limited, 2, pp. 1–21. doi: 10.1038/nrdp.2016.74.

van de Beek, D. *et al.* (2021) ‘Community-acquired bacterial meningitis’, *The Lancet*. Elsevier Ltd, 398(10306), pp. 1171–1183. doi: 10.1016/S0140-6736(21)00883-7.

Behrens, M. *et al.* (2014) ‘ORA1, a zebrafish olfactory receptor ancestral to all mammalian V1R genes, recognizes 4-hydroxyphenylacetic acid, a putative reproductive pheromone’, *Journal of*

Biological Chemistry, 289(28), pp. 19778–19788. doi: 10.1074/jbc.M114.573162.

Beilharz, K. *et al.* (2015) 'Red fluorescent proteins for gene expression and protein localization studies in Streptococcus pneumoniae and efficient transformation with DNA assembled via the gibson assembly method', *Applied and Environmental Microbiology*, 81(20), pp. 7244–7252. doi: 10.1128/AEM.02033-15.

Di Bella, D. J. *et al.* (2019) 'Ascl1 Balances Neuronal versus Ependymal Fate in the Spinal Cord Central Canal', *Cell Reports*, 28(9), pp. 2264-2274.e3. doi: 10.1016/j.celrep.2019.07.087.

Belmonte, C. *et al.* (1991) 'Excitation by irritant chemical substances of sensory afferent units in the cat's cornea', *Journal of Physiology*, 437(1), pp. 709–725. doi: 10.1113/jphysiol.1991.sp018621.

Bernardos, R. L. and Raymond, P. A. (2006) 'GFAP transgenic zebrafish', *Gene Expression Patterns*, 6(8), pp. 1007–1013. doi: 10.1016/j.modgep.2006.04.006.

Bernhardt, R. R. *et al.* (1992) 'Axonal trajectories and distribution of GABAergic spinal neurons in wildtype and mutant zebrafish lacking floor plate cells', *Journal of Comparative Neurology*, 326(2), pp. 263–272. doi: 10.1002/cne.903260208.

Bertini, R. *et al.* (1999) 'Thioredoxin, a redox enzyme released in infection and inflammation, is a unique chemoattractant for neutrophils, monocytes, and T cells', *Journal of Experimental Medicine*, 189(11), pp. 1783–1789. doi: 10.1084/jem.189.11.1783.

Bessou, P. and Perl, E. R. (1969) 'Response of cutaneous sensory units with unmyelinated fibers to noxious stimuli', *Journal of neurophysiology*, 32(6), pp. 1025–1043. doi: 10.1152/jn.1969.32.6.1025.

Bijlsma, M. W. *et al.* (2016) 'Community-acquired bacterial meningitis in adults in the Netherlands, 2006-14: A prospective cohort study', *The Lancet Infectious Diseases*. Elsevier Ltd, 16(3), pp. 339–347. doi: 10.1016/S1473-3099(15)00430-2.

Binor, E. and Heathcote, R. D. (2001) 'Development of GABA-immunoreactive neuron patterning in the spinal cord', *Journal of Comparative Neurology*, 438(1), pp. 1–11. doi: 10.1002/cne.1298.

Biran, J. *et al.* (2012) 'Neurokinin Bs and neurokinin B receptors in zebrafish-potential role in controlling fish reproduction', *Proceedings of the National Academy of Sciences*, 109(26), pp. 10269–10274. doi: 10.1073/pnas.1119165109.

Bjorefeldt, A. *et al.* (2018) 'Neuromodulation via the cerebrospinal fluid: Insights from recent in vitro studies', *Frontiers in Neural Circuits*, 12(February), pp. 1–12. doi: 10.3389/fncir.2018.00005.

Böhm, U. L. *et al.* (2016) 'CSF-contacting neurons regulate locomotion by relaying mechanical stimuli to spinal circuits', *Nature Communications*, 7. doi: 10.1038/ncomms10866.

Böhm, U. L. (2017) *Physiological inputs to cerebrospinal fluid-contacting neurons*. Univeristé Pierre et Marie Curie - Paris VI.

Bos, L. D. J., Sterk, P. J. and Schultz, M. J. (2013) 'Volatile Metabolites of Pathogens: A Systematic Review', *PLoS Pathogens*, 9(5), pp. 1–8. doi: 10.1371/journal.ppat.1003311.

Boyd, I. A. (1962) 'The structure and innervation of the nuclear bag muscle fibre system and the nuclear chain muscle fibre system in mammalian muscle spindles', *Royal Society*, 245(720). doi: 10.1098/rstb.1962.0007.

Brand, M. *et al.* (1996) 'Mutations affecting development of the midline and general body shape during zebrafish embryogenesis', *Development*, 123(June 2014), pp. 129–142. doi: 10.1242/dev.123.1.129.

Braubach, O. R., Fine, A. and Croll, R. P. (2012) 'Distribution and functional organization of glomeruli in the olfactory bulbs of zebrafish (Danio rerio)', *Journal of Comparative Neurology*, 520(11), pp. 2317–2339. doi: 10.1002/cne.23075.

Brisben, A. J., Hsiao, S. S. and Johnson, K. O. (1999) 'Detection of vibration transmitted through an object grasped in the hand', *Journal of Neurophysiology*, 81(4), pp. 1548–1558. doi: 10.1152/jn.1999.81.4.1548.

Brown, A. G. and Iggo, A. (1967) 'A quantitative study of cutaneous receptors and afferent fibres in the cat and rabbit', *The Journal of Physiology*, 193(3), pp. 707–733. doi: 10.1113/jphysiol.1967.sp008390.

Brunger, A. T., Jin, R. and Breidenbach, M. A. (2008) 'Highly specific interactions between botulinum neurotoxins and synaptic vesicle proteins', *Cellular and Molecular Life Sciences*, 65(15), pp. 2296–2306. doi: 10.1007/s00018-008-8088-0.

Buchanan, J. T. *et al.* (1987) 'Survey of neuropeptide-like immunoreactivity in the lamprey spinal cord', *Brain Research*, 408(1–2), pp. 299–302. doi: 10.1016/0006-8993(87)90392-1.

Buck, L. B. (2000) 'The molecular architecture of odor and pheromone sensing in mammals', *Cell*, 100(6), pp. 611–618. doi: 10.1016/S0092-8674(00)80698-4.

Budick, S. A. and O'Malley, D. M. (2000) 'Locomotor repertoire of the larval zebrafish: Swimming, turning and prey capture', *Journal of Experimental Biology*, 203(17), pp. 2565–2579. doi: 10.1242/jeb.203.17.2565.

Burgess, P. R., Petit, D. and Warren, R. M. (1968) 'Receptor types in cat hairy skin supplied by myelinated fibers.', *Journal of neurophysiology*, 31(6), pp. 833–848. doi: 10.1152/jn.1968.31.6.833.

Burke, D., Gandevia, S. C. and Macefield, G. (1988) 'Responses to passive movement of receptors in joint, skin and muscle of the human hand', *Journal of Pain*, 402, pp. 347–361. doi: 10.1113/jphysiol.1988.sp017208.

Byrd, C. A. and Brunjes, P. C. (1995) ‘Organization of the olfactory system in the adult zebrafish: Histological, immunohistochemical, and quantitative analysis’, *Journal of Comparative Neurology*, 358(2), pp. 247–259. doi: 10.1002/cne.903580207.

Caceres, A. I. *et al.* (2009) ‘A sensory neuronal ion channel essential for airway inflammation and hyperreactivity in asthma’, *Proceedings of the National Academy of Sciences of the United States of America*, 106(22), pp. 9099–9104. doi: 10.1073/pnas.0900591106.

Calvo-Ochoa, E. and Byrd-Jacobs, C. A. (2019) ‘The olfactory system of zebrafish as a model for the study of neurotoxicity and injury: Implications for neuroplasticity and disease’, *International Journal of Molecular Sciences*, 20(7). doi: 10.3390/ijms20071639.

Campero, M. *et al.* (2001) ‘Slowly conducting afferents activated by innocuous low temperature in human skin’, *Journal of Physiology*, 535(3), pp. 855–865. doi: 10.1111/j.1469-7793.2001.t01-1-00855.x.

Cantaut-Belarif, Y. *et al.* (2018) ‘The Reissner Fiber in the Cerebrospinal Fluid Controls Morphogenesis of the Body Axis’, *Current Biology*. Elsevier Ltd., pp. 1–8. doi: 10.1016/j.cub.2018.05.079.

Cantaut-Belarif, Y. *et al.* (2020) ‘Adrenergic activation modulates the signal from the reissner fiber to cerebrospinal fluid-contacting neurons during development’, *eLife*, 9, pp. 1–25. doi: 10.7554/eLife.59469.

Caspary, T. and Anderson, K. V. (2003) ‘Patterning cell types in the dorsal spinal cord: What the mouse mutants say’, *Nature Reviews Neuroscience*, 4(4), pp. 290–298. doi: 10.1038/nrn1073.

Caterina, M. J. *et al.* (1997) ‘The capsaicin receptor: A heat-activated ion channel in the pain pathway’, *Nature*, 389(6653), pp. 816–824. doi: 10.1038/39807.

Caterina, M. J. *et al.* (1999) ‘A capsaicin-receptor homologue with a high threshold for noxious heat’, *Nature*, 398(6726), pp. 436–441. doi: 10.1038/18906.

Caterina, M. J. *et al.* (2000) ‘Impaired Nociception and Pain Sensation in Mice Lacking the Capsaicin Receptor’, *Science*, 288(April), pp. 306–313. doi: 10.1126/science.288.5464.306.

Chalermkitpanit, P. *et al.* (2017) ‘Noradrenaline, Serotonin, GABA, and Glycine in Cerebrospinal Fluid during Labor Pain: A Cross-Sectional Prospective Study’, *Pain Research and Management*. Hindawi, 2017. doi: 10.1155/2017/2752658.

Chalfie, M. and Sulston, J. (1981) ‘Developmental genetics of the mechanosensory neurons of Caenorhabditis elegans’, *Developmental Biology*, 82(2), pp. 358–370. doi: 10.1016/0012-1606(81)90459-0.

Chambers, D., Huang, C. and Matthews, G. (2015) 'The spinal cord', in *Basic Physiology for Anaesthetists*. Cambridge: Cambridge University Press, pp. 207–216. doi: 10.1017/CBO9781139226394.049.

Chandrashekar, J. *et al.* (2000) 'T2Rs function as bitter taste receptors', *Cell*, 100(6), pp. 703–711. doi: 10.1016/S0092-8674(00)80706-0.

Chandrashekar, J. *et al.* (2006) 'The receptors and cells for mammalian taste', *Nature*, 444(7117), pp. 288–294. doi: 10.1038/nature05401.

Chandrashekar, J. *et al.* (2009) 'The taste of carbonation', *Science*, 326(5951), pp. 443–445. doi: 10.1126/science.1174601.

Chang, J. T., Lehtinen, M. K. and Sive, H. (2016) 'Zebrafish cerebrospinal fluid mediates cell survival through a retinoid signaling pathway', *Developmental Neurobiology*, 76(1), pp. 75–92. doi: 10.1002/dneu.22300.

Chang, W. *et al.* (2016) 'Merkel disc is a serotonergic synapse in the epidermis for transmitting tactile signals in mammals', *Proceedings of the National Academy of Sciences of the United States of America*, 113(37), pp. E5491–E5500. doi: 10.1073/pnas.1610176113.

Chatzigeorgiou, M. *et al.* (2010) 'Specific roles for DEG/ENaC and TRP channels in touch and thermosensation in C. elegans nociceptors', *Nature Neuroscience*, 13(7), pp. 861–868. doi: 10.1038/nn.2581.

Chau, K. F. *et al.* (2015) 'Progressive Differentiation and Instructive Capacities of Amniotic Fluid and Cerebrospinal Fluid Proteomes following Neural Tube Closure', *Developmental Cell*, 35(6), pp. 789–802. doi: 10.1016/j.devcel.2015.11.015.

Chen, C. C. *et al.* (2002) 'A role for ASIC3 in the modulation of high-intensity pain stimuli', *Proceedings of the National Academy of Sciences of the United States of America*, 99(13), pp. 8992–8997. doi: 10.1073/pnas.122245999.

Chen, G. *et al.* (2014) 'C-type natriuretic peptide attenuates LPS-induced endothelial activation: Involvement of p38, Akt, and NF-κB pathways', *Amino Acids*, 46(12), pp. 2653–2663. doi: 10.1007/s00726-014-1816-x.

Chen, G., Ning, B. and Shi, T. (2019) 'Single-cell RNA-seq technologies and related computational data analysis', *Frontiers in Genetics*, 10(APR), pp. 1–13. doi: 10.3389/fgene.2019.00317.

Chiu, I. M. *et al.* (2013) 'Bacteria activate sensory neurons that modulate pain and inflammation', *Nature*. Nature Publishing Group, 501(7465), pp. 52–57. doi: 10.1038/nature12479.

Christenson, J. *et al.* (1991) 'Co-localized GABA and somatostatin use different ionic mechanisms to

hyperpolarize target neurons in the lamprey spinal cord', *Neuroscience Letters*, 134(1), pp. 93–97. doi: 10.1016/0304-3940(91)90516-V.

Colburn, R. W. *et al.* (2007) 'Attenuated Cold Sensitivity in TRPM8 Null Mice', *Neuron*, 54(3), pp. 379–386. doi: 10.1016/j.neuron.2007.04.017.

Collaborators, G. 2016 M. (2018) 'Global, regional, and national burden of meningitis, 1990–2016: a systematic analysis for the Global Burden of Disease Study 2016', *The Lancet Neurology*, 17(12), pp. 1061–1082. doi: 10.1016/S1474-4422(18)30387-9.

Concordet, J. P. and Haeussler, M. (2018) 'CRISPOR: Intuitive guide selection for CRISPR/Cas9 genome editing experiments and screens', *Nucleic Acids Research*. Oxford University Press, 46(W1), pp. W242–W245. doi: 10.1093/nar/gky354.

Conwey, B. A., Hultborn, H. and Kiehn, O. (1987) 'Proprioceptive input resets central locomotor rhythm in the spinal cat', *Experimental Brain Research*, 68, pp. 643–656. doi: 10.1007/BF00249807.

Corns, L. F. *et al.* (2015) 'Cholinergic Enhancement of Cell Proliferation in the Postnatal Neurogenic Niche of the Mammalian Spinal Cord', *STEM CELLS*, 33(9), pp. 2864–2876. doi: 10.1002/stem.2077.

Cox, J. J. *et al.* (2006) 'An SCN9A channelopathy causes congenital inability to experience pain', *Nature*, 444(7121), pp. 894–898. doi: 10.1038/nature05413.

Cropper, E. C. *et al.* (2018) 'Peptide Cotransmitters as Dynamic, Intrinsic Modulators of Network Activity', *Frontiers in Neural Circuits*, 12(October), pp. 1–7. doi: 10.3389/fncir.2018.00078.

Dale, N. *et al.* (1987) 'The Development of a Population of Spinal Cord Neurons and their Axonal Projections Revealed by GABA Immunocytochemistry in Frog Embryos', *Proceedings of the Royal Society B: Biological Sciences*, 232(1267), pp. 205–215. doi: 10.1098/rspb.1987.0069.

Dalm, V. A. S. H. *et al.* (2003) 'Expression of somatostatin, cortistatin, and somatostatin receptors in human monocytes, macrophages, and dendritic cells', *American Journal of Physiology - Endocrinology and Metabolism*, 285(2 48-2), pp. 344–353. doi: 10.1152/ajpendo.00048.2003.

Damkier, H. H., Brown, P. D. and Praetorius, J. (2013) 'Cerebrospinal fluid secretion by the choroid plexus', *Physiological Reviews*, 93(4), pp. 1847–1892. doi: 10.1152/physrev.00004.2013.

Darian-Smith, I. *et al.* (1979) 'Warm fibers innervating palmar and digital skin of the monkey: Responses to thermal stimuli', *Journal of Neurophysiology*, 42(5), pp. 1297–1315. doi: 10.1152/jn.1979.42.5.1297.

Daroff, R. and Aminoff, M. (eds) (2014) *Encyclopedia of the Neurological Sciences, Second Edition*. 2nd edn.

Davis, J. B. *et al.* (2000) 'Vanilloid receptor-1 is essential for inflammatory thermal hyperalgesia', *Nature*, 405(6783), pp. 183–187. doi: 10.1038/35012076.

De-Doncker, L. *et al.* (2003) 'Characterization of spindle afferents in rat soleus muscle using ramp-and-hold and sinusoidal stretches', *Journal of Neurophysiology*, 89(1), pp. 442–449. doi: 10.1152/jn.00153.2002.

DeFazio, R. A. *et al.* (2006) 'Separate populations of receptor cells and presynaptic cells in mouse taste buds', *Journal of Neuroscience*, 26(15), pp. 3971–3980. doi: 10.1523/JNEUROSCI.0515-06.2006.

Deisenhammer, F. *et al.* (2006) 'Guidelines on routine cerebrospinal fluid analysis. Report from an EFNS task force', *European Journal of Neurology*, 13(9), pp. 913–922. doi: 10.1111/j.1468-1331.2006.01493.x.

Delneste, Y., Beauvillain, C. and Jeannin, P. (2007) 'Innate immunity: structure and function of TLRs', *Médecine/Sciences*, 23(1), pp. 67–74. doi: 10.1051/medsci/200723167.

DeMaria, S. *et al.* (2013) 'Role of a ubiquitously expressed receptor in the vertebrate olfactory system', *Journal of Neuroscience*, 33(38), pp. 15235–15247. doi: 10.1523/JNEUROSCI.2339-13.2013.

Desban, L. *et al.* (2019) 'Regulation of the apical extension morphogenesis tunes the mechanosensory response of microvilliated neurons', *PLoS Biology*, 17(4), pp. 1–27. doi: 10.1371/journal.pbio.3000235.

Dhaka, A. *et al.* (2007) 'TRPM8 Is Required for Cold Sensation in Mice', *Neuron*, 54(3), pp. 371–378. doi: 10.1016/j.neuron.2007.02.024.

Dib-Hajj, S. D., Yang, Y. and Waxman, S. G. (2008) *Chapter 4 Genetics and Molecular Pathophysiology of Nav1.7-Related Pain Syndromes*. 1st edn, *Advances in Genetics*. 1st edn. Elesvier Inc. doi: 10.1016/S0065-2660(08)01004-3.

Djenoune, L. *et al.* (2014) 'Investigation of spinal cerebrospinal fluid-contacting neurons expressing PKD2L1: evidence for a conserved system from fish to primates.', *Frontiers in neuroanatomy*, 8(May), p. 26. doi: 10.3389/fnana.2014.00026.

Djenoune, L. *et al.* (2017) 'The dual developmental origin of spinal cerebrospinal fluid- contacting neurons gives rise to distinct functional subtypes', *Scientific Reports*. Springer US, 7(719), pp. 1–14. doi: 10.1038/s41598-017-00350-1.

Drew, L. J. *et al.* (2004) 'Acid-sensing ion channels ASIC2 and ASIC3 do not contribute to mechanically activated currents in mammalian sensory neurones', *Journal of Physiology*, 556(3), pp. 691–710. doi: 10.1113/jphysiol.2003.058693.

Driscoll, M. and Chalfie, M. (1991) ‘The mec-4 gene is a member of a family of Caenorhabditis elegans genes that can mutate to induce neuronal degeneration’, *Nature*, 349, pp. 588–593. doi: 10.1038/349588a0.

Du, J. *et al.* (2009) ‘Expression of TRPM8 in the distal cerebrospinal fluid-contacting neurons in the brain mesencephalon of rats’, *Cerebrospinal Fluid Research*, 6. doi: 10.1186/1743-8454-6-3.

Dubyak, G. R. (2003) ‘Knock-out mice reveal tissue-specific roles of P2Y receptor subtypes in different epithelia’, *Molecular Pharmacology*, 63(4), pp. 773–776. doi: 10.1124/mol.63.4.773.

Dvoryanchikov, G., Tomchik, S. M. and Chaudhari, N. (2007) ‘Biogenic amine synthesis and uptake in rodent taste buds’, *The Journal of Comparative Neurology*, 505(3), pp. 302–313. doi: 10.1002/cne.21494.

Eccles, J. C. (1946) ‘Synaptic potentials of motoneurones’, *Physiology*. doi: 10.1152/jn.1946.9.2.87.

Eccles, J. C. and Sherrington, C. S. (1930) ‘Numbers and contraction-values of individual motor-units examined in some muscles of the limb’, *Royal Society*, 106(745), pp. 326–357. doi: 10.1098/rspb.1930.0032.

Eccles, R. M. and Lundberg, A. (1958) ‘Integrative pattern of Ia synaptic actions on motoneurones of hip and knee muscles’, *The Journal of Physiology*, 144(2), pp. 271–298. doi: 10.1113/jphysiol.1958.sp006101.

Eftekhari, S. *et al.* (2013) ‘Differentiation of nerve fibers storing CGRP and CGRP receptors in the peripheral trigeminovascular system’, *The Journal of Pain*. Elsevier Ltd, 14(11), pp. 1289–1303. doi: 10.1016/j.jpain.2013.03.010.

Eisthen, H. L. (1992) ‘Phylogeny of the vomeronasal system and of receptor cell types in the olfactory and vomeronasal epithelia of vertebrates’, *Microscopy Research and Technique*, 23(1), pp. 1–21. doi: 10.1002/jemt.1070230102.

England, S. J. *et al.* (2017) ‘Identification and Expression Analysis of the Complete Family of Zebrafish pkd Genes’, *Frontiers in Cell and Developmental Biology*, 5(February). doi: 10.3389/fcell.2017.00005.

Estacion, M. *et al.* (2008) ‘NaV1.7 gain-of-function mutations as a continuum: A1632E displays physiological changes associated with erythromelalgia and paroxysmal extreme pain disorder mutations and produces symptoms of both disorders’, *Journal of Neuroscience*, 28(43), pp. 11079–11088. doi: 10.1523/JNEUROSCI.3443-08.2008.

Fang, X. *et al.* (2005) ‘trkA is expressed in nociceptive neurons and influences electrophysiological properties via Nav1.8 expression in rapidly conducting nociceptors’, *Journal of Neuroscience*, 25(19), pp. 4868–4878. doi: 10.1523/JNEUROSCI.0249-05.2005.

Ferrell, W. R. (1980) ‘The adequacy of stretch receptors in the cat knee joint for signalling joint angle throughout a full range of movement’, *The Journal of Physiology*, 299(1), pp. 85–99. doi: 10.1113/jphysiol.1980.sp013112.

Fertleman, C. R. *et al.* (2006) ‘SCN9A Mutations in Paroxysmal Extreme Pain Disorder: Allelic Variants Underlie Distinct Channel Defects and Phenotypes’, *Neuron*, 52(5), pp. 767–774. doi: 10.1016/j.neuron.2006.10.006.

Fettiplace, R. and Hackney, C. M. (2006) ‘The sensory and motor roles of auditory hair cells’, *Nature Reviews Neuroscience*, 7(1), pp. 19–29. doi: 10.1038/nrn1828.

Fidelin, K. *et al.* (2015) ‘State-dependent modulation of locomotion by GABAergic spinal sensory neurons’, *Current Biology*. Elsevier, 25(23), pp. 3035–3047. doi: 10.1016/j.cub.2015.09.070.

Filipiak, W. *et al.* (2012) ‘Characterization of volatile metabolites taken up by or released from Streptococcus pneumoniae and Haemophilus influenzae by using GC-MS’, *Microbiology (United Kingdom)*, 158(12), pp. 3044–3053. doi: 10.1099/mic.0.062687-0.

Finger, T. E. (1997) ‘Evolution of Taste and Solitary Chemoreceptor Cell Systems’, *Brain, Behavior and Evolution*, 50(4), pp. 234–243. doi: 10.1159/000113337.

Finger, T. E. *et al.* (2003) ‘Solitary chemoreceptor cells in the nasal cavity serve as sentinels of respiration’, *Proceedings of the National Academy of Sciences of the United States of America*, 100(15), pp. 8981–8986. doi: 10.1073/pnas.1531172100.

Finger, T. E. *et al.* (2005) ‘Neuroscience: ATP signalling is crucial for communication from taste buds to gustatory nerves’, *Science*, 310(5753), pp. 1495–1499. doi: 10.1126/science.1118435.

Firestein, S., Darrow, B. and Shepherd, G. M. (1991) ‘Activation of the sensory current in salamander olfactory receptor neurons depends on a G protein-mediated cAMP second messenger system’, *Neuron*, 6(5), pp. 825–835. doi: 10.1016/0896-6273(91)90178-3.

Fisher, S. *et al.* (2006) ‘Evaluating the biological relevance of putative enhancers using Tol2 transposon-mediated transgenesis in zebrafish’, *Nature Protocols*, 1(3), pp. 1297–1305. doi: 10.1038/nprot.2006.230.

Folgueira, M., Anadón, R. and Yañez, J. (2003) ‘Experimental study of the connections of the gustatory system in the rainbow trout, Oncorhynchus mykiss’, *Journal of Comparative Neurology*, 465(4), pp. 604–619. doi: 10.1002/cne.10879.

Foster, S. L. *et al.* (2017) ‘Sense and immunity: Context-dependent neuro-immune interplay’, *Frontiers in Immunology*, 8(NOV), pp. 1–11. doi: 10.3389/fimmu.2017.01463.

Freund, J. R. *et al.* (2018) ‘Activation of airway epithelial bitter taste receptors by pseudomonas

aeruginosa quinolones modulates calcium, cyclic-amp, and nitric oxide signaling', *Journal of Biological Chemistry*, 293(25), pp. 9824–9840. doi: 10.1074/jbc.RA117.001005.

Friedrich, R. W. and Korsching, S. I. (1998) 'Representations in the Olfactory Bulb Revealed Using a Voltage-Sensitive Axon Tracer', *The Journal of neuroscience*, 18(23), pp. 9977–9988.

Fuller, C. L., Yettaw, H. K. and Byrd, C. A. (2006) 'Mitral cells in the olfactory bulb of adult zebrafish (Danio rerio): Morphology and distribution', *The Journal of Comparative Neurology*, 499(2), pp. 218–230. doi: 10.1002/cne.21091.

Ganju, P. *et al.* (1998) 'Differential regulation of SHC proteins by nerve growth factor in sensory neurons and PC12 cells', *European Journal of Neuroscience*, 10(6), pp. 1995–2008. doi: 10.1046/j.1460-9568.1998.00209.x.

Gardner, E. D. (1942) 'Nerve terminals associated with the knee joint of the mouse', *The Anatomical Record*, 83(3), pp. 401–419. doi: 10.1002/ar.1090830309.

Gato, Á. *et al.* (2005) 'Embryonic cerebrospinal fluid regulates neuroepithelial survival, proliferation, and neurogenesis in chick embryos', *Anatomical Record - Part A Discoveries in Molecular, Cellular, and Evolutionary Biology*, 284(1), pp. 475–484. doi: 10.1002/ar.a.20185.

Gawel, K. *et al.* (2020) 'Seizing the moment: Zebrafish epilepsy models', *Neuroscience and Biobehavioral Reviews*. Elsevier Ltd, 116, pp. 1–20. doi: 10.1016/j.neubiorev.2020.06.010.

Ghitani, N. *et al.* (2017) 'Specialized Mechanosensory Nociceptors Mediating Rapid Responses to Hair-Pull', *Neuron*, 95(4), pp. 944-954.e4. doi: 10.1016/j.neuron.2017.07.024.

Goldberg, D. W. *et al.* (2018) 'Neurological sequelae of adult meningitis in Africa: A systematic literature review', *Open Forum Infectious Diseases*, 5(1). doi: 10.1093/ofid/ofx246.

Gossard, J. P. *et al.* (1994) 'Transmission in a locomotor-related group Ib pathway from hindlimb extensor muscles in the cat', *Experimental Brain Research*, 98(2), pp. 213–228. doi: 10.1007/BF00228410.

Grigg, P. and Greenspan, B. J. (1977) 'Response of primate joint afferent neurons to mechanical stimulation of knee joint', *Journal of Neurophysiology*, 40(1). doi: 10.1152/jn.1977.40.1.1.

Grillner, S., Williams, T. and Lagerbäck, P. Å. (1984) 'The edge cell, a possible intraspinal mechanoreceptor', *Science*, 223(4635), pp. 500–503. doi: 10.1126/science.6691161.

Guertin, P. *et al.* (1995) 'Ankle extensor group I afferents excite extensors throughout the hindlimb during fictive locomotion in the cat', *The Journal of Physiology*, 487(1), pp. 197–209. doi: 10.1113/jphysiol.1995.sp020871.

Gulbransen, B. D. *et al.* (2008) 'Nasal Solitary Chemoreceptor Cell Responses to Bitter and Trigeminal Stimulants In Vitro', *Journal of Neurophysiology*, 99(6), pp. 2929–2937. doi: 10.1152/jn.00066.2008.

Güler, A. D. *et al.* (2002) 'Heat-Evoked Activation of the Ion Channel, TRPV4', *The Journal of Neuroscience*, 22(15), pp. 6408–6414. doi: 10.1016/S0003-2670(01)85240-5.

Hagen-Torn, O. (1882) 'Entwicklung und Bau der Synoviamembranen.', *Arch. Mikros. Anat.*, 21, pp. 591–663.

Halata, Z., Grim, M. and Bauman, K. I. (2003) 'Friedrich Sigmund Merkel and his "Merkel cell", morphology, development, and physiology: Review and new results', *Anatomical Record - Part A Discoveries in Molecular, Cellular, and Evolutionary Biology*, 271(1), pp. 225–239. doi: 10.1002/ar.a.10029.

Handler, A. and Ginty, D. D. (2021) 'The mechanosensory neurons of touch and their mechanisms of activation', *Nature Reviews Neuroscience*. Springer US, 22(9), pp. 521–537. doi: 10.1038/s41583-021-00489-x.

Hansen, A. *et al.* (1999) 'Ultrastructure of the olfactory epithelium in intact, axotomized, and bulbectomized goldfish, Carassius auratus', *Microscopy Research and Technique*, 45(4–5), pp. 325–338. doi: 10.1002/(SICI)1097-0029(19990515/01)45:4/5<325::AID-JEMT16>3.0.CO;2-V.

Hansen, A. *et al.* (2003) 'Correlation between Olfactory Receptor Cell Type and Function in the Channel Catfish', *Journal of Neuroscience*, 23(28), pp. 9328–9339. doi: 10.1523/jneurosci.23-28-09328.2003.

Hansen, A., Reutter, K. and Zeiske, E. (2002) 'Taste bud development in the zebrafish, Danio rerio', *Developmental Dynamics*, 223(4), pp. 483–496. doi: 10.1002/dvdy.10074.

Hansen, A. and Zeiske, E. (1998) 'The peripheral olfactory organ of the zebrafish, Danio rerio: An ultrastructural study', *Chemical Senses*, 23(1), pp. 39–48. doi: 10.1093/chemse/23.1.39.

Hansen, A. and Zielinski, B. S. (2005) 'Diversity in the olfactory epithelium of bony fishes: Development, lamellar arrangement, sensory neuron cell types and transduction components', *Journal of Neurocytology*, 34(3–5), pp. 183–208. doi: 10.1007/s11068-005-8353-1.

Harden, T. K. *et al.* (2010) 'Signalling and pharmacological properties of the P2Y14 receptor', *Acta Physiologica*, 199(2), pp. 149–160. doi: 10.1111/j.1748-1716.2010.02116.x.

Hatta, T. *et al.* (2006) 'Quantitative analyses of leukemia inhibitory factor in the cerebrospinal fluid in mouse embryos', *NeuroReport*, 17(18), pp. 1863–1866. doi: 10.1097/WNR.0b013e3280113962.

Higashijima, S. I., Mandel, G. and Fetcho, J. R. (2004) 'Distribution of prospective glutamatergic, glycinergic, and gabaergic neurons in embryonic and larval zebrafish', *Journal of Comparative*

Neurology, 480(1), pp. 1–18. doi: 10.1002/cne.20278.

Higashijima, S. I., Schaefer, M. and Fetcho, J. R. (2004) 'Neurotransmitter properties of spinal interneurons in embryonic and larval zebrafish', *Journal of Comparative Neurology*, 480(1), pp. 19–37. doi: 10.1002/cne.20279.

Hoegg, S. *et al.* (2004) 'Phylogenetic timing of the fish-specific genome duplication correlates with the diversification of teleost fish', *Journal of Molecular Evolution*, 59(2), pp. 190–203. doi: 10.1007/s00239-004-2613-z.

Hökfelt, T. *et al.* (1976) 'Immunohistochemical evidence for separate populations of somatostatin-containing and substance P-containing primary afferent neurons in the rat', *Neuroscience*, 1(2), pp. 131–136. doi: 10.1016/0306-4522(76)90006-3.

Hoogman, M. *et al.* (2007) 'Cognitive outcome in adults after bacterial meningitis', *Journal of Neurology, Neurosurgery and Psychiatry*, 78(10), pp. 1092–1096. doi: 10.1136/jnnp.2006.110023.

Howell, M. *et al.* (1994) 'Cloning and functional expression of a tetrabenazine sensitive vesicular monoamine transporter from bovine chromaffin granules', *FEBS Letters*, 338(1), pp. 16–22. doi: 10.1016/0014-5793(94)80108-8.

Huang, A. L. *et al.* (2006) 'The cells and logic for mammalian sour taste detection', *Nature*, 442(7105), pp. 934–938. doi: 10.1038/nature05084.

Huang, J. *et al.* (2014) 'Gain-of-function mutations in sodium channel NaV1.9 in painful neuropathy', *Brain*, 137(6), pp. 1627–1642. doi: 10.1093/brain/awu079.

Huang, M. and Chalfie, M. (1994) 'Gene interactions affecting mechanosensory transduction in Caenorhabditis elegans', *Nature*, 367(6462), pp. 467–470. doi: 10.1038/367467a0.

Huang, P. *et al.* (2012) 'Attenuation of Notch and hedgehog signaling is required for fate specification in the spinal cord', *PLoS Genetics*, 8(6). doi: 10.1371/journal.pgen.1002762.

Huang, S. M. *et al.* (2011) 'TRPV3 and TRPV4 ion channels are not major contributors to mouse heat sensation', *Molecular Pain*, 7, pp. 1–11. doi: 10.1186/1744-8069-7-37.

Huang, X. *et al.* (2010) 'Transventricular delivery of sonic hedgehog is essential to cerebellar ventricular zone development', *Proceedings of the National Academy of Sciences of the United States of America*, 107(18), pp. 8422–8427. doi: 10.1073/pnas.0911838107.

Huang, Y. A. *et al.* (2008) 'Presynaptic (Type III) cells in mouse taste buds sense sour (acid) taste', *Journal of Physiology*, 586(12), pp. 2903–2912. doi: 10.1113/jphysiol.2008.151233.

Hubbard, J. M. *et al.* (2016) 'Intraspinal Sensory Neurons Provide Powerful Inhibition to Motor Circuits

Ensuring Postural Control during Locomotion', *Current Biology*, 26(21), pp. 2841–2853. doi: 10.1016/j.cub.2016.08.026.

Hull, M., Parnes, M. and Jankovic, J. (2021) 'Botulinum Neurotoxin Injections in Childhood Opisthotonus', *Toxins*, 13(2), pp. 1–9. doi: 10.3390/toxins13020137.

Hultborn, H. (1972) 'Convergence on interneurones in the reciprocal Ia inhibitory pathway to motoneurones', *Acta Physiologica Scandinavica Supplementum*, 375, pp. 1–42. doi: 10.1111/j.1748-1716.1972.tb05298.x.

Hunt, C. C. (1954) 'RELATION OF FUNCTION TO DIAMETER IN AFFERENT FIBERS OF MUSCLE NERVES', *Journal of General Physiology*, 38(1), pp. 117–131. doi: 10.1085/jgp.38.1.117.

Iggo, A. and Muir, A. R. (1969) 'The structure and function of a slowly adapting touch corpuscle in hairy skin', *The Journal of Physiology*, 200(3), pp. 763–796. doi: 10.1113/jphysiol.1969.sp008721.

Immke, D. C. and McCleskey, E. W. (2001) 'Lactate enhances the acid-sensing NA+ channel on ischemia-sensing neurons', *Nature Neuroscience*, 4(9), pp. 869–870. doi: 10.1038/nn0901-869.

Ishimaru, Y. *et al.* (2005) 'Two families of candidate taste receptors in fishes', *Mechanisms of Development*, 122(12), pp. 1310–1321. doi: 10.1016/j.mod.2005.07.005.

Jaeger, C. B. *et al.* (1983) 'Some Neurons of the Rat Central Nervous System Contain Aromatic-L-Amino-Acid Decarboxylase But Not Monoamines', *Science*, 219(4589), pp. 1233–1235. doi: 10.1126/science.6131537.

Jakutis, G. and Stainier, D. Y. R. (2021) 'Genotype–Phenotype Relationships in the Context of Transcriptional Adaptation and Genetic Robustness', *Annual Review of Genetics*, 55(1), pp. 71–91. doi: 10.1146/annurev-genet-071719-020342.

Jalalvand, E. *et al.* (2014) 'Laterally projecting cerebrospinal fluid-contacting cells in the lamprey spinal cord are of two distinct types', *Journal of Comparative Neurology*, 522(8), pp. 1753–1768. doi: 10.1002/cne.23542.

Jalalvand, E., Robertson, B., Wallén, P., *et al.* (2016) 'Ciliated neurons lining the central canal sense both fluid movement and pH through ASIC3', *Nature Communications*, 7, p. 10002. doi: 10.1038/ncomms10002.

Jalalvand, E., Robertson, B., Tostivint, H., *et al.* (2016) 'The spinal cord has an intrinsic system for the control of pH', *Current Biology*, 26(10), pp. 1346–1351. doi: 10.1016/j.cub.2016.03.048.

Jalalvand, E. *et al.* (2018) 'Cerebrospinal fluid-contacting neurons sense pH changes and motion in the hypothalamus', *Journal of Neuroscience*, 38(35), pp. 7713–7724. doi: 10.1523/JNEUROSCI.3359-17.2018.

Jim, K. K. *et al.* (2016) 'Infection of zebrafish embryos with live fluorescent Streptococcus pneumoniae as a real-time pneumococcal meningitis model', *Journal of Neuroinflammation*. Journal of Neuroinflammation, 13(1), pp. 1–13. doi: 10.1186/s12974-016-0655-y.

Johansson, R. S., Landström, U. and Lundström, R. (1982) 'Responses of mechanoreceptive afferent units in the glabrous skin of the human hand to sinusoidal skin displacements', *Brain Research*, 244(1), pp. 17–25. doi: 10.1016/0006-8993(82)90899-X.

Johnson, E. *et al.* (2020) 'Graded calcium spikes differentially signal neurotransmitter input in cerebrospinal fluid contacting neurons of mouse spinal cord', *bioRxiv*. doi: 10.1101/2020.09.18.303347.

Johnson, K. *et al.* (2016) 'Gfap-positive radial glial cells are an essential progenitor population for later-born neurons and glia in the zebrafish spinal cord', *Glia*, 64(7), pp. 1170–1189. doi: 10.1002/glia.22990.

Johnson, K. O. and Hsiao, S. S. (1992) 'Neural Mechanisms of Tactual form and Texture Perception', *Annual Review of Neuroscience*, 15(1), pp. 227–250. doi: 10.1146/annurev.ne.15.030192.001303.

de Jong, E. K. *et al.* (2008) 'Expression, transport, and axonal sorting of neuronal CCL21 in large dense-core vesicles.', *FASEB journal : official publication of the Federation of American Societies for Experimental Biology*, 22(12), pp. 4136–45. doi: 10.1096/fj.07-101907.

Jordt, S. E. *et al.* (2004) 'Mustard oils and cannabinoids excite sensory nerve fibres through the TRP channel ANKTM1', *Nature*, 427(6971), pp. 260–265. doi: 10.1038/nature02282.

Joselevitch, C. and Zenisek, D. (2009) 'Imaging exocytosis in retinal bipolar cells with TIRF microscopy', *Journal of Visualized Experiments*, (28), pp. 1–6. doi: 10.3791/1305.

Kadioglu, A. *et al.* (2008) 'The role of Streptococcus pneumoniae virulence factors in host respiratory colonization and disease', *Nature Reviews Microbiology*, 6(4), pp. 288–301. doi: 10.1038/nrmicro1871.

Kandel, E. R. *et al.* (2012) *Principle of Neural Science, Fifth Edtion*. New York: McGraw-Hill.

Karashima, Y. *et al.* (2007) 'Bimodal action of menthol on the transient receptor potential channel TRPA1', *Journal of Neuroscience*, 27(37), pp. 9874–9884. doi: 10.1523/JNEUROSCI.2221-07.2007.

Karashima, Y. *et al.* (2009) 'TRPA1 acts as a cold sensor in vitro and in vivo', *Proceedings of the National Academy of Sciences of the United States of America*, 106(4), pp. 1273–1278. doi: 10.1073/pnas.0808487106.

Kashem, S. W. *et al.* (2015) 'Nociceptive Sensory Fibers Drive Interleukin-23 Production from CD301b+ Dermal Dendritic Cells and Drive Protective Cutaneous Immunity', *Immunity*. Elsevier Inc., 43(3), pp. 515–526. doi: 10.1016/j.immuni.2015.08.016.

Kasumyan, A. O. (2019) ‘The taste system in fishes and the effects of environmental variables’, *Journal of Fish Biology*, 95(1), pp. 155–178. doi: 10.1111/jfb.13940.

Kasumyan, A. O. and Døving, K. B. (2003) ‘Taste preferences in fishes’, *Fish and Fisheries*, 4(4), pp. 289–347. doi: 10.1046/j.1467-2979.2003.00121.x.

Kennedy, W. R., Webster, H. de F. and Yoon, K. S. (1975) ‘Human muscle spindles: fine structure of the primary sensory ending’, *Journal of Neurocytology*, 4(6), pp. 675–695. doi: 10.1007/BF01181630.

Khakh, B. S. and North, R. A. (2012) ‘Neuromodulation by Extracellular ATP and P2X Receptors in the CNS’, *Neuron*, 76(1), pp. 51–69. doi: 10.1016/j.neuron.2012.09.024.

Kieser, K. J. and Kagan, J. C. (2017) ‘Multi-receptor detection of individual bacterial products by the innate immune system’, *Nature Reviews Immunology*. Nature Publishing Group, 17(6), pp. 376–390. doi: 10.1038/nri.2017.25.

Kim, J. H., Creekmore, E. and Vezina, P. (2003) ‘Microinjection of CART peptide 55-102 into the nucleus accumbens blocks amphetamine-induced locomotion’, *Neuropeptides*, 37(6), pp. 369–373. doi: 10.1016/j.npep.2003.10.001.

Kirino, M. *et al.* (2013) ‘Evolutionary origins of taste buds: Phylogenetic analysis of purinergic neurotransmission in epithelial chemosensors’, *Open Biology*, 3(MAR). doi: 10.1098/rsob.130015.

Kleene, S. J. and Gesteland, R. C. (1991) ‘Calcium-activated chloride conductance in frog olfactory cilia’, *Journal of Neuroscience*, 11(11), pp. 3624–3629. doi: 10.1523/jneurosci.11-11-03624.1991.

Knibestöl, M. (1975) ‘Stimulus-response functions of slowly adapting mechanoreceptors in the human glabrous skin area.’, *The Journal of Physiology*, 245(1), pp. 63–80. doi: 10.1113/jphysiol.1975.sp010835.

Koedel, U. *et al.* (2009) ‘Apoptosis is essential for neutrophil functional shutdown and determines tissue damage in experimental pneumococcal meningitis’, *PLoS Pathogens*, 5(5). doi: 10.1371/journal.ppat.1000461.

Koide, T. *et al.* (2009) ‘Olfactory neural circuitry for attraction to amino acids revealed by transposon-mediated gene trap approach in zebrafish’, *Proceedings of the National Academy of Sciences of the United States of America*, 106(24), pp. 9884–9889. doi: 10.1073/pnas.0900470106.

Kolmer, W. (1921) ‘Das ,,Sagittalorgan" der Wirbeltiere.’, *Anatomy and Embryology*, 60(3), pp. 652–717.

Kolmer, W. (1931) ‘Über das Sagittalorgan, ein zentrales Sinnesorgan der Wirbeltiere, insbesondere beim Affen.’, *Zeitschrift für Zellforschung und Mikroskopische Anatomie*, 13(1), pp. 236–248. doi: 10.1007/BF00406356.

Koltzenburg, M., Stucky, C. L. and Lewin, G. R. (1997) 'Receptive properties of mouse sensory neurons innervating hairy skin', *Journal of Neurophysiology*, 78(4), pp. 1841–1850. doi: 10.1152/jn.1997.78.4.1841.

Konieczny, M. R., Senyurt, H. and Krauspe, R. (2013) 'Epidemiology of adolescent idiopathic scoliosis', *Journal of Children's Orthopaedics*, 7(1), pp. 3–9. doi: 10.1007/s11832-012-0457-4.

Korsching, S. I. (2020) *Taste and Smell in Zebrafish*. Second Edi, *The Senses: A Comprehensive Reference*. Second Edi. Elsevier. doi: 10.1016/b978-0-12-809324-5.24155-2.

Koshimizu, T. A. *et al.* (2000) 'Characterization of calcium signaling by purinergic receptor-channels expressed in excitable cells', *Molecular Pharmacology*, 58(5), pp. 936–945. doi: 10.1124/mol.58.5.936.

Kotrschal, K. (1996) 'Solitary chemosensory cells: Why do primary aquatic vertebrates need another taste system?', *Trends in Ecology and Evolution*, 11(3), pp. 110–114. doi: 10.1016/0169-5347(96)81088-3.

Kotrschal, K., Krautgartner, W. D. and Hansen, A. (1997) 'Ontogeny of the solitary chemosensory cells in the zebrafish, Danio rerio', *Chemical Senses*, 22(2), pp. 111–118. doi: 10.1093/chemse/22.2.111.

Kramer-Zucker, A. G. *et al.* (2005) 'Cilia-driven fluid flow in the zebrafish pronephros, brain and Kupffer's vesicle is required for normal organogenesis', *Development*, 132(8), pp. 1907–1921. doi: 10.1242/dev.01772.

Krantic, S. (2000) 'Peptides as regulators of the immune system: Emphasis on somatostatin', *Peptides*, 21(12), pp. 1941–1964. doi: 10.1016/S0196-9781(00)00347-8.

Kútna, V. *et al.* (2014) 'Enigmatic cerebrospinal fluid-contacting neurons arise even after the termination of neurogenesis in the rat spinal cord during embryonic development and retain their immature-like characteristics until adulthood', *Acta Histochemica*, 116(1), pp. 278–285. doi: 10.1016/j.acthis.2013.08.004.

Kwan, K. M. *et al.* (2007) 'The Tol2kit: A multisite gateway-based construction Kit for Tol2 transposon transgenesis constructs', *Developmental Dynamics*, 236(11), pp. 3088–3099. doi: 10.1002/dvdy.21343.

Kwan, K. Y. *et al.* (2006) 'TRPA1 Contributes to Cold, Mechanical, and Chemical Nociception but Is Not Essential for Hair-Cell Transduction', *Neuron*, 50(2), pp. 277–289. doi: 10.1016/j.neuron.2006.03.042.

Lai, N. Y. *et al.* (2020) 'Gut-Innervating Nociceptor Neurons Regulate Peyer's Patch Microfold Cells and SFB Levels to Mediate Salmonella Host Defense', *Cell*. Elsevier Inc., 180(1), pp. 1–17. doi: 10.1016/j.cell.2019.11.014.

Lamotte, C. C. (1987) ‘Vasoactive Intestinal Polypeptide Cerebrospinal Fluid-Contacting Neurons of the Monkey and Cat Spinal Central Canal’, *Journal of Comparative Neurology*, 258(4), pp. 527–541. doi: 10.1002/cne.902580405.

LaMotte, R. H. and Campbell, J. N. (1978) ‘Comparison of responses of warm and nociceptive C-fiber afferents in monkey with human judgments of thermal pain’, *Journal of Neurophysiology*, 41(2), pp. 509–528. doi: 10.1152/jn.1978.41.2.509.

Langevin, C. *et al.* (2013) ‘The antiviral innate immune response in fish: Evolution and conservation of the IFN system’, *Journal of Molecular Biology*. Elsevier Ltd, 425(24), pp. 4904–4920. doi: 10.1016/j.jmb.2013.09.033.

Lawrence, C. (2011) ‘Advances in zebrafish husbandry and management’, *Methods in Cell Biology*, 104, pp. 429–451. doi: 10.1016/B978-0-12-374814-0.00023-9.

Lawrence, C. (2016) *New frontiers for zebrafish management*, *Methods in Cell Biology*. Elsevier Ltd. doi: 10.1016/bs.mcb.2016.04.015.

Lee, R. J. *et al.* (2012) ‘T2R38 taste receptor polymorphisms underlie susceptibility to upper respiratory infection’, *Journal of Clinical Investigation*, 122(11), pp. 4145–4159. doi: 10.1172/JCI64240.

Lee, R. J., Kofonow, J. M., *et al.* (2014) ‘Bitter and sweet taste receptors regulate human upper respiratory innate immunity’, *Journal of Clinical Investigation*, 124(3), pp. 1393–1405. doi: 10.1172/JCI72094.

Lee, R. J., Chen, B., *et al.* (2014) ‘Mouse nasal epithelial innate immune responses to Pseudomonas aeruginosa quorum-sensing molecules require taste signaling components’, *Innate Immunity*, 20(6), pp. 606–617. doi: 10.1177/1753425913503386.

Lee, R. J. *et al.* (2017) ‘Bacterial D-amino acids suppress sinonasal innate immunity through sweet taste receptors in solitary chemosensory cells’, *Science Signaling*, 10(495), pp. 1–12. doi: 10.1126/scisignal.aam7703.

Lee, W. *et al.* (2014) ‘Endocan elicits severe vascular inflammatory responses in vitro and in vivo’, *Journal of Cellular Physiology*, 229(5), pp. 620–630. doi: 10.1002/jcp.24485.

Lehtinen, M. K. *et al.* (2011) ‘The Cerebrospinal Fluid Provides a Proliferative Niche for Neural Progenitor Cells’, *Neuron*. Elsevier Inc., 69(5), pp. 893–905. doi: 10.1016/j.neuron.2011.01.023.

Leipold, E. *et al.* (2013) ‘A de novo gain-of-function mutation in SCN11A causes loss of pain perception’, *Nature Genetics*, 45(11), pp. 1399–1407. doi: 10.1038/ng.2767.

Lerner, R. A. *et al.* (1994) ‘Cerebrodiene: A brain lipid isolated from sleep-deprived cats’, *Proceedings*

of the National Academy of Sciences of the United States of America, 91(20), pp. 9505–9508. doi: 10.1073/pnas.91.20.9505.

Lewin, G. R. and McMahon, S. B. (1991) 'Physiological properties of primary sensory neurons appropriately and inappropriately innervating skin in the adult rat', *Journal of Neurophysiology*, 66(4), pp. 1205–1217. doi: 10.1152/jn.1991.66.4.1205.

Li, F. (2013) 'Taste perception: From the tongue to the testis', *Molecular Human Reproduction*, 19(6), pp. 349–360. doi: 10.1093/molehr/gat009.

Li, L. *et al.* (2011) 'The Functional Organization of Cutaneous Low-Threshold Mechanosensory Neurons', *Cell*, 147(7), pp. 1615–1627. doi: 10.1016/j.cell.2011.11.027.

Li, W. *et al.* (2011) 'The neural circuits and sensory channels mediating harsh touch sensation in Caenorhabditis elegans', *Nature Communications*, 2(1), p. 315. doi: 10.1038/ncomms1308.

Liljencrantz, J. and Olausson, H. (2014) 'Tactile C fibers and their contributions to pleasant sensations and to tactile allodynia', *Frontiers in Behavioral Neuroscience*, 8(MAR), pp. 6–11. doi: 10.3389/fnbeh.2014.00037.

Lloyd, D. P. C. (1943a) 'CONDUCTION AND SYNAPTIC TRANSMISSION OF THE REFLEX RESPONSE TO STRETCH IN SPINAL CATS', *Journal of Neurophysiology*, 6(4), pp. 317–326. doi: 10.1152/jn.1943.6.4.317.

Lloyd, D. P. C. (1943b) 'NEURON PATTERNS CONTROLLING TRANSMISSION OF IPSILATERAL HIND LIMB REFLEXES IN CAT', *Journal of Neurophysiology*, 6(4), pp. 293–315. doi: 10.1152/jn.1943.6.4.293.

Lloyd, David P C (1946) 'FACILITATION AND INHIBITION OF SPINAL MOTONEURONS', *Journal of Neurophysiology*, 9(6), pp. 421–438. doi: 10.1152/jn.1946.9.6.421.

Lloyd, David P. C. (1946) 'INTEGRATIVE PATTERN OF EXCITATION AND INHIBITION IN TWO-NEURON REFLEX ARCS', *Journal of Neurophysiology*, 9(6), pp. 439–444. doi: 10.1152/jn.1946.9.6.439.

Löken, L. S. *et al.* (2009) 'Coding of pleasant touch by unmyelinated afferents in humans', *Nature Neuroscience*, 12(5), pp. 547–548. doi: 10.1038/nn.2312.

Louati, K. and Berenbaum, F. (2015) 'Fatigue in chronic inflammation - a link to pain pathways', *Arthritis Research and Therapy*. Arthritis Research & Therapy, 17(1), pp. 1–10. doi: 10.1186/s13075-015-0784-1.

Lu, H. *et al.* (2020) 'Reissner fibre-induced urotensin signalling from cerebrospinal fluid-contacting neurons prevents scoliosis of the vertebrate spine', *Biology Open*, 9(5). doi: 10.1242/bio.052027.

Lun, M. P. *et al.* (2015) 'Spatially heterogeneous choroid plexus transcriptomes encode positional identity and contribute to regional CSF production', *Journal of Neuroscience*, 35(12), pp. 4903–4916. doi: 10.1523/JNEUROSCI.3081-14.2015.

Ly, N. P. *et al.* (2005) 'Netrin-1 inhibits leukocyte migration in vitro and in vivo', *Proceedings of the National Academy of Sciences of the United States of America*, 102(41), pp. 14729–14734. doi: 10.1073/pnas.0506233102.

Ma, L. and Michel, W. C. (1998) 'Drugs affecting phospholipase C-mediated signal transduction block the olfactory cyclic nucleotide-gated current of adult zebrafish', *Journal of Neurophysiology*, 79(3), pp. 1183–1192. doi: 10.1152/jn.1998.79.3.1183.

Mainen, Z. F. and Sejnowski, T. J. (1996) 'Influence of dendritic structure on firing pattern in model neocortical neurons', *Nature*, pp. 363–366. doi: 10.1038/382363a0.

Maksimovic, S., Baba, Y. and Lumpkin, E. A. (2013) 'Neurotransmitters and synaptic components in the Merkel cell-neurite complex, a gentle-touch receptor', *Annals of the New York Academy of Sciences*, 1279(1), pp. 13–21. doi: 10.1111/nyas.12057.

Manoli, M. and Driever, W. (2012) 'Fluorescence-activated cell sorting (FACS) of fluorescently tagged cells from zebrafish larvae for RNA isolation', *Cold Spring Harbor Protocols*, 7(8), pp. 879–886. doi: 10.1101/pdb.prot069633.

Marichal, N. *et al.* (2009) 'Enigmatic central canal contacting cells: Immature neurons in "standby mode"?', *Journal of Neuroscience*, 29(32), pp. 10010–10024. doi: 10.1523/JNEUROSCI.6183-08.2009.

Marnas, H. *et al.* (no date) 'Diverse chemosensory cues can activate sensory neurons in contact with the cerebrospinal fluid'.

Marquart, G. D. *et al.* (2015) 'A 3D searchable database of transgenic zebrafish gal4 and cre lines for functional neuroanatomy studies', *Frontiers in Neural Circuits*, 9(November), pp. 1–17. doi: 10.3389/fncir.2015.00078.

Martin, B. *et al.* (1995) 'The recA gene of Streptococcus pneumoniae is part of a competence- induced operon and controls lysogenic induction', *Molecular Microbiology*, 15(2), pp. 367–379. doi: 10.1111/j.1365-2958.1995.tb02250.x.

Martín, C. *et al.* (2006) 'FGF2 plays a key role in embryonic cerebrospinal fluid trophic properties over chick embryo neuroepithelial stem cells', *Developmental Biology*, 297(2), pp. 402–416. doi: 10.1016/j.ydbio.2006.05.010.

Martin, J. *et al.* (2014) 'Vasopressin and oxytocin in CSF and plasma of patients with aneurysmal subarachnoid haemorrhage', *Neuropeptides*. Elsevier Ltd, 48(2), pp. 91–96. doi:

10.1016/j.npep.2013.12.004.

Matsumae, M. *et al.* (2016) 'Research into the physiology of cerebrospinal fluid reaches a new horizon: Intimate exchange between cerebrospinal fluid and interstitial fluid may contribute to maintenance of homeostasis in the central nervous system', *Neurologia Medico-Chirurgica*, 56(7), pp. 416–441. doi: 10.2176/nmc.ra.2016-0020.

Matsumoto, I., Ohmoto, M. and Abe, K. (2013) 'Functional diversification of taste cells in vertebrates', *Seminars in Cell and Developmental Biology*. Elsevier Ltd, 24(3), pp. 210–214. doi: 10.1016/j.semcdb.2012.10.004.

Matta, J. A. *et al.* (2008) 'General anesthetics activate a nociceptive ion channel to enhance pain and inflammation', *Proceedings of the National Academy of Sciences of the United States of America*, 105(25), pp. 8784–8789. doi: 10.1073/pnas.0711038105.

Maxwell Lawton, D. *et al.* (2000) 'Localization of the glutamate-aspartate transporter, GLAST, in rat taste buds', *European Journal of Neuroscience*, 12(9), pp. 3163–3171. doi: 10.1046/j.1460-9568.2000.00207.x.

McKemy, D. D., Neuhausser, W. M. and Julius, D. (2002) 'Identification of a cold receptor reveals a general role for TRP channels in thermosensation', *Nature*, 416(6876), pp. 52–58. doi: 10.1038/nature719.

McPherson, D. R. and Kemnitz, C. P. (1994) 'Modulation of lamprey fictive swimming and motoneuron physiology by dopamine, and its immunocytochemical localization in the spinal cord', *Neuroscience Letters*, 166(1), pp. 23–26. doi: 10.1016/0304-3940(94)90831-1.

Megías, M., Álvarez-Otero, R. and Pombal, M. A. (2003) 'Calbindin and calretinin immunoreactivities identify different types of neurons in the adult lamprey spinal cord', *Journal of Comparative Neurology*, 455(1), pp. 72–85. doi: 10.1002/cne.10473.

Meletti, S. *et al.* (2017) 'Decreased allopregnanolone levels in cerebrospinal fluid obtained during status epilepticus', *Epilepsia*, 58(2), pp. e16–e20. doi: 10.1111/epi.13625.

Merkel, F. (1875) 'Tastzellen und Tastkörperchen bei den Hausthieren und beim Menschen', *Archiv für Mikroskopische Anatomie*, 11(S1), pp. 636–652. doi: 10.1007/BF02933819.

Miao, E. A. *et al.* (2007) 'TLR5 and Ipaf: Dual sensors of bacterial flagellin in the innate immune system', *Seminars in Immunopathology*, 29(3), pp. 275–288. doi: 10.1007/s00281-007-0078-z.

Michel, W. C. and Derbidge, D. S. (1997) 'Evidence of distinct amino acid and bile salt receptors in the olfactory system of the zebrafish, Danio rerio', *Brain Research*, 764(1–2), pp. 179–187. doi: 10.1016/S0006-8993(97)00454-X.

Miesenböck, G., De Angelis, D. a and Rothman, J. E. (1998) 'Visualizing secretion and synaptic transmission with pH-sensitive green fluorescent proteins.', *Nature*, 394(6689), pp. 192–5. doi: 10.1038/28190.

Millard, C. L. and Woolf, C. J. (1988) 'Sensory innervation of the hairs of the rat hindlimb: A light microscopic analysis', *Journal of Comparative Neurology*, 277(2), pp. 183–194. doi: 10.1002/cne.902770203.

Mirat, O. *et al.* (2013) 'ZebraZoom: An automated program for high-throughput behavioral analysis and categorization', *Frontiers in Neural Circuits*, 7(JUNE), pp. 1–12. doi: 10.3389/fncir.2013.00107.

Miyasaka, N. *et al.* (2009) 'From the olfactory bulb to higher brain Centers: Genetic visualization of secondary olfactory pathways in zebrafish', *Journal of Neuroscience*, 29(15), pp. 4756–4767. doi: 10.1523/JNEUROSCI.0118-09.2009.

Mombaerts, P. (2004) 'Genes and ligands for odorant, vomeronasal and taste receptors', *Nature Reviews Neuroscience*, 5(4), pp. 263–278. doi: 10.1038/nrn1365.

Moqbel, R. and Coughlin, J. J. (2006) 'Differential secretion of cytokines.', *Science's STKE : signal transduction knowledge environment*, 2006(338), pp. 1–5. doi: 10.1126/stke.3382006pe26.

Moqrich, A. *et al.* (2005) 'Impaired thermosensation in mice lacking TRPV3, a heat and camphor sensor in the skin', *Science*, 307(5714), pp. 1468–1472. doi: 10.1126/science.1108609.

Morita, Y. and Finger, T. E. (1998) 'Differential projections of ciliated and microvillous olfactory receptor cells in the catfish, Ictalurus punctatus', *Journal of Comparative Neurology*, 398(4), pp. 539–550. doi: 10.1002/(SICI)1096-9861(19980907)398:4<539::AID-CNE6>3.0.CO;2-3.

Morris, C. A., Benson, E. and White-Cooper, H. (2009) 'Determination of gene expression patterns using in situ hybridization to Drosophila testes', *Nature Protocols*. Nature Publishing Group, 4(12), pp. 1807–1819. doi: 10.1038/nprot.2009.192.

Muraki, K. *et al.* (2003) 'TRPV2 Is a Component of Osmotically Sensitive Cation Channels in Murine Aortic Myocytes', *Circulation Research*, 93(9), pp. 829–838. doi: 10.1161/01.RES.0000097263.10220.0C.

Murray, R. Z. and Stow, J. L. (2014) 'Cytokine secretion in macrophages: SNAREs, Rabs, and membrane trafficking', *Frontiers in Immunology*, 5(OCT), pp. 1–10. doi: 10.3389/fimmu.2014.00538.

Nagatsu, I. *et al.* (1988) 'Aromatic l-amino acid decarboxylase-immunoreactive neurons in and around the cerebrospinal fluid-contacting neurons of the central canal do not contain dopamine or serotonin in the mouse and rat spinal cord', *Brain Research*, 475(1), pp. 91–102. doi: 10.1016/0006-8993(88)90202-8.

Nagy, J. I. and Hunt, S. P. (1982) ‘Fluoride-resistant acid phosphatase-containing neurones in dorsal root ganglia are separate from those containing substance P or somatostatin’, *Neuroscience*, 7(1), pp. 89–97. doi: 10.1016/0306-4522(82)90155-5.

Nave, K. A. and Werner, H. B. (2014) ‘Myelination of the nervous system: Mechanisms and functions’, *Annual Review of Cell and Developmental Biology*, 30, pp. 503–533. doi: 10.1146/annurev-cellbio-100913-013101.

Navone, F. *et al.* (1986) ‘Protein p38: An integral membrane protein specific for small vesicles of neurons and neuroendocrine cells’, *Journal of Cell Biology*, 103(6), pp. 2511–2527. doi: 10.1083/jcb.103.6.2511.

Nelson, G. *et al.* (2001) ‘Mammalian Sweet Taste Receptors’, *Cell*, 106(3), pp. 381–390. doi: 10.1016/S0092-8674(01)00451-2.

Nemeroff, C. B. *et al.* (1984) ‘Elevated concentrations of CSF corticotropin-releasing factor-like immunoreactivity in depressed patients’, *Science*, 226(4680), pp. 1342–1344. doi: 10.1126/science.6334362.

Nilsson, C. L. *et al.* (2001) ‘Processing of neuropeptide Y, galanin, and somatostatin in the cerebrospinal fluid of patients with Alzheimer’s disease and frontotemporal dementia’, *Peptides*, 22(12), pp. 2105–2112. doi: 10.1016/S0196-9781(01)00571-X.

North, R. A. (2002) ‘Molecular physiology of P2X receptors’, *Physiological Reviews*, 82(4), pp. 1013–1067. doi: 10.1152/physrev.00015.2002.

Ochi, J., Yamamoto, T. and Hosoya, Y. (1979) ‘Comparative study of the monoamine neuron system in the spinal cord of the lamprey and hagfish’, *Arch Histol Jpn*, 42(3), pp. 327–336. doi: 10.1679/aohc1950.42.327.

Ogura, T. *et al.* (2010) ‘Chemoreception regulates chemical access to mouse vomeronasal organ: Role of solitary chemosensory cells’, *PLoS ONE*, 5(7). doi: 10.1371/journal.pone.0011924.

Ohmoto, M. *et al.* (2008) ‘Genetic tracing of the gustatory and trigeminal neural pathways originating from T1R3-expressing taste receptor cells and solitary chemoreceptor cells’, *Molecular and Cellular Neuroscience*, 38(4), pp. 505–517. doi: 10.1016/j.mcn.2008.04.011.

Ohmoto, M. *et al.* (2011) ‘Mutually exclusive expression of Gαia and Gα14 reveals diversification of taste receptor cells in zebrafish’, *Journal of Comparative Neurology*, 519(8), pp. 1616–1629. doi: 10.1002/cne.22589.

Oike, H. *et al.* (2007) ‘Characterization of ligands for fish taste receptors’, *Journal of Neuroscience*, 27(21), pp. 5584–5592. doi: 10.1523/JNEUROSCI.0651-07.2007.

Oka, Y. and Korsching, S. I. (2011) ‘Shared and unique G alpha proteins in the zebrafish versus mammalian senses of taste and smell’, *Chemical Senses*, 36(4), pp. 357–365. doi: 10.1093/chemse/bjq138.

Oka, Y., Saraiva, L. R. and Korsching, S. I. (2012) ‘Crypt neurons express a single v1r-related ora gene’, *Chemical Senses*, 37(3), pp. 219–227. doi: 10.1093/chemse/bjr095.

Omdal, R. (2020) ‘The biological basis of chronic fatigue: neuroinflammation and innate immunity’, *Current opinion in neurology*, 33(3), pp. 391–396. doi: 10.1097/WCO.0000000000000817.

Orts-Del’Immagine, A. *et al.* (2012) ‘Properties of subependymal cerebrospinal fluid contacting neurones in the dorsal vagal complex of the mouse brainstem’, *Journal of Physiology*, 590(16), pp. 3719–3741. doi: 10.1113/jphysiol.2012.227959.

Orts-Del’Immagine, A. *et al.* (2014) ‘Morphology, distribution and phenotype of polycystin kidney disease 2-like 1-positive cerebrospinal fluid contacting neurons in the brainstem of adult mice’, *PLoS ONE*, 9(2). doi: 10.1371/journal.pone.0087748.

Orts-Del’Immagine, A. *et al.* (2016) ‘A single polycystic kidney disease 2-like 1 channel opening acts as a spike generator in cerebrospinal fluid-contacting neurons of adult mouse brainstem’, *Neuropharmacology*, 101, pp. 549–565. doi: 10.1016/j.neuropharm.2015.07.030.

Orts-Del’Immagine, A. *et al.* (2020) ‘Sensory Neurons Contacting the Cerebrospinal Fluid Require the Reissner Fiber to Detect Spinal Curvature In Vivo’, *Current Biology*, 30(5), pp. 827-839.e4. doi: 10.1016/j.cub.2019.12.071.

Orts-Del’Immagine, A. and Wyart, C. (2017) ‘Cerebrospinal-fluid-contacting neurons’, *Current Biology*. Elsevier, 27(22), pp. R1198–R1200. doi: 10.1016/j.cub.2017.09.017.

Park, H.-C., Shin, J. and Appel, B. (2004) ‘Spatial and temporal regulation of ventral spinal cord precursor specification by Hedgehog signaling’, *Development*, 131(23), pp. 5959–5969. doi: 10.1242/dev.01456.

Park, U. *et al.* (2011) ‘TRP vanilloid 2 knock-out mice are susceptible to perinatal lethality but display normal thermal and mechanical nociception’, *Journal of Neuroscience*, 31(32), pp. 11425–11436. doi: 10.1523/JNEUROSCI.1384-09.2011.

Pei, X. *et al.* (2014) ‘PC3-Secreted Microprotein Is a Novel Chemoattractant Protein and Functions as a High-Affinity Ligand for CC Chemokine Receptor 2’, *The Journal of Immunology*, 192(4), pp. 1878–1886. doi: 10.4049/jimmunol.1300758.

Peier, A. M. *et al.* (2002) ‘A TRP channel that senses cold stimuli and menthol’, *Cell*, 108(5), pp. 705–715. doi: 10.1016/S0092-8674(02)00652-9.

Perez, D. M. (2006) *The adrenergic receptors in the 21st century*. Totowa, New Jersey: Humana Press.

Petracca, Y. L. *et al.* (2016a) 'The late and dual origin of cerebrospinal fluid-contacting neurons in the mouse spinal cord', *The Company of Biologists Development*, 143(5), pp. 880–891. doi: 10.1242/dev.129254.

Petracca, Y. L. *et al.* (2016b) 'The late and dual origin of cerebrospinal fluid-contacting neurons in the mouse spinal cord', *Development*, 143(5), pp. 880–891. doi: 10.1242/dev.129254.

Pfister, P. and Rodriguez, I. (2005) 'Olfactory expression of a single and highly variable V1r pheromone receptor-like gene in fish species', *Proceedings of the National Academy of Sciences of the United States of America*, 102(15), pp. 5489–5494. doi: 10.1073/pnas.0402581102.

Polfliet, M. M. J. *et al.* (2001) 'Meningeal and Perivascular Macrophages of the Central Nervous System Play a Protective Role During Bacterial Meningitis', *The Journal of Immunology*, 167(8), pp. 4644–4650. doi: 10.4049/jimmunol.167.8.4644.

Prendergast, A. *et al.* (2019) 'Central Sensory Neurons Detect and Combat Pathogens Invading the Cerebrospinal Fluid', *SSRN Electronic Journal*. doi: 10.2139/ssrn.3404255.

Price, M. P. *et al.* (2000) 'The mammalian sodium channel BNC1 is required for normal touch sensation', *Nature*, 407(6807), pp. 1007–1011. doi: 10.1038/35039512.

Proske, U. and Gandevia, S. C. (2012) 'The proprioceptive senses: Their roles in signaling body shape, body position and movement, and muscle force', *Physiological Reviews*, 92(4), pp. 1651–1697. doi: 10.1152/physrev.00048.2011.

Purves, D. *et al.* (eds) (2001) *Neuroscience, Second Edition*. 2nd edn. Sinauer Associates.

Quan, F. B. *et al.* (2015) 'Comparative distribution and in vitro activities of the urotensin II-related peptides URP1 and URP2 in zebrafish: Evidence for their colocalization in spinal cerebrospinal fluid-contacting neurons', *PLoS ONE*, 10(3), pp. 1–21. doi: 10.1371/journal.pone.0119290.

Quan, F. B. *et al.* (2020) 'Somatostatin 1.1 contributes to the innate exploration of zebrafish larva', *Scientific Reports*. Nature Publishing Group UK, 10(1), pp. 1–12. doi: 10.1038/s41598-020-72039-x.

Reali, C. *et al.* (2011) 'GABAergic signalling in a neurogenic niche of the turtle spinal cord', *Journal of Physiology*, 589(23), pp. 5633–5647. doi: 10.1113/jphysiol.2011.214312.

Renshaw, S. A. *et al.* (2006) 'A transgenic zebrafish model of neutrophilic inflammation', *Blood*, 108(13), pp. 3976–3978. doi: 10.1182/blood-2006-05-024075.

Reutter, K., Boudriot, F. and Witt, M. (2000) 'Heterogeneity of fish taste bud ultrastructure as

demonstrated in the holosteans Amia calva and Lepisosteus oculatus', *Philosophical Transactions of the Royal Society B: Biological Sciences*, 355(1401), pp. 1225–1228. doi: 10.1098/rstb.2000.0672.

Rink, E. and Wullimann, M. F. (1998) 'Some forebrain connections of the gustatory system in the goldfish Carassius auratus visualized by separate DiI application to the hypothalamic inferior lobe and the torus lateralis', *Journal of Comparative Neurology*, 394(2), pp. 152–170. doi: 10.1002/(SICI)1096-9861(19980504)394:2<152::AID-CNE2>3.0.CO;2-1.

Roberts, B. L. *et al.* (1995) 'Dopaminergic and GABAergic cerebrospinal fluid- contacting neurons along the central canal of the spinal cord of the Eel and Trout', *Journal of Comparative Neurology*, 354(3), pp. 423–437. doi: 10.1002/cne.903540310.

Robinson, D. R. and Gebhart, G. F. (2008) 'Inside information: The unique features of visceral sensation', *Molecular Interventions*, 8(5), pp. 242–253. doi: 10.1124/mi.8.5.9.

Robles, E., Laurell, E. and Baier, H. (2014) 'The retinal projectome reveals brain-area-specific visual representations generated by ganglion cell diversity', *Current Biology*. Elsevier Ltd, 24(18), pp. 2085–2096. doi: 10.1016/j.cub.2014.07.080.

Romigi, A. *et al.* (2010) 'Cerebrospinal fluid levels of the endocannabinoid anandamide are reduced in patients with untreated newly diagnosed temporal lobe epilepsy', *Epilepsia*, 51(5), pp. 768–772. doi: 10.1111/j.1528-1167.2009.02334.x.

Rose, C. D. *et al.* (2020) 'SCO-Spondin Defects and Neuroinflammation Are Conserved Mechanisms Driving Spinal Deformity across Genetic Models of Idiopathic Scoliosis', *Current Biology*, 30(12), pp. 2363-2373.e6. doi: 10.1016/j.cub.2020.04.020.

Ruffini, A. (1894) 'Di un novo organo nervoso terminale, e sulla presenza dei corpuscoli Golgi-Mazzoni nel connettivo sottocutaneo dei polpastrelli delle dita dell-uomo', *Attl Dell Accademia Nazionale dei Lincet*, 7, pp. 398–410.

Russo, R. E. *et al.* (2004) 'Functional and molecular clues reveal precursor-like cells and immature neurones in the turtle spinal cord', *Journal of Physiology*, 560(3), pp. 831–838. doi: 10.1113/jphysiol.2004.072405.

Sainburg, R. L. *et al.* (1995) 'Control of limb dynamics in normal subjects and patients without proprioception', *Journal of Neurophysiology*, 73(2), pp. 820–835. doi: 10.1152/jn.1995.73.2.820.

Salvatierra, J. *et al.* (2018) 'NaV1.1 inhibition can reduce visceral hypersensitivity', *JCI insight*, 3(11), pp. 1–13. doi: 10.1172/jci.insight.121000.

Sato, K. and Suzuki, N. (2001) 'Whole-cell response characteristics of ciliated and microvillous olfactory receptor neurons to amino acids, pheromone candidates and urine in rainbow trout', *Chemical Senses*, 26(9), pp. 1145–1156. doi: 10.1093/chemse/26.9.1145.

Sato, Y., Miyasaka, N. and Yoshihara, Y. (2005) ‘Mutually exclusive glomerular innervation by two distinct types of olfactory sensory neurons revealed in transgenic zebrafish’, *Journal of Neuroscience*, 25(20), pp. 4889–4897. doi: 10.1523/JNEUROSCI.0679-05.2005.

Sato, Y., Miyasaka, N. and Yoshihara, Y. (2007) ‘Hierarchical regulation of odorant receptor gene choice and subsequent axonal projection of olfactory sensory neurons in zebrafish’, *Journal of Neuroscience*, 27(7), pp. 1606–1615. doi: 10.1523/JNEUROSCI.4218-06.2007.

Saunders, C. J. *et al.* (2014) ‘Cholinergic neurotransmission links solitary chemosensory cells to nasal inflammation’, *Proceedings of the National Academy of Sciences of the United States of America*, 111(16), pp. 6075–6080. doi: 10.1073/pnas.1402251111.

Sawamoto, K. *et al.* (2006) ‘New Neurons Follow the Flow of Cerebrospinal Fluid in the Adult Brain’, *Science*, 311(5761), pp. 629–632. doi: 10.1126/science.1119133.

Schepers, R. J. and Ringkamp, M. (2009) ‘Thermoreceptors and thermosensitive afferents’, *Neuroscience and Biobehavioral Reviews*, 33(3), pp. 205–212. doi: 10.1016/j.neubiorev.2008.07.009.

Schindelin, J. *et al.* (2012) ‘Fiji: An open-source platform for biological-image analysis’, *Nature Methods*, 9(7), pp. 676–682. doi: 10.1038/nmeth.2019.

Schmachtenberg, O. (2006) ‘Histological and electrophysiological properties of crypt cells from the olfactory epithelium of the marine teleost Trachurus symmetricus’, *Journal of Comparative Neurology*, 495(1), pp. 113–121. doi: 10.1002/cne.20847.

Schmidt, A. P. *et al.* (2015) ‘Changes in Purines Concentration in the Cerebrospinal Fluid of Pregnant Women Experiencing Pain During Active Labor’, *Neurochemical Research*, 40(11), pp. 2262–2269. doi: 10.1007/s11064-015-1716-9.

Schmidt, R. *et al.* (1995) ‘Novel classes of responsive and unresponsive C nociceptors in human skin’, *The Journal of Neuroscience*, 15(1), pp. 333–341. doi: 10.1523/jneurosci.15-01-00333.1995.

Schotland, J. L. *et al.* (1996) ‘Synaptic and nonsynaptic monoaminergic neuron systems in the lamprey spinal cord’, *Journal of Comparative Neurology*, 372(2), pp. 229–244. doi: 10.1002/(SICI)1096-9861(19960819)372:2<229::AID-CNE6>3.0.CO;2-5.

Schröder, J. M. *et al.* (1989) ‘Scanning electron microscopy of teased intrafusal muscle fibers from rat muscle spindles’, *Muscle & Nerve*, 12(3), pp. 221–232. doi: 10.1002/mus.880120311.

Schueren, A. M. and DeSantis, M. (1985) ‘Cellular heterogeneity in the ependymal layer of the chicken’s lumbosacral spinal cord’, *Experimental Neurology*, 87(2), pp. 387–391. doi: 10.1016/0014-4886(85)90230-4.

Sfameni, A. (1902) ‘Recherches anatomiques sur l’existence des i m f S e t sur leur mode de 88

terminer d a m le tissu adipeux, dam le perioste, dans le periehondre e t dans les tissus qui renforcent les articulations.', *Arch. ital. di Biol.*, 38, pp. 49–101.

Shah, A. S. *et al.* (2009) 'Motile cilia of human airway epithelia are chemosensory', *Science*, 325(5944), pp. 1131–1134. doi: 10.1126/science.1173869.

Sherrington, C. S. (1906) *The integrative action of the nervous system*. New York: C Scribner and Sons.

Shimosegawa, T. *et al.* (1986) 'An immunohistochemical study of methionine-enkephalin-Arg6-Gly7-Leu8-like immunoreactivity-containing liquor-contacting neurons (LCNs) in the rat spinal cord', *Brain Research*, 379(1), pp. 1–9. doi: 10.1016/0006-8993(86)90249-0.

Shin, J. *et al.* (2007) 'Notch signaling regulates neural precursor allocation and binary neuronal fate decisions in zebrafish', *Development*, 134(10), pp. 1911–1920. doi: 10.1242/dev.001602.

Shiriagin, V. and Korsching, S. I. (2018) 'Massive expansion of bitter taste receptors in blind cavefish, Astyanax mexicanus', *Chemical Senses*. doi: 10.1093/chemse/bjy062.

Shooshtarizadeh, P. *et al.* (2010) 'The antimicrobial peptides derived from chromogranin/secretogranin family, new actors of innate immunity', *Regulatory Peptides*. Elsevier B.V., 165(1), pp. 102–110. doi: 10.1016/j.regpep.2009.11.014.

Shu, X. and Mendell, L. M. (1999) 'Nerve growth factor acutely sensitizes the response of adult rat sensory neurons to capsaicin', *Neuroscience Letters*, 274(3), pp. 159–162. doi: 10.1016/S0304-3940(99)00701-6.

Siegel, G. *et al.* (1999) 'Chapter 13: Serotonin Receptors', in *Basic Neurochemistry: Molecular, Cellular, and Medical Aspects.* Philadelphia: Lippincott-Raven, pp. 263–292.

Silverman, J. D. and Kruger, L. (1990) 'Selective neuronal glycoconjugate expression in sensory and autonomic ganglia: relation of lectin reactivity to peptide and enzyme markers', *Journal of Neurocytology*, 19(5), pp. 789–801. doi: 10.1007/BF01188046.

Sims, T. J. (1977) 'The development of monoamine-containing neurons in the brain and spinal cord of the salamander, Ambystoma mexicanum', *The Journal of Comparative Neurology*, 173(2), pp. 319–335. doi: 10.1002/cne.901730208.

Slager, J., Aprianto, R. and Veening, J.-W. (2018) 'Deep genome annotation of the opportunistic human pathogen Streptococcus pneumoniae D39', *Nucleic Acids Research*. Oxford University Press, 46(19), pp. 9971–9989. doi: 10.1093/nar/gky725.

Smith, G. D. *et al.* (2002) 'TRPV3 is a temperature-sensitive vanilloid receptor-like protein', *Nature*, 418(6894), pp. 186–190. doi: 10.1038/nature00894.

Sonner, M. J., Walters, M. C. and Ladle, D. R. (2017) ‘Analysis of proprioceptive sensory innervation of the mouse soleus: A whole-mount muscle approach’, *PLoS ONE*, 12(1), pp. 1–18. doi: 10.1371/journal.pone.0170751.

Spitzer, N. C. and Lamborghini, J. E. (1976) ‘The development of the action potential mechanism of amphibian neurons isolated in culture’, *Proceedings of the National Academy of Sciences of the United States of America*, 73(5), pp. 1641–1645. doi: 10.1073/pnas.73.5.1641.

Spitzer, N. C., Vincent, A. and Lautermilch, N. J. (2000) ‘Differentiation of electrical excitability in motoneurons’, *Brain Research Bulletin*, 53(5), pp. 547–552. doi: 10.1016/S0361-9230(00)00388-9.

Sternberg, J. R. (2016) *Neuronal populations underlying locomotion in zebrafish*. Université Pierre et Marie Curie - Paris VI.

Sternberg, J. R. *et al.* (2016) ‘Optimization of a Neurotoxin to Investigate the Contribution of Excitatory Interneurons to Speed Modulation In Vivo’, *Current Biology*. Elsevier Ltd., 26(17), pp. 2319–2328. doi: 10.1016/j.cub.2016.06.037.

Sternberg, J. R. *et al.* (2018) ‘Pkd2l1 is required for mechanoception in cerebrospinal fluid-contacting neurons and maintenance of spine curvature’, *Nature Communications*, 9(1), pp. 1–10. doi: 10.1038/s41467-018-06225-x.

Stoeckel, M. E. *et al.* (2003) ‘Cerebrospinal fluid-contacting neurons in the rat spinal cord, a γ-aminobutyric acidergic system expressing the P2X2 subunit of purinergic receptors, PSA-NCAM, and GAP-43 immunoreactivities: Light and electron microscopic study’, *Journal of Comparative Neurology*, 457(2), pp. 159–174. doi: 10.1002/cne.10565.

Story, G. M. *et al.* (2003) ‘ANKTM1, a TRP-like channel expressed in nociceptive neurons, is activated by cold temperatures’, *Cell*, 112(6), pp. 819–829. doi: 10.1016/S0092-8674(03)00158-2.

Strittmatter, M. *et al.* (1997) ‘Cerebrospinal fluid neuropeptides and monoaminergic transmitters in patients with trigeminal neuralgia’, *Headache*, 37(4), pp. 211–216. doi: 10.1046/j.1526-4610.1997.3704211.x.

Sueiro, C. *et al.* (2004) ‘Distribution and development of glutamic acid decarboxylase immunoreactivity in the spinal cord of the dogfish Scyliorhinus canicula (Elasmobranchs)’, *Journal of Comparative Neurology*, 478(2), pp. 189–206. doi: 10.1002/cne.20285.

Talbot, S. *et al.* (2015) ‘Silencing Nociceptor Neurons Reduces Allergic Airway Inflammation’, *Neuron*, 87(2), pp. 341–354. doi: 10.1016/j.neuron.2015.06.007.

Tan, C. H. and McNaughton, P. A. (2016) ‘The TRPM2 ion channel is required for sensitivity to warmth’, *Nature*, 536(7617), pp. 460–463. doi: 10.1038/nature19074.

Di Terlizzi, R. and Platt, S. (2006) 'The function, composition and analysis of cerebrospinal fluid in companion animals: Part I - Function and composition', *Veterinary Journal*, 172(3), pp. 422–431. doi: 10.1016/j.tvjl.2005.07.021.

Thisse, C. and Thisse, B. (2008) 'High-resolution in situ hybridization to whole-mount zebrafish embryos', *Nature Protocols*, 3(1), pp. 59–69. doi: 10.1038/nprot.2007.514.

Thompson, A. and R. Lummis, S. (2006) '5-HT3 Receptors', *Current Pharmaceutical Design*, 12(28), pp. 3615–3630. doi: 10.2174/138161206778522029.

Thouvenin, O. *et al.* (2020) 'Origin and role of the cerebrospinal fluid bidirectional flow in the central canal', *eLife*, 9, pp. 1–37. doi: 10.7554/eLife.47699.

Tizzano, M. *et al.* (2010) 'Nasal chemosensory cells use bitter taste signaling to detect irritants and bacterial signals', *Proceedings of the National Academy of Sciences of the United States of America*, 107(7), pp. 3210–3215. doi: 10.1073/pnas.0911934107.

Tizzano, M. *et al.* (2011) 'Expression of taste receptors in Solitary Chemosensory Cells of rodent airways', *BMC Pulmonary Medicine*, 11, pp. 1–12. doi: 10.1186/1471-2466-11-3.

Todaka, H. *et al.* (2004) 'Warm temperature-sensitive transient receptor potential vanilloid 4 (TRPV4) plays an essential role in thermal hyperalgesia', *Journal of Biological Chemistry*. Â© 2004 ASBMB. Currently published by Elsevier Inc; originally published by American Society for Biochemistry and Molecular Biology., 279(34), pp. 35133–35138. doi: 10.1074/jbc.M406260200.

Tomasiuk, R. *et al.* (2016) 'Higher level of NT-proCNP in cerebrospinal fluid of patients with meningitis', *Neuroscience Letters*. Elsevier Ireland Ltd, 614, pp. 29–32. doi: 10.1016/j.neulet.2015.12.053.

Tomchik, S. M. *et al.* (2007) 'Breadth of tuning and taste coding in mammalian taste buds', *Journal of Neuroscience*, 27(40), pp. 10840–10848. doi: 10.1523/JNEUROSCI.1863-07.2007.

Tominaga, M. *et al.* (1998) 'The cloned capsaicin receptor integrates multiple pain-producing stimuli', *Neuron*, 21(3), pp. 531–543. doi: 10.1016/S0896-6273(00)80564-4.

Tracey, W. D. *et al.* (2003) 'painless, a Drosophila gene essential for nociception', *Cell*, 113(2), pp. 261–273. doi: 10.1016/S0092-8674(03)00272-1.

Treede, R. D., Meyer, R. A. and Campbell, J. N. (1998) 'Myelinated mechanically insensitive afferents from monkey hairy skin: Heat-response properties', *Journal of Neurophysiology*, 80(3), pp. 1082–1093. doi: 10.1152/jn.1998.80.3.1082.

Trostdorf, F. *et al.* (1999) 'Reduction of meningeal macrophages does not decrease migration of granulocytes into the CSF and brain parenchyma in experimental pneumococcal meningitis', *Journal*

of Neuroimmunology, 99(2), pp. 205–210. doi: 10.1016/S0165-5728(99)00121-6.

Troutwine, B. R. *et al.* (2020) 'The Reissner Fiber Is Highly Dynamic In Vivo and Controls Morphogenesis of the Spine', *Current Biology*. Elsevier Ltd., 30(12), pp. 2353-2362.e3. doi: 10.1016/j.cub.2020.04.015.

Tsujikawa, M. and Malicki, J. (2004) 'Intraflagellar transport genes are essential for differentiation and survival of vertebrate sensory neurons', *Neuron*, 42(5), pp. 703–716. doi: 10.1016/S0896-6273(04)00268-5.

Tuomanen, E. *et al.* (1985) 'The induction of meningeal inflammation by components of the pneumococcal cell wall', *Journal of Infectious Diseases*, 151(5), pp. 859–868. doi: 10.1093/infdis/151.5.859.

Tuthill, J. C. and Azim, E. (2018) 'Proprioception', *Current Biology*, 28(5), pp. R194–R203. doi: 10.1016/j.cub.2018.01.064.

Vandenbeuch, A., Clapp, T. R. and Kinnamon, S. C. (2008) 'Amiloride-sensitive channels in type I fungiform taste cells in mouse', *BMC Neuroscience*, 9, pp. 1–13. doi: 10.1186/1471-2202-9-1.

Vaudry, H. *et al.* (2010) 'Urotensin II, from fish to human', *Annals of the New York Academy of Sciences*, 1200, pp. 53–66. doi: 10.1111/j.1749-6632.2010.05514.x.

Verbeurgt, C. *et al.* (2017) 'The human bitter taste receptor T2R38 is broadly tuned for bacterial compounds', *PLoS ONE*, 12(9). doi: 10.1371/journal.pone.0181302.

Vielma, A. *et al.* (2008) 'The elusive crypt olfactory receptor neuron: Evidence for its stimulation by amino acids and cAMP pathway agonists', *Journal of Experimental Biology*, 211(15), pp. 2417–2422. doi: 10.1242/jeb.018796.

Vígh, B. *et al.* (2004) 'The system of cerebrospinal fluid-contacting neurons. Its supposed role in the nonsynaptic signal transmission of the brain', *Histology and Histopathology*, 19(2), pp. 607–628. doi: 10.1002/brb3.218.

Vigh, B. and Vigh-Teichmann, I. (1973) 'Comparative Ultrastructure of the Cerebrospinal Fluid-Contacting Neurons', *International Review of Cytology*, 35(C), pp. 189–251. doi: 10.1016/S0074-7696(08)60355-1.

Vigh, B. and Vigh-Teichmann, I. (1981) 'Light- and electron-microscopic demonstration of immunoreactive opsin in the pinealocytes of various vertebrates', *Cell And Tissue Research*, 221(2), pp. 451–463. doi: 10.1007/BF00216748.

Vigh, B. and Vigh-Teichmann, I. (1998) 'Actual problems of the cerebrospinal fluid-contacting neurons', *Microscopy Research and Technique*, 41(1), pp. 57–83. doi: 10.1002/(SICI)1097-

0029(19980401)41:1<57::AID-JEMT6>3.0.CO;2-R.

Vigh, B., Vigh-Teichmann, I. and Aros, B. (1977) ‘Special dendritic and axonal endings formed by the cerebrospinal fluid contacting neurons of the spinal cord’, *Cell and Tissue Research*, 183(4), pp. 541–552. doi: 10.1007/BF00225666.

Vize, P. D., McCoy, K. E. and Zhou, X. (2009) ‘Multichannel wholemount fluorescent and fluorescent/chromogenic in situ hybridization in xenopus embryos’, *Nature Protocols*, 4(6), pp. 975–983. doi: 10.1038/nprot.2009.69.

Vriens, J. *et al.* (2011) ‘TRPM3 Is a Nociceptor Channel Involved in the Detection of Noxious Heat’, *Neuron*. Elsevier Inc., 70(3), pp. 482–494. doi: 10.1016/j.neuron.2011.02.051.

Vriens, J., Nilius, B. and Voets, T. (2014) ‘Peripheral thermosensation in mammals’, *Nature Reviews Neuroscience*. Nature Publishing Group, 15(9), pp. 573–589. doi: 10.1038/nrn3784.

Wakisaka, N. *et al.* (2017) ‘An Adenosine Receptor for Olfaction in Fish’, *Current Biology*. Elsevier Ltd., 27(10), pp. 1437-1447.e4. doi: 10.1016/j.cub.2017.04.014.

Waxman, S. G. (1980) ‘Determinants of conduction velocity in myelinated nerve fibers’, *Muscle & Nerve*, 3(2), pp. 141–150. doi: 10.1002/mus.880030207.

Weber, A. I. *et al.* (2013) ‘Spatial and temporal codes mediate the tactile perception of natural textures’, *Proceedings of the National Academy of Sciences of the United States of America*, 110(42), pp. 17107–17112. doi: 10.1073/pnas.1305509110.

Welch, M. J., Markham, C. H. and Jenden, D. J. (1976) ‘Acetylcholine and choline in cerebrospinal fluid of patients with Parkinson’s disease and Huntington’s chorea’, *Journal of Neurology, Neurosurgery, and Psychiatry*, 39(4), pp. 367–374. doi: 10.1136/jnnp.39.4.367.

Westerfield, M. (2000) *The zebrafish book. A guide for the laboratory use of zebrafish (Danio rerio), Fourth Edition*. 4th edn. Eugene: Univ. of Oregon Press.

Wilkinson, K. A., Kloefkorn, H. E. and Hochman, S. (2012) ‘Characterization of muscle spindle afferents in the adult mouse using an in vitro muscle-nerve preparation’, *PLoS ONE*, 7(6). doi: 10.1371/journal.pone.0039140.

Woehrl, B. *et al.* (2011) ‘Complement component 5 contributes to poor disease outcome in humans and mice with pneumococcal meningitis’, *Journal of Clinical Investigation*, 121(10), pp. 3943–3953. doi: 10.1172/JCI57522.

Woodbury, C. J. and Koerber, H. R. (2007) ‘Central and peripheral anatomy of slowly adapting type I low-threshold mechanoreceptors innervating trunk skin of neonatal mice’, *The Journal of Comparative Neurology*, 505(5), pp. 547–561. doi: 10.1002/cne.21517.

Wu, M.-Y. *et al.* (2021) ‘Spinal sensory neurons project onto the hindbrain to stabilize posture and enhance locomotor speed’, *Current Biology*, 31(15), pp. 3315–3329. doi: 10.1016/j.cub.2021.05.042.

Wyart, C. *et al.* (2009) ‘Optogenetic dissection of a behavioural module in the vertebrate spinal cord’, *Nature*. Nature Publishing Group, 461(7262), pp. 407–410. doi: 10.1038/nature08323.

Wyart, C. *et al.* (no date) ‘Understanding the spinal cord’s intrinsic polymodal sensory system’, *Nature Reviews Neuroscience*.

Xie, L. *et al.* (2013) ‘Sleep drives metabolite clearance from the adult brain’, *Science*, 342(6156), pp. 373–377. doi: 10.1126/science.1241224.

Yagi, J. *et al.* (2006) ‘Sustained currents through ASIC3 ion channels at the modest pH changes that occur during myocardial ischemia’, *Circulation Research*, 99(5), pp. 501–509. doi: 10.1161/01.RES.0000238388.79295.4c.

Yang, L., Rastegar, S. and Strähle, U. (2010) ‘Regulatory interactions specifying Kolmer-Agduhr interneurons’, *Development*, 137(16), pp. 2713–2722. doi: 10.1242/dev.048470.

Yasuoka, A. *et al.* (2004) ‘Phospholipase C-beta 2 as a mammalian taste signaling marker is expressed in the multiple gustatory tissues of medaka fish, Oryzias latipes’, *Mechanisms of Development*, 121(7–8), pp. 985–989. doi: 10.1016/j.mod.2004.03.009.

Yoshida, Y. *et al.* (2007) ‘Transient receptor potential channel M5 and phospholipaseC-β2 colocalizing in zebrafish taste receptor cells’, *NeuroReport*, 18(15), pp. 1517–1520. doi: 10.1097/WNR.0b013e3282ec6874.

Yu, Y. X. *et al.* (2015) ‘Odor fingerprinting of listeria monocytogenes recognized by SPME-GC-MS and E-nose’, *Canadian Journal of Microbiology*, 61(5), pp. 367–372. doi: 10.1139/cjm-2014-0652.

Yulis, C. R. and Lederis, K. (1988) ‘Relationship between urotensin II- and somatostatin-immunoreactive spinal cord neurons of Catostomus commersoni and Oncorhynchus kisutch (Teleostei)’, *Cell and Tissue Research*, 254(3), pp. 539–542. doi: 10.1007/BF00226503.

Zappaterra, M. W. and Lehtinen, M. K. (2012) ‘The cerebrospinal fluid: Regulator of neurogenesis, behavior, and beyond’, *Cellular and Molecular Life Sciences*, 69(17), pp. 2863–2878. doi: 10.1007/s00018-012-0957-x.

Zhang, X. (2015) ‘Molecular sensors and modulators of thermoreception’, *Channels*, 9(2), pp. 73–81. doi: 10.1080/19336950.2015.1025186.

Zhang, X. *et al.* (2018a) ‘Cilia-driven cerebrospinal fluid flow directs expression of urotensin neuropeptides to straighten the vertebrate body axis’, *Nature Genetics*. Springer US, 50(12), pp. 1666–1673. doi: 10.1038/s41588-018-0260-3.

Zhang, X. *et al.* (2018b) ‘Cilia-driven cerebrospinal fluid flow directs expression of urotensin neuropeptides to straighten the vertebrate body axis’, *Nature Genetics*. Springer US, 50(12), pp. 1666–1673. doi: 10.1038/s41588-018-0260-3.

Zhang, X. Y. *et al.* (2013) ‘Gain-of-Function mutations in SCN11A cause familial episodic pain’, *American Journal of Human Genetics*. The American Society of Human Genetics, 93(5), pp. 957–966. doi: 10.1016/j.ajhg.2013.09.016.

Zhang, Y. *et al.* (2003) ‘Coding of sweet, bitter, and umami tastes: Different receptor cells sharing similar signaling pathways’, *Cell*, 112(3), pp. 293–301. doi: 10.1016/S0092-8674(03)00071-0.

Zhao, G. Q. *et al.* (2003) ‘The receptors for mammalian sweet and umami taste’, *Cell*, 115(3), pp. 255–266. doi: 10.1016/S0092-8674(03)00844-4.

Zhou, W. *et al.* (2012) ‘The evolution of tachykinin/tachykinin receptor (TAC/TACR) in vertebrates and molecular identification of the TAC3/TACR3 system in zebrafish (Danio rerio)’, *Molecular and Cellular Endocrinology*. Elsevier Ireland Ltd, 361(1–2), pp. 202–212. doi: 10.1016/j.mce.2012.04.007.

Zimmermann, K. *et al.* (2007) ‘Sensory neuron sodium channel Nav1.8 is essential for pain at low temperatures’, *Nature*, 447(7146), pp. 855–858. doi: 10.1038/nature05880.

Zoons, E. *et al.* (2008) ‘Seizures in adults with bacterial meningitis.’, *Neurology*, 70(22 Pt 2), pp. 2109–2115. doi: 10.1212/01.wnl.0000288178.91614.5d.

Discussion and perspectives

The goal of my PhD has been to investigate the chemosensory functions of spinal neurons in contact with the cerebrospinal fluid (CSF-cNs). To do so, I adapted spinal CSF-cNs culture protocols (Böhm *et al.*, 2016; Sternberg *et al.*, 2018) to conceive a new protocol of primary cell culture of spinal CSF-cNs enabling to investigate spinal CSF-cNs responses to potential chemical agonists. To find out receptors of spinal CSF-cNs to chemical cues, I analyzed a transcriptome of spinal CSF-cNs from 3 dpf zebrafish larvae that revealed expression of different families of receptors such as receptors for neuromodulators, neuropeptides or hormones. Interestingly, I found that receptors for immune-related factors such as interleukins or interferons, suggesting a role for spinal CSF-cNs in innate immunity. In primary cultures, I found that spinal CSF-cNs detect bacterial metabolites that act as bitter compounds, and that in turn these cells up-regulate the expression of cytokines and complement components involved in innate immunity to increase host survival during pneumococcal CSF infection. Altogether, my work showed that spinal CSF-cNs are interoceptive chemosensory neurons detecting bacteria in the CSF to promote innate immunity, and also carrying different families of receptors for detection of other chemical cues from the CSF.

1) Spinal CSF-cNs as sensors for neuromodulators in the CSF

Classically, the CSF has been known to play a role of mechanical protection for the brain, as well as maintain brain homeostasis. The CSF transport biomolecules crucial for the central nervous system development (Gato *et al.*, 2005; Lehtinen *et al.*, 2011). The CSF also clears metabolites during sleep in mice (Xie *et al.*, 2013). The CSF composition reflects physiological states of the central nervous system such as sleep (Lerner *et al.*, 1994), and conditions such as depression (Nemeroff *et al.*, 1984). The CSF contains a large variety of active neuromodulators and neurotransmitters such as dopamine, noradrenaline and serotonin (Strittmatter *et al.*, 1997), acetylcholine (Welch, Markham and Jenden, 1976), purines (Schmidt *et al.*, 2015), and neuropeptides such as somatostatin, neuropeptide Y (Nilsson *et al.*, 2001), vasopressin and oxytocin (Martin *et al.*, 2014). Because spinal CSF-cNs are ideally located at the interface between the CSF and the central nervous system, we hypothesized that they could sense the chemical content from the CSF, which is changing depending on physiological states.

Thus, we monitored whether spinal CSF-cNs carry receptors to sense the active chemical cues from the CSF. An investigation of the spinal CSF-cNs transcriptome revealed the expression of different families of neurotransmitter and neuromodulator receptors such as purinergic, glutamatergic, serotonergic, GABAergic, cholinergic and adrenergic receptors, suggesting that spinal CSF-cNs could sense the chemical content of the CSF.

Spinal CSF-cNs respond to ATP pressure-application (Johnson *et al.*, 2020) in mice and express the ionotropic receptor $P2X_2$ in rat (Stoeckel *et al.*, 2003). Using an approach of transcriptomic after fluorescent activated cell sorting in zebrafish, I did not find that $P2X_2$ receptor expressed in spinal CSF-cNs, and spinal CSF-cNs in primary cultures did not respond to pressure-application of ATP. In addition, I did not observe that spinal CSF-cNs *in vitro* respond to pressure-application of neither epinephrine, norepinephrine nor serotonin. As exposed in Chapter II, different possibilities could explain these results, one being that spinal CSF-cN properties may differ across species (my PhD is focused on zebrafish, while other studies involved mice and rat), or stages of development (larval zebrafish versus adult mice/rats). Furthermore, spinal CSF-cNs could exhibit different expressions of receptors to chemical cues *in vivo* compared to *in vitro*. We found that spinal CSF-cNs cultured *in vitro* conserved their GABAergic and Pkd2l1 molecular identity, but receptors for neuromodulators such as purinergic receptors, and neurotransmitters such as adrenergic, serotonergic and cholinergic receptors are weakly expressed and could not be labeled by immunocytochemistry. Then, spinal CSF-cNs could not express adrenergic, purinergic and serotonergic receptors *in vitro*. In addition, dorsolateral and ventral subpopulations of spinal CSF-cNs exhibit different molecular identities. Dorsolateral spinal CSF-cNs express the Somatostatin1.1 paralog in zebrafish (Wyart *et al.*, 2009; Djenoune *et al.*, 2017). Ventral spinal CSF-cNs express the transient serotonin in zebrafish (Djenoune *et al.*, 2017), as well as the protein Msmp2 (Prendergast *et al.*, 2019), Urp1 and Urp2 (Quan *et al.*, 2015). Similarly, dorsolateral and ventral subpopulations of spinal CSF-cNs could differ in terms of the chemoreceptors they express in order to confer them sensitivities to different molecules. In the future, it would be interesting to monitor whether the two subpopulations of spinal CSF-cNs are conserved in culture, using specific markers of dorsolateral and ventral spinal CSF-cNs, such as Somatostastin1.1 for dorsolateral spinal CSF-cNs, and Msmp2, Urp1 and Urp2 for ventral spinal CSF-cNs.

Spinal CSF-cNs could also exhibit different firing properties *in vitro*, compared to *in vivo*. We found that all spinal CSF-cNs recorded *in vitro* (n = 7) exhibited tonic firing upon current injection. As explained in Chapter I, two physiological populations of spinal CSF-cNs were described in fish (Orts-Del'Immagine *et al.*, 2020), turtle (Russo *et al.*, 2004; Reali *et al.*,

2011) and rodents (Orts-Del'Immagine *et al.*, 2012, 2016; Petracca *et al.*, 2016b): one exhibited tonic firing while the other showed phasic firing. Different interpretations can explain this difference in firing patterns between *in vivo* and *in vitro*. Spinal CSF-cNs in culture could exhibit a difference of expression of voltage-dependent channels due to cell dissociation and plating. The cell culture protocol could also promote growth and survival of tonic firing spinal CSF-cNs subpopulation exclusively, missing the phasic firing neurons. A model of neocortical neurons showed a correlation between the cell dendritic structure and firing properties (Mainen and Sejnowski, 1996), suggesting that the structure of the dendrite can influence the firing properties of a neuron. Spinal CSF-cNs bear an apical extension protruding into the CSF. Depending on the species, spinal CSF-cNs apical extension exhibits or not multiple microvilli (Vigh and Vigh-Teichmann, 1973), as well as a cilium for some species such as *Xenopus* (Dale *et al.*, 1987), mice (Alfaro-Cervello *et al.*, 2012) and fish (Djenoune *et al.*, 2017). In zebrafish, it has been shown that the shape of spinal CSF-cNs apical extension tunes the amplitude of the mechanosensory response to spinal bending (Desban *et al.*, 2019). Thus, this apical extension structure could influence the firing properties of spinal CSF-cNs. Further analysis of spinal CSF-cNs dendritic morphology in culture, using a dendritic marker such as MAP2, is required to assess whether cell culture affected the apical extension morphology. Another possibility could be to stimulate *in vivo* the spinal CSF-cNs and see whether we can see an activation. To do so, we could perform hindbrain injections of caged neuromodulators such as norepinephrine, and uncage the neuromodulator locally in the spinal cord to stimulate the spinal CSF-cNs.

An alternative explanation for the discrepancy between the transcriptome and response to chemical cues is that spinal CSF-cNs *in vitro* could also express the receptors to ATP, the monoamines epinephrine and norepinephrine, as well as serotonin, but lack the key elements on the transduction path that lead to calcium entry, such as the phospholipase C or the phosphatidylinositol 4,5-bisphosphate. In addition, the transduction paths for multiple adrenergic, purinergic and serotonergic receptors were described as calcium-independent. Thus, a response of spinal CSF-cNs for these receptors should be monitored via electrophysiological recordings, as they cannot be detected with calcium imaging.

Finally, the lack of response to ATP, epinephrine/norepinephrine and serotonin could be imputed to artifacts in the transcriptome analysis after fluorescent-activated cell sorting (FACS) of green cells in the *Tg(pkd2l1:GAL4;UAS:GFP)* transgenic line. The transcriptome compared fluorescent spinal CSF-cNs to the other (dark) cells of the trunk of zebrafish larvae. For example, spinal CSF-cN receptors found in the transcriptome could result in some cases from sorting along with CSF-cNs, motor neurons, floor plate cells or immune

cells sorted by fluorescence. Another possibility is that receptors were specifically expressed in subpopulations of spinal CSF-cNs, information missing in our current transcriptome as all spinal CSF-cNs were pooled prior to RNA-sequencing. To conserve the heterogeneity of spinal CSF-cNs subpopulations, as well as to maintain the specificity of the transcriptome, I am pursuing a single-cell RNA-sequencing is currently ongoing together with the engineer Julian Roussel in the lab and collaborators from the Jean-Pierre Levraud's lab (Pasteur Institute). We gain in specificity using this technique as we can investigate the gene expression of individual CSF-cNs and verify specific gene expressions of spinal CSF-cNs such as Pkd2l1, but we will lose in depth/sensitivity. Single-cell RNA-sequencing should inform us about heterogeneity in gene expression of individual CSF-cNs, highlighting potential subpopulations of spinal CSF-cNs based on their pattern of expression of receptors. However, the loss in sensitivity by monitoring gene expression of individual spinal CSF-cNs might not reveal receptors expressed at a low level.

2) Spinal CSF-cNs are interoceptive chemosensory neurons involved in innate immunity

2.1) Spinal CSF-cNs detect bacterial metabolites during bacterial infection

We found in our transcriptome for spinal CSF-cNs transcripts for two taste receptors, tas2r3a/b. These taste receptors were highly enriched in spinal CSF-cNs, suggesting a predominant role for these receptors. Initially, taste receptors of type 2 (T2Rs) were described as G protein-coupled receptors (GPCRs) detecting bitterness (Li, 2013). Interestingly, T2Rs were also described in ciliated cells of the upper airway to detect bacterial quorum-sensing metabolites such as acyl-homoserine lactone (AHL) (Lee *et al.*, 2012) or quinolones (Freund *et al.*, 2018). In addition, to taste receptors, we found that spinal CSF-cNs express the receptor Tlr5 involved in the detection of flagellin (Miao *et al.*, 2007), the principal component of the bacterial flagella. Thus, we hypothesized that spinal CSF-cNs can sense bacterial metabolites, potentially during a bacterial infection of the CSF.

Taking advantage of a meningitis model of larval zebrafish (Jim *et al.*, 2016), we showed that spinal CSF-cNs exhibit large and long responses to pneumococcal bacterial infection of the CSF *in vivo*. These calcium transients were recurrent in individual cells over hours without apparent cell death, suggesting that large spinal CSF-cNs activity was not pre-apoptotic. We showed that spinal CSF-cNs *in vivo* do not respond to heat-killed bacteria and nonvirulent bacteria, suggesting that either metabolites released by living bacteria in the CSF, or

proinflammatory cues from cells infected by the pathogenic bacteria, are required to activate spinal CSF-cNs. To assess whether spinal CSF-cNs activation relies on direct detection of bacterial chemical cues as described in ciliated cells of the upper airway (Lee *et al.*, 2012; Freund *et al.*, 2018), we pressure-applied *in vitro* bacterial metabolites and found that spinal CSF-cNs respond to pneumolysin, a virulence factor of Streptococcus pneumoniae, as well as to DMDS and 2-pentanone, microbial volatile organic compounds (mVOCs) acting as bitter compounds. The response of spinal CSF-cNs to bitter metabolites was stronger than what was observed with pneumolysin, suggesting that bacterial metabolites acting as bitter compounds could directly trigger the response of spinal CSF-cNs as it was observed *in vivo*.

However, the responses to pneumococcal infection of the CSF *in vivo* were stronger and longer compared to *in vitro*. A combination of different bacterial metabolites *in vivo*, such as mVOCs and the virulence factor pneumolysin forming pores in the cell membrane, could lead to large calcium responses to bacteria. In addition, bacteria produce a large variety of mVOCs that can act as bitter compounds (Bos, Sterk and Schultz, 2013). The taste receptor T2R38 has been shown to respond to at least 7 bacterial metabolites (Verbeurgt *et al.*, 2017), suggesting that taste 2 receptors are susceptible to detect a large variety of bacterial metabolites. Thus, we can also hypothesize that taste 2 receptors expressed in spinal CSF-cNs could detect other bacterial bitter metabolites that could recapitulate the responses observed *in vivo*.

Interestingly, the bacterial pathogen *in vivo* induced response of a subset of spinal CSF-cNs during infection. This result can be explained as heterogeneity in taste 2 receptors expression in spinal CSF-cNs, leading to activation of a subpopulation of spinal CSF-cNs during infection. Ongoing single-cell RNA-sequencing of spinal CSF-cNs will inform about this hypothesis. As we found that spinal CSF-cNs express receptors for GABA and somatostatin, another possibility is that non-activated spinal CSF-cNs receive inhibitory cues reducing their neuronal excitability. The release of large dense-core granules containing peptides requires a sustained neuronal activation (Cropper *et al.*, 2018), as observed in spinal CSF-cNs in response to bacterial infection *in vivo*. Thus, we can hypothesize that spinal CSF-cNs activated by bacterial infection *in vivo* lead to the secretion of inhibitors such as GABA or somatostatin to inhibit the neighboring spinal CSF-cNs. Inhibitory signals could also come from cells infected by the bacteria and releasing chemical inhibitors detected by a subpopulation of spinal CSF-cNs.

2.2) Spinal CSF-cNs increase host survival during bacterial infection

We showed that spinal CSF-cNs conferred a threefold host survival benefit during bacterial CSF infection. When we blocked the spinal CSF-cN neurosecretion after bacterial infection of the CSF, we found a reduction of host survival as well as an elevated bacterial load. Spinal CSF-cNs transcriptome of Dr. Laura Desban and Dr. Andrew Prendergast highlighted expression of numerous peptides acting as antimicrobial peptides (secretogranin 2a) or modulating inflammatory signaling (microseminoprotein, prostate associated 2, endothelial cell specific molecule 1 or natriuretic peptide C). In addition, we performed transcriptomes of control versus infected zebrafish larvae and found that CSF bacterial infection leads to upregulation of cytokines and complement factor components. Thus, we hypothesized that spinal CSF-cNs neurosecretion could promote the survival host. Accordingly, spinal CSF-cNs sustained activation in response to bacterial infection *in vivo* correspond to the typical neuronal activation leading to the release of large dense-core granules containing peptides (Cropper *et al.*, 2018). In addition, electron microscopy revealed clear vesicles (containing neurotransmitters) and dense core granules (containing neuropeptides and secreted proteins) at both apical extension and axonal projections (Vigh, Vigh-Teichmann and Aros, 1977; Djenoune *et al.*, 2017). However, we have not monitored the exocytosis at the CSF-cN membrane in the context of infection *in vivo*.

To monitor the secretion of spinal CSF-cNs, we could take advantage of the pHluorin, a pH-sensitive fluorescent protein derived from the GFP (Miesenböck, De Angelis and Rothman, 1998). We could combine pHluorin with vesicle proteins to visualize exocytosis of the vesicle: pHluorin fluorescence is quenched inside the vesicle due to the acidic intra-vesicular pH (~5.5), and pHluorin express fluorescence when exposed to the extracellular pH during exocytosis. I engineered two different UAS constructs combining pHluorin to two proteins: a marker of dense-core granules containing peptides, the synaptic vesicle proteins vesicular monoamine transporter 2 (VMAT2) (Howell *et al.*, 1994); and one marker of clear synaptic vesicles, the synaptic vesicle protein Synaptophysin (Navone *et al.*, 1986). I injected these two constructs in one-cell stage embryos to generate *Tg(UAS:synaptophysin-pHluorin)*^{icm49} and *Tg(UAS:VMAT2-pHluorin)*^{icm50} transgenic lines. The expression of the two transgenes is under the control of the *pkd2l1* promoter, to restrain their expression to spinal CSF-cNs. These tools could be used in the soon future to monitor the spinal CSF-cNs exocytosis of clear vesicle and dense granules upon bacterial infection of the CSF *in vivo*, as well as test whether activation of spinal CSF-cNs with bacterial metabolites acting as bitter compounds, such as DMDS or 2-pentanone, triggers exocytosis *in vitro*. More imaging experiments will be required to observe exocytosis using these pHluorin transgenic lines.

2.3) What other immune-related metabolites are detected by spinal CSF-cNs?

In addition to taste 2 receptors detecting bacterial metabolites acting as bitter compounds, our transcriptome analysis revealed multiple immune-related receptors. We found receptors for tumor necrosis factors (TNFs) such as TNF-α, as well as interleukins (ILs) such as IL-13 and IL-14. These proinflammatory cues and cytokines could be secreted by infected cells during bacterial infection, and detected by spinal CSF-cNs to potentially secrete peptides, cytokines and complement factor components. We also showed the expression of Toll-like receptors (TLRs), which are proteins expressed in the membrane of leukocytes, as well as non-immune cells such as epithelial cells, endothelial cells and fibroblasts (Delneste, Beauvillain and Jeannin, 2007), and involved in innate immunity. Notably, we found that spinal CSF-cNs express the Tlr5 receptor involved in flagellin detection (Miao *et al.*, 2007), suggesting that spinal CSF-cNs could detect flagellated bacteria. I tested this hypothesis and found that pressure-application of flagellin 1 µg/mL failed to trigger spinal CSF-cNs calcium responses (**Figure 1, n = 9 cells**), indicating that spinal CSF-cNs do not detect bacterial flagella. The absence of spinal CSF-cNs response could also be explained by one of the interpretations exposed in part I of this discussion.

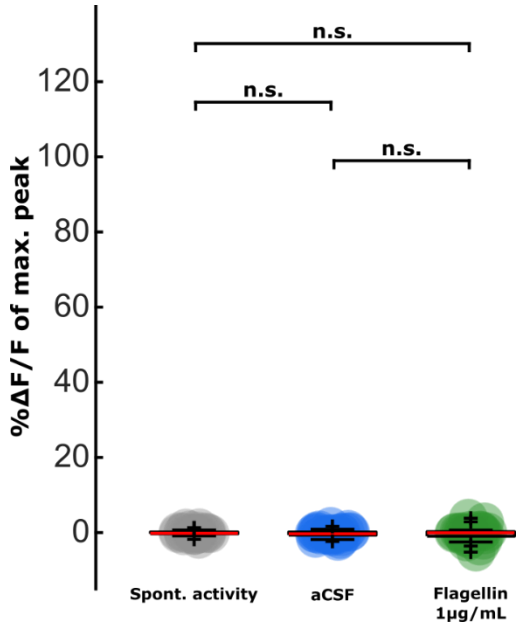

Figure 1. Spinal CSF-cNs do not respond *in vitro* to pressure-applied flagellin. Quantification of calcium transients in spontaneous activity (grey circle), or after aCSF (blue circle) and flagellin 1µg/mL (green circle) pressure-application. 1-factor ANOVA, $p > 0.05$. n.s. = not significant. Red bar: median ΔF/F (median spontaneous activity = -0.19%, median aCSF = -0.33% and median flagellin 1µg/mL = -0.07%, 0 responding cells out of 9.

Surprisingly, we found that spinal CSF-cNs also express the cytokine receptors Crfb1 and Crfb2, activated by virus-induced interferons (IFNs) in zebrafish (Langevin *et al.*, 2013), suggesting that spinal CSF-cNs could detect viral pathogen as well in the CSF. I test this hypothesis using interferon (IFN) phi 1, an agonist of the Crfb1 receptors that we found more expressed in spinal CSF-cNs than Crfb2 in our transcriptome (1015 F.P.K.M for Crfb1 versus 148 F.P.K.M for Crfb2, ~6.86 fold difference). I found that IFN phi 1 at 0.1 mg/mL failed to trigger spinal CSF-cNs calcium response (**Figure 2, n = 10 cells**), suggesting that spinal CSF-cNs do not detect virus-induced IFN.

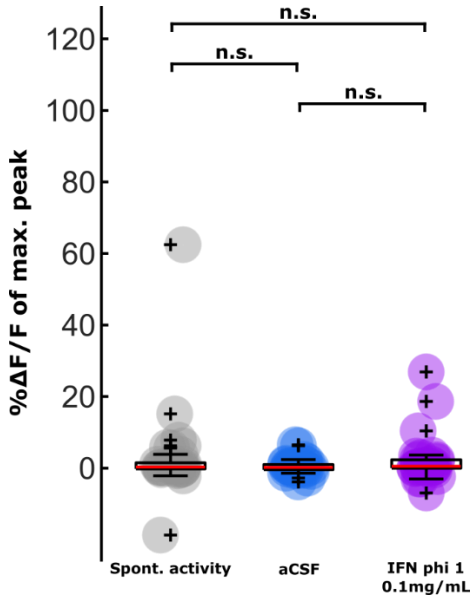

Figure 2. Spinal CSF-cNs do not respond *in vitro* to pressure-applied interferon (IFN) phi 1. Quantification of calcium transients in spontaneous activity (grey circle), or after aCSF (blue circle) and IFN phi 1 0.1mg/mL (purple circle) pressure-application. 1-factor ANOVA, $p > 0.05$. n.s. = not significant. Red bar: median ΔF/F (median spontaneous activity = 0.52%, median aCSF = -0.37% and median flagellin 1µg/mL = 0.18%, 0 responding cells out of 10.

However, we hypothesized that spinal CSF-cNs could detect chemical cues secreted by infected cells during viral infection. To test this hypothesis, collaborators from Jean-Pierre Levraud's lab infected baby hamster kidney (BHK) cells with the Sindbis virus expressing mCherry fluorescent protein. After 48 hours of incubation, infected cells showed red fluorescence and started to detach from the support, while non-infected control cells were still attached to the support. Then, supernatants of control and infected cells were collected and inactivated using UVs. Preliminary data showed that if spinal CSF-cNs failed to respond to supernatant from control cells *in vitro*, they were activated by supernatant from infected cells, suggesting that spinal CSF-cNs detect chemical cues released by infected cells after

viral infection. These preliminary results are the first data suggesting that spinal CSF-cNs could detect chemical cues in the context of viral infection. Analysis of the two supernatants, using a technique such as high-performance liquid chromatography (HPLC), is required to decipher the chemical cues activating the spinal CSF-cNs. Another possibility is that the spinal CSF-cNs responses come from the inactivated virus itself. Then, we could test to pressure-apply the inactivated virus *in vitro* in a neutral medium to observe whether it triggers spinal CSF-cNs activation.

3) Spinal CSF-cNs chemosensory functions in the regulation of locomotion

During the last decade, investigations showed that spinal CSF-cNs are mechanosensory cells detecting spinal bending (Böhm *et al.*, 2016; Hubbard *et al.*, 2016), and modulating in response to locomotion and posture of zebrafish (Fidelin *et al.*, 2015; Hubbard *et al.*, 2016; Quan *et al.*, 2020; Wu *et al.*, 2021) and lamprey (Jalalvand, Robertson, Wallén, *et al.*, 2016). Spinal CSF-cNs modulate locomotion through the release of the neurotransmitter GABA (Fidelin *et al.*, 2015) as well as the neuropeptide Somatostatin1.1 (Christenson *et al.*, 1991; Wyart *et al.*, 2009; Jalalvand, Robertson, Wallén, *et al.*, 2016; Quan *et al.*, 2020). We found in our transcriptome that spinal CSF-cNs express receptors for GABA and somatostatin. This suggests that spinal CSF-cNs carry receptors to sense the extracellular concentration of inhibitory molecules such as GABA and Somatostatin1.1, in order to finely regulate in an autocrine manner the release of neurotransmitters and neuropeptides to modulate the locomotion.

Other chemical cues could also be detected by spinal CSF-cNs that could shape the kinematics of locomotion or modulate its occurrence. Chronic inflammatory disease can increase levels of proinflammatory cytokines, such as IL-1, IL−6 and TNF-α, leading to fatigue (Louati and Berenbaum, 2015). We found that spinal CSF-cNs express receptors for interleukins and tumor necrosis factors, suggesting that spinal CSF-cNs could detect those cytokines and in response inhibit locomotion in fatigue. Fatigue can also be linked to depression (Louati and Berenbaum, 2015). The CSF composition was shown to reflect conditions such as depression (Nemeroff *et al.*, 1984). Thus, we can hypothesize that spinal CSF-cNs could detect chemical cues from the CSF to inhibit locomotion in the context of depression. Then, spinal CSF-cNs could detect chemical cues, in addition to mechanical cues from spinal bending, to modulate locomotion. Further investigations are required to demonstrate the link between chemical cues detection and regulation of locomotion in the context of fatigue or depression.

4) Spinal CSF-cNs contribute to morphogenesis

The sensory interface between the central canal of the spinal cord and the CSF has been shown to be important for morphogenesis during embryonic and post-embryonic development. In zebrafish embryos, CSF flows bi-directionally in the central canal of the spinal cord (Cantaut-Belarif *et al.*, 2018; Sternberg *et al.*, 2018; Thouvenin *et al.*, 2020). Indeed, the analysis of the displacement of particles flowing in the brain and spinal cord cavities allowed to characterize a displacement of fluid towards the head of the animal in the dorsal part of the central canal accompanied by an opposite movement towards the tail in the ventral part. This bidirectional flow of CSF originates from the asymmetric motility of cilia projecting from the ventral wall of the central canal (Thouvenin *et al.*, 2020). During embryogenesis, zebrafish mutants defective for cilia function or motility exhibit a curled-down body axis (Brand *et al.*, 1996; Tsujikawa and Malicki, 2004; Kramer-Zucker *et al.*, 2005). This suggested that the cilia-dependent generation of CSF flow is involved in body axis morphogenesis.
Recent investigations on the Reissner fiber (RF), an acellular polymer bathing in the CSF formed by the aggregation of the SCO-spondin protein, showed that *scospondin* mutants develop a curled-down body axis (Cantaut-Belarif *et al.*, 2018). These mutants deprived of the RF exhibit intact motile cilia and bidirectional CSF flow in the central canal. Interestingly, mutants with defective cilia do not form a proper fiber in the central canal (Cantaut-Belarif *et al.*, 2018). Thus, the formation of the RF in the CSF depends on cilia and controls the straightening of the body axis.

In the central canal, the RF is located at the interface with CSF-cNs. Recent work showed that the RF is required for the spontaneous calcium transients generated in ventral spinal CSF-cNs during the embryonic period (Cantaut-Belarif *et al.*, 2020). In zebrafish, ventral spinal CSF-cNs express specifically the Urotensin-related peptides 1 and 2 (URP1, URP2) from the embryonic stage to adulthood (Quan *et al.*, 2015). Cilia-defective mutants exhibit decreased expression levels of *urp1* and *urp2* transcripts (Zhang *et al.*, 2018b), and *scospondin* mutants exhibit a decreased expression of *urp2* (Cantaut-Belarif *et al.*, 2020), suggesting that the RF triggers body morphogenesis by controlling peptidergic expression in ventral CSF-cNs.

Two ligands present in the CSF and transported by the RF, epinephrine and norepinephrine, have been shown to compensate for the defective body axis geometry and URP expression

level in *scospondin* mutants (Cantaut-Belarif *et al.*, 2020). In addition, hindbrain ventricle injections of epinephrine and norepinephrine restore calcium variations defects observed in ventral CSF-cNs in *scospondin* mutants (Cantaut-Belarif *et al.*, 2020). Altogether, these results suggest that epinephrine and norepinephrine could be involved in the mechanisms by which the RF triggers URP expression in spinal CSF-cNs.

Our transcriptome revealed that adrenergic receptors are expressed in spinal CSF-cNs (**Table 1**). Thus, we could hypothesize that the RF facilitates the detection of monoamines by CSF-cNs to enhance the expression of URP peptides. However, I showed that spinal CSF-cNs fail to trigger calcium transients in response to pressure-application of epinephrine and norepinephrine *in vitro*. This suggests that spinal CSF-cNs are not involved in the direct detection of these monoamines. Adrb2 is one adrenergic receptor for epinephrine and norepinephrine that has recently been shown to be expressed in a population of cuboidal cells located at the interface with the CSF in the ventral midline of the embryonic neural tube (Cantaut-Belarif *et al.*, 2020). Thus, it is likely that the mechanism by which monoamines trigger the expression of URP in spinal CSF-cNs is indirect. We could rather propose that the activation of Adrb2-expressing cells could induce the release of chemical cues acting as second messengers on spinal CSF-cNs. More investigations are required to decipher the mechanisms linking the RF, monoamines and URP expression in spinal CSF-cNs.

	Receptor	Full name (ZFIN)	Enriched	logFC	Mean dark (F.P.K.M.)	Mean GFP (F.P.K.M.)
Adrenoceptors	*adrb3a*	adrenoceptor beta 3a	No	0,45	1972	1917
	adra2c	adrenoceptor alpha 2C	No	0,22	552,4	477
	adra1a	adrenoceptor alpha 1Aa	No	0,20	153,2	118
	adrb2a	adrenoceptor beta 2, surface a	No	-0,10	984,8	718
	adra2a	adrenoceptor alpha 2A	No	-0,22	624,6	438
	adrb1	adrenoceptor beta 1	No	-0,70	126,4	59
	adra2da	adrenergic, alpha-2D-, receptor a	No	-1,95	524	106
	adra1d	adrenoceptor alpha 1D	No	-2,16	288,2	55

Table 1. Summary of adrenergic receptors expressed in spinal CSF-cNs. Hits are grouped by families and then ranked by log fold change (logFC) between GFP- reference and GFP+ CSF-cN RNA pools.

In juvenile and adult zebrafish, mutants for the Pkd2l1 channel exhibit an exaggerated spine curvature referred as to hyper-kyphosis (Sternberg *et al.*, 2018). This suggests that the Pkd2l1-dependent activity of spinal CSF-cNs contributes to maintain a correct alignment of the spine. In addition, zebrafish animals deprived of the RF develop three-dimensional

torsions of the spine (Lu *et al.*, 2020; Rose *et al.*, 2020; Troutwine *et al.*, 2020) reminiscent of idiopathic scoliosis in humans. Recently, it has been found that overexpressing *urp2* specifically in CSF-cNs rescues the scoliosis-like phenotype of *scospondin* mutants (Lu *et al.*, 2020). Moreover, mutants for URP receptors expressed in smooth muscle (Zhang *et al.*, 2018b) have been reported to develop spine alignment defects in zebrafish. Hence, URP signaling is involved in late-stage morphogenesis. These results suggest that the sensory interface in the central canal involving the RF and peptidergic signaling in spinal CSF-cNs is crucial for body axis morphogenesis from embryonic to adult stages.

5) Can spinal CSF-cNs detect or respond to sex hormones?

As explained in Chapter II, we found transcripts of receptors for hormones involved in reproduction, such as the luteinizing hormone (LH), the estrogen or the prolactin, suggesting a role of spinal CSF-cNs in reproduction. In our transcriptome of spinal CSF-cNs, we found enriched *tac3a*, a gene encoding for the precursor of two peptides: the Neurokinins Ba (NKBa) and NKB-Related Peptide a (NKB-RPa, also named NKF) (Prendergast *et al.*, 2019). Single intraperitoneal injection of NKBa and NKBRPa peptides in adult female zebrafish significantly increased luteinizing hormone levels (Biran *et al.*, 2012). Moreover, estrogen treatment of pre-pubertal fish elicited increases of Tac3a and Tacr3a/b in the brain (Biran *et al.*, 2012). Interestingly, we also found in our transcriptome expression of the Tac receptor *tacr1a* in CSF-cNs. Altogether, the results suggest that spinal CSF-cNs could detect sexual hormones through tachykinin, LH and estrogen receptors, and in turn potentially release NKBa and NKB-RPa peptides.

In addition, it has been shown that idiopathic scoliosis in adolescents affects predominantly females, with ranges of female to male ratio from 1.5:1 to 3:1, and this ratio increases with age (Konieczny, Senyurt and Krauspe, 2013). As developed in part IV, spinal CSF-cNs contribute to the maintenance of the natural curvature of the spine. Thus, we could hypothesize that spinal CSF-cNs detection of female sex hormones such as estrogen could be linked to a proper maintenance of spine curvature. As idiopathic scoliosis affects predominantly females, we could imagine that female hormonal changes, especially during adolescence, could impact the activity of the spinal CSF-cNs, leading to impaired spine curvature.

Conclusion and Perspectives

During my PhD, I focused on investigating the chemosensory functions of spinal CSF-cNs. I analyzed a transcriptome of spinal CSF-cNs and found receptors for chemical cues involved in different physiological contexts. We found that spinal CSF-cNs respond to bacteria *in vivo*, in the context of bacterial infection of the CSF. Taking advantage of a primary cell culture protocol of spinal CSF-cNs that I developed, we showed that spinal CSF-cNs directly respond to bacterial metabolites such as the virulence factor pneumolysin or microbial volatile organic compounds acting as bitter compounds. During bacterial infection, spinal CSF-cNs up-regulate the expression of cytokines and complement components involved in innate immunity in order to increase host survival. Altogether, we showed that spinal CSF-cNs are interoceptive chemosensory neurons that detect bacterial metabolites to enhance innate immunity.

We have evidence that spinal CSF-cNs exhibit clear vesicles and dense-core granules (Vigh, Vigh-Teichmann and Aros, 1977; Djenoune *et al.*, 2017). Furthermore, spinal CSF-cNs showed vigorous activation in response to bacterial infection, typical of dense-core granules release (Cropper *et al.*, 2018). Further investigations are required to decipher the neurosecretion of spinal CSF-cNs in the context of CSF bacterial infection. A strategy based on the pHluorin fluorescent protein could be used to monitor exocytosis of spinal CSF-cNs *in vivo* and *in vitro*. In addition, we found a large variety of receptors for chemical cues expressed in spinal CSF-cNs.

As discussed, these receptors could be involved in different physiological contexts, such as locomotion, morphogenesis or reproduction. To better understand the physiological chemosensory functions of spinal CSF-cNs, a first step could be to confirm the expression of receptors for chemical cues by performing an additional single-cell RNA-sequencing of spinal CSF-cNs. Then, we could monitor the spinal CSF-cNs responses *in vitro* to pressure-applications of receptor ligands. Ligands activating the spinal CSF-cNs could be tested *in vivo* and investigated more intensively to understand their physiological roles.

Finally, we found first evidence that in addition to bacterial metabolites, spinal CSF-cNs could detect metabolites from infected cells in the context of virus infection. Further investigations will be required to decipher the chemical molecules detected by spinal CSF-cNs during viral infection, as well the physiological role of this detection *in vivo*.

References

Abraira, V. E. and Ginty, D. D. (2013) 'The sensory neurons of touch', *Neuron*. Elsevier Inc., 79(4), pp. 618–639. doi: 10.1016/j.neuron.2013.07.051.

Acerbo, M. J., Hellmann, B. and Güntürkün, O. (2003) 'Catecholaminergic and dopamine-containing neurons in the spinal cord of pigeons: an immunohistochemical study', *Journal of Chemical Neuroanatomy*, 25, pp. 19–27. doi: 10.1016/S0891-0618(02)00072-8.

Adler, E. *et al.* (2000) 'A novel family of mammalian taste receptors', *Cell*, 100(6), pp. 693–702. doi: 10.1016/S0092-8674(00)80705-9.

Agduhr, E. (1922) 'Über ein zentrales Sinnesorgan (?) bei den Vertebraten.', *Zeitschrift für Anatomie und Entwicklungsgeschichte*, 66(3), pp. 223–360.

Ahuja, G. *et al.* (2015) 'Kappe neurons, a novel population of olfactory sensory neurons', *Scientific Reports*, 4, pp. 1–8. doi: 10.1038/srep04037.

Akopian, A. N. *et al.* (1999) 'The tetrodotoxin-resistant sodium channel SNS has a specialized function in pain pathways', *Nature Neuroscience*, 2(6), pp. 541–548. doi: 10.1038/9195.

Albayar, A. A. *et al.* (2019) 'Biomarkers in spinal cord injury: Prognostic insights and future potentials', *Frontiers in Neurology*, 10(JAN). doi: 10.3389/fneur.2019.00027.

Albeg, A. *et al.* (2011) 'C. elegans multi-dendritic sensory neurons: Morphology and function', *Molecular and Cellular Neuroscience*, 46(1), pp. 308–317. doi: 10.1016/j.mcn.2010.10.001.

Alfaro-Cervello, C. *et al.* (2012) 'Biciliated ependymal cell proliferation contributes to spinal cord growth', *Journal of Comparative Neurology*, 520(15), pp. 3528–3552. doi: 10.1002/cne.23104.

Alibardi, L. (1990) 'Cerebrospinal fluid contacting neurons inside the regenerating caudal spinal cord of xenopus tadpoles', *Bolletino di zoologia*, 57(4), pp. 309–315. doi: 10.1080/11250009009355713.

Allardyce, R. A. *et al.* (2006) 'Detection of volatile metabolites produced by bacterial growth in blood culture media by selected ion flow tube mass spectrometry (SIFT-MS)', *Journal of Microbiological Methods*, 65(2), pp. 361–365. doi: 10.1016/j.mimet.2005.09.003.

Andrzejczuk, L. A. *et al.* (2018) 'Tal1, Gata2a, and Gata3 have distinct functions in the development of V2b and cerebrospinal fluid-contacting KA spinal neurons', *Frontiers in Neuroscience*, 12(MAR), pp. 1–24. doi: 10.3389/fnins.2018.00170.

Arbeille, E. *et al.* (2015) 'Cerebrospinal fluid-derived Semaphorin3B orients neuroepithelial cell

divisions in the apicobasal axis', *Nature Communications*, 6. doi: 10.1038/ncomms7366.

Auer, T. O. *et al.* (2015) 'Deletion of a kinesin I motor unmasks a mechanism of homeostatic branching control by neurotrophin-3', *eLife*, 4(JUNE), pp. 1–26. doi: 10.7554/eLife.05061.

Avery, O. T., MacLeod, C. M. and McCarty, M. (1979) 'Studies Nature Inducing of on of the the Chemical Transformation Types', *Journal of Experimental Medicine*, 149, pp. 297–326.

Baker, C. V. H. and Bronner-Fraser, M. (2001) 'Vertebrate cranial placodes. I. Embryonic induction', *Developmental Biology*, 232(1), pp. 1–61. doi: 10.1006/dbio.2001.0156.

Bandell, M. *et al.* (2004) 'Noxious Cold Ion Channel TRPA1 Is Activated by Pungent Compounds and Bradykinin', *Neuron*, 41, pp. 849–857. doi: 10.1016/s0896-6273(04)00150-3.

Banks, R. W. *et al.* (2009) 'A comparative analysis of the encapsulated end-organs of mammalian skeletal muscles and of their sensory nerve endings', *Journal of Anatomy*, 214(6), pp. 859–887. doi: 10.1111/j.1469-7580.2009.01072.x.

Barber, R. P., Vaughn, J. E. and Roberts, E. (1982) 'The cytoarchitecture of GABAergic neurons in rat spinal cord', *Brain Research*, 238, pp. 305–328. doi: 10.1016/0006-8993(82)90107-X.

Barham, H. P. *et al.* (2013) 'Solitary chemosensory cells and bitter taste receptor signaling in human sinonasal mucosa', *International Forum of Allergy & Rhinology*, 3(6), pp. 450–457. doi: 10.1002/alr.21149.

Bartel, D. L. *et al.* (2006) 'Nucleoside triphosphate diphosphohydrolase-2 is the ecto-ATPase of type I cells in taste buds', *The Journal of Comparative Neurology*, 497(1), pp. 1–12. doi: 10.1002/cne.20954.

Bautista, D. M. *et al.* (2006) 'TRPA1 Mediates the Inflammatory Actions of Environmental Irritants and Proalgesic Agents', *Cell*, 124(6), pp. 1269–1282. doi: 10.1016/j.cell.2006.02.023.

Bautista, D. M. *et al.* (2007) 'The menthol receptor TRPM8 is the principal detector of environmental cold', *Nature*, 448(7150), pp. 204–208. doi: 10.1038/nature05910.

Bazáes, A. and Schmachtenberg, O. (2012) 'Odorant tuning of olfactory crypt cells from juvenile and adult rainbow trout', *Journal of Experimental Biology*, 215(10), pp. 1740–1748. doi: 10.1242/jeb.067264.

van de Beek, D. *et al.* (2004) 'Clinical Features and Prognostic Factors in Adults with Bacterial Meningitis', *New England Journal of Medicine*, 351(18), pp. 1849–1859. doi: 10.1056/nejmoa040845.

van de Beek, D. *et al.* (2006) 'Community-Acquired Bacterial Meningitis in Adults', *New England Journal of Medicine*, 354(1), pp. 44–53. doi: 10.1056/NEJMra052116.

van de Beek, D. *et al.* (2016) 'Community-acquired bacterial meningitis', *Nature Reviews Disease*

Primers. Macmillan Publishers Limited, 2, pp. 1–21. doi: 10.1038/nrdp.2016.74.

van de Beek, D. *et al.* (2021) 'Community-acquired bacterial meningitis', *The Lancet*. Elsevier Ltd, 398(10306), pp. 1171–1183. doi: 10.1016/S0140-6736(21)00883-7.

Behrens, M. *et al.* (2014) 'ORA1, a zebrafish olfactory receptor ancestral to all mammalian V1R genes, recognizes 4-hydroxyphenylacetic acid, a putative reproductive pheromone', *Journal of Biological Chemistry*, 289(28), pp. 19778–19788. doi: 10.1074/jbc.M114.573162.

Beilharz, K. *et al.* (2015) 'Red fluorescent proteins for gene expression and protein localization studies in Streptococcus pneumoniae and efficient transformation with DNA assembled via the gibson assembly method', *Applied and Environmental Microbiology*, 81(20), pp. 7244–7252. doi: 10.1128/AEM.02033-15.

Di Bella, D. J. *et al.* (2019) 'Ascl1 Balances Neuronal versus Ependymal Fate in the Spinal Cord Central Canal', *Cell Reports*, 28(9), pp. 2264-2274.e3. doi: 10.1016/j.celrep.2019.07.087.

Belmonte, C. *et al.* (1991) 'Excitation by irritant chemical substances of sensory afferent units in the cat's cornea', *Journal of Physiology*, 437(1), pp. 709–725. doi: 10.1113/jphysiol.1991.sp018621.

Bernardos, R. L. and Raymond, P. A. (2006) 'GFAP transgenic zebrafish', *Gene Expression Patterns*, 6(8), pp. 1007–1013. doi: 10.1016/j.modgep.2006.04.006.

Bernhardt, R. R. *et al.* (1992) 'Axonal trajectories and distribution of GABAergic spinal neurons in wildtype and mutant zebrafish lacking floor plate cells', *Journal of Comparative Neurology*, 326(2), pp. 263–272. doi: 10.1002/cne.903260208.

Bertini, R. *et al.* (1999) 'Thioredoxin, a redox enzyme released in infection and inflammation, is a unique chemoattractant for neutrophils, monocytes, and T cells', *Journal of Experimental Medicine*, 189(11), pp. 1783–1789. doi: 10.1084/jem.189.11.1783.

Bessou, P. and Perl, E. R. (1969) 'Response of cutaneous sensory units with unmyelinated fibers to noxious stimuli', *Journal of neurophysiology*, 32(6), pp. 1025–1043. doi: 10.1152/jn.1969.32.6.1025.

Bijlsma, M. W. *et al.* (2016) 'Community-acquired bacterial meningitis in adults in the Netherlands, 2006-14: A prospective cohort study', *The Lancet Infectious Diseases*. Elsevier Ltd, 16(3), pp. 339–347. doi: 10.1016/S1473-3099(15)00430-2.

Binor, E. and Heathcote, R. D. (2001) 'Development of GABA-immunoreactive neuron patterning in the spinal cord', *Journal of Comparative Neurology*, 438(1), pp. 1–11. doi: 10.1002/cne.1298.

Biran, J. *et al.* (2012) 'Neurokinin Bs and neurokinin B receptors in zebrafish-potential role in controlling fish reproduction', *Proceedings of the National Academy of Sciences*, 109(26), pp. 10269–10274. doi: 10.1073/pnas.1119165109.

Bjorefeldt, A. *et al.* (2018) 'Neuromodulation via the cerebrospinal fluid: Insights from recent in vitro studies', *Frontiers in Neural Circuits*, 12(February), pp. 1–12. doi: 10.3389/fncir.2018.00005.

Böhm, U. L. *et al.* (2016) 'CSF-contacting neurons regulate locomotion by relaying mechanical stimuli to spinal circuits', *Nature Communications*, 7. doi: 10.1038/ncomms10866.

Böhm, U. L. (2017) *Physiological inputs to cerebrospinal fluid-contacting neurons*. Univeristé Pierre et Marie Curie - Paris VI.

Bos, L. D. J., Sterk, P. J. and Schultz, M. J. (2013) 'Volatile Metabolites of Pathogens: A Systematic Review', *PLoS Pathogens*, 9(5), pp. 1–8. doi: 10.1371/journal.ppat.1003311.

Boyd, I. A. (1962) 'The structure and innervation of the nuclear bag muscle fibre system and the nuclear chain muscle fibre system in mammalian muscle spindles', *Royal Society*, 245(720). doi: 10.1098/rstb.1962.0007.

Brand, M. *et al.* (1996) 'Mutations affecting development of the midline and general body shape during zebrafish embryogenesis', *Development*, 123(June 2014), pp. 129–142. doi: 10.1242/dev.123.1.129.

Braubach, O. R., Fine, A. and Croll, R. P. (2012) 'Distribution and functional organization of glomeruli in the olfactory bulbs of zebrafish (Danio rerio)', *Journal of Comparative Neurology*, 520(11), pp. 2317–2339. doi: 10.1002/cne.23075.

Brisben, A. J., Hsiao, S. S. and Johnson, K. O. (1999) 'Detection of vibration transmitted through an object grasped in the hand', *Journal of Neurophysiology*, 81(4), pp. 1548–1558. doi: 10.1152/jn.1999.81.4.1548.

Brown, A. G. and Iggo, A. (1967) 'A quantitative study of cutaneous receptors and afferent fibres in the cat and rabbit', *The Journal of Physiology*, 193(3), pp. 707–733. doi: 10.1113/jphysiol.1967.sp008390.

Brunger, A. T., Jin, R. and Breidenbach, M. A. (2008) 'Highly specific interactions between botulinum neurotoxins and synaptic vesicle proteins', *Cellular and Molecular Life Sciences*, 65(15), pp. 2296–2306. doi: 10.1007/s00018-008-8088-0.

Buchanan, J. T. *et al.* (1987) 'Survey of neuropeptide-like immunoreactivity in the lamprey spinal cord', *Brain Research*, 408(1–2), pp. 299–302. doi: 10.1016/0006-8993(87)90392-1.

Buck, L. B. (2000) 'The molecular architecture of odor and pheromone sensing in mammals', *Cell*, 100(6), pp. 611–618. doi: 10.1016/S0092-8674(00)80698-4.

Budick, S. A. and O'Malley, D. M. (2000) 'Locomotor repertoire of the larval zebrafish: Swimming, turning and prey capture', *Journal of Experimental Biology*, 203(17), pp. 2565–2579. doi: 10.1242/jeb.203.17.2565.

Burgess, P. R., Petit, D. and Warren, R. M. (1968) 'Receptor types in cat hairy skin supplied by myelinated fibers.', *Journal of neurophysiology*, 31(6), pp. 833–848. doi: 10.1152/jn.1968.31.6.833.

Burke, D., Gandevia, S. C. and Macefield, G. (1988) 'Responses to passive movement of receptors in joint, skin and muscle of the human hand', *Journal of Pain*, 402, pp. 347–361. doi: 10.1113/jphysiol.1988.sp017208.

Byrd, C. A. and Brunjes, P. C. (1995) 'Organization of the olfactory system in the adult zebrafish: Histological, immunohistochemical, and quantitative analysis', *Journal of Comparative Neurology*, 358(2), pp. 247–259. doi: 10.1002/cne.903580207.

Caceres, A. I. *et al.* (2009) 'A sensory neuronal ion channel essential for airway inflammation and hyperreactivity in asthma', *Proceedings of the National Academy of Sciences of the United States of America*, 106(22), pp. 9099–9104. doi: 10.1073/pnas.0900591106.

Calvo-Ochoa, E. and Byrd-Jacobs, C. A. (2019) 'The olfactory system of zebrafish as a model for the study of neurotoxicity and injury: Implications for neuroplasticity and disease', *International Journal of Molecular Sciences*, 20(7). doi: 10.3390/ijms20071639.

Campero, M. *et al.* (2001) 'Slowly conducting afferents activated by innocuous low temperature in human skin', *Journal of Physiology*, 535(3), pp. 855–865. doi: 10.1111/j.1469-7793.2001.t01-1-00855.x.

Cantaut-Belarif, Y. *et al.* (2018) 'The Reissner Fiber in the Cerebrospinal Fluid Controls Morphogenesis of the Body Axis', *Current Biology*. Elsevier Ltd., pp. 1–8. doi: 10.1016/j.cub.2018.05.079.

Cantaut-Belarif, Y. *et al.* (2020) 'Adrenergic activation modulates the signal from the reissner fiber to cerebrospinal fluid-contacting neurons during development', *eLife*, 9, pp. 1–25. doi: 10.7554/eLife.59469.

Caspary, T. and Anderson, K. V. (2003) 'Patterning cell types in the dorsal spinal cord: What the mouse mutants say', *Nature Reviews Neuroscience*, 4(4), pp. 290–298. doi: 10.1038/nrn1073.

Caterina, M. J. *et al.* (1997) 'The capsaicin receptor: A heat-activated ion channel in the pain pathway', *Nature*, 389(6653), pp. 816–824. doi: 10.1038/39807.

Caterina, M. J. *et al.* (1999) 'A capsaicin-receptor homologue with a high threshold for noxious heat', *Nature*, 398(6726), pp. 436–441. doi: 10.1038/18906.

Caterina, M. J. *et al.* (2000) 'Impaired Nociception and Pain Sensation in Mice Lacking the Capsaicin Receptor', *Science*, 288(April), pp. 306–313. doi: 10.1126/science.288.5464.306.

Chalermkitpanit, P. *et al.* (2017) 'Noradrenaline, Serotonin, GABA, and Glycine in Cerebrospinal Fluid

during Labor Pain: A Cross-Sectional Prospective Study', *Pain Research and Management*. Hindawi, 2017. doi: 10.1155/2017/2752658.

Chalfie, M. and Sulston, J. (1981) 'Developmental genetics of the mechanosensory neurons of Caenorhabditis elegans', *Developmental Biology*, 82(2), pp. 358–370. doi: 10.1016/0012-1606(81)90459-0.

Chambers, D., Huang, C. and Matthews, G. (2015) 'The spinal cord', in *Basic Physiology for Anaesthetists*. Cambridge: Cambridge University Press, pp. 207–216. doi: 10.1017/CBO9781139226394.049.

Chandrashekar, J. *et al.* (2000) 'T2Rs function as bitter taste receptors', *Cell*, 100(6), pp. 703–711. doi: 10.1016/S0092-8674(00)80706-0.

Chandrashekar, J. *et al.* (2006) 'The receptors and cells for mammalian taste', *Nature*, 444(7117), pp. 288–294. doi: 10.1038/nature05401.

Chandrashekar, J. *et al.* (2009) 'The taste of carbonation', *Science*, 326(5951), pp. 443–445. doi: 10.1126/science.1174601.

Chang, J. T., Lehtinen, M. K. and Sive, H. (2016) 'Zebrafish cerebrospinal fluid mediates cell survival through a retinoid signaling pathway', *Developmental Neurobiology*, 76(1), pp. 75–92. doi: 10.1002/dneu.22300.

Chang, W. *et al.* (2016) 'Merkel disc is a serotonergic synapse in the epidermis for transmitting tactile signals in mammals', *Proceedings of the National Academy of Sciences of the United States of America*, 113(37), pp. E5491–E5500. doi: 10.1073/pnas.1610176113.

Chatzigeorgiou, M. *et al.* (2010) 'Specific roles for DEG/ENaC and TRP channels in touch and thermosensation in C. elegans nociceptors', *Nature Neuroscience*, 13(7), pp. 861–868. doi: 10.1038/nn.2581.

Chau, K. F. *et al.* (2015) 'Progressive Differentiation and Instructive Capacities of Amniotic Fluid and Cerebrospinal Fluid Proteomes following Neural Tube Closure', *Developmental Cell*, 35(6), pp. 789–802. doi: 10.1016/j.devcel.2015.11.015.

Chen, C. C. *et al.* (2002) 'A role for ASIC3 in the modulation of high-intensity pain stimuli', *Proceedings of the National Academy of Sciences of the United States of America*, 99(13), pp. 8992–8997. doi: 10.1073/pnas.122245999.

Chen, G. *et al.* (2014) 'C-type natriuretic peptide attenuates LPS-induced endothelial activation: Involvement of p38, Akt, and NF-κB pathways', *Amino Acids*, 46(12), pp. 2653–2663. doi: 10.1007/s00726-014-1816-x.

Chen, G., Ning, B. and Shi, T. (2019) 'Single-cell RNA-seq technologies and related computational data analysis', *Frontiers in Genetics*, 10(APR), pp. 1–13. doi: 10.3389/fgene.2019.00317.

Chiu, I. M. *et al.* (2013) 'Bacteria activate sensory neurons that modulate pain and inflammation', *Nature*. Nature Publishing Group, 501(7465), pp. 52–57. doi: 10.1038/nature12479.

Christenson, J. *et al.* (1991) 'Co-localized GABA and somatostatin use different ionic mechanisms to hyperpolarize target neurons in the lamprey spinal cord', *Neuroscience Letters*, 134(1), pp. 93–97. doi: 10.1016/0304-3940(91)90516-V.

Colburn, R. W. *et al.* (2007) 'Attenuated Cold Sensitivity in TRPM8 Null Mice', *Neuron*, 54(3), pp. 379–386. doi: 10.1016/j.neuron.2007.04.017.

Collaborators, G. 2016 M. (2018) 'Global, regional, and national burden of meningitis, 1990–2016: a systematic analysis for the Global Burden of Disease Study 2016', *The Lancet Neurology*, 17(12), pp. 1061–1082. doi: 10.1016/S1474-4422(18)30387-9.

Concordet, J. P. and Haeussler, M. (2018) 'CRISPOR: Intuitive guide selection for CRISPR/Cas9 genome editing experiments and screens', *Nucleic Acids Research*. Oxford University Press, 46(W1), pp. W242–W245. doi: 10.1093/nar/gky354.

Conwey, B. A., Hultborn, H. and Kiehn, O. (1987) 'Proprioceptive input resets central locomotor rhythm in the spinal cat', *Experimental Brain Research*, 68, pp. 643–656. doi: 10.1007/BF00249807.

Corns, L. F. *et al.* (2015) 'Cholinergic Enhancement of Cell Proliferation in the Postnatal Neurogenic Niche of the Mammalian Spinal Cord', *STEM CELLS*, 33(9), pp. 2864–2876. doi: 10.1002/stem.2077.

Cox, J. J. *et al.* (2006) 'An SCN9A channelopathy causes congenital inability to experience pain', *Nature*, 444(7121), pp. 894–898. doi: 10.1038/nature05413.

Cropper, E. C. *et al.* (2018) 'Peptide Cotransmitters as Dynamic, Intrinsic Modulators of Network Activity', *Frontiers in Neural Circuits*, 12(October), pp. 1–7. doi: 10.3389/fncir.2018.00078.

Dale, N. *et al.* (1987) 'The Development of a Population of Spinal Cord Neurons and their Axonal Projections Revealed by GABA Immunocytochemistry in Frog Embryos', *Proceedings of the Royal Society B: Biological Sciences*, 232(1267), pp. 205–215. doi: 10.1098/rspb.1987.0069.

Dalm, V. A. S. H. *et al.* (2003) 'Expression of somatostatin, cortistatin, and somatostatin receptors in human monocytes, macrophages, and dendritic cells', *American Journal of Physiology - Endocrinology and Metabolism*, 285(2 48-2), pp. 344–353. doi: 10.1152/ajpendo.00048.2003.

Damkier, H. H., Brown, P. D. and Praetorius, J. (2013) 'Cerebrospinal fluid secretion by the choroid plexus', *Physiological Reviews*, 93(4), pp. 1847–1892. doi: 10.1152/physrev.00004.2013.

Darian-Smith, I. *et al.* (1979) 'Warm fibers innervating palmar and digital skin of the monkey: Responses to thermal stimuli', *Journal of Neurophysiology*, 42(5), pp. 1297–1315. doi: 10.1152/jn.1979.42.5.1297.

Daroff, R. and Aminoff, M. (eds) (2014) *Encyclopedia of the Neurological Sciences, Second Edition*. 2nd edn.

Davis, J. B. *et al.* (2000) 'Vanilloid receptor-1 is essential for inflammatory thermal hyperalgesia', *Nature*, 405(6783), pp. 183–187. doi: 10.1038/35012076.

De-Doncker, L. *et al.* (2003) 'Characterization of spindle afferents in rat soleus muscle using ramp-and-hold and sinusoidal stretches', *Journal of Neurophysiology*, 89(1), pp. 442–449. doi: 10.1152/jn.00153.2002.

DeFazio, R. A. *et al.* (2006) 'Separate populations of receptor cells and presynaptic cells in mouse taste buds', *Journal of Neuroscience*, 26(15), pp. 3971–3980. doi: 10.1523/JNEUROSCI.0515-06.2006.

Deisenhammer, F. *et al.* (2006) 'Guidelines on routine cerebrospinal fluid analysis. Report from an EFNS task force', *European Journal of Neurology*, 13(9), pp. 913–922. doi: 10.1111/j.1468-1331.2006.01493.x.

Delneste, Y., Beauvillain, C. and Jeannin, P. (2007) 'Innate immunity: structure and function of TLRs', *Médecine/Sciences*, 23(1), pp. 67–74. doi: 10.1051/medsci/200723167.

DeMaria, S. *et al.* (2013) 'Role of a ubiquitously expressed receptor in the vertebrate olfactory system', *Journal of Neuroscience*, 33(38), pp. 15235–15247. doi: 10.1523/JNEUROSCI.2339-13.2013.

Desban, L. *et al.* (2019) 'Regulation of the apical extension morphogenesis tunes the mechanosensory response of microvilliated neurons', *PLoS Biology*, 17(4), pp. 1–27. doi: 10.1371/journal.pbio.3000235.

Dhaka, A. *et al.* (2007) 'TRPM8 Is Required for Cold Sensation in Mice', *Neuron*, 54(3), pp. 371–378. doi: 10.1016/j.neuron.2007.02.024.

Dib-Hajj, S. D., Yang, Y. and Waxman, S. G. (2008) *Chapter 4 Genetics and Molecular Pathophysiology of Nav1.7-Related Pain Syndromes*. 1st edn, *Advances in Genetics*. 1st edn. Elesvier Inc. doi: 10.1016/S0065-2660(08)01004-3.

Djenoune, L. *et al.* (2014) 'Investigation of spinal cerebrospinal fluid-contacting neurons expressing PKD2L1: evidence for a conserved system from fish to primates.', *Frontiers in neuroanatomy*, 8(May), p. 26. doi: 10.3389/fnana.2014.00026.

Djenoune, L. *et al.* (2017) 'The dual developmental origin of spinal cerebrospinal fluid- contacting

neurons gives rise to distinct functional subtypes', *Scientific Reports*. Springer US, 7(719), pp. 1–14. doi: 10.1038/s41598-017-00350-1.

Drew, L. J. *et al.* (2004) 'Acid-sensing ion channels ASIC2 and ASIC3 do not contribute to mechanically activated currents in mammalian sensory neurones', *Journal of Physiology*, 556(3), pp. 691–710. doi: 10.1113/jphysiol.2003.058693.

Driscoll, M. and Chalfie, M. (1991) 'The mec-4 gene is a member of a family of Caenorhabditis elegans genes that can mutate to induce neuronal degeneration', *Nature*, 349, pp. 588–593. doi: 10.1038/349588a0.

Du, J. *et al.* (2009) 'Expression of TRPM8 in the distal cerebrospinal fluid-contacting neurons in the brain mesencephalon of rats', *Cerebrospinal Fluid Research*, 6. doi: 10.1186/1743-8454-6-3.

Dubyak, G. R. (2003) 'Knock-out mice reveal tissue-specific roles of P2Y receptor subtypes in different epithelia', *Molecular Pharmacology*, 63(4), pp. 773–776. doi: 10.1124/mol.63.4.773.

Dvoryanchikov, G., Tomchik, S. M. and Chaudhari, N. (2007) 'Biogenic amine synthesis and uptake in rodent taste buds', *The Journal of Comparative Neurology*, 505(3), pp. 302–313. doi: 10.1002/cne.21494.

Eccles, J. C. (1946) 'Synaptic potentials of motoneurones', *Physiology*. doi: 10.1152/jn.1946.9.2.87.

Eccles, J. C. and Sherrington, C. S. (1930) 'Numbers and contraction-values of individual motor-units examined in some muscles of the limb', *Royal Society*, 106(745), pp. 326–357. doi: 10.1098/rspb.1930.0032.

Eccles, R. M. and Lundberg, A. (1958) 'Integrative pattern of Ia synaptic actions on motoneurones of hip and knee muscles', *The Journal of Physiology*, 144(2), pp. 271–298. doi: 10.1113/jphysiol.1958.sp006101.

Eftekhari, S. *et al.* (2013) 'Differentiation of nerve fibers storing CGRP and CGRP receptors in the peripheral trigeminovascular system', *The Journal of Pain*. Elsevier Ltd, 14(11), pp. 1289–1303. doi: 10.1016/j.jpain.2013.03.010.

Eisthen, H. L. (1992) 'Phylogeny of the vomeronasal system and of receptor cell types in the olfactory and vomeronasal epithelia of vertebrates', *Microscopy Research and Technique*, 23(1), pp. 1–21. doi: 10.1002/jemt.1070230102.

England, S. J. *et al.* (2017) 'Identification and Expression Analysis of the Complete Family of Zebrafish pkd Genes', *Frontiers in Cell and Developmental Biology*, 5(February). doi: 10.3389/fcell.2017.00005.

Estacion, M. *et al.* (2008) 'NaV1.7 gain-of-function mutations as a continuum: A1632E displays physiological changes associated with erythromelalgia and paroxysmal extreme pain disorder

mutations and produces symptoms of both disorders', *Journal of Neuroscience*, 28(43), pp. 11079–11088. doi: 10.1523/JNEUROSCI.3443-08.2008.

Fang, X. *et al.* (2005) 'trkA is expressed in nociceptive neurons and influences electrophysiological properties via Nav1.8 expression in rapidly conducting nociceptors', *Journal of Neuroscience*, 25(19), pp. 4868–4878. doi: 10.1523/JNEUROSCI.0249-05.2005.

Ferrell, W. R. (1980) 'The adequacy of stretch receptors in the cat knee joint for signalling joint angle throughout a full range of movement', *The Journal of Physiology*, 299(1), pp. 85–99. doi: 10.1113/jphysiol.1980.sp013112.

Fertleman, C. R. *et al.* (2006) 'SCN9A Mutations in Paroxysmal Extreme Pain Disorder: Allelic Variants Underlie Distinct Channel Defects and Phenotypes', *Neuron*, 52(5), pp. 767–774. doi: 10.1016/j.neuron.2006.10.006.

Fettiplace, R. and Hackney, C. M. (2006) 'The sensory and motor roles of auditory hair cells', *Nature Reviews Neuroscience*, 7(1), pp. 19–29. doi: 10.1038/nrn1828.

Fidelin, K. *et al.* (2015) 'State-dependent modulation of locomotion by GABAergic spinal sensory neurons', *Current Biology*. Elsevier, 25(23), pp. 3035–3047. doi: 10.1016/j.cub.2015.09.070.

Filipiak, W. *et al.* (2012) 'Characterization of volatile metabolites taken up by or released from Streptococcus pneumoniae and Haemophilus influenzae by using GC-MS', *Microbiology (United Kingdom)*, 158(12), pp. 3044–3053. doi: 10.1099/mic.0.062687-0.

Finger, T. E. (1997) 'Evolution of Taste and Solitary Chemoreceptor Cell Systems', *Brain, Behavior and Evolution*, 50(4), pp. 234–243. doi: 10.1159/000113337.

Finger, T. E. *et al.* (2003) 'Solitary chemoreceptor cells in the nasal cavity serve as sentinels of respiration', *Proceedings of the National Academy of Sciences of the United States of America*, 100(15), pp. 8981–8986. doi: 10.1073/pnas.1531172100.

Finger, T. E. *et al.* (2005) 'Neuroscience: ATP signalling is crucial for communication from taste buds to gustatory nerves', *Science*, 310(5753), pp. 1495–1499. doi: 10.1126/science.1118435.

Firestein, S., Darrow, B. and Shepherd, G. M. (1991) 'Activation of the sensory current in salamander olfactory receptor neurons depends on a G protein-mediated cAMP second messenger system', *Neuron*, 6(5), pp. 825–835. doi: 10.1016/0896-6273(91)90178-3.

Fisher, S. *et al.* (2006) 'Evaluating the biological relevance of putative enhancers using Tol2 transposon-mediated transgenesis in zebrafish', *Nature Protocols*, 1(3), pp. 1297–1305. doi: 10.1038/nprot.2006.230.

Folgueira, M., Anadón, R. and Yañez, J. (2003) 'Experimental study of the connections of the

gustatory system in the rainbow trout, Oncorhynchus mykiss', *Journal of Comparative Neurology*, 465(4), pp. 604–619. doi: 10.1002/cne.10879.

Foster, S. L. *et al.* (2017) 'Sense and immunity: Context-dependent neuro-immune interplay', *Frontiers in Immunology*, 8(NOV), pp. 1–11. doi: 10.3389/fimmu.2017.01463.

Freund, J. R. *et al.* (2018) 'Activation of airway epithelial bitter taste receptors by pseudomonas aeruginosa quinolones modulates calcium, cyclic-amp, and nitric oxide signaling', *Journal of Biological Chemistry*, 293(25), pp. 9824–9840. doi: 10.1074/jbc.RA117.001005.

Friedrich, R. W. and Korsching, S. I. (1998) 'Representations in the Olfactory Bulb Revealed Using a Voltage-Sensitive Axon Tracer', *The Journal of neuroscience*, 18(23), pp. 9977–9988.

Fuller, C. L., Yettaw, H. K. and Byrd, C. A. (2006) 'Mitral cells in the olfactory bulb of adult zebrafish (Danio rerio): Morphology and distribution', *The Journal of Comparative Neurology*, 499(2), pp. 218–230. doi: 10.1002/cne.21091.

Ganju, P. *et al.* (1998) 'Differential regulation of SHC proteins by nerve growth factor in sensory neurons and PC12 cells', *European Journal of Neuroscience*, 10(6), pp. 1995–2008. doi: 10.1046/j.1460-9568.1998.00209.x.

Gardner, E. D. (1942) 'Nerve terminals associated with the knee joint of the mouse', *The Anatomical Record*, 83(3), pp. 401–419. doi: 10.1002/ar.1090830309.

Gato, Á. *et al.* (2005) 'Embryonic cerebrospinal fluid regulates neuroepithelial survival, proliferation, and neurogenesis in chick embryos', *Anatomical Record - Part A Discoveries in Molecular, Cellular, and Evolutionary Biology*, 284(1), pp. 475–484. doi: 10.1002/ar.a.20185.

Gawel, K. *et al.* (2020) 'Seizing the moment: Zebrafish epilepsy models', *Neuroscience and Biobehavioral Reviews*. Elsevier Ltd, 116, pp. 1–20. doi: 10.1016/j.neubiorev.2020.06.010.

Ghitani, N. *et al.* (2017) 'Specialized Mechanosensory Nociceptors Mediating Rapid Responses to Hair-Pull', *Neuron*, 95(4), pp. 944-954.e4. doi: 10.1016/j.neuron.2017.07.024.

Goldberg, D. W. *et al.* (2018) 'Neurological sequelae of adult meningitis in Africa: A systematic literature review', *Open Forum Infectious Diseases*, 5(1). doi: 10.1093/ofid/ofx246.

Gossard, J. P. *et al.* (1994) 'Transmission in a locomotor-related group Ib pathway from hindlimb extensor muscles in the cat', *Experimental Brain Research*, 98(2), pp. 213–228. doi: 10.1007/BF00228410.

Grigg, P. and Greenspan, B. J. (1977) 'Response of primate joint afferent neurons to mechanical stimulation of knee joint', *Journal of Neurophysiology*, 40(1). doi: 10.1152/jn.1977.40.1.1.

Grillner, S., Williams, T. and Lagerbäck, P. Å. (1984) 'The edge cell, a possible intraspinal mechanoreceptor', *Science*, 223(4635), pp. 500–503. doi: 10.1126/science.6691161.

Guertin, P. *et al.* (1995) 'Ankle extensor group I afferents excite extensors throughout the hindlimb during fictive locomotion in the cat', *The Journal of Physiology*, 487(1), pp. 197–209. doi: 10.1113/jphysiol.1995.sp020871.

Gulbransen, B. D. *et al.* (2008) 'Nasal Solitary Chemoreceptor Cell Responses to Bitter and Trigeminal Stimulants In Vitro', *Journal of Neurophysiology*, 99(6), pp. 2929–2937. doi: 10.1152/jn.00066.2008.

Güler, A. D. *et al.* (2002) 'Heat-Evoked Activation of the Ion Channel, TRPV4', *The Journal of Neuroscience*, 22(15), pp. 6408–6414. doi: 10.1016/S0003-2670(01)85240-5.

Hagen-Torn, O. (1882) 'Entwicklung und Bau der Synoviamembranen.', *Arch. Mikros. Anat.*, 21, pp. 591–663.

Halata, Z., Grim, M. and Bauman, K. I. (2003) 'Friedrich Sigmund Merkel and his "Merkel cell", morphology, development, and physiology: Review and new results', *Anatomical Record - Part A Discoveries in Molecular, Cellular, and Evolutionary Biology*, 271(1), pp. 225–239. doi: 10.1002/ar.a.10029.

Handler, A. and Ginty, D. D. (2021) 'The mechanosensory neurons of touch and their mechanisms of activation', *Nature Reviews Neuroscience*. Springer US, 22(9), pp. 521–537. doi: 10.1038/s41583-021-00489-x.

Hansen, A. *et al.* (1999) 'Ultrastructure of the olfactory epithelium in intact, axotomized, and bulbectomized goldfish, Carassius auratus', *Microscopy Research and Technique*, 45(4–5), pp. 325–338. doi: 10.1002/(SICI)1097-0029(19990515/01)45:4/5<325::AID-JEMT16>3.0.CO;2-V.

Hansen, A. *et al.* (2003) 'Correlation between Olfactory Receptor Cell Type and Function in the Channel Catfish', *Journal of Neuroscience*, 23(28), pp. 9328–9339. doi: 10.1523/jneurosci.23-28-09328.2003.

Hansen, A., Reutter, K. and Zeiske, E. (2002) 'Taste bud development in the zebrafish, Danio rerio', *Developmental Dynamics*, 223(4), pp. 483–496. doi: 10.1002/dvdy.10074.

Hansen, A. and Zeiske, E. (1998) 'The peripheral olfactory organ of the zebrafish, Danio rerio: An ultrastructural study', *Chemical Senses*, 23(1), pp. 39–48. doi: 10.1093/chemse/23.1.39.

Hansen, A. and Zielinski, B. S. (2005) 'Diversity in the olfactory epithelium of bony fishes: Development, lamellar arrangement, sensory neuron cell types and transduction components', *Journal of Neurocytology*, 34(3–5), pp. 183–208. doi: 10.1007/s11068-005-8353-1.

Harden, T. K. *et al.* (2010) 'Signalling and pharmacological properties of the P2Y14 receptor', *Acta*

Physiologica, 199(2), pp. 149–160. doi: 10.1111/j.1748-1716.2010.02116.x.

Hatta, T. *et al.* (2006) 'Quantitative analyses of leukemia inhibitory factor in the cerebrospinal fluid in mouse embryos', *NeuroReport*, 17(18), pp. 1863–1866. doi: 10.1097/WNR.0b013e3280113962.

Higashijima, S. I., Mandel, G. and Fetcho, J. R. (2004) 'Distribution of prospective glutamatergic, glycinergic, and gabaergic neurons in embryonic and larval zebrafish', *Journal of Comparative Neurology*, 480(1), pp. 1–18. doi: 10.1002/cne.20278.

Higashijima, S. I., Schaefer, M. and Fetcho, J. R. (2004) 'Neurotransmitter properties of spinal interneurons in embryonic and larval zebrafish', *Journal of Comparative Neurology*, 480(1), pp. 19–37. doi: 10.1002/cne.20279.

Hoegg, S. *et al.* (2004) 'Phylogenetic timing of the fish-specific genome duplication correlates with the diversification of teleost fish', *Journal of Molecular Evolution*, 59(2), pp. 190–203. doi: 10.1007/s00239-004-2613-z.

Hökfelt, T. *et al.* (1976) 'Immunohistochemical evidence for separate populations of somatostatin-containing and substance P-containing primary afferent neurons in the rat', *Neuroscience*, 1(2), pp. 131–136. doi: 10.1016/0306-4522(76)90006-3.

Hoogman, M. *et al.* (2007) 'Cognitive outcome in adults after bacterial meningitis', *Journal of Neurology, Neurosurgery and Psychiatry*, 78(10), pp. 1092–1096. doi: 10.1136/jnnp.2006.110023.

Howell, M. *et al.* (1994) 'Cloning and functional expression of a tetrabenazine sensitive vesicular monoamine transporter from bovine chromaffin granules', *FEBS Letters*, 338(1), pp. 16–22. doi: 10.1016/0014-5793(94)80108-8.

Huang, A. L. *et al.* (2006) 'The cells and logic for mammalian sour taste detection', *Nature*, 442(7105), pp. 934–938. doi: 10.1038/nature05084.

Huang, J. *et al.* (2014) 'Gain-of-function mutations in sodium channel NaV1.9 in painful neuropathy', *Brain*, 137(6), pp. 1627–1642. doi: 10.1093/brain/awu079.

Huang, M. and Chalfie, M. (1994) 'Gene interactions affecting mechanosensory transduction in Caenorhabditis elegans', *Nature*, 367(6462), pp. 467–470. doi: 10.1038/367467a0.

Huang, P. *et al.* (2012) 'Attenuation of Notch and hedgehog signaling is required for fate specification in the spinal cord', *PLoS Genetics*, 8(6). doi: 10.1371/journal.pgen.1002762.

Huang, S. M. *et al.* (2011) 'TRPV3 and TRPV4 ion channels are not major contributors to mouse heat sensation', *Molecular Pain*, 7, pp. 1–11. doi: 10.1186/1744-8069-7-37.

Huang, X. *et al.* (2010) 'Transventricular delivery of sonic hedgehog is essential to cerebellar

ventricular zone development', *Proceedings of the National Academy of Sciences of the United States of America*, 107(18), pp. 8422–8427. doi: 10.1073/pnas.0911838107.

Huang, Y. A. *et al.* (2008) 'Presynaptic (Type III) cells in mouse taste buds sense sour (acid) taste', *Journal of Physiology*, 586(12), pp. 2903–2912. doi: 10.1113/jphysiol.2008.151233.

Hubbard, J. M. *et al.* (2016) 'Intraspinal Sensory Neurons Provide Powerful Inhibition to Motor Circuits Ensuring Postural Control during Locomotion', *Current Biology*, 26(21), pp. 2841–2853. doi: 10.1016/j.cub.2016.08.026.

Hull, M., Parnes, M. and Jankovic, J. (2021) 'Botulinum Neurotoxin Injections in Childhood Opisthotonus', *Toxins*, 13(2), pp. 1–9. doi: 10.3390/toxins13020137.

Hultborn, H. (1972) 'Convergence on interneurones in the reciprocal Ia inhibitory pathway to motoneurones', *Acta Physiologica Scandinavica Supplementum*, 375, pp. 1–42. doi: 10.1111/j.1748-1716.1972.tb05298.x.

Hunt, C. C. (1954) 'RELATION OF FUNCTION TO DIAMETER IN AFFERENT FIBERS OF MUSCLE NERVES', *Journal of General Physiology*, 38(1), pp. 117–131. doi: 10.1085/jgp.38.1.117.

Iggo, A. and Muir, A. R. (1969) 'The structure and function of a slowly adapting touch corpuscle in hairy skin', *The Journal of Physiology*, 200(3), pp. 763–796. doi: 10.1113/jphysiol.1969.sp008721.

Immke, D. C. and McCleskey, E. W. (2001) 'Lactate enhances the acid-sensing NA+ channel on ischemia-sensing neurons', *Nature Neuroscience*, 4(9), pp. 869–870. doi: 10.1038/nn0901-869.

Ishimaru, Y. *et al.* (2005) 'Two families of candidate taste receptors in fishes', *Mechanisms of Development*, 122(12), pp. 1310–1321. doi: 10.1016/j.mod.2005.07.005.

Jaeger, C. B. *et al.* (1983) 'Some Neurons of the Rat Central Nervous System Contain Aromatic-L-Amino-Acid Decarboxylase But Not Monoamines', *Science*, 219(4589), pp. 1233–1235. doi: 10.1126/science.6131537.

Jakutis, G. and Stainier, D. Y. R. (2021) 'Genotype–Phenotype Relationships in the Context of Transcriptional Adaptation and Genetic Robustness', *Annual Review of Genetics*, 55(1), pp. 71–91. doi: 10.1146/annurev-genet-071719-020342.

Jalalvand, E. *et al.* (2014) 'Laterally projecting cerebrospinal fluid-contacting cells in the lamprey spinal cord are of two distinct types', *Journal of Comparative Neurology*, 522(8), pp. 1753–1768. doi: 10.1002/cne.23542.

Jalalvand, E., Robertson, B., Wallén, P., *et al.* (2016) 'Ciliated neurons lining the central canal sense both fluid movement and pH through ASIC3', *Nature Communications*, 7, p. 10002. doi: 10.1038/ncomms10002.

Jalalvand, E., Robertson, B., Tostivint, H., *et al.* (2016) 'The spinal cord has an intrinsic system for the control of pH', *Current Biology*, 26(10), pp. 1346–1351. doi: 10.1016/j.cub.2016.03.048.

Jalalvand, E. *et al.* (2018) 'Cerebrospinal fluid-contacting neurons sense pH changes and motion in the hypothalamus', *Journal of Neuroscience*, 38(35), pp. 7713–7724. doi: 10.1523/JNEUROSCI.3359-17.2018.

Jim, K. K. *et al.* (2016) 'Infection of zebrafish embryos with live fluorescent Streptococcus pneumoniae as a real-time pneumococcal meningitis model', *Journal of Neuroinflammation*. Journal of Neuroinflammation, 13(1), pp. 1–13. doi: 10.1186/s12974-016-0655-y.

Johansson, R. S., Landström, U. and Lundström, R. (1982) 'Responses of mechanoreceptive afferent units in the glabrous skin of the human hand to sinusoidal skin displacements', *Brain Research*, 244(1), pp. 17–25. doi: 10.1016/0006-8993(82)90899-X.

Johnson, E. *et al.* (2020) 'Graded calcium spikes differentially signal neurotransmitter input in cerebrospinal fluid contacting neurons of mouse spinal cord', *bioRxiv*. doi: 10.1101/2020.09.18.303347.

Johnson, K. *et al.* (2016) 'Gfap-positive radial glial cells are an essential progenitor population for later-born neurons and glia in the zebrafish spinal cord', *Glia*, 64(7), pp. 1170–1189. doi: 10.1002/glia.22990.

Johnson, K. O. and Hsiao, S. S. (1992) 'Neural Mechanisms of Tactual form and Texture Perception', *Annual Review of Neuroscience*, 15(1), pp. 227–250. doi: 10.1146/annurev.ne.15.030192.001303.

de Jong, E. K. *et al.* (2008) 'Expression, transport, and axonal sorting of neuronal CCL21 in large dense-core vesicles.', *FASEB journal : official publication of the Federation of American Societies for Experimental Biology*, 22(12), pp. 4136–45. doi: 10.1096/fj.07-101907.

Jordt, S. E. *et al.* (2004) 'Mustard oils and cannabinoids excite sensory nerve fibres through the TRP channel ANKTM1', *Nature*, 427(6971), pp. 260–265. doi: 10.1038/nature02282.

Joselevitch, C. and Zenisek, D. (2009) 'Imaging exocytosis in retinal bipolar cells with TIRF microscopy', *Journal of Visualized Experiments*, (28), pp. 1–6. doi: 10.3791/1305.

Kadioglu, A. *et al.* (2008) 'The role of Streptococcus pneumoniae virulence factors in host respiratory colonization and disease', *Nature Reviews Microbiology*, 6(4), pp. 288–301. doi: 10.1038/nrmicro1871.

Kandel, E. R. *et al.* (2012) *Principle of Neural Science, Fifth Edtion*. New York: McGraw-Hill.

Karashima, Y. *et al.* (2007) 'Bimodal action of menthol on the transient receptor potential channel TRPA1', *Journal of Neuroscience*, 27(37), pp. 9874–9884. doi: 10.1523/JNEUROSCI.2221-07.2007.

Karashima, Y. *et al.* (2009) 'TRPA1 acts as a cold sensor in vitro and in vivo', *Proceedings of the National Academy of Sciences of the United States of America*, 106(4), pp. 1273–1278. doi: 10.1073/pnas.0808487106.

Kashem, S. W. *et al.* (2015) 'Nociceptive Sensory Fibers Drive Interleukin-23 Production from CD301b+ Dermal Dendritic Cells and Drive Protective Cutaneous Immunity', *Immunity*. Elsevier Inc., 43(3), pp. 515–526. doi: 10.1016/j.immuni.2015.08.016.

Kasumyan, A. O. (2019) 'The taste system in fishes and the effects of environmental variables', *Journal of Fish Biology*, 95(1), pp. 155–178. doi: 10.1111/jfb.13940.

Kasumyan, A. O. and Døving, K. B. (2003) 'Taste preferences in fishes', *Fish and Fisheries*, 4(4), pp. 289–347. doi: 10.1046/j.1467-2979.2003.00121.x.

Kennedy, W. R., Webster, H. de F. and Yoon, K. S. (1975) 'Human muscle spindles: fine structure of the primary sensory ending', *Journal of Neurocytology*, 4(6), pp. 675–695. doi: 10.1007/BF01181630.

Khakh, B. S. and North, R. A. (2012) 'Neuromodulation by Extracellular ATP and P2X Receptors in the CNS', *Neuron*, 76(1), pp. 51–69. doi: 10.1016/j.neuron.2012.09.024.

Kieser, K. J. and Kagan, J. C. (2017) 'Multi-receptor detection of individual bacterial products by the innate immune system', *Nature Reviews Immunology*. Nature Publishing Group, 17(6), pp. 376–390. doi: 10.1038/nri.2017.25.

Kim, J. H., Creekmore, E. and Vezina, P. (2003) 'Microinjection of CART peptide 55-102 into the nucleus accumbens blocks amphetamine-induced locomotion', *Neuropeptides*, 37(6), pp. 369–373. doi: 10.1016/j.npep.2003.10.001.

Kirino, M. *et al.* (2013) 'Evolutionary origins of taste buds: Phylogenetic analysis of purinergic neurotransmission in epithelial chemosensors', *Open Biology*, 3(MAR). doi: 10.1098/rsob.130015.

Kleene, S. J. and Gesteland, R. C. (1991) 'Calcium-activated chloride conductance in frog olfactory cilia', *Journal of Neuroscience*, 11(11), pp. 3624–3629. doi: 10.1523/jneurosci.11-11-03624.1991.

Knibestöl, M. (1975) 'Stimulus-response functions of slowly adapting mechanoreceptors in the human glabrous skin area.', *The Journal of Physiology*, 245(1), pp. 63–80. doi: 10.1113/jphysiol.1975.sp010835.

Koedel, U. *et al.* (2009) 'Apoptosis is essential for neutrophil functional shutdown and determines tissue damage in experimental pneumococcal meningitis', *PLoS Pathogens*, 5(5). doi: 10.1371/journal.ppat.1000461.

Koide, T. *et al.* (2009) 'Olfactory neural circuitry for attraction to amino acids revealed by transposon-mediated gene trap approach in zebrafish', *Proceedings of the National Academy of Sciences of the*

United States of America, 106(24), pp. 9884–9889. doi: 10.1073/pnas.0900470106.

Kolmer, W. (1921) 'Das ,,Sagittalorgan" der Wirbeltiere.', *Anatomy and Embryology*, 60(3), pp. 652–717.

Kolmer, W. (1931) 'Über das Sagittalorgan, ein zentrales Sinnesorgan der Wirbeltiere, insbesondere beim Affen.', *Zeitschrift für Zellforschung und Mikroskopische Anatomie*, 13(1), pp. 236–248. doi: 10.1007/BF00406356.

Koltzenburg, M., Stucky, C. L. and Lewin, G. R. (1997) 'Receptive properties of mouse sensory neurons innervating hairy skin', *Journal of Neurophysiology*, 78(4), pp. 1841–1850. doi: 10.1152/jn.1997.78.4.1841.

Konieczny, M. R., Senyurt, H. and Krauspe, R. (2013) 'Epidemiology of adolescent idiopathic scoliosis', *Journal of Children's Orthopaedics*, 7(1), pp. 3–9. doi: 10.1007/s11832-012-0457-4.

Korsching, S. I. (2020) *Taste and Smell in Zebrafish*. Second Edi, *The Senses: A Comprehensive Reference*. Second Edi. Elsevier. doi: 10.1016/b978-0-12-809324-5.24155-2.

Koshimizu, T. A. *et al.* (2000) 'Characterization of calcium signaling by purinergic receptor-channels expressed in excitable cells', *Molecular Pharmacology*, 58(5), pp. 936–945. doi: 10.1124/mol.58.5.936.

Kotrschal, K. (1996) 'Solitary chemosensory cells: Why do primary aquatic vertebrates need another taste system?', *Trends in Ecology and Evolution*, 11(3), pp. 110–114. doi: 10.1016/0169-5347(96)81088-3.

Kotrschal, K., Krautgartner, W. D. and Hansen, A. (1997) 'Ontogeny of the solitary chemosensory cells in the zebrafish, Danio rerio', *Chemical Senses*, 22(2), pp. 111–118. doi: 10.1093/chemse/22.2.111.

Kramer-Zucker, A. G. *et al.* (2005) 'Cilia-driven fluid flow in the zebrafish pronephros, brain and Kupffer's vesicle is required for normal organogenesis', *Development*, 132(8), pp. 1907–1921. doi: 10.1242/dev.01772.

Krantic, S. (2000) 'Peptides as regulators of the immune system: Emphasis on somatostatin', *Peptides*, 21(12), pp. 1941–1964. doi: 10.1016/S0196-9781(00)00347-8.

Kútna, V. *et al.* (2014) 'Enigmatic cerebrospinal fluid-contacting neurons arise even after the termination of neurogenesis in the rat spinal cord during embryonic development and retain their immature-like characteristics until adulthood', *Acta Histochemica*, 116(1), pp. 278–285. doi: 10.1016/j.acthis.2013.08.004.

Kwan, K. M. *et al.* (2007) 'The Tol2kit: A multisite gateway-based construction Kit for Tol2 transposon transgenesis constructs', *Developmental Dynamics*, 236(11), pp. 3088–3099. doi:

10.1002/dvdy.21343.

Kwan, K. Y. *et al.* (2006) 'TRPA1 Contributes to Cold, Mechanical, and Chemical Nociception but Is Not Essential for Hair-Cell Transduction', *Neuron*, 50(2), pp. 277–289. doi: 10.1016/j.neuron.2006.03.042.

Lai, N. Y. *et al.* (2020) 'Gut-Innervating Nociceptor Neurons Regulate Peyer's Patch Microfold Cells and SFB Levels to Mediate Salmonella Host Defense', *Cell*. Elsevier Inc., 180(1), pp. 1–17. doi: 10.1016/j.cell.2019.11.014.

Lamotte, C. C. (1987) 'Vasoactive Intestinal Polypeptide Cerebrospinal Fluid-Contacting Neurons of the Monkey and Cat Spinal Central Canal', *Journal of Comparative Neurology*, 258(4), pp. 527–541. doi: 10.1002/cne.902580405.

LaMotte, R. H. and Campbell, J. N. (1978) 'Comparison of responses of warm and nociceptive C-fiber afferents in monkey with human judgments of thermal pain', *Journal of Neurophysiology*, 41(2), pp. 509–528. doi: 10.1152/jn.1978.41.2.509.

Langevin, C. *et al.* (2013) 'The antiviral innate immune response in fish: Evolution and conservation of the IFN system', *Journal of Molecular Biology*. Elsevier Ltd, 425(24), pp. 4904–4920. doi: 10.1016/j.jmb.2013.09.033.

Lawrence, C. (2011) 'Advances in zebrafish husbandry and management', *Methods in Cell Biology*, 104, pp. 429–451. doi: 10.1016/B978-0-12-374814-0.00023-9.

Lawrence, C. (2016) *New frontiers for zebrafish management*, *Methods in Cell Biology*. Elsevier Ltd. doi: 10.1016/bs.mcb.2016.04.015.

Lee, R. J. *et al.* (2012) 'T2R38 taste receptor polymorphisms underlie susceptibility to upper respiratory infection', *Journal of Clinical Investigation*, 122(11), pp. 4145–4159. doi: 10.1172/JCI64240.

Lee, R. J., Kofonow, J. M., *et al.* (2014) 'Bitter and sweet taste receptors regulate human upper respiratory innate immunity', *Journal of Clinical Investigation*, 124(3), pp. 1393–1405. doi: 10.1172/JCI72094.

Lee, R. J., Chen, B., *et al.* (2014) 'Mouse nasal epithelial innate immune responses to Pseudomonas aeruginosa quorum-sensing molecules require taste signaling components', *Innate Immunity*, 20(6), pp. 606–617. doi: 10.1177/1753425913503386.

Lee, R. J. *et al.* (2017) 'Bacterial D-amino acids suppress sinonasal innate immunity through sweet taste receptors in solitary chemosensory cells', *Science Signaling*, 10(495), pp. 1–12. doi: 10.1126/scisignal.aam7703.

Lee, W. *et al.* (2014) 'Endocan elicits severe vascular inflammatory responses in vitro and in vivo', *Journal of Cellular Physiology*, 229(5), pp. 620–630. doi: 10.1002/jcp.24485.

Lehtinen, M. K. *et al.* (2011) 'The Cerebrospinal Fluid Provides a Proliferative Niche for Neural Progenitor Cells', *Neuron*. Elsevier Inc., 69(5), pp. 893–905. doi: 10.1016/j.neuron.2011.01.023.

Leipold, E. *et al.* (2013) 'A de novo gain-of-function mutation in SCN11A causes loss of pain perception', *Nature Genetics*, 45(11), pp. 1399–1407. doi: 10.1038/ng.2767.

Lerner, R. A. *et al.* (1994) 'Cerebrodiene: A brain lipid isolated from sleep-deprived cats', *Proceedings of the National Academy of Sciences of the United States of America*, 91(20), pp. 9505–9508. doi: 10.1073/pnas.91.20.9505.

Lewin, G. R. and McMahon, S. B. (1991) 'Physiological properties of primary sensory neurons appropriately and inappropriately innervating skin in the adult rat', *Journal of Neurophysiology*, 66(4), pp. 1205–1217. doi: 10.1152/jn.1991.66.4.1205.

Li, F. (2013) 'Taste perception: From the tongue to the testis', *Molecular Human Reproduction*, 19(6), pp. 349–360. doi: 10.1093/molehr/gat009.

Li, L. *et al.* (2011) 'The Functional Organization of Cutaneous Low-Threshold Mechanosensory Neurons', *Cell*, 147(7), pp. 1615–1627. doi: 10.1016/j.cell.2011.11.027.

Li, W. *et al.* (2011) 'The neural circuits and sensory channels mediating harsh touch sensation in Caenorhabditis elegans', *Nature Communications*, 2(1), p. 315. doi: 10.1038/ncomms1308.

Liljencrantz, J. and Olausson, H. (2014) 'Tactile C fibers and their contributions to pleasant sensations and to tactile allodynia', *Frontiers in Behavioral Neuroscience*, 8(MAR), pp. 6–11. doi: 10.3389/fnbeh.2014.00037.

Lloyd, D. P. C. (1943a) 'CONDUCTION AND SYNAPTIC TRANSMISSION OF THE REFLEX RESPONSE TO STRETCH IN SPINAL CATS', *Journal of Neurophysiology*, 6(4), pp. 317–326. doi: 10.1152/jn.1943.6.4.317.

Lloyd, D. P. C. (1943b) 'NEURON PATTERNS CONTROLLING TRANSMISSION OF IPSILATERAL HIND LIMB REFLEXES IN CAT', *Journal of Neurophysiology*, 6(4), pp. 293–315. doi: 10.1152/jn.1943.6.4.293.

Lloyd, David P C (1946) 'FACILITATION AND INHIBITION OF SPINAL MOTONEURONS', *Journal of Neurophysiology*, 9(6), pp. 421–438. doi: 10.1152/jn.1946.9.6.421.

Lloyd, David P. C. (1946) 'INTEGRATIVE PATTERN OF EXCITATION AND INHIBITION IN TWO-NEURON REFLEX ARCS', *Journal of Neurophysiology*, 9(6), pp. 439–444. doi: 10.1152/jn.1946.9.6.439.

Löken, L. S. *et al.* (2009) 'Coding of pleasant touch by unmyelinated afferents in humans', *Nature Neuroscience*, 12(5), pp. 547–548. doi: 10.1038/nn.2312.

Louati, K. and Berenbaum, F. (2015) 'Fatigue in chronic inflammation - a link to pain pathways', *Arthritis Research and Therapy*. Arthritis Research & Therapy, 17(1), pp. 1–10. doi: 10.1186/s13075-015-0784-1.

Lu, H. *et al.* (2020) 'Reissner fibre-induced urotensin signalling from cerebrospinal fluid-contacting neurons prevents scoliosis of the vertebrate spine', *Biology Open*, 9(5). doi: 10.1242/bio.052027.

Lun, M. P. *et al.* (2015) 'Spatially heterogeneous choroid plexus transcriptomes encode positional identity and contribute to regional CSF production', *Journal of Neuroscience*, 35(12), pp. 4903–4916. doi: 10.1523/JNEUROSCI.3081-14.2015.

Ly, N. P. *et al.* (2005) 'Netrin-1 inhibits leukocyte migration in vitro and in vivo', *Proceedings of the National Academy of Sciences of the United States of America*, 102(41), pp. 14729–14734. doi: 10.1073/pnas.0506233102.

Ma, L. and Michel, W. C. (1998) 'Drugs affecting phospholipase C-mediated signal transduction block the olfactory cyclic nucleotide-gated current of adult zebrafish', *Journal of Neurophysiology*, 79(3), pp. 1183–1192. doi: 10.1152/jn.1998.79.3.1183.

Mainen, Z. F. and Sejnowski, T. J. (1996) 'Influence of dendritic structure on firing pattern in model neocortical neurons', *Nature*, pp. 363–366. doi: 10.1038/382363a0.

Maksimovic, S., Baba, Y. and Lumpkin, E. A. (2013) 'Neurotransmitters and synaptic components in the Merkel cell-neurite complex, a gentle-touch receptor', *Annals of the New York Academy of Sciences*, 1279(1), pp. 13–21. doi: 10.1111/nyas.12057.

Manoli, M. and Driever, W. (2012) 'Fluorescence-activated cell sorting (FACS) of fluorescently tagged cells from zebrafish larvae for RNA isolation', *Cold Spring Harbor Protocols*, 7(8), pp. 879–886. doi: 10.1101/pdb.prot069633.

Marichal, N. *et al.* (2009) 'Enigmatic central canal contacting cells: Immature neurons in "standby mode"?', *Journal of Neuroscience*, 29(32), pp. 10010–10024. doi: 10.1523/JNEUROSCI.6183-08.2009.

Marnas, H. *et al.* (no date) 'Diverse chemosensory cues can activate sensory neurons in contact with the cerebrospinal fluid'.

Marquart, G. D. *et al.* (2015) 'A 3D searchable database of transgenic zebrafish gal4 and cre lines for functional neuroanatomy studies', *Frontiers in Neural Circuits*, 9(November), pp. 1–17. doi: 10.3389/fncir.2015.00078.

Martin, B. *et al.* (1995) 'The recA gene of Streptococcus pneumoniae is part of a competence-induced operon and controls lysogenic induction', *Molecular Microbiology*, 15(2), pp. 367–379. doi: 10.1111/j.1365-2958.1995.tb02250.x.

Martín, C. *et al.* (2006) 'FGF2 plays a key role in embryonic cerebrospinal fluid trophic properties over chick embryo neuroepithelial stem cells', *Developmental Biology*, 297(2), pp. 402–416. doi: 10.1016/j.ydbio.2006.05.010.

Martin, J. *et al.* (2014) 'Vasopressin and oxytocin in CSF and plasma of patients with aneurysmal subarachnoid haemorrhage', *Neuropeptides*. Elsevier Ltd, 48(2), pp. 91–96. doi: 10.1016/j.npep.2013.12.004.

Matsumae, M. *et al.* (2016) 'Research into the physiology of cerebrospinal fluid reaches a new horizon: Intimate exchange between cerebrospinal fluid and interstitial fluid may contribute to maintenance of homeostasis in the central nervous system', *Neurologia Medico-Chirurgica*, 56(7), pp. 416–441. doi: 10.2176/nmc.ra.2016-0020.

Matsumoto, I., Ohmoto, M. and Abe, K. (2013) 'Functional diversification of taste cells in vertebrates', *Seminars in Cell and Developmental Biology*. Elsevier Ltd, 24(3), pp. 210–214. doi: 10.1016/j.semcdb.2012.10.004.

Matta, J. A. *et al.* (2008) 'General anesthetics activate a nociceptive ion channel to enhance pain and inflammation', *Proceedings of the National Academy of Sciences of the United States of America*, 105(25), pp. 8784–8789. doi: 10.1073/pnas.0711038105.

Maxwell Lawton, D. *et al.* (2000) 'Localization of the glutamate-aspartate transporter, GLAST, in rat taste buds', *European Journal of Neuroscience*, 12(9), pp. 3163–3171. doi: 10.1046/j.1460-9568.2000.00207.x.

McKemy, D. D., Neuhausser, W. M. and Julius, D. (2002) 'Identification of a cold receptor reveals a general role for TRP channels in thermosensation', *Nature*, 416(6876), pp. 52–58. doi: 10.1038/nature719.

McPherson, D. R. and Kemnitz, C. P. (1994) 'Modulation of lamprey fictive swimming and motoneuron physiology by dopamine, and its immunocytochemical localization in the spinal cord', *Neuroscience Letters*, 166(1), pp. 23–26. doi: 10.1016/0304-3940(94)90831-1.

Megías, M., Álvarez-Otero, R. and Pombal, M. A. (2003) 'Calbindin and calretinin immunoreactivities identify different types of neurons in the adult lamprey spinal cord', *Journal of Comparative Neurology*, 455(1), pp. 72–85. doi: 10.1002/cne.10473.

Meletti, S. *et al.* (2017) 'Decreased allopregnanolone levels in cerebrospinal fluid obtained during status epilepticus', *Epilepsia*, 58(2), pp. e16–e20. doi: 10.1111/epi.13625.

Merkel, F. (1875) ‘Tastzellen und Tastkörperchen bei den Hausthieren und beim Menschen’, *Archiv für Mikroskopische Anatomie*, 11(S1), pp. 636–652. doi: 10.1007/BF02933819.

Miao, E. A. *et al.* (2007) ‘TLR5 and Ipaf: Dual sensors of bacterial flagellin in the innate immune system’, *Seminars in Immunopathology*, 29(3), pp. 275–288. doi: 10.1007/s00281-007-0078-z.

Michel, W. C. and Derbidge, D. S. (1997) ‘Evidence of distinct amino acid and bile salt receptors in the olfactory system of the zebrafish, Danio rerio’, *Brain Research*, 764(1–2), pp. 179–187. doi: 10.1016/S0006-8993(97)00454-X.

Miesenböck, G., De Angelis, D. a and Rothman, J. E. (1998) ‘Visualizing secretion and synaptic transmission with pH-sensitive green fluorescent proteins.’, *Nature*, 394(6689), pp. 192–5. doi: 10.1038/28190.

Millard, C. L. and Woolf, C. J. (1988) ‘Sensory innervation of the hairs of the rat hindlimb: A light microscopic analysis’, *Journal of Comparative Neurology*, 277(2), pp. 183–194. doi: 10.1002/cne.902770203.

Mirat, O. *et al.* (2013) ‘ZebraZoom: An automated program for high-throughput behavioral analysis and categorization’, *Frontiers in Neural Circuits*, 7(JUNE), pp. 1–12. doi: 10.3389/fncir.2013.00107.

Miyasaka, N. *et al.* (2009) ‘From the olfactory bulb to higher brain Centers: Genetic visualization of secondary olfactory pathways in zebrafish’, *Journal of Neuroscience*, 29(15), pp. 4756–4767. doi: 10.1523/JNEUROSCI.0118-09.2009.

Mombaerts, P. (2004) ‘Genes and ligands for odorant, vomeronasal and taste receptors’, *Nature Reviews Neuroscience*, 5(4), pp. 263–278. doi: 10.1038/nrn1365.

Moqbel, R. and Coughlin, J. J. (2006) ‘Differential secretion of cytokines.’, *Science’s STKE : signal transduction knowledge environment*, 2006(338), pp. 1–5. doi: 10.1126/stke.3382006pe26.

Moqrich, A. *et al.* (2005) ‘Impaired thermosensation in mice lacking TRPV3, a heat and camphor sensor in the skin’, *Science*, 307(5714), pp. 1468–1472. doi: 10.1126/science.1108609.

Morita, Y. and Finger, T. E. (1998) ‘Differential projections of ciliated and microvillous olfactory receptor cells in the catfish, Ictalurus punctatus’, *Journal of Comparative Neurology*, 398(4), pp. 539–550. doi: 10.1002/(SICI)1096-9861(19980907)398:4<539::AID-CNE6>3.0.CO;2-3.

Morris, C. A., Benson, E. and White-Cooper, H. (2009) ‘Determination of gene expression patterns using in situ hybridization to Drosophila testes’, *Nature Protocols*. Nature Publishing Group, 4(12), pp. 1807–1819. doi: 10.1038/nprot.2009.192.

Muraki, K. *et al.* (2003) ‘TRPV2 Is a Component of Osmotically Sensitive Cation Channels in Murine Aortic Myocytes’, *Circulation Research*, 93(9), pp. 829–838. doi:

10.1161/01.RES.0000097263.10220.0C.

Murray, R. Z. and Stow, J. L. (2014) 'Cytokine secretion in macrophages: SNAREs, Rabs, and membrane trafficking', *Frontiers in Immunology*, 5(OCT), pp. 1–10. doi: 10.3389/fimmu.2014.00538.

Nagatsu, I. *et al.* (1988) 'Aromatic l-amino acid decarboxylase-immunoreactive neurons in and around the cerebrospinal fluid-contacting neurons of the central canal do not contain dopamine or serotonin in the mouse and rat spinal cord', *Brain Research*, 475(1), pp. 91–102. doi: 10.1016/0006-8993(88)90202-8.

Nagy, J. I. and Hunt, S. P. (1982) 'Fluoride-resistant acid phosphatase-containing neurones in dorsal root ganglia are separate from those containing substance P or somatostatin', *Neuroscience*, 7(1), pp. 89–97. doi: 10.1016/0306-4522(82)90155-5.

Nave, K. A. and Werner, H. B. (2014) 'Myelination of the nervous system: Mechanisms and functions', *Annual Review of Cell and Developmental Biology*, 30, pp. 503–533. doi: 10.1146/annurev-cellbio-100913-013101.

Navone, F. *et al.* (1986) 'Protein p38: An integral membrane protein specific for small vesicles of neurons and neuroendocrine cells', *Journal of Cell Biology*, 103(6), pp. 2511–2527. doi: 10.1083/jcb.103.6.2511.

Nelson, G. *et al.* (2001) 'Mammalian Sweet Taste Receptors', *Cell*, 106(3), pp. 381–390. doi: 10.1016/S0092-8674(01)00451-2.

Nemeroff, C. B. *et al.* (1984) 'Elevated concentrations of CSF corticotropin-releasing factor-like immunoreactivity in depressed patients', *Science*, 226(4680), pp. 1342–1344. doi: 10.1126/science.6334362.

Nilsson, C. L. *et al.* (2001) 'Processing of neuropeptide Y, galanin, and somatostatin in the cerebrospinal fluid of patients with Alzheimer's disease and frontotemporal dementia', *Peptides*, 22(12), pp. 2105–2112. doi: 10.1016/S0196-9781(01)00571-X.

North, R. A. (2002) 'Molecular physiology of P2X receptors', *Physiological Reviews*, 82(4), pp. 1013–1067. doi: 10.1152/physrev.00015.2002.

Ochi, J., Yamamoto, T. and Hosoya, Y. (1979) 'Comparative study of the monoamine neuron system in the spinal cord of the lamprey and hagfish', *Arch Histol Jpn*, 42(3), pp. 327–336. doi: 10.1679/aohc1950.42.327.

Ogura, T. *et al.* (2010) 'Chemoreception regulates chemical access to mouse vomeronasal organ: Role of solitary chemosensory cells', *PLoS ONE*, 5(7). doi: 10.1371/journal.pone.0011924.

Ohmoto, M. *et al.* (2008) 'Genetic tracing of the gustatory and trigeminal neural pathways originating

from T1R3-expressing taste receptor cells and solitary chemoreceptor cells', *Molecular and Cellular Neuroscience*, 38(4), pp. 505–517. doi: 10.1016/j.mcn.2008.04.011.

Ohmoto, M. *et al.* (2011) 'Mutually exclusive expression of Gαia and Gα14 reveals diversification of taste receptor cells in zebrafish', *Journal of Comparative Neurology*, 519(8), pp. 1616–1629. doi: 10.1002/cne.22589.

Oike, H. *et al.* (2007) 'Characterization of ligands for fish taste receptors', *Journal of Neuroscience*, 27(21), pp. 5584–5592. doi: 10.1523/JNEUROSCI.0651-07.2007.

Oka, Y. and Korsching, S. I. (2011) 'Shared and unique G alpha proteins in the zebrafish versus mammalian senses of taste and smell', *Chemical Senses*, 36(4), pp. 357–365. doi: 10.1093/chemse/bjq138.

Oka, Y., Saraiva, L. R. and Korsching, S. I. (2012) 'Crypt neurons express a single v1r-related ora gene', *Chemical Senses*, 37(3), pp. 219–227. doi: 10.1093/chemse/bjr095.

Omdal, R. (2020) 'The biological basis of chronic fatigue: neuroinflammation and innate immunity', *Current opinion in neurology*, 33(3), pp. 391–396. doi: 10.1097/WCO.0000000000000817.

Orts-Del'Immagine, A. *et al.* (2012) 'Properties of subependymal cerebrospinal fluid contacting neurones in the dorsal vagal complex of the mouse brainstem', *Journal of Physiology*, 590(16), pp. 3719–3741. doi: 10.1113/jphysiol.2012.227959.

Orts-Del'Immagine, A. *et al.* (2014) 'Morphology, distribution and phenotype of polycystin kidney disease 2-like 1-positive cerebrospinal fluid contacting neurons in the brainstem of adult mice', *PLoS ONE*, 9(2). doi: 10.1371/journal.pone.0087748.

Orts-Del'Immagine, A. *et al.* (2016) 'A single polycystic kidney disease 2-like 1 channel opening acts as a spike generator in cerebrospinal fluid-contacting neurons of adult mouse brainstem', *Neuropharmacology*, 101, pp. 549–565. doi: 10.1016/j.neuropharm.2015.07.030.

Orts-Del'Immagine, A. *et al.* (2020) 'Sensory Neurons Contacting the Cerebrospinal Fluid Require the Reissner Fiber to Detect Spinal Curvature In Vivo', *Current Biology*, 30(5), pp. 827-839.e4. doi: 10.1016/j.cub.2019.12.071.

Orts-Del'Immagine, A. and Wyart, C. (2017) 'Cerebrospinal-fluid-contacting neurons', *Current Biology*. Elsevier, 27(22), pp. R1198–R1200. doi: 10.1016/j.cub.2017.09.017.

Park, H.-C., Shin, J. and Appel, B. (2004) 'Spatial and temporal regulation of ventral spinal cord precursor specification by Hedgehog signaling', *Development*, 131(23), pp. 5959–5969. doi: 10.1242/dev.01456.

Park, U. *et al.* (2011) 'TRP vanilloid 2 knock-out mice are susceptible to perinatal lethality but display

normal thermal and mechanical nociception', *Journal of Neuroscience*, 31(32), pp. 11425–11436. doi: 10.1523/JNEUROSCI.1384-09.2011.

Pei, X. *et al.* (2014) 'PC3-Secreted Microprotein Is a Novel Chemoattractant Protein and Functions as a High-Affinity Ligand for CC Chemokine Receptor 2', *The Journal of Immunology*, 192(4), pp. 1878–1886. doi: 10.4049/jimmunol.1300758.

Peier, A. M. *et al.* (2002) 'A TRP channel that senses cold stimuli and menthol', *Cell*, 108(5), pp. 705–715. doi: 10.1016/S0092-8674(02)00652-9.

Perez, D. M. (2006) *The adrenergic receptors in the 21st century*. Totowa, New Jersey: Humana Press.

Petracca, Y. L. *et al.* (2016a) 'The late and dual origin of cerebrospinal fluid-contacting neurons in the mouse spinal cord', *The Company of Biologists Development*, 143(5), pp. 880–891. doi: 10.1242/dev.129254.

Petracca, Y. L. *et al.* (2016b) 'The late and dual origin of cerebrospinal fluid-contacting neurons in the mouse spinal cord', *Development*, 143(5), pp. 880–891. doi: 10.1242/dev.129254.

Pfister, P. and Rodriguez, I. (2005) 'Olfactory expression of a single and highly variable V1r pheromone receptor-like gene in fish species', *Proceedings of the National Academy of Sciences of the United States of America*, 102(15), pp. 5489–5494. doi: 10.1073/pnas.0402581102.

Polfliet, M. M. J. *et al.* (2001) 'Meningeal and Perivascular Macrophages of the Central Nervous System Play a Protective Role During Bacterial Meningitis', *The Journal of Immunology*, 167(8), pp. 4644–4650. doi: 10.4049/jimmunol.167.8.4644.

Prendergast, A. *et al.* (2019) 'Central Sensory Neurons Detect and Combat Pathogens Invading the Cerebrospinal Fluid', *SSRN Electronic Journal*. doi: 10.2139/ssrn.3404255.

Price, M. P. *et al.* (2000) 'The mammalian sodium channel BNC1 is required for normal touch sensation', *Nature*, 407(6807), pp. 1007–1011. doi: 10.1038/35039512.

Proske, U. and Gandevia, S. C. (2012) 'The proprioceptive senses: Their roles in signaling body shape, body position and movement, and muscle force', *Physiological Reviews*, 92(4), pp. 1651–1697. doi: 10.1152/physrev.00048.2011.

Purves, D. *et al.* (eds) (2001) *Neuroscience, Second Edition*. 2nd edn. Sinauer Associates.

Quan, F. B. *et al.* (2015) 'Comparative distribution and in vitro activities of the urotensin II-related peptides URP1 and URP2 in zebrafish: Evidence for their colocalization in spinal cerebrospinal fluid-contacting neurons', *PLoS ONE*, 10(3), pp. 1–21. doi: 10.1371/journal.pone.0119290.

Quan, F. B. *et al.* (2020) 'Somatostatin 1.1 contributes to the innate exploration of zebrafish larva', *Scientific Reports*. Nature Publishing Group UK, 10(1), pp. 1–12. doi: 10.1038/s41598-020-72039-x.

Reali, C. *et al.* (2011) 'GABAergic signalling in a neurogenic niche of the turtle spinal cord', *Journal of Physiology*, 589(23), pp. 5633–5647. doi: 10.1113/jphysiol.2011.214312.

Renshaw, S. A. *et al.* (2006) 'A transgenic zebrafish model of neutrophilic inflammation', *Blood*, 108(13), pp. 3976–3978. doi: 10.1182/blood-2006-05-024075.

Reutter, K., Boudriot, F. and Witt, M. (2000) 'Heterogeneity of fish taste bud ultrastructure as demonstrated in the holosteans Amia calva and Lepisosteus oculatus', *Philosophical Transactions of the Royal Society B: Biological Sciences*, 355(1401), pp. 1225–1228. doi: 10.1098/rstb.2000.0672.

Rink, E. and Wullimann, M. F. (1998) 'Some forebrain connections of the gustatory system in the goldfish Carassius auratus visualized by separate DiI application to the hypothalamic inferior lobe and the torus lateralis', *Journal of Comparative Neurology*, 394(2), pp. 152–170. doi: 10.1002/(SICI)1096-9861(19980504)394:2<152::AID-CNE2>3.0.CO;2-1.

Roberts, B. L. *et al.* (1995) 'Dopaminergic and GABAergic cerebrospinal fluid-contacting neurons along the central canal of the spinal cord of the Eel and Trout', *Journal of Comparative Neurology*, 354(3), pp. 423–437. doi: 10.1002/cne.903540310.

Robinson, D. R. and Gebhart, G. F. (2008) 'Inside information: The unique features of visceral sensation', *Molecular Interventions*, 8(5), pp. 242–253. doi: 10.1124/mi.8.5.9.

Robles, E., Laurell, E. and Baier, H. (2014) 'The retinal projectome reveals brain-area-specific visual representations generated by ganglion cell diversity', *Current Biology*. Elsevier Ltd, 24(18), pp. 2085–2096. doi: 10.1016/j.cub.2014.07.080.

Romigi, A. *et al.* (2010) 'Cerebrospinal fluid levels of the endocannabinoid anandamide are reduced in patients with untreated newly diagnosed temporal lobe epilepsy', *Epilepsia*, 51(5), pp. 768–772. doi: 10.1111/j.1528-1167.2009.02334.x.

Rose, C. D. *et al.* (2020) 'SCO-Spondin Defects and Neuroinflammation Are Conserved Mechanisms Driving Spinal Deformity across Genetic Models of Idiopathic Scoliosis', *Current Biology*, 30(12), pp. 2363-2373.e6. doi: 10.1016/j.cub.2020.04.020.

Ruffini, A. (1894) 'Di un novo organo nervoso terminale, e sulla presenza dei corpuscoli Golgi-Mazzoni nel connettivo sottocutaneo dei polpastrelli delle dita dell-uomo', *Attl Dell Accademia Nazionale dei Lincet*, 7, pp. 398–410.

Russo, R. E. *et al.* (2004) 'Functional and molecular clues reveal precursor-like cells and immature neurones in the turtle spinal cord', *Journal of Physiology*, 560(3), pp. 831–838. doi: 10.1113/jphysiol.2004.072405.

Sainburg, R. L. *et al.* (1995) 'Control of limb dynamics in normal subjects and patients without proprioception', *Journal of Neurophysiology*, 73(2), pp. 820–835. doi: 10.1152/jn.1995.73.2.820.

Salvatierra, J. *et al.* (2018) 'NaV1.1 inhibition can reduce visceral hypersensitivity', *JCI insight*, 3(11), pp. 1–13. doi: 10.1172/jci.insight.121000.

Sato, K. and Suzuki, N. (2001) 'Whole-cell response characteristics of ciliated and microvillous olfactory receptor neurons to amino acids, pheromone candidates and urine in rainbow trout', *Chemical Senses*, 26(9), pp. 1145–1156. doi: 10.1093/chemse/26.9.1145.

Sato, Y., Miyasaka, N. and Yoshihara, Y. (2005) 'Mutually exclusive glomerular innervation by two distinct types of olfactory sensory neurons revealed in transgenic zebrafish', *Journal of Neuroscience*, 25(20), pp. 4889–4897. doi: 10.1523/JNEUROSCI.0679-05.2005.

Sato, Y., Miyasaka, N. and Yoshihara, Y. (2007) 'Hierarchical regulation of odorant receptor gene choice and subsequent axonal projection of olfactory sensory neurons in zebrafish', *Journal of Neuroscience*, 27(7), pp. 1606–1615. doi: 10.1523/JNEUROSCI.4218-06.2007.

Saunders, C. J. *et al.* (2014) 'Cholinergic neurotransmission links solitary chemosensory cells to nasal inflammation', *Proceedings of the National Academy of Sciences of the United States of America*, 111(16), pp. 6075–6080. doi: 10.1073/pnas.1402251111.

Sawamoto, K. *et al.* (2006) 'New Neurons Follow the Flow of Cerebrospinal Fluid in the Adult Brain', *Science*, 311(5761), pp. 629–632. doi: 10.1126/science.1119133.

Schepers, R. J. and Ringkamp, M. (2009) 'Thermoreceptors and thermosensitive afferents', *Neuroscience and Biobehavioral Reviews*, 33(3), pp. 205–212. doi: 10.1016/j.neubiorev.2008.07.009.

Schindelin, J. *et al.* (2012) 'Fiji: An open-source platform for biological-image analysis', *Nature Methods*, 9(7), pp. 676–682. doi: 10.1038/nmeth.2019.

Schmachtenberg, O. (2006) 'Histological and electrophysiological properties of crypt cells from the olfactory epithelium of the marine teleost Trachurus symmetricus', *Journal of Comparative Neurology*, 495(1), pp. 113–121. doi: 10.1002/cne.20847.

Schmidt, A. P. *et al.* (2015) 'Changes in Purines Concentration in the Cerebrospinal Fluid of Pregnant Women Experiencing Pain During Active Labor', *Neurochemical Research*, 40(11), pp. 2262–2269. doi: 10.1007/s11064-015-1716-9.

Schmidt, R. *et al.* (1995) 'Novel classes of responsive and unresponsive C nociceptors in human skin', *The Journal of Neuroscience*, 15(1), pp. 333–341. doi: 10.1523/jneurosci.15-01-00333.1995.

Schotland, J. L. *et al.* (1996) 'Synaptic and nonsynaptic monoaminergic neuron systems in the lamprey spinal cord', *Journal of Comparative Neurology*, 372(2), pp. 229–244. doi:

10.1002/(SICI)1096-9861(19960819)372:2<229::AID-CNE6>3.0.CO;2-5.

Schröder, J. M. *et al.* (1989) 'Scanning electron microscopy of teased intrafusal muscle fibers from rat muscle spindles', *Muscle & Nerve*, 12(3), pp. 221–232. doi: 10.1002/mus.880120311.

Schueren, A. M. and DeSantis, M. (1985) 'Cellular heterogeneity in the ependymal layer of the chicken's lumbosacral spinal cord', *Experimental Neurology*, 87(2), pp. 387–391. doi: 10.1016/0014-4886(85)90230-4.

Sfameni, A. (1902) 'Recherches anatomiques sur l'existence des i m f S e t sur leur mode de 88 terminer d a m le tissu adipeux, dam le perioste, dans le periehondre e t dans les tissus qui renforcent les articulations.', *Arch. ital. di Biol.*, 38, pp. 49–101.

Shah, A. S. *et al.* (2009) 'Motile cilia of human airway epithelia are chemosensory', *Science*, 325(5944), pp. 1131–1134. doi: 10.1126/science.1173869.

Sherrington, C. S. (1906) *The integrative action of the nervous system*. New York: C Scribner and Sons.

Shimosegawa, T. *et al.* (1986) 'An immunohistochemical study of methionine-enkephalin-Arg6-Gly7-Leu8-like immunoreactivity-containing liquor-contacting neurons (LCNs) in the rat spinal cord', *Brain Research*, 379(1), pp. 1–9. doi: 10.1016/0006-8993(86)90249-0.

Shin, J. *et al.* (2007) 'Notch signaling regulates neural precursor allocation and binary neuronal fate decisions in zebrafish', *Development*, 134(10), pp. 1911–1920. doi: 10.1242/dev.001602.

Shiriagin, V. and Korsching, S. I. (2018) 'Massive expansion of bitter taste receptors in blind cavefish, Astyanax mexicanus', *Chemical Senses*. doi: 10.1093/chemse/bjy062.

Shooshtarizadeh, P. *et al.* (2010) 'The antimicrobial peptides derived from chromogranin/secretogranin family, new actors of innate immunity', *Regulatory Peptides*. Elsevier B.V., 165(1), pp. 102–110. doi: 10.1016/j.regpep.2009.11.014.

Shu, X. and Mendell, L. M. (1999) 'Nerve growth factor acutely sensitizes the response of adult rat sensory neurons to capsaicin', *Neuroscience Letters*, 274(3), pp. 159–162. doi: 10.1016/S0304-3940(99)00701-6.

Siegel, G. *et al.* (1999) 'Chapter 13: Serotonin Receptors', in *Basic Neurochemistry: Molecular, Cellular, and Medical Aspects.* Philadelphia: Lippincott-Raven, pp. 263–292.

Silverman, J. D. and Kruger, L. (1990) 'Selective neuronal glycoconjugate expression in sensory and autonomic ganglia: relation of lectin reactivity to peptide and enzyme markers', *Journal of Neurocytology*, 19(5), pp. 789–801. doi: 10.1007/BF01188046.

Sims, T. J. (1977) ‘The development of monoamine-containing neurons in the brain and spinal cord of the salamander, Ambystoma mexicanum’, *The Journal of Comparative Neurology*, 173(2), pp. 319–335. doi: 10.1002/cne.901730208.

Slager, J., Aprianto, R. and Veening, J.-W. (2018) ‘Deep genome annotation of the opportunistic human pathogen Streptococcus pneumoniae D39’, *Nucleic Acids Research*. Oxford University Press, 46(19), pp. 9971–9989. doi: 10.1093/nar/gky725.

Smith, G. D. *et al.* (2002) ‘TRPV3 is a temperature-sensitive vanilloid receptor-like protein’, *Nature*, 418(6894), pp. 186–190. doi: 10.1038/nature00894.

Sonner, M. J., Walters, M. C. and Ladle, D. R. (2017) ‘Analysis of proprioceptive sensory innervation of the mouse soleus: A whole-mount muscle approach’, *PLoS ONE*, 12(1), pp. 1–18. doi: 10.1371/journal.pone.0170751.

Spitzer, N. C. and Lamborghini, J. E. (1976) ‘The development of the action potential mechanism of amphibian neurons isolated in culture’, *Proceedings of the National Academy of Sciences of the United States of America*, 73(5), pp. 1641–1645. doi: 10.1073/pnas.73.5.1641.

Spitzer, N. C., Vincent, A. and Lautermilch, N. J. (2000) ‘Differentiation of electrical excitability in motoneurons’, *Brain Research Bulletin*, 53(5), pp. 547–552. doi: 10.1016/S0361-9230(00)00388-9.

Sternberg, J. R. (2016) *Neuronal populations underlying locomotion in zebrafish*. Université Pierre et Marie Curie - Paris VI.

Sternberg, J. R. *et al.* (2016) ‘Optimization of a Neurotoxin to Investigate the Contribution of Excitatory Interneurons to Speed Modulation In Vivo’, *Current Biology*. Elsevier Ltd., 26(17), pp. 2319–2328. doi: 10.1016/j.cub.2016.06.037.

Sternberg, J. R. *et al.* (2018) ‘Pkd2l1 is required for mechanoception in cerebrospinal fluid-contacting neurons and maintenance of spine curvature’, *Nature Communications*, 9(1), pp. 1–10. doi: 10.1038/s41467-018-06225-x.

Stoeckel, M. E. *et al.* (2003) ‘Cerebrospinal fluid-contacting neurons in the rat spinal cord, a γ-aminobutyric acidergic system expressing the P2X2 subunit of purinergic receptors, PSA-NCAM, and GAP-43 immunoreactivities: Light and electron microscopic study’, *Journal of Comparative Neurology*, 457(2), pp. 159–174. doi: 10.1002/cne.10565.

Story, G. M. *et al.* (2003) ‘ANKTM1, a TRP-like channel expressed in nociceptive neurons, is activated by cold temperatures’, *Cell*, 112(6), pp. 819–829. doi: 10.1016/S0092-8674(03)00158-2.

Strittmatter, M. *et al.* (1997) ‘Cerebrospinal fluid neuropeptides and monoaminergic transmitters in patients with trigeminal neuralgia’, *Headache*, 37(4), pp. 211–216. doi: 10.1046/j.1526-4610.1997.3704211.x.

Sueiro, C. *et al.* (2004) 'Distribution and development of glutamic acid decarboxylase immunoreactivity in the spinal cord of the dogfish Scyliorhinus canicula (Elasmobranchs)', *Journal of Comparative Neurology*, 478(2), pp. 189–206. doi: 10.1002/cne.20285.

Talbot, S. *et al.* (2015) 'Silencing Nociceptor Neurons Reduces Allergic Airway Inflammation', *Neuron*, 87(2), pp. 341–354. doi: 10.1016/j.neuron.2015.06.007.

Tan, C. H. and McNaughton, P. A. (2016) 'The TRPM2 ion channel is required for sensitivity to warmth', *Nature*, 536(7617), pp. 460–463. doi: 10.1038/nature19074.

Di Terlizzi, R. and Platt, S. (2006) 'The function, composition and analysis of cerebrospinal fluid in companion animals: Part I - Function and composition', *Veterinary Journal*, 172(3), pp. 422–431. doi: 10.1016/j.tvjl.2005.07.021.

Thisse, C. and Thisse, B. (2008) 'High-resolution in situ hybridization to whole-mount zebrafish embryos', *Nature Protocols*, 3(1), pp. 59–69. doi: 10.1038/nprot.2007.514.

Thompson, A. and R. Lummis, S. (2006) '5-HT3 Receptors', *Current Pharmaceutical Design*, 12(28), pp. 3615–3630. doi: 10.2174/138161206778522029.

Thouvenin, O. *et al.* (2020) 'Origin and role of the cerebrospinal fluid bidirectional flow in the central canal', *eLife*, 9, pp. 1–37. doi: 10.7554/eLife.47699.

Tizzano, M. *et al.* (2010) 'Nasal chemosensory cells use bitter taste signaling to detect irritants and bacterial signals', *Proceedings of the National Academy of Sciences of the United States of America*, 107(7), pp. 3210–3215. doi: 10.1073/pnas.0911934107.

Tizzano, M. *et al.* (2011) 'Expression of taste receptors in Solitary Chemosensory Cells of rodent airways', *BMC Pulmonary Medicine*, 11, pp. 1–12. doi: 10.1186/1471-2466-11-3.

Todaka, H. *et al.* (2004) 'Warm temperature-sensitive transient receptor potential vanilloid 4 (TRPV4) plays an essential role in thermal hyperalgesia', *Journal of Biological Chemistry*. Â© 2004 ASBMB. Currently published by Elsevier Inc; originally published by American Society for Biochemistry and Molecular Biology., 279(34), pp. 35133–35138. doi: 10.1074/jbc.M406260200.

Tomasiuk, R. *et al.* (2016) 'Higher level of NT-proCNP in cerebrospinal fluid of patients with meningitis', *Neuroscience Letters*. Elsevier Ireland Ltd, 614, pp. 29–32. doi: 10.1016/j.neulet.2015.12.053.

Tomchik, S. M. *et al.* (2007) 'Breadth of tuning and taste coding in mammalian taste buds', *Journal of Neuroscience*, 27(40), pp. 10840–10848. doi: 10.1523/JNEUROSCI.1863-07.2007.

Tominaga, M. *et al.* (1998) 'The cloned capsaicin receptor integrates multiple pain-producing stimuli', *Neuron*, 21(3), pp. 531–543. doi: 10.1016/S0896-6273(00)80564-4.

Tracey, W. D. *et al.* (2003) ‘painless, a Drosophila gene essential for nociception’, *Cell*, 113(2), pp. 261–273. doi: 10.1016/S0092-8674(03)00272-1.

Treede, R. D., Meyer, R. A. and Campbell, J. N. (1998) ‘Myelinated mechanically insensitive afferents from monkey hairy skin: Heat-response properties’, *Journal of Neurophysiology*, 80(3), pp. 1082–1093. doi: 10.1152/jn.1998.80.3.1082.

Trostdorf, F. *et al.* (1999) ‘Reduction of meningeal macrophages does not decrease migration of granulocytes into the CSF and brain parenchyma in experimental pneumococcal meningitis’, *Journal of Neuroimmunology*, 99(2), pp. 205–210. doi: 10.1016/S0165-5728(99)00121-6.

Troutwine, B. R. *et al.* (2020) ‘The Reissner Fiber Is Highly Dynamic In Vivo and Controls Morphogenesis of the Spine’, *Current Biology*. Elsevier Ltd., 30(12), pp. 2353-2362.e3. doi: 10.1016/j.cub.2020.04.015.

Tsujikawa, M. and Malicki, J. (2004) ‘Intraflagellar transport genes are essential for differentiation and survival of vertebrate sensory neurons’, *Neuron*, 42(5), pp. 703–716. doi: 10.1016/S0896-6273(04)00268-5.

Tuomanen, E. *et al.* (1985) ‘The induction of meningeal inflammation by components of the pneumococcal cell wall’, *Journal of Infectious Diseases*, 151(5), pp. 859–868. doi: 10.1093/infdis/151.5.859.

Tuthill, J. C. and Azim, E. (2018) ‘Proprioception’, *Current Biology*, 28(5), pp. R194–R203. doi: 10.1016/j.cub.2018.01.064.

Vandenbeuch, A., Clapp, T. R. and Kinnamon, S. C. (2008) ‘Amiloride-sensitive channels in type I fungiform taste cells in mouse’, *BMC Neuroscience*, 9, pp. 1–13. doi: 10.1186/1471-2202-9-1.

Vaudry, H. *et al.* (2010) ‘Urotensin II, from fish to human’, *Annals of the New York Academy of Sciences*, 1200, pp. 53–66. doi: 10.1111/j.1749-6632.2010.05514.x.

Verbeurgt, C. *et al.* (2017) ‘The human bitter taste receptor T2R38 is broadly tuned for bacterial compounds’, *PLoS ONE*, 12(9). doi: 10.1371/journal.pone.0181302.

Vielma, A. *et al.* (2008) ‘The elusive crypt olfactory receptor neuron: Evidence for its stimulation by amino acids and cAMP pathway agonists’, *Journal of Experimental Biology*, 211(15), pp. 2417–2422. doi: 10.1242/jeb.018796.

Vígh, B. *et al.* (2004) ‘The system of cerebrospinal fluid-contacting neurons. Its supposed role in the nonsynaptic signal transmission of the brain’, *Histology and Histopathology*, 19(2), pp. 607–628. doi: 10.1002/brb3.218.

Vigh, B. and Vigh-Teichmann, I. (1973) ‘Comparative Ultrastructure of the Cerebrospinal Fluid-

Contacting Neurons', *International Review of Cytology*, 35(C), pp. 189–251. doi: 10.1016/S0074-7696(08)60355-1.

Vigh, B. and Vigh-Teichmann, I. (1981) 'Light- and electron-microscopic demonstration of immunoreactive opsin in the pinealocytes of various vertebrates', *Cell And Tissue Research*, 221(2), pp. 451–463. doi: 10.1007/BF00216748.

Vigh, B. and Vigh-Teichmann, I. (1998) 'Actual problems of the cerebrospinal fluid-contacting neurons', *Microscopy Research and Technique*, 41(1), pp. 57–83. doi: 10.1002/(SICI)1097-0029(19980401)41:1<57::AID-JEMT6>3.0.CO;2-R.

Vigh, B., Vigh-Teichmann, I. and Aros, B. (1977) 'Special dendritic and axonal endings formed by the cerebrospinal fluid contacting neurons of the spinal cord', *Cell and Tissue Research*, 183(4), pp. 541–552. doi: 10.1007/BF00225666.

Vize, P. D., McCoy, K. E. and Zhou, X. (2009) 'Multichannel wholemount fluorescent and fluorescent/chromogenic in situ hybridization in xenopus embryos', *Nature Protocols*, 4(6), pp. 975–983. doi: 10.1038/nprot.2009.69.

Vriens, J. *et al.* (2011) 'TRPM3 Is a Nociceptor Channel Involved in the Detection of Noxious Heat', *Neuron*. Elsevier Inc., 70(3), pp. 482–494. doi: 10.1016/j.neuron.2011.02.051.

Vriens, J., Nilius, B. and Voets, T. (2014) 'Peripheral thermosensation in mammals', *Nature Reviews Neuroscience*. Nature Publishing Group, 15(9), pp. 573–589. doi: 10.1038/nrn3784.

Wakisaka, N. *et al.* (2017) 'An Adenosine Receptor for Olfaction in Fish', *Current Biology*. Elsevier Ltd., 27(10), pp. 1437-1447.e4. doi: 10.1016/j.cub.2017.04.014.

Waxman, S. G. (1980) 'Determinants of conduction velocity in myelinated nerve fibers', *Muscle & Nerve*, 3(2), pp. 141–150. doi: 10.1002/mus.880030207.

Weber, A. I. *et al.* (2013) 'Spatial and temporal codes mediate the tactile perception of natural textures', *Proceedings of the National Academy of Sciences of the United States of America*, 110(42), pp. 17107–17112. doi: 10.1073/pnas.1305509110.

Welch, M. J., Markham, C. H. and Jenden, D. J. (1976) 'Acetylcholine and choline in cerebrospinal fluid of patients with Parkinson's disease and Huntington's chorea', *Journal of Neurology, Neurosurgery, and Psychiatry*, 39(4), pp. 367–374. doi: 10.1136/jnnp.39.4.367.

Westerfield, M. (2000) *The zebrafish book. A guide for the laboratory use of zebrafish (Danio rerio), Fourth Edition*. 4th edn. Eugene: Univ. of Oregon Press.

Wilkinson, K. A., Kloefkorn, H. E. and Hochman, S. (2012) 'Characterization of muscle spindle afferents in the adult mouse using an in vitro muscle-nerve preparation', *PLoS ONE*, 7(6). doi:

10.1371/journal.pone.0039140.

Woehrl, B. *et al.* (2011) 'Complement component 5 contributes to poor disease outcome in humans and mice with pneumococcal meningitis', *Journal of Clinical Investigation*, 121(10), pp. 3943–3953. doi: 10.1172/JCI57522.

Woodbury, C. J. and Koerber, H. R. (2007) 'Central and peripheral anatomy of slowly adapting type I low-threshold mechanoreceptors innervating trunk skin of neonatal mice', *The Journal of Comparative Neurology*, 505(5), pp. 547–561. doi: 10.1002/cne.21517.

Wu, M.-Y. *et al.* (2021) 'Spinal sensory neurons project onto the hindbrain to stabilize posture and enhance locomotor speed', *Current Biology*, 31(15), pp. 3315–3329. doi: 10.1016/j.cub.2021.05.042.

Wyart, C. *et al.* (2009) 'Optogenetic dissection of a behavioural module in the vertebrate spinal cord', *Nature*. Nature Publishing Group, 461(7262), pp. 407–410. doi: 10.1038/nature08323.

Wyart, C. *et al.* (no date) 'Understanding the spinal cord's intrinsic polymodal sensory system', *Nature Reviews Neuroscience*.

Xie, L. *et al.* (2013) 'Sleep drives metabolite clearance from the adult brain', *Science*, 342(6156), pp. 373–377. doi: 10.1126/science.1241224.

Yagi, J. *et al.* (2006) 'Sustained currents through ASIC3 ion channels at the modest pH changes that occur during myocardial ischemia', *Circulation Research*, 99(5), pp. 501–509. doi: 10.1161/01.RES.0000238388.79295.4c.

Yang, L., Rastegar, S. and Strähle, U. (2010) 'Regulatory interactions specifying Kolmer-Agduhr interneurons', *Development*, 137(16), pp. 2713–2722. doi: 10.1242/dev.048470.

Yasuoka, A. *et al.* (2004) 'Phospholipase C-beta 2 as a mammalian taste signaling marker is expressed in the multiple gustatory tissues of medaka fish, Oryzias latipes', *Mechanisms of Development*, 121(7–8), pp. 985–989. doi: 10.1016/j.mod.2004.03.009.

Yoshida, Y. *et al.* (2007) 'Transient receptor potential channel M5 and phospholipaseC-β2 colocalizing in zebrafish taste receptor cells', *NeuroReport*, 18(15), pp. 1517–1520. doi: 10.1097/WNR.0b013e3282ec6874.

Yu, Y. X. *et al.* (2015) 'Odor fingerprinting of listeria monocytogenes recognized by SPME-GC-MS and E-nose', *Canadian Journal of Microbiology*, 61(5), pp. 367–372. doi: 10.1139/cjm-2014-0652.

Yulis, C. R. and Lederis, K. (1988) 'Relationship between urotensin II- and somatostatin-immunoreactive spinal cord neurons of Catostomus commersoni and Oncorhynchus kisutch (Teleostei)', *Cell and Tissue Research*, 254(3), pp. 539–542. doi: 10.1007/BF00226503.

Zappaterra, M. W. and Lehtinen, M. K. (2012) ‘The cerebrospinal fluid: Regulator of neurogenesis, behavior, and beyond’, *Cellular and Molecular Life Sciences*, 69(17), pp. 2863–2878. doi: 10.1007/s00018-012-0957-x.

Zhang, X. (2015) ‘Molecular sensors and modulators of thermoreception’, *Channels*, 9(2), pp. 73–81. doi: 10.1080/19336950.2015.1025186.

Zhang, X. *et al.* (2018a) ‘Cilia-driven cerebrospinal fluid flow directs expression of urotensin neuropeptides to straighten the vertebrate body axis’, *Nature Genetics*. Springer US, 50(12), pp. 1666–1673. doi: 10.1038/s41588-018-0260-3.

Zhang, X. *et al.* (2018b) ‘Cilia-driven cerebrospinal fluid flow directs expression of urotensin neuropeptides to straighten the vertebrate body axis’, *Nature Genetics*. Springer US, 50(12), pp. 1666–1673. doi: 10.1038/s41588-018-0260-3.

Zhang, X. Y. *et al.* (2013) ‘Gain-of-Function mutations in SCN11A cause familial episodic pain’, *American Journal of Human Genetics*. The American Society of Human Genetics, 93(5), pp. 957–966. doi: 10.1016/j.ajhg.2013.09.016.

Zhang, Y. *et al.* (2003) ‘Coding of sweet, bitter, and umami tastes: Different receptor cells sharing similar signaling pathways’, *Cell*, 112(3), pp. 293–301. doi: 10.1016/S0092-8674(03)00071-0.

Zhao, G. Q. *et al.* (2003) ‘The receptors for mammalian sweet and umami taste’, *Cell*, 115(3), pp. 255–266. doi: 10.1016/S0092-8674(03)00844-4.

Zhou, W. *et al.* (2012) ‘The evolution of tachykinin/tachykinin receptor (TAC/TACR) in vertebrates and molecular identification of the TAC3/TACR3 system in zebrafish (Danio rerio)’, *Molecular and Cellular Endocrinology*. Elsevier Ireland Ltd, 361(1–2), pp. 202–212. doi: 10.1016/j.mce.2012.04.007.

Zimmermann, K. *et al.* (2007) ‘Sensory neuron sodium channel Nav1.8 is essential for pain at low temperatures’, *Nature*, 447(7146), pp. 855–858. doi: 10.1038/nature05880.

Zoons, E. *et al.* (2008) ‘Seizures in adults with bacterial meningitis.’, *Neurology*, 70(22 Pt 2), pp. 2109–2115. doi: 10.1212/01.wnl.0000288178.91614.5d.